



**This electronic thesis or dissertation has been
downloaded from Explore Bristol Research,
<http://research-information.bristol.ac.uk>**

Author:

King, Logan

Title:

**Macroevolutionary and Ontogenetic Trends in the Anatomy and Morphology of the
Non-Avian Dinosaur Endocranium**

General rights

Access to the thesis is subject to the Creative Commons Attribution - NonCommercial-No Derivatives 4.0 International Public License. A copy of this may be found at <https://creativecommons.org/licenses/by-nc-nd/4.0/legalcode>. This license sets out your rights and the restrictions that apply to your access to the thesis so it is important you read this before proceeding.

Take down policy

Some pages of this thesis may have been removed for copyright restrictions prior to having it been deposited in Explore Bristol Research. However, if you have discovered material within the thesis that you consider to be unlawful e.g. breaches of copyright (either yours or that of a third party) or any other law, including but not limited to those relating to patent, trademark, confidentiality, data protection, obscenity, defamation, libel, then please contact collections-metadata@bristol.ac.uk and include the following information in your message:

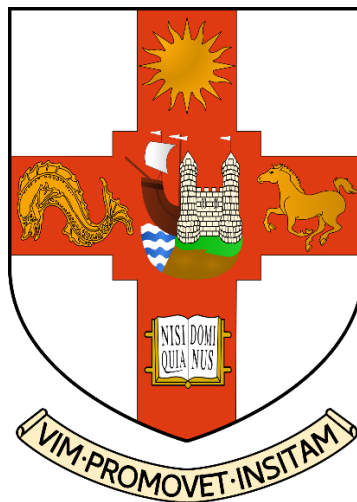
- Your contact details
- Bibliographic details for the item, including a URL
- An outline nature of the complaint

Your claim will be investigated and, where appropriate, the item in question will be removed from public view as soon as possible.

Macroevolutionary and Ontogenetic Trends in the Anatomy and Morphology of the Non-Avian Dinosaur Endocranium

by

Logan King



A dissertation submitted to the University of Bristol in accordance with the requirements for award of the degree of Doctor of Philosophy in the Faculty of Science.

June 2021

Word count: 59,189

Abstract

The subfield of dinosaur palaeoneurology describes and compares the function and form of neuroanatomy in non-avian dinosaur taxa. Currently, palaeoneurologists have collected nearly 100 partial and complete reconstructed endocrasts – the internal soft tissue space of the braincase (Chapter 1). From these endocrania, palaeontologists have been able to explore the relationship between the brain, behaviour, palaeoecology, and trophic ecology of adult non-avian dinosaurs (Chapter 2). However, immature specimens from an ontogenetic series are rarely published upon due to their rarity in the fossil record. Similarly, our understanding of postnatal ontogenetic development in extant taxa is frequently referred to in the literature, but very few studies describe or compare full ontogenetic series of modern archosaur endocrania. By understanding how the morphology and relative sizes of endocrania change with developmental age in modern taxa, palaeoneurologists can apply the same methods to interpret extinct taxa (Chapter 3). Surprisingly, when a complete ontogenetic series of a non-avian dinosaur (*Psittacosaurus lujiatunensis*) endocrania is compared to patterns in modern archosaurs, the endocrasts diverge from established avian or crocodilian developmental patterns (Chapter 4). This indicates limitations in our understanding of how the brains or endocrasts change shape, flexure, and anatomical size with age in extinct taxa. This shows the importance of determining the age of endocranial specimens – and especially if the endocrast is being used in macroevolutionary studies. To emphasize this point, the juvenile endocrast of *P. lujiatunensis* is convergent in form with bird endocrasts (Chapter 5). This underlines how little is known about the relationship between the non-avian endocranium, paedomorphosis, and heterochrony when comparing adult bird endocrasts to non-avian dinosaurs.

The aims of this thesis are to show the relationship between an endocrast, palaeoecology, and postcranial fossils (Chapter 2); demonstrate the difference between modern exemplar archosaur endocrasts and discuss what the differences mean for non-avian dinosaurs (Chapter 3); describe the ontogenetic changes that occur in the basal ceratopsian *P. lujiatunensis* (Chapter 4); and compare the shape of the endocrast from the juvenile-most *P. lujiatunensis* with other archosaurs (Chapter 5). Broadly, I found that while endocrania are helpful in supporting functions of the brain and palaeoecological interpretations for a species; the form of the non-avian dinosaur is not easily predictable. Ontogeny was found to be a large driver of endocranial shape change in *P. lujiatunensis* – meaning that knowing the ontogenetic stage is crucial for palaeoneurology studies. Furthermore, the juvenile endocrast of *P. lujiatunensis* was found to share paedomorphic characters found in birds, therefore supporting previous work that demonstrated birds have paedomorphic characteristics attributable to non-avian dinosaurs.

Acknowledgements

Firstly, I owe unfathomable amounts of gratitude to my supervisors – Professor Michael Benton and Professor Emily Rayfield – who have helped to guide my thesis, provide feedback, establish collaborations, and generally put up with my academic shenanigans these past few years. Without their input and guidance, I would have had a much more difficult time during my thesis and would not have had the good fortunes that I did throughout my PhD. I would also like to thank my annual progress mentors, Professor Phil Donoghue and Professor Daniela Schmidt, whose advice and practical criticisms of my work have been instrumental in helping to focus my efforts, resources, and time. Equally, I wish to thank my external reviewer, Dr. Stephan Lautenschlager (University of Birmingham), for taking the time to provide feedback on my thesis.

During the course of my PhD, I also planned and had my own wedding with my wonderful wife, Theresa Gayle Bauer. She has been an outstanding source of keeping me grounded, involved with non-academic life, and has helped to keep me from being burned out throughout my time at Bristol. Without her, my life in Bristol would have been nowhere nearly as fulfilling as it was with her here with me.

The ever-revolving door of postdocs, PhD students, and MSc students at Bristol have provided an almost innumerable amount of friendships, collaborations, and new research views that I would have never had by myself. I owe enormous amounts of gratitude to all that I have come into contact with during my time at The University of Bristol (even Rhys Charles and Liz Martin-Silverstone, I guess). I will take all of these new experiences and ideas into all of my future palaeontological endeavors and, indeed, life.

Chief among all my acknowledgements are my parents and late grandparents. My interests have been shaped, nurtured, and supported since the first day I decided I wanted to pursue palaeontology. Their support has not wavered no matter what degree level I was at any given time – my PhD included. This PhD has been the keystone achievement that began in a small home in Alabama with two parents that put up with a child full of unending dinosaur questions and an unconventional life goal.

COVID-19 Statement

Due to the global COVID-19 pandemic, I was unable to scan and reconstruct as many modern taxa for comparative purposes as I would have liked for my thesis. To work around this, I utilised collaborators and their collections of pre-made endocasts rather than segmenting my own, previously unsegmented specimens. Thankfully, I focused on fossil taxa first before the outbreak and the pandemic did not impact my ability to locate, scan, and recreate the non-avian dinosaur taxa that were so important in the making of this thesis.

Author's Declaration

I declare that the work in this dissertation was carried out in accordance with the requirements of the University's *Regulations and Code of Practice for Research Degree Programmes* and that it has not been submitted for any other academic award. Except where indicated by specific reference in the text, the work is the candidate's own work. Work done in collaboration with, or with the assistance of, others, is indicated as such. Any views expressed in the dissertation are those of the author.

SIGNED: DATE:.....

Table of Contents	Page
Abstract	i
Acknowledgements	ii
COVID-19 Statement	iii
Author's Declaration	iv
Table of Contents	v-viii
List of Figures	ix-xiii
List of Tables	xiv
Chapter 1: Introduction	1
1.1 Palaeoneurology	1
1.2 Thesis Importance, Reasoning, Research Goals	1
1.3 Development of Non-Avian Dinosaur Palaeoneurology	3
1.3.1 Othniel Marsh	3
1.3.2 Tilly Edinger	4
1.3.3 Harry Jerison	6
1.4 Endocast Reconstruction Methods	7
1.4.1 Steinkerns	7
1.4.2 Sectioning	8
1.4.3 Latex casting	9
1.4.4 Computed tomography	10
1.5 Research Trends	11
1.6 Anatomy of the non-avian dinosaur endocast	14
1.6.1 General endocast anatomy	14
1.6.2 Dural envelope	17
1.6.3 Olfactory bulbs and tract	17
1.6.4 Cerebral hemispheres	20
1.6.5 Optic lobes	22
1.6.6 Pituitary	24
1.6.7 Cerebellum and floccular lobes	26
1.6.8 Cranial nerves	28
1.6.9 Endosseous labyrinths	28
1.6.10 Flexure	31
1.7 Dinosaur Palaeobiology and Palaeoneurology	33
1.7.1 Encephalization quotients	33
1.7.2 Sensory perception and palaeoecology	37
1.7.3 Ontogeny	38

Chapter 2: The endocranium and trophic ecology of <i>Velociraptor mongoliensis</i>	41
2.1 Collaborative Statement	41
2.2 Abstract	41
2.3 Introduction	41
2.4 Materials, Methods, and Abbreviations	43
2.5 Results	45
2.5.1 Cranial endocast	45
2.5.2 Cranial nerves and vasculature	46
2.5.3 Endosseous labyrinth	47
2.6 Discussion and Palaeobiological Interpretations	49
2.6.1 Sensory abilities of <i>Velociraptor</i>	49
2.6.2 The trophic ecology of <i>Velociraptor</i>	52
2.7 Conclusions	54
Chapter 3: Ontogenetic endocranial shape change in alligators and ostriches and implications for the development of the non-avian dinosaur endocranium	55
3.1 Collaborative Statement	55
3.2 Abstract	55
3.3 Introduction	56
3.4 Materials and Methods	57
3.4.1 Describing fossil brains: terminology	57
3.4.2 Sample: Source and age composition	57
3.4.3 3D reconstruction	59
3.4.4 Measurements and morphometrics	59
3.5 Results	63
3.5.1 Surface anatomy of the adult alligator endocast	63
3.5.2 Surface anatomy of the adult ostrich brain	64
3.5.3 Comparative anatomy of adult alligator and ostrich endocasts	65
3.6 Cephalic and Pontine Flexure Angles	65
3.7 Ontogenetic Development of the Alligator Endocranium	66
3.7.1 Forebrain	66
3.7.2 Midbrain	73
3.7.3 Hindbrain	73
3.8. Ontogenetic Development of the Ostrich Endocranium	73

3.8.1 Forebrain	73
3.8.2 Midbrain	80
3.8.3 Hindbrain	80
3.9 Brain Growth with Age and Body Mass	80
3.10 Geometric Morphometrics	83
3.11 Discussion	85
3.11.1 Endocranial change through ontogeny	85
3.11.2 Heterochrony and the archosaur endocranium	86
3.11.3 Implications for non-avian dinosaurs	89
3.12 Conclusions	89
Chapter 4: Ontogenetic trends in the endocranium of <i>Psittacosaurus</i>	91
<i>lujiatunensis</i>	
4.1 Collaborative Statement	91
4.2 Abstract	91
4.3 Introduction	90
4.4 Materials, Methods, and Institutional Abbreviations	94
4.5 Anatomy of the Developing Endocranial Form of <i>Psittacosaurus lujiatunensis</i>	96
4.5.1 IVPP V15451: Sub-yearling (<1-year-old)	96
4.5.2 IVPP V12731: Juvenile (2-years-old)	100
4.5.3 PKUP V1053: Sub-adult (7-years-old)	103
4.5.4 PKUP V1054: Sub-adult (8-years-old)	105
4.5.5 IVPP V12617: Adult (10-years-old)	107
4.6 Olfactory, Cerebral, and Cerebellar Shifts in the Species and Their Implications	109
4.6.1 Olfactory growth	109
4.6.2 Cerebrum development	112
4.6.3 Growth of the cerebellum	116
4.7 Endocranial Flexure and the Variable Morphology of the <i>Psittacosaurus</i> Endocast	119
4.8 Conclusions	122
Chapter 5: The avian nature of the juvenile <i>Psittacosaurus lujiatunensis</i> endocast and its implications	126
5.1 Collaborative Statement	126
5.2 Abstract	126
5.3 Introduction	126

5.4 Materials and Methods	128
5.4.1 Endocasts	128
5.4.2 Scanning and segmentation	128
5.4.3 Age estimation	129
5.4.4 Linear measurements	130
5.5 Results	130
5.6 Discussion	138
5.7 Conclusions	141
Chapter 6: Conclusions, Impact, and Future Work	143
6.1 Conclusions	143
6.2 Broad impact	146
6.3 Future work	148
Chapter 7: References	149
Supplementary Information	162

List of Figures	Page
Figure 1.1 – Visualization of attenuation in fossilized skulls. Skulls with high metallic mineral content, such as pyrite, become attenuated and lose detail in their cross-sectional anatomy. This is best demonstrated by comparing a cross-section of a <i>Scelidosaurus harrisonii</i> skull (left) with high pyrite content with the cross-section of a <i>Psittacosaurus lujiatunensis</i> skull (right) that has a lower metal content in the fossil.	11
Figure 1.2 – Cladogram of all dinosaurian taxa and their relationship to each other. Note that Saurischia is comparably oversampled when compared to Ornithischia – thus leaving many questions about the nature of ornithischian palaeoneurology. Regardless, palaeoneurology spans almost the entirety of Dinosauria from some of their earliest Triassic forms to those found at the K/Pg extinction event.	14
Figure 1.3 – Examples of commonly preserved anatomy on a non-avian dinosaur endocast in dorsal (A) and lateral (B) views. Abbreviations: P, pituitary; CB, cerebrum; CE, cerebellar area; CN, various cranial nerves (trigeminal (CN V), facial (VII), and hypoglossal (XII) nerves depicted); DE, dural expansion; FL, floccular lobe; IC, internal carotid arteries; IF, infundibulum; MO, medulla oblongata; NC, cast of the nasal cavity. Scale bars = 5 mm.	16
Figure 1.4 – Dorsal view of CT data (A) and endocast (B) of the sauropodomorph <i>Massospondylus carinatus</i> . Anatomy is labelled to locate and show the location of the olfactory apparatus. Abbreviations: CB, cerebrum; CE, cerebellum; NC, nasal cavity; OB, olfactory bulbs; OT, olfactory tract.	19
Figure 1.5 – CT data and endocasts that show differences in cerebral anatomy in basal archosaurs/non-avian dinosaurs (<i>Massospondylus carinatus</i> ; A, C) and avians (<i>Gymnogyps californianus</i> ; B, D). Non-avians lack the specialised dorsal expansion called the hyperpallium (named the Wulst along reconstructed endocasts). The presence of fissures is frequently obscured on basal archosaur endocasts due to thick dural coverings. Abbreviations: W, Wulst; CB, cerebrum; CE, cerebellum; HP, hyperpallium; LF, longitudinal fissure; SS, dorsal sinus; TF, transverse fissure.	21
Figure 1.6 – Comparative optic lobes between <i>Psittacosaurus lujiatunensis</i> (A,C) and <i>Gallus gallus</i> (B,D). Optic lobes are located along the midbrain (as shown laterally; B,C) and are much more exaggerated in avians than non-avian dinosaurs (as shown dorsally; B,D). They are rarely visible on non-theropod dinosaurs and usually on young specimens (A,C). Scale bars = 5 mm.	23
Figure 1.7 – Complete endocast (A) of the non-ceratopsid ceratopsian dinosaur <i>Psittacosaurus lujiatunensis</i> with the pituitary area detailed (B) and the pituitary area in prior to reconstruction (C). Abbreviations: P, pituitary; IC, internal carotid; IN, infundibulum; CN VI, abducens nerve.	25
Figure 1.8 – Cerebral endocranial space within the braincase (dorsal view; A) and digitally reconstructed cerebellum (CE), flocculus (FL), medulla oblongata (MO) and endosseous labyrinth (LAB) of <i>Thecodontosaurus antiquus</i> (lateral view; B). The flocculi, when present along the endocast, fit into the labyrinths as shown in B	27
Figure 1.9 – Reconstructed right endosseous labyrinth of <i>Velociraptor mongoliensis</i> in right lateral (A) and dorsal (B) views. ASC, anterior semicircular canal; ASCA, ampulla of the anterior semicircular canal; CC, crus communis; CD, endosseous cochlear duct; FV/FC, fenestra vestibuli and fenestra cochleae (the division between the two cannot be identified); LSC, lateral semicircular canal; LSCA, ampulla of the	30

lateral semicircular canal; PSC, posterior semicircular canal. See Figure 2.1 and 2.2. Scale bar = 5 mm.

Figure 1.10 – Examples of cephalic (CF) and pontine (PF) flexure angles between different archosaurian taxa: alligators (*Alligator mississippiensis*), chickens (*Gallus gallus*), and a basal ceratopsian (*Psittacosaurus lujiatunensis*). 32

Figure 1.11 – Graph showing the ratios between brain weight and body mass in modern birds, mammals, reptiles, and fish. This visually shows the difference between what is defined as “higher” and “lower” vertebrates defined by Harry Jerison. Black circles are mammals, black triangles are birds, white triangles are reptiles, and white circles are fish. Modified from Jerison (1969). 34

Figure 1.12 – Graph based on Hurlburt (1996) showing the locations of non-avian dinosaurs and pterosaurs plotted on top of areas already defined by extant mammals, birds, and reptiles. Dinosaurs (black circles) have brains that are expected for reptiles of their size; the same as pterosaurs (white stars) sampled for Hurlburt’s dissertation. Notably, *Archaeopteryx* (white circle) already had an above average brain for its size, further delineating it from dinosaurs. *Troodon* breaks the pattern of dinosaurs in that although it is a non-avian dinosaur, its brain-to-body size value was already more similar to birds than reptiles or non-avian dinosaurs. 35

Figure 2.1 – The braincase and endocranium of *Velociraptor mongoliensis* IGM 100/976. Partial braincase in anterolateral view (A). Braincase rendered transparent (B), revealing the in situ endocast in anterolateral view. The labelled endocast is presented in the right, (C), and left (D) lateral, dorsal (E), and posterior (F) views. Brain endocast is shown in blue, veins in dark blue, cranial nerves in yellow, and endosseous labyrinth in pink. Scale bars: 5 mm. CE, cerebellum; PVCm, posterior middle cerebral vein; FL, floccular lobes; CN V, trigeminal nerve; CN VI, abducens nerve; CN VII, facial nerve; CN X–XI, shared foramina for the vagus and accessory nerves 44

Figure 2.2 – The endosseous labyrinth of IGM 100/976. Labelled right labyrinth (A) in lateral (left) and dorsal (right) views. The right (B–E) and left (F–I) labyrinths of IGM 100/976 shown in lateral (B,F), posterior (C,G), anterior (D,H), and dorsal (E,I) views. Scale bars: 5 mm. ASC, anterior semicircular canal; ASCA, ampulla of the anterior semicircular canal; CC, crus communis; ECD, endosseous cochlear duct; FV/FC, fenestra vestibuli and fenestra cochleae (the division between the two cannot be identified); LSC, lateral semicircular canal; LSCA, ampulla of the lateral semicircular canal; PSC, posterior semicircular canal 48

Figure 2.3 – Scaled endosseous cochlear duct (ECD) length against scaled ECD anteroposterior width, with some taxa highlighted. *Velociraptor mongoliensis* grouped more closely with birds rather than with Crocodyliformes and non-archosaurs. The scaled measurements of IGM 100/976 most closely resembled the upper range of vocal/social neognath birds. A.n, *Ahaetulla nasuta*; C.j, *Crocodylus johnstoni*; C.n, *Ciconia nigra*; C.o, *Cygnus olor*; C.s, *Chelydra serpentina*; Ci.c, *Ciconia ciconia*; Co.c, *Corvus corax*; D.n, *Dromaius novaehollandiae*; G.g, *Gymnodactylus geckoides*; L.m, *Luscinia megarhynchos*; M.u, *Melopsittacus undulatus*; P.e, *Psittacus erithacus*; S.c, *Struthio camelus*; S.p, *Sphenodon punctatus*; T.a, *Tyto alba*; T.s, *Tomistoma schlegelii*; V.m, *Velociraptor mongoliensis*. Modified from Walsh et al. (2009) 51

Figure 3.1 – Left lateral and dorsal views of an *Alligator mississippiensis* (A, C) and *Struthio camelus* (B, D) endocast. Relevant anatomy has been labelled on 61

each specimen to demonstrate key differences between each endocast. P, pituitary body/gland; CE, cerebellum; CB, cerebral hemispheres/cerebrum; HP, hyperpallium; IN, infundibulum; OB, olfactory bulb; OT, olfactory tract. Note that the hyperpallium is unique to birds. Endocasts are not to scale

Figure 3.2 – Landmarks used for specimens in this chapter. Numbered natural landmarks are orange; semilandmarks are green. 62

Figure 3.3 – A neonatal alligator endocast in (A) lateral, (B) dorsal, (C) ventral, (D) anterior, and (E) posterior views. Scale bar = 5 mm 68

Figure 3.4 – A 10-month-old alligator endocast in (A) lateral, (B) dorsal, (C) ventral, (D) anterior, and (E) posterior views. Scale bar = 5 mm 69

Figure 3.5 – A 1-year-old alligator endocast in (A) lateral, (B) dorsal, (C) ventral, (D) anterior, and (E) posterior views. Scale bar = 5 mm 70

Figure 3.6 – A subadult (3 to 4-year-old) alligator endocast in (A) lateral, (B) dorsal, (C) ventral, (D) anterior, and (E) posterior views. Scale bar = 5 mm 71

Figure 3.7 – A large adult (≥ 5 -year-old) alligator endocast in (A) lateral, (B) dorsal, (C) ventral, (D) anterior, and (E) posterior views. Scale bar = 5 mm 72

Figure 3.8 – Two-week-old posthatching ostrich endocast in (A) lateral, (B) dorsal, (C) ventral, (D) anterior, and (E) posterior views. Scale bar = 5 mm 75

Figure 3.9 – Four-week-old posthatching ostrich endocast in (A) lateral, (B) dorsal, (C) ventral, (D) anterior, and (E) posterior views. Scale bar = 5 mm 76

Figure 3.10 – Twelve-week-old posthatching ostrich endocast in (A) lateral, (B) dorsal, (C) ventral, (D) anterior, and (E) posterior views. Scale bar = 5 mm 77

Figure 3.11 – Five-month-old posthatching ostrich endocast in (A) lateral, (B) dorsal, (C) ventral, (D) anterior, and (E) posterior views. Scale bar = 5 mm 78

Figure 3.12 – A 36-month-old posthatching ostrich endocast in (A) lateral, (B) dorsal, (C) ventral, (D) anterior, and (E) posterior views. Scale bar = 5 mm 79

Figure 3.13 – Growth in body size and brain shape for alligators and ostriches. Body size growth curves for ostriches and alligators (A). The question mark and dotted line on the alligator growth curve indicates a projected growth pattern, as they continue to increase their body size throughout their lifetime. The endocasts of alligators (B) and ostriches (C) shown to uniform length so shape changes are highlighted 82

Figure 3.14 – Brain shape change trajectories in morphospace based on landmark data. Brain shape for both ostrich (left) and alligator (right) are always distinctive and do not occupy the same portions of morphospace. The trajectory for the ostrich (left, blue) is tight and curves round, suggesting brain shape in the adult is most similar to that of the hatchling. The trajectory for the alligator (right, yellow) is open and unidirectional, showing continuing shape change in uniform directions, particularly the unfolding of the posterior part of the brain and overall substantial rostrocaudal elongation. Youngest specimens marked with an asterisk. Grey arrow indicated age increase in alligators. Endocasts not to scale. 84

Figure 3.15 – Graphs showing how the logarithmically transformed olfactory bulb, cerebral hemisphere, and cerebellum widths of birds (A) and alligators (B) change with age. In order to better understand what these endocranial width transformations mean, ratios between the olfactory bulbs and cerebral 88

hemispheres (C) and cerebellum and cerebral hemispheres (D) were made for both taxa

Figure 4.1 – Line drawings of a juvenile and adult *Psittacosaurus lujiatunensis* braincase in posterior (A) and left lateral (B) views. Changes in bone size or form are summarised as a shrinking of the supraoccipital (pink; a), an increase in the width (green; b) and height (green; c) of the basal tubera, lateral expansion of the paroccipital processes (yellow; d) elongation of the laterosphenoids (blue; e), and lengthening of the parietals (red; f). Braincases not to scale. Modified from Bullar et al. (2019). 93

Figure 4.2 – Skulls of a posthatchling (A), juvenile (B), and adult (C) *Psittacosaurus lujiatunensis* with their respective calculated head angles. Note how the angle becomes smaller with age signifying a change in how *P. lujiatunensis* held its head throughout life. Figure modified from Bullar et al. (2019). Skulls not to scale. 94

Figure 4.3 – Lateral (A), dorsal (B), anterior (C), and posterior (D) views of the segmented endocast of IVPP V15451. P, pituitary; CB, cerebellum; CE, cerebrum; IC, internal carotid artery; IN, infundibulum; FL, flocculus; LF, longitudinal fissure; MO, medulla oblongata; OB, olfactory bulb; OT, olfactory tract; TF, transverse fissure; CEP, cerebral protuberance; CN XII, hypoglossal nerve 99

Figure 4.4 – Lateral (A), dorsal (B), anterior (C), and posterior (D) views of the segmented endocast of IVPP V12731. P, pituitary; CB, cerebellum; CE, cerebrum; IC, internal carotid artery; IN, infundibulum; FL, flocculus; MO, medulla oblongata; OB, olfactory bulb; OL?, optic lobe?, OT, olfactory tract; CEP, cerebral protuberance 102

Figure 4.5 – Lateral (A), dorsal (B), anterior (C), and posterior (D) views of the segmented endocast of PKUP V1053. P, pituitary; CB, cerebellum; CE, cerebrum; IC, internal carotid artery; IN, infundibulum; FL, flocculus; MO, medulla oblongata; OB, olfactory bulb; OT, olfactory tract; CEP, cerebral protuberance; CMCV, caudal middle cerebral vein; CN V, trigeminal nerve; CN VI, abducens nerve; CN VII, facial nerve; CN XII?, hypoglossal nerve? 104

Figure 4.6 – Lateral (A), dorsal (B), anterior (C), and posterior (D) views of the segmented endocast of PKUP V1054. CB, cerebellum; CE, cerebrum; IN, infundibulum; FL, flocculus; MO, medulla oblongata; OB, olfactory bulb; OT, olfactory tract; CEP, cerebral protuberance; CN II, olfactory nerve 106

Figure 4.7 – Lateral (A), dorsal (B), anterior (C), and posterior (D) views of the segmented endocast of IVPP V12617. P, pituitary; CB, cerebellum; CE, cerebrum; IC, internal carotid artery; IN, infundibulum; FL, flocculus; MO, medulla oblongata; OB, olfactory bulb; OT, olfactory tract; CEP, cerebral protuberance; CN V, trigeminal nerve; CN VI, abducens nerve; CN VII, facial nerve; CN XII, hypoglossal nerve 108

Figure 4.8 – Logarithmically normalised widths of *Psittacosaurus lujiatunensis* olfactory bulbs compared with birds (*Struthio camelus* and *Gallus gallus*) and crocodilians (*Alligator mississippiensis* and *Caiman crocodilus*). The tyrannosaurid *Tyrannosaurus rex* was added to give a sense of how the olfactory bulbs from *P. lujiatunensis* developed when compared to large-bodied, predacious theropod. 111

Figure 4.9 – Logarithmically normalised widths of *Psittacosaurus lujiatunensis* cerebra compared with birds (*Struthio camelus* and *Gallus gallus*) and crocodilians (*Alligator mississippiensis* and *Caiman crocodilus*). 115

Figure 4.10 – Logarithmically normalised widths of *Psittacosaurus lujiatunensis* cerebellar regions compared with birds (*Struthio camelus* and *Gallus gallus*) and crocodilians (*Alligator mississippiensis* and *Caiman crocodilus*). 118

Figure 4.11 – Cephalic flexure angles (in degrees) plotted against logarithmically corrected ages of crocodilians, birds, and non-avian dinosaurs – *P. lujiatunensis* included. 120

Figure 4.12 – Pontine flexure angles (in degrees) plotted against logarithmically corrected ages of crocodilians, birds, and non-avian dinosaurs – *P. lujiatunensis* included. Note that angles are similar between cephalic flexure angles from the same species of the same ontogenetic stages, however, neither flexure angle of non-avian dinosaurs do not always reliably favour other archosaur taxa. 121

Figure 4.13 – Cladogram modified from Zhou et al. (2007) that shows how PKUP V1053's endocast fits with others within Ceratopsia. PKUP V1053 has been found to be a subadult based on osteohistology and does not reflect the morphology that should be expected in an adult such as IVPP V12617 (blue). 122

Figure 5.1 – Line-drawing of a sub-yearling *Psittacosaurus lujiatunensis* (A) and the segmented braincase of IVPP V15451 (B). The segmented endocast of IVPP V15451 is shown in right lateral (C), dorsal (D), and posterior (E) views to show anatomy relevant to this study. Braincase abbreviations: BO – basioccipital, FR – frontal, LS – laterosphenoid, PA – parietal, PP – paroccipital process, PR – prootic, SO – supraoccipital, BPC – basisphenoid-parasphenoid process. Endocast abbreviations: CB – cerebellum, CN V – trigeminal nerve, CN XII – hypoglossal nerve, FL – floccular lobe, IC – internal carotid arteries, LF – longitudinal fissure, MO – medulla oblongata, OL – optic lobe, OT – olfactory tract, P – pituitary, TF – transverse fissure. Skeletal artwork (A) of *P. lujiatunensis* credited to Simon Powell. The segmented braincase (B) was adapted from Bullar et al. (2019). Scale bar = 5 mm 132

Figure 5.2 – Normalized widest diameter measurements of olfactory bulbs (A), cerebral hemispheres (B), and cerebellum (C) along ontogenetic series of endocasts from *Alligator mississippiensis* (red), *Psittacosaurus lujiatunensis* (green), and *Struthio camelus* (blue). Neuroanatomy development is variable across taxa with no clear comparison that can be drawn between exemplar non-avian archosaurs, birds, and the extinct ceratopsian *P. lujiatunensis* throughout growth 134

Figure 5.3 – Archosaur brains through ontogeny: *Alligator mississippiensis* (first row), *Psittacosaurus lujiatunensis* (second row), *Struthio camelus* (third row), and *Gallus gallus* (fourth row). The endocast of *Psittacosaurus* demonstrates growth patterns that are most similar to avians early in life (e.g. expanded cerebrum, $\leq 90^\circ$ flexure angles) but incorporates more non-avian archosaur traits with age (e.g. endocranial elongation, enlarged olfactory bulbs). Ontogenetic development of the *P. lujiatunensis* endocast ends with a refolded form that superficially resembles both avian and non-avian archosaur endocranial morphologies. Age increases from juveniles (left) to adults (right). The older *P. lujiatunensis* endocasts were made from a 7-years-old individual (PKUP V1053; middle) and 10-years-old individual (IVPP V12617; right). Endocasts and outlines are not to scale 137

Figure 5.4 – Comparative endocasts from a juvenile non-theropod, non-avian dinosaurs (*Psittacosaurus lujiatunensis*, IVPP V15451), an avialan (*Archaeopteryx lithographica*), an extinct avian (*Cerebavis cenomanica*), and an extant avian (*Gallus gallus*). Note the enlarged cerebrum and optic lobe location on each specimen. Scale bars = 5mm 139

List of Tables	Page
Table 1.1 – List of all cranial nerves found along the non-avian dinosaur endocast and the sensory data transmitted associated with each nerve.	28
Table 2.1 – Measurements taken from the endocast of IGM 100/976. Volumes do not account for vascularization, endosseous labyrinths or cranial nerves.	46
Table 3.1 – Master list of specimens used for this study and the relevant scan parameters. Specimens noted with superscript were either specifically made for this project ¹ or used for the PCA ² . All were used for comparative anatomy	58
Table 3.2 – Cephalic and pontine flexure angles measured from select ostrich and alligator endocasts	66
Table 4.1 – Scan parameters used for all psittacosaurus used throughout this chapter	95
Table 4.2 – List of measurements from identifiable sources of brain anatomy across the entire ontogenetic series of <i>P. lujiatunensis</i> endocasts.	96
Table 4.3 – List of all cephalic and pontine flexure angles from the entire ontogenetic series of <i>P. lujiatunensis</i> endocasts.	97
Table 4.4 – Age and olfactory bulb width data (with logarithmically corrected values for both) for ostriches, chickens, alligators, caiman, and <i>Psittacosaurus</i> , respectively, used throughout this project. Another dinosaur, <i>Tyrannosaurus</i> , was added to test how closely the absolute and normalised widths of large-bodied predacious theropods compare with those of <i>P. lujiatunensis</i> .	110
Table 4.5 – Age and cerebral width data (with logarithmically corrected values for both) for ostriches, chickens, alligators, caiman, and <i>Psittacosaurus</i> , respectively, used throughout this project.	114
Table 4.6 – Age and cerebellar width data (with logarithmically corrected values for both) for ostriches, chickens, alligators, caiman, and <i>Psittacosaurus</i> , respectively, used throughout this project.	117
Table 5.1 – Master list of the specimen flexure angles and ages used for this chapter	130
Table 5.2 – Master list of the total length of their endocast, maximal olfactory bulb width, maximal cerebral hemisphere width, and maximal cerebellum width. Ratios of the maximal widths were made by comparing them to the widest aspect of the cerebral hemispheres ¹ or the total length of the endocast ²	135
Table S1 – Comprehensive table of named taxa from which cranial endocasts are known. Taxa are separated into genus and species, first appearance in the fossil record (FAD), last appearance in the fossil record (LAD), clade, the lowest phylogenetic level available that groups large amounts of taxa, and continent where the species is found.	162

Chapter 1: Introduction

1.1 Palaeoneurology

Palaeoneurology is a subfield of vertebrate palaeontology that specializes in the study of the anatomy and evolution of neuroanatomical systems in extinct organisms (Buchholtz and Seyfarth, 1999, 2001); dinosaur palaeoneurology is simply the subfield of palaeoneurology applied to ornithischian and saurischian dinosaurs. The goal of dinosaur palaeoneurology (simply referred to as “palaeoneurology” in this overview unless otherwise specified) is to describe the gross neuroanatomy and to elucidate how the nervous system changed within dinosaur lineages through time. The importance of anatomical changes or morphological trends within the neuroanatomy of non-avian archosaurs and extinct avians cannot be understated since they are sometimes our only glimpse into the behaviour or neurosensory abilities of Dinosauria.

For over a century, palaeoneurology has refined our understanding of neuroanatomy in extinct taxa, methodologies for exposing or reconstructing endocasts – the restored soft anatomy found inside the endocast, and observable macroevolutionary trends found in non-avian dinosaurs. The purpose of this chapter is to provide a historical perspective of dinosaur palaeoneurology; describe current methodologies of endocranial reconstruction; establish research trends within the Dinosauria; address methods of – and issues with – quantifying trends in endocranial anatomy; and to set the groundwork for ontogenetic palaeoneurology research for the rest of the thesis.

1.2 Thesis Importance, Reasoning, Research Goals

In this thesis, I broadly use comparative anatomy to understand how behaviour or anatomical/morphological changes in non-avian dinosaur endocasts can be related to modern archosaurs. The primary importance of this thesis is that it offers the first descriptions of a full ontogenetic series of cranial endocasts and postulates what the morphology of juvenile non-avian, non-theropod dinosaurs mean for our understanding of archosaur endocranial evolution. To do this, CT datasets of non-avian dinosaurs were segmented with Avizo (v9.7.0) and measured in ImageJ (v1.48). All measurements and anatomical comparisons made from non-avian dinosaur endocasts were based on extant archosaur analogues.

Comparative anatomy was decided upon over more quantitative methods (e.g. deriving encephalization quotients, comparing endocranial volumes) due to the uncertain nature of brain-to-braincase volumes in extinct archosaurs. As stated above, the variable nature of the dura and sinuses between archosaurs and at different developmental stages makes

estimating the true endocranial volume dubious. I have elected to use maximal widths of select areas of the endocast to represent changes in size relative to the length of the endocast and the age of the specimen.

Broadly, this thesis seeks to incorporate ontogeny into palaeoneurology. How do behaviours and ecology relate to the endocast? What do palaeontologists know about anatomical and morphological trends in modern exemplar archosaur taxa? What does a complete set of endocasts from a non-avian, non-theropod ontogenetic series look like? And, potentially most importantly, what can palaeontologists learn from the underrepresented endocranial anatomy and morphology of a juvenile non-avian dinosaur? I seek to answer all of these questions by using digitally reconstructed endocasts, geometric morphometrics, and comparative anatomy.

My specific research goals are as follows:

- Briefly explain the history and methodologies of palaeoneurology as a science
- Use a well-known, but poorly understood (from a palaeoneurology standpoint), non-avian dinosaur to demonstrate how the endocranium can be used alongside postcranial remains to predict behaviour
- Describe the morphological and anatomical differences between the endocasts of two exemplar taxa, alligators (*Alligator mississippiensis*) and ostriches (*Struthio camelus*), to establish broad trends in postnatal development of the modern archosaur endocranium
- Describe the morphological and anatomical differences in the endocast of *Psittacosaurus lujiatunensis* from a complete ontogenetic series
- Discuss how the endocast of *P. lujiatunensis* compares with modern archosaur taxa throughout postnatal development
- Compare the aesthetically avian endocast of a sub-yearling *P. lujiatunensis* to those of extinct and modern birds to broadly understand what the morphological similarities mean for avian palaeoneurology
- Link all the information together to explain endocast's and ontogeny's role in our understanding of form, function, and morphological variation in dinosaur palaeoneurology

This thesis seeks to fill gaps in our understanding, or lack thereof, of ontogenetic trends in endocranial anatomy and morphology in non-avian dinosaurs. Furthermore, this thesis also explores the relationship between heterochrony or paedomorphosis and the evolution of the archosaur endocranium.

1.3 Development of Non-Avian Dinosaur Palaeoneurology

The actual foundation of palaeoneurology can be debated depending on how far back in time one wants to search and what one defines as "neuroanatomical research". Early descriptions of fossilized endocasts stretches back to the end of the 1700s (Cuvier, 1835) with broad evolutionary questions about brain and body size dating almost half a century earlier than that (von Haller, 1762).

1.3.1 Othniel Marsh

The framework of modern dinosaur palaeoneurology can be traced back to American palaeontologist Othniel Marsh (1831-1899) between 1874 and 1895 (Marsh, 1874, 1881, 1884a, 1884b, 1886, 1889, 1890, 1891). Most famous for his descriptions and excavations of dinosaurs from the western United States, Marsh was one of the premier dinosaur palaeontologists of the late 19th century alongside others such as Joseph Leidy and Edward Cope (though probably to Marsh's dismay). Marsh can be considered the founder of modern dinosaur palaeoneurology – not because of the long-lasting impacts his research had upon the subject, but because he was the first to start thinking about the braincases of dinosaurs and began slowly relating their neuroanatomy to palaeoneurology within Dinosauria. His study of braincases, endocasts, and brains of extinct taxa led to the derivation and refinement of eight rules for brain evolution:

1. All Tertiary (Cenozoic) mammals had small brains.
2. There was a gradual increase in the size of the brain during this period.
3. This increase was confined mainly to the cerebral hemispheres, or higher portions of the brain.
4. In some groups, the convolutions of the brain have gradually become more complex.
5. In some, the cerebellum and the olfactory bulbs have even diminished in size.
6. There is some evidence that the same general law of brain growth holds good for Bird and Reptiles from the Cretaceous to the present time.
7. The brain of a mammal belonging to a vigorous race, fitted for a long survival, is larger than the average brain, of that period, in the same group.
8. The brain of a mammal of a declining race is smaller than the average of its contemporaries of the same group (Marsh, 1886; p. 58-59).

While the laws were later found to be false, Marsh's laws showed that a concentrated effort to study endocasts was one of his primary focuses—at least in theory. Marsh's greatest, and perhaps only, long-term contribution to the field of palaeoneurology was the observation that brains were not a consistent shape or a static size throughout the fossil record and clearly changed through time. Apart from a few cases, most animals trend towards encephalisation

rather than losing brain volume (Jerison, 1955, 1961) which Marsh had noticed while studying Cenozoic mammal endocasts and surmised in his laws. However, his laws were based solely on the stratigraphic position of each endocast and did not account for the body size of the animal the endocast belonged to in life. The size of the brain relative to an animal's body size is not an indicator of a "vigorous" or "declining" race (Jerison, 1973).

Marsh's sixth law stood out since it concerned non-mammalian taxa. This law was in reference to his discovery and description of the Late Cretaceous birds *Ichthyornis dispar* (Marsh, 1873) and *Hesperornis regalis* (Marsh, 1880), how he thought their brains should look, and how the brains *I. dispar* of *H. regalis* related to the brain size and shape in dinosaurs:

“More recent research renders it probable that the same general law of brain-growth holds good for birds and reptiles from the Mesozoic to the present time. The Cretaceous birds, that have been investigated with reference to this point, had brains only about one-third as large in proportion as those nearest allied among living species. The Dinosaurs from our Western Jurassic follow the same law, and had brain cavities vastly smaller than any existing reptiles. (Schuchert, 1938; p. 56-57)”

In the above quote, Marsh concluded that Cretaceous aged birds would have shared the same pattern of brain-to-endocast volume as non-avian dinosaurs. By doing so, Marsh connected the phylogenetic relationship between birds and non-avian dinosaurs and begins the first academic thought into how dinosaur palaeoneurology evolved throughout the Mesozoic. Interestingly, Marsh's claims that dinosaurs and Cretaceous birds would not have had a braincase filled with neural tissue were made approximately 30 years prior to Arthur Dendy's similar claims (Dendy, 1910).

In hindsight, Othniel Marsh contributed much less than some of his successors would in the decades to follow. Saying this, Marsh had two profound effects on general and dinosaur palaeoneurology. He was one of the first naturalists to bring attention to the palaeontological resources of the American West and its wealth of well-preserved taxa (Schuchert, 1938). And due to the specimens he and others found throughout the western half of the United States, the first broad trends in endocranial evolution were described in mammals (Marsh, 1874) and fossil birds (Marsh, 1880) – thus allowing the first palaeoneurological implications to be applied to dinosaurs.

1.3.2 Tilly Edinger

While Marsh can be credited as the first to start conceptualizing the evolution of dinosaur brains, he is not considered the founder of current modern paleoneurology (Buchholtz and

Seyfarth, 2001). Much of Othniel Marsh's work on fossil brains was challenged and, eventually, falsified (Jerison, 1973; Franzosa, 2004) by the first true palaeoneurologist: Johanna Gabriele Ottilie "Tilly" Edinger (1897-1967). Tilly Edinger was a German emigrant that dedicated her academic career to describing the endocrania of fossil and modern organisms (Edinger, 1929, 1942, 1948, 1955, 1975; Cobb and Edinger, 1962; Buchholtz and Seyfarth, 2001). It was Edinger's work on bats that disproved Marsh's rules for brain evolution in mammals and her investigations into Marsh's work on *Hesperornis* found that he actually did not have any endocasts—he was purely hypothesizing what a *Hesperornis* brain would have looked like in life (Buchholtz and Seyfarth, 1999). Edinger noticed that the size of the brains of animals did not always scale equally with body size and certain portions of the brain expanded or shrank throughout a lineage:

"...the absolute increase and elaboration of the cerebrum in the Equidae was not at all times closely correlated with progress in body size, limb or tooth structure in the manner that the so-called 'scale' of extant mammals would suggest if regarded as representing steps in evolution; but the fact that enlargement was greater in the cerebrum and its neocortex, i.e. in the neencephalon than in the palaeoencephalon, and greater also in the neocerebellum than in the palaeocerebellum, brilliantly justifies these distinctions which my father derived from comparing brains of lower and higher extant animals (Edinger, 1962; p. 62) "

Edinger's above observation meant that the size of the brain was not a driver in the success of a group of animals; the specialization of a brain for an organism's environment was more of a survival factor (Edinger, 1948; Cobb and Edinger, 1962). This was in direct contradiction to almost half of Marsh's laws – which Edinger often associated with his background being in earth sciences rather than comparative anatomy (Buchholtz and Seyfarth, 1999). While Edinger's assessment of brain size not being a predictor of evolutionary success does not directly utilise dinosaur endocasts, it does set the foundation for understanding how dinosaurs – especially those typified outside of natural sciences as being “small-brained” like *Stegosaurus* (Ruse, 2019) – proliferated without the need for a large brain-to-body size ratio.

Tilly Edinger did not support the quantitative study of endocrania (Buchholtz and Seyfarth, 1999). She feared that misrepresentation of an organism due to such a fragmentary fossil record—specifically those with endocranial remains that could not have a reliable body size or weight reconstructed (Buchholtz and Seyfarth, 1999).

1.3.3 Harry Jerison

It was Harry Jerison, a colleague and close friend of Tilly Edinger, that laid the foundation for quantitative palaeoneurology research, especially in his publications "Brain evolution and dinosaur brains" (Jerison, 1969) and "Evolution of the brain and intelligence" (Jerison, 1973), by investigating the relationships between the total brain volume and expected body size in both modern organisms and dinosaurs. The results of Jerison and co-authors resulted in his own eight "orderliness to brain evolution" laws:

1. "A basal lower vertebrate grade of encephalisation evolved in the earliest bony fish, amphibians and reptiles and has continued to the present as a steady-state or equilibrium maintained for at least 350 million years. Since about two-thirds of living vertebrate species are members of these three classes of vertebrates, this basal grade is the norm for vertebrates.
2. There are variations in encephalisation within the lower vertebrate groups, the most interesting being between herbivorous and carnivorous dinosaurs. The carnivores were apparently significantly more encephalized.
3. The earliest fossil birds and mammals with known endocasts had evolved to a higher grade, representing at least three or four times as much brain as in lower vertebrate species of comparable body size. This progressive or "anagenetic" evolution occurred at least 150 million years ago, and in the case of the mammals may have begun with their reptilian ancestors at least 50 million years earlier.
4. Within the mammals there is a good fossil record of the brain, which is consistent with a picture of steady-states punctuated by rapid evolution to higher grades. However, many grades of encephalisation are represented in living mammalian species, with some (opossum, hedgehog) at the same grade as the earliest of the mammals.
5. Two unusual conclusions are evident in the history of encephalisation in primates. First, primates have always been a brainy order, perhaps doing with their brains what many other species did by morphological specializations. Second, the evolution of encephalisation in the primates followed rather than preceded or even accompanied other adaptations by primates to their niches.
6. The highest grade of encephalisation is shared by humans and bottlenose dolphins (*Tursiops truncatus*). The sapient grade was attained about 200,000 years ago, but cetaceans may have reached their highest grade 18 million years ago.
7. Encephalisation in the hominids is a phenomenon of the past three to five million years, and its rapidity appears to have been unique in vertebrate evolution.
8. These results suggest two complementary conclusions. First, the long steady-states that occurred in most groups indicate that, on the whole, encephalisation was not a major element in vertebrate evolution. A particular grade of encephalisation tended to

be maintained once it was achieved. On the other hand, its appearance in many different and distantly related groups is evidence of some Darwinian "fitness" for encephalisation." (Jerison et al., 1985; p. 24-25)

The above listed modified laws of encephalisation echo those originally defined by Marsh, but in a much more quantitative and phylogenetically diverse way. Specifically, this new and improved set of laws and observations quantitatively dispelled the "bigger is more successful" idea proposed by Marsh by noting that there is variability within encephalisation – with the most notable examples being among dinosaurs. Moreover, Jerison noted that diet or ecomorphology played a significant role in the encephalisation grade in dinosaurs, thus establishing that brain size was not independent of the environment or postcranial anatomy among Dinosauria. These laws, both in totality and when specifically applied to dinosaurs, gave evidence for a complex mosaic of evolutionary pressures that influence brain size.

In addition to his own refined laws Jerison developed the idea of the encephalisation quotient – a measurement of brain size based on an animal's body size (see 1.6.1 for details). Jerison was one of the first to apply quantification to the endocranium of extant and extinct animals. By being able to calculate and quantify the endocranial volume of organisms, Jerison allowed for behavioural (see 1.6.1) and morphological changes to be mathematically traced throughout deep time. Insight to how and when changes to the endocast occur has allowed palaeoneurologists to understand broad neuroanatomical macroevolutionary themes as they appear within the fossil record.

1.4 Endocast Reconstruction Methods

The most straightforward way to study palaeoneurology is to directly describe and measure the cranial endocast (here referred to as "endocast"). Endocasts are the sum total of all soft tissue within the braincase. Endocrania reflect the surface anatomy and general morphology that has been lithified and turned into a cast with time and burial (Hopson, 1979). Methodologies used to expose and describe endocranial anatomy have evolved dramatically in both complexity and number since the conceptualization of palaeoneurology. These methods have trended away from destructive procedures towards more detailed non-intrusive techniques. As time has passed, more methods have become more complex and allowed for more detail to be described off endocasts. Methods for exposing or reconstructing the endocast are varied and are briefly described below.

1.4.1 Steinkerns

Initially, palaeontologists measured the proportions of steinkerns—incredibly rare naturally occurring stone endocasts—to compare the overall size and volume of fossilized brains. Steinkerns are formed when sediments fill-in the spaces left behind when the soft tissues of the cranium decompose (Hopson, 1979). In instances that produce steinkerns, the minerals that replace the soft anatomy of the cranium (e.g. phosphates and carbonates) are more resistant to weathering than the bones that surround the brain (Newton, 1888; Brasier et al., 2016). Once the bones that comprise the braincase erode away, the steinkern is an internal cast of the cranial cavity and can give insight into the gross anatomy of both the endocast and the dura mater (Brasier et al., 2016; Carabajal et al., 2018). While using a natural endocast is not destructive in a traditional sense, the observations and measurements of the steinkern cannot be assigned to a genus or species unless the steinkern is associated with a particular specimen.

1.4.2 Sectioning

Sectioning originally started as a method to grind down fossil in incremental layers in order to expose their internal structure (Sollas, 1904). Each layer would be extremely small ($<100\mu\text{m}$) so each internal layer could be photographed, drawn, scanned, or otherwise imaged. Images obtained from the serial grinding are then reconstructed in a medium (e.g. wax) to make a three-dimensional (3D) image. However, as demonstrated in Jarvik (1954), this method is extremely time consuming and wholly destructive to the specimen. Jarvik (1954) described the skeletal anatomy of Devonian fishes by grinding them down and reconstructing each slice with wax. This method produced a highly detailed reproduction of *Eusthenopteron* with 500 wax slices but took 25 years to complete. As a braincase methodology, serial thin sectioning is impractical due to the differences between the fossilized bone that comprises the braincase and the sediment that has replaced the soft anatomy of the endocrania. Serial grinding a braincase would result in the uneven grinding of fossil bone and sediment that fills the cranial cavity. Instead, the braincase of fossil organisms can be sectioned down the midline of the braincase to produce two halves. These halves can then be cleaned of sediment and cast in either plaster or latex to form half endocasts that can then be glued together. This method was preferred for larger dinosaur braincases in the early 1900s as evidenced by Henry Osborn and his work on *Tyrannosaurus rex* braincases. Osborn would use a diamond saw to bisect the braincase and use plaster to replicate the endocast of *Tyrannosaurus* (Larsson et al., 2000)—one of the first of its kind for its species.

1.4.3 Latex Casting

Latex endocasts are created by injecting the endocranial spaces with silicone or latex to give a better view of the undersurface of the bones that comprise the braincase. This method requires that the braincase of a specimen be incomplete, sectioned, or meticulously prepared so the internal matrix can be removed and to allow access to the interior portions of the braincase (Jerison 1973). In more modern extinct organisms, latex is poured through the foramen magnum and the skull is rotated to coat the inside of the skull with a thin layer of latex. The initial coat of latex fills in all foramen and canals and allows for subsequent pourings of latex that will fill in the rest of the cranial cavity to form a soft endocast that can be pulled out of the braincase after solidifying (Edinger 1968). When this method is used with more modern fossils, there is a chance of damaging the endocranium, foramen magnum, basioccipitals, occipital condyles, or any other number of bones located at or near the base of the skull. If not properly removed, the entirety of the posterior cranium can be destroyed when removing the latex cast through the foramen magnum. Latex casting has been used to show the evolution of horse brains (Edinger, 1948) and prosimian primates (Radinsky, 1968) but has a limited use when it comes to dinosaurs. Ancient, infilled braincases require a different method to receive a latex impression of the endocranial anatomy. In order to make a cast of a skull that has been infilled with sediment, the braincase must have the matrix prepped out of the area that will be the mould. Once cleared of matrix, the walls of the braincase can be coated in latex, cured, and removed to give a surface view of the endodural or endocranial mould. This method has been used to help support the presence of vascular valliculae in lambeosaurine and hadrosaurine dinosaurs (Evans, 2005) by showing evidence for vascular canals along the frontals of hadrosaur skulls along.

While latex is easy to use, commercially affordable, and, when properly used, has a low risk of damaging the specimen, there are a few drawbacks. Latex casting material can be photosensitive and will degrade when in direct light. Casts must be properly stored in light resistant or opaque housing to prevent light damage (Radinsky 1968) and degradation of the outward appearance of the cast. Additionally, latex casting materials used for endocranial extraction are pliable and lose their shape if not supported by another material—usually plaster of Paris (Edinger 1948; Radinsky 1968). If left without support, the original form will become warped or otherwise distorted and lose its shape. Similarly, latex casts can shrink or expand over time (Edinger 1948) as their curing process continues outside of the mould thus limiting the use of latex casts for morphometric, volumetric, or other any other size dependent forms of research.

1.4.4 Computed Tomography

It was the development and refining of computed tomographic (CT) scanning that led to the revival and revolutionizing of palaeoneurology (Witmer & Ridgely 2009) and the importance of CT scanning as a palaeontological and preparatory tool cannot be overstated. CT scanners and 3D manipulation software offer all the benefits that removing the matrix surrounding an endocast and without any of the destructive testing. This was first carried out in dinosaur palaeoneurology in Rogers (2000) where the endocast of *Allosaurus fragilis* was compared with modern taxa. Scanners provide the first truly reliable non-destructive methods of modelling internal structures of fossils. At its most basic level, CT scanning uses an X-ray beam to generate a series of 2D images that can be stitched together into a digital 3D image. The resolution of the resulting images is dependent on the size and location of the focal point and intensity of the X-ray beam generated by the CT scanner. Medical-grade scanners used by hospitals usually have a focal point between 0.3 and 1.2 mm and an intensity range between 5 and 120 kilo-electronvolts (keV). Stronger research-grade scanners can reduce the focal point of the X-rays and boost the intensity of the beam to 0.5 and 220 μm and 10 and 450 kV, respectively; this results in better overall resolution in research scanners than medical scanners (Racicot 2016).

Attenuation, the blocking or distorting of X-rays, is the most common issue that can be called a "drawback" to CT scanning (Figure 1.1). The degree of attenuation is dependent on the geological makeup of the matrix surrounding a fossil. Higher concentrations of dense or metallic minerals will block or scatter lower energy X-ray beams from CT scanners thus resulting in unclear or uninterpretable scan images. This is measured by a signal-to-noise ratio (SNR) where "signals" are photons and "noise" is the deviation of pixels from normal. A high SNR means that the image will be clearer and have less artefacts. Conversely, the higher the attenuation, the lower the signal-to-noise ratio will be, and artefacts will occur more frequently in the resulting scans or segmented 3D models.

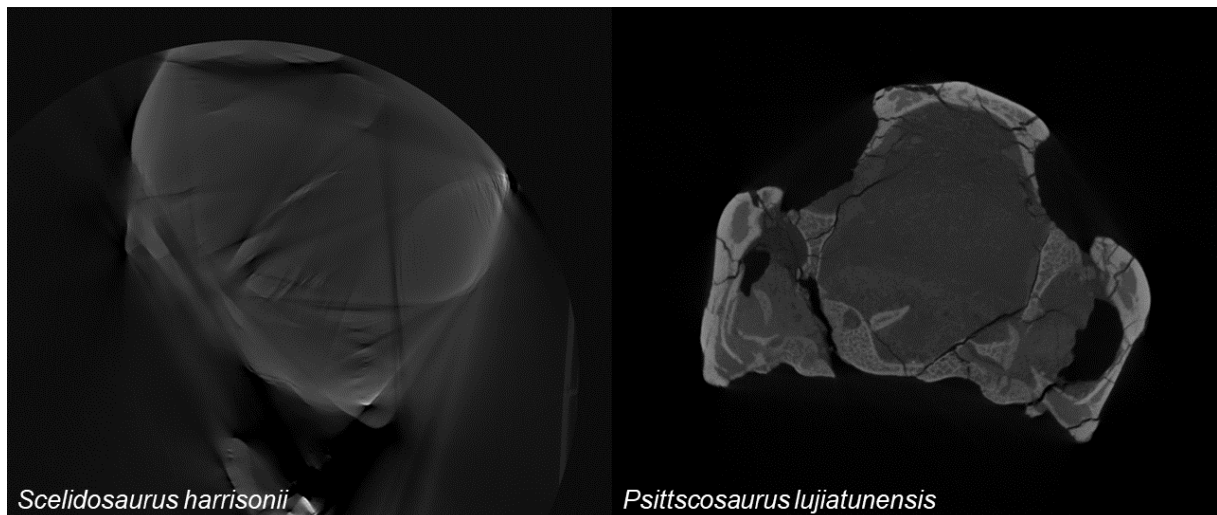


Figure 1.1 – Visualization of attenuation in fossilized skulls. Skulls with high metallic mineral content, such as pyrite, become attenuated and lose detail in their cross-sectional anatomy. This is best demonstrated by comparing a cross-section of a *Scelidosaurus harrisonii* skull (left) with high pyrite content with the cross-section of a *Psittacosaurus lujiatunensis* skull (right) that has a lower metal content in the fossil.

Current research relies heavily on the use of CT scanning and its benefits. Many fossils are too fragile to send long distances or rare to use with potentially destructive analyses. Sending 3D specimens electronically allows for faithful reproductions to be delivered without the worry of damage to the original fossil. Analyses such as Geometric Morphometrics, linear and volumetric measurements, and qualitative descriptions can be performed without fear of measuring a specimen that has been deformed or is undergoing degradation. Unlike latex casts, the scans do not degrade with time and are easily reproduced digitally. The accessibility of scanners and cost to use vary by location but scanners are becoming more common and their usage for research purposes is becoming cheaper with time thus allowing CT scanning and digital reconstruction to be used more frequently.

1.5 Research Trends

Palaeoneurological research from the late 1970s to the current day has evolved in ways that were inconceivable when Tilly Edinger first founded palaeoneurology as a subfield of palaeontology. Many papers are still purely descriptive and discuss the gross anatomy of fossil endocasts; however, new methods and specimens have allowed for an extensive number of taxa to be described. A cursory scan of literature from the past two decades shows that ornithischian (Zhou et al., 2007; Lauters et al., 2013; Cruzado-Caballero et al., 2015; Brasier et al., 2016; Carabajal et al., 2016; Sakagami and Kawabe, 2020) and saurischian dinosaurs (Rogers, 1998; Larsson et al., 2000; Franzosa and Rowe, 2005; Sanders and Smith, 2005;

Sampson and Witmer, 2007; Knoll and Schwarz-Wings, 2009; Witmer and Ridgely, 2009; Bever et al., 2011; Bronzati et al., 2017; Müller et al., 2020), avians (Dominguez et al., 2004), extinct ornithurine birds (Walsh et al., 2016) have been extensively sampled and described in an attempt to better understand the gross morphology of their endocranial anatomy. The main findings of papers from the past 20 years have been to model, describe, and understand how the non-avian dinosaur endocast changed through time and what impact changes in size had on neurosensory abilities at the species and clade level. The overarching goal of qualitative work has been to create a baseline of endocasts to compare neuroanatomy interspecifically and intraspecifically throughout Dinosauria as a way to directly explore cranial soft tissues.

It is not fair to say that all neuroanatomical work is focused on the qualitative descriptions of fossil endocasts. Numerous studies and theses have used the large influx of available endocasts and taken the next logical step – a quantitative or functional analysis that focuses on the evolution of endocrania; usually with a phylogenetic point-of-view. The partitioning of neuroanatomy in birds and dinosaurs, especially those near the theropod-bird transition have been the focus of most recent studies (Balanoff et al., 2013, 2016). Descriptive work has created an explosion of new endocasts to compare since the inception of palaeoneurology with nearly 100 endocrania now known from named non-avian dinosaurs (Figure 1.2). Aside from descriptive work, recent research has trended towards asking broad questions about how total brain morphology or specific lobes of the brain change through time. One such example that blends morphology and lobe anatomy together is a new technique called Gross Anatomical Brain Region Approximation (GABRA) (Morhardt et al., 2017). GABRA uses soft tissues – as defined by impressions along the interior surface of the braincase – to define locations of discernible landmarks along brain regions (e.g. olfactory bulbs, cerebrum, cerebellum, etc.). Landmarks along the braincase were correlated with actual soft tissue stained with iodine in modern taxa. Knowing that the osteological impressions accurately match with iodine-stained soft tissue, GABRA provides evidence for mosaic evolution in which the pituitary and olfactory bulbs evolve independently from the rest of the brain. The results of GABRA need further testing on lineages of non-avian dinosaurs to observe if the same results hold true at the clade-level. Prior research suggests that modular evolution is observable within some clades of non-avian dinosaur – though this has yet to be tested beyond theropods (Balanoff et al., 2016; Beyrand et al., 2019).

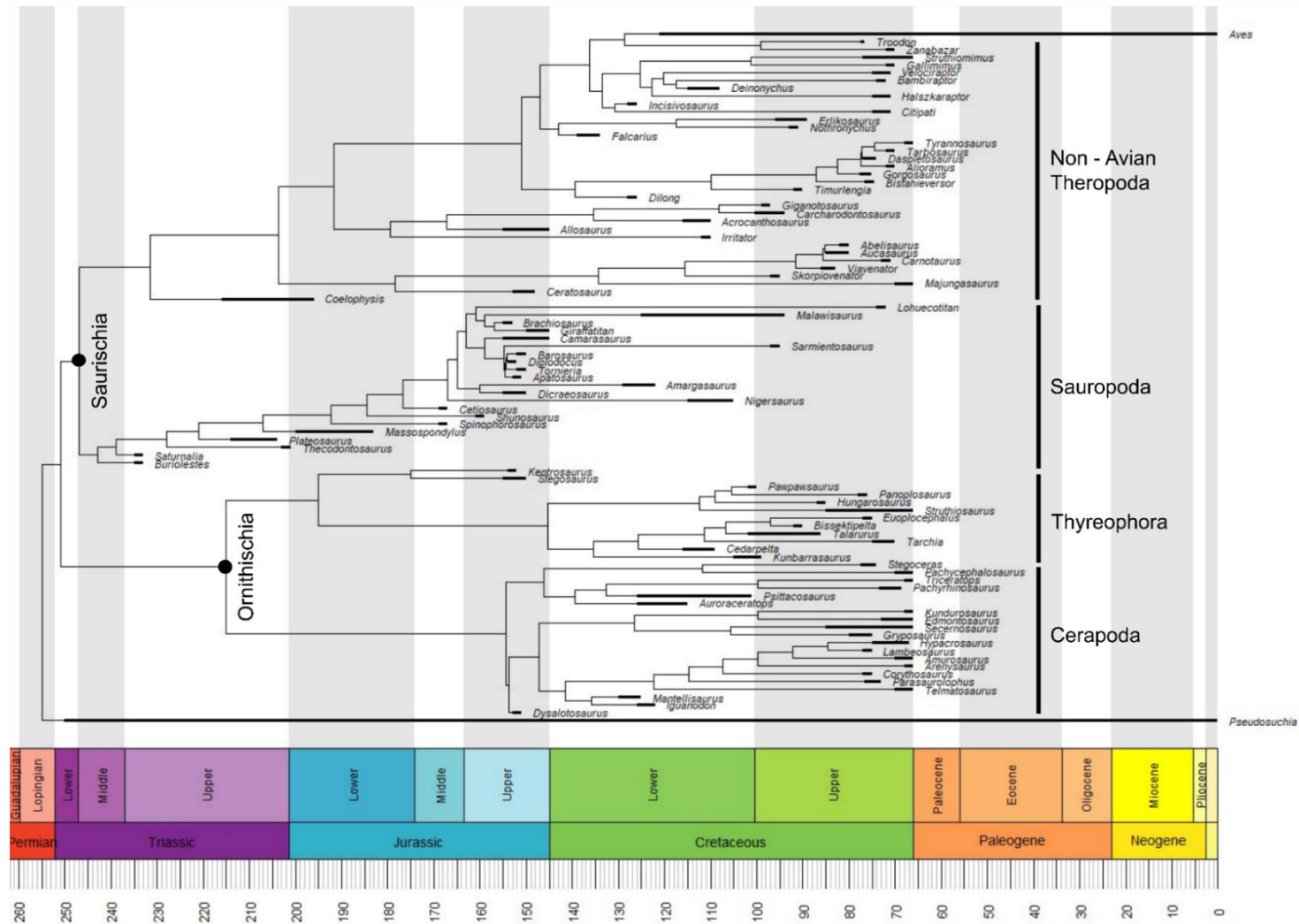


Figure 1.2 – Cladogram of all dinosaurian taxa and their relationship to each other. Note that Saurischia is comparably oversampled when compared to Ornithischia – thus leaving many questions about the nature of ornithischian palaeoneurology. Regardless, palaeoneurology spans almost the entirety of Dinosauria from some of their earliest Triassic forms to those found at the K/Pg extinction event. A full breakdown of species, phylogeny, and geographic range can be found in Table S1.

1.6 Anatomy of the Non-Avian Dinosaur Endocast

Now that a brief overview of past and present research highlights has been given, it would be wise to technically define what an endocast is and is not. It would be easy to say that an endocast is the brain; however, this definition is simplified to the point of being incorrect. An endocast is, by definition, the area inside the braincase that held soft anatomy during the life of an animal and excludes the surrounding bones (Balanoff and Bever, 2017). This soft anatomy decomposes extremely quickly after death and leaves behind a hollow area inside of the braincase. Sometime during the fossilization process, the hollow area is filled with sediments and the sediments become lithified over time to become a physical cast of the soft endocranial anatomy of a skull. It is true that the original anatomical structures cannot be directly viewed and are lost to time; however, the internal braincase anatomy of modern animals is so much more complex than “just the brain”. For simplicity, the soft tissue of the internal braincase anatomy will be restricted to the brain itself, cranial nerves that receive and distribute cephalic and somatic impulses, arteries that supplied the endocast with blood flow in life, and the internal lining of the braincase.

Taphonomic processes and lithification only preserve the fossae that housed the internal anatomy. This is to say that what all that is observable is the hollow space in which the brain and all its related anatomy was located. Only in very specific and extraordinarily rare circumstances are actual endocranial tissues preserved in the fossil record (Brasier et al., 2016). The fossae that are present in digital reconstructions generally housed the anatomy along with an anatomical cushion of sorts and cannot be trusted to be a true representation of the endocast’s original volume. When digital reconstructions of endocrania are made or a cast is made from a braincase, the result is always comprised of the dura mater, brain, cranial nerves, arteries, endosseous labyrinths, and varying amounts of cartilage—endocasts are never just the brain and should not be thought of or researched as such.

1.6.1 General Endocast Anatomy

The size and shape of dinosaur endocasts have been the subject of a multitude of papers over many years (Jerison, 1955, 1969; Hopson, 1979; Giffin, 1989; Brochu, 2003; Witmer and Ridgely, 2009; Balanoff et al., 2016; Müller et al., 2020; Sakagami and Kawabe, 2020). The general divisions of the brain have been described in detail before; here, I will discuss the location and function of specific lobes of the brain and their role in neurosensory detection and/or interpretation. While the morphology of an endocast changes with time, the general anatomy is the same: olfactory bulbs, olfactory tract, cerebral hemispheres, optic lobe, pituitary, and cerebellum. The names of the gross anatomy described throughout this thesis

reflect either the surface anatomy that can be observed on the endocast or the fossae that housed specific anatomy in life. For example, the floccular lobes of any given dinosaur have not been preserved, but rather the floccular fossae are preserved and a digital cast has been made of the interior surface upon segmentation.

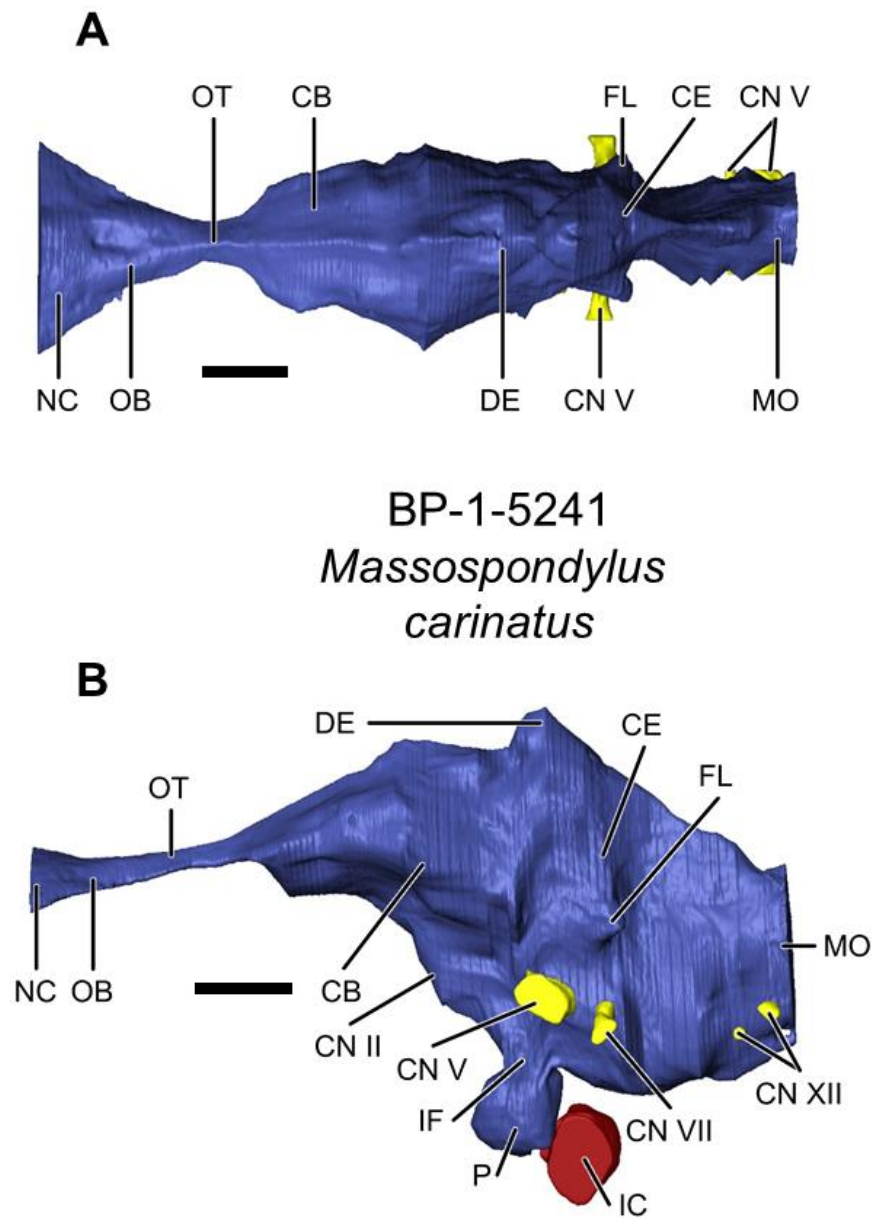


Figure 1.3 – Examples of commonly preserved anatomy on a non-avian dinosaur endocranium in dorsal (A) and lateral (B) views. Abbreviations: P, pituitary; CB, cerebrum; CE, cerebellar area; CN, various cranial nerves (trigeminal (CN V), facial (VII), and hypoglossal (XII) nerves depicted); DE, dural expansion; FL, floccular lobe; IC, internal carotid arteries; IF, infundibulum; MO, medulla oblongata; NC, cast of the nasal cavity. Scale bars = 5 mm.

1.6.2 Dural envelope

The dural envelope (also the dura mater or dural covering) can be defined in two ways. Anatomically, the dural envelope consists of up to three major parts (in birds and mammals – reptiles such as alligators have fewer) that surround the brain proper: the pia mater, arachnoid mater, and dura mater (Kondrashova et al., 2020). These three parts form a protective covering around the brain that houses vasculature, cranial sinuses, and cerebrospinal fluid. However, the subdivisions of the dural envelope are not identifiable in fossil endocasts. Instead of defining the layers by their anatomical names, they are lumped together as the dural envelope.

The external most layer, the dura mater, is the thickest and located closest to the skull. Functionally, the dura mater provides protection to the brain and supports sinuses along the neurocranium. This layer is the thickest and is typically what obscures the surface anatomy of brains in endocasts. Below the dura mater is the arachnoid mater. The arachnoid mater, so called for the spiderweb like appearance of fibrous filaments within the arachnoid, uses cerebrospinal fluid to act as a cushion in the space between the arachnoid and the next dural layer – the pia mater. Lastly, the pia mater is located closest to the brain and surrounds the surface gyri and fissures. In life, the pia mater is responsible for protection of the brain and production of cerebrospinal fluid. All of these layers mesh with the rest of a reconstructed endocast and only dura mater can be considered observable in endocasts made from traditionally prepared skulls (i.e. non-iodine stained or skulls from fresh cadavers).

Since the dural envelope surrounds the brain, it comes in contact with all the bones of the braincase.

1.6.3 Olfactory Bulbs and Tract

The olfactory bulbs and tract (together called the olfactory apparatus) are always the anteriormost neurosensory portions of the brain or endocast (Figure 1.4). In life, the olfactory bulbs gather scent and chemoreception data from across the olfactory epithelium via nerve axons. Data collected in the olfactory bulbs are transmitted along mitral cells to deeper within the brain.

In the fossil record, the size of the olfactory bulbs is interpreted as an organism's reliance on olfaction (Zelenitsky et al., 2009, 2011). Larger olfactory bulbs translate to more olfactory receptor cells along the epithelium in the nasal cavity and more glomerular cells, structures that transmit receptor data from neurons to mitral cells, to gather and send, respectively,

olfactory data. Usually associated with dinosaurs like tyrannosaurs (Witmer and Ridgely, 2009; Zelenitsky et al., 2009), large olfactory bulbs are not limited to predators. Some herbivores, such as sub-adult and adult psittacosaur, have olfactory bulbs that are large for the body size of the animal (Zhou et al., 2007; Hughes and Finarelli, 2019) – though the exact use for an acute sense of smell in herbivores is debated.

The olfactory apparatus is bound by the frontals and sphenethmoid (Franzosa, 2004) – sometimes by the orbitosphenoids (Brochu, 2003; Franzosa, 2004).

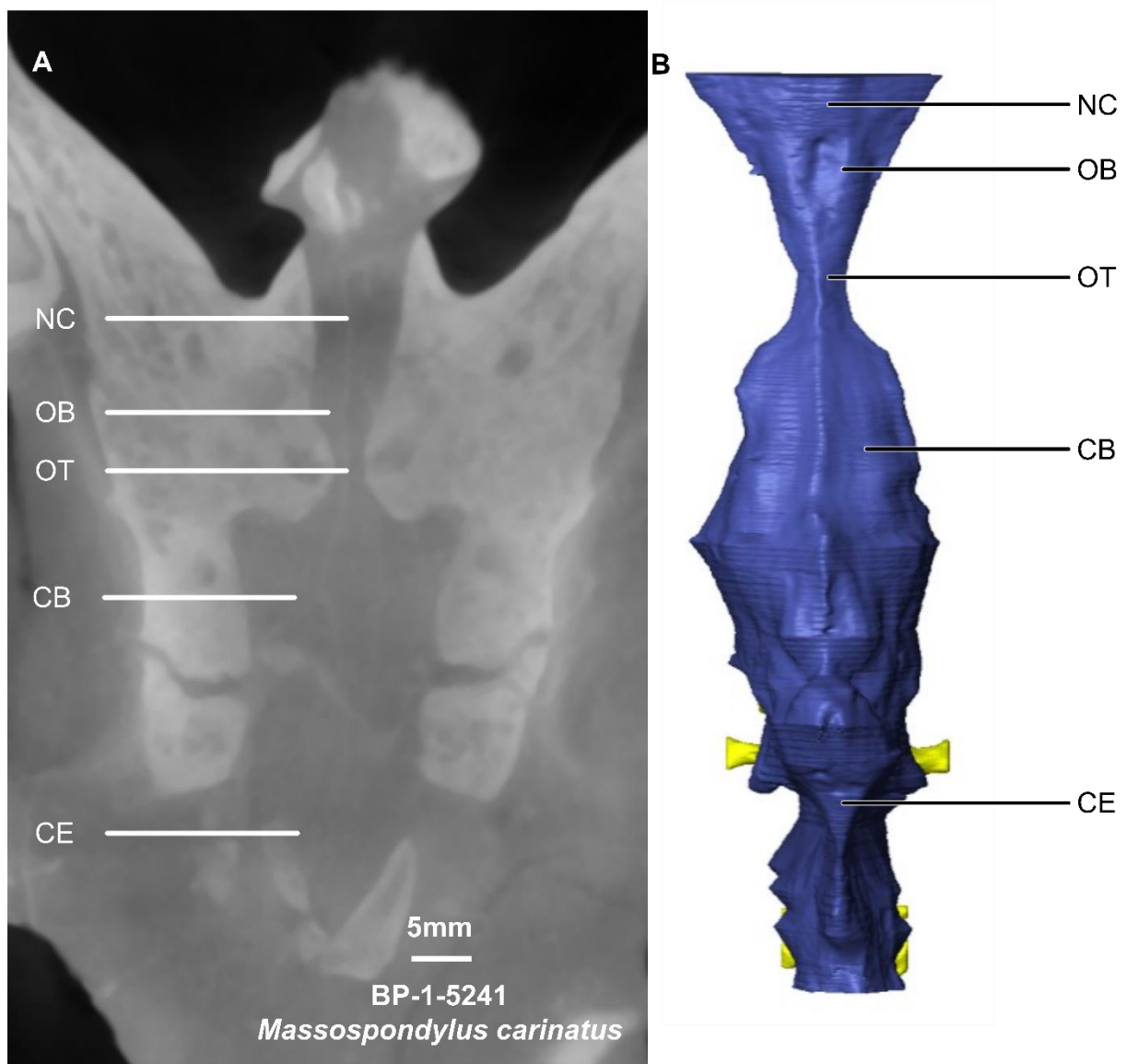


Figure 1.4 – Dorsal view of CT data (A) and endocast (B) of the sauropodomorph *Massospondylus carinatus*. Anatomy is labelled to located and show the location of the olfactory apparatus. Abbreviations: CB, cerebrum; CE, cerebellum; NC, nasal cavity; OB, olfactory bulbs; OT, olfactory tract.

1.6.4 Cerebral Hemispheres

Both cerebral hemispheres (frequently referred to as the cerebrum) are located together just posterior to the olfactory apparatus. The cerebral hemispheres form a pyriform or diamond shape when viewed dorsally (Figure 1.5). Medially, the hemispheres are separated by the longitudinal fissure and are separated from the cerebellum by the transverse fissure. In modern archosaurs, the soft tissues of the left and right hemisphere are connected by a bundle of nerves called the corpus callosum. The cerebrum is almost invariably the widest aspect of the endocast in archosaurs with the broadest part being the posterior section closest to the transverse fissure. The cerebra of non-avian dinosaurs differ from birds in that the cerebral hemispheres of dinosaurs are uniformly rounded along the dorsal margin whereas birds have what is called a hyperpallium – a secondary ridge on the dorsal surface of the cerebrum used for extra optical data processing. This is represented as a Wulst on reconstructed endocasts and is wholly absent on non-avian dinosaurs (Beyrand et al., 2019).

Functionally, the cerebral hemispheres are responsible for interpreting the details gathered by the rest of the brain. Evidence shows that each hemisphere specialises in different forms of sensory or tactile information processing in mammals (Bianki, 1983). Franzosa (2004) points out that reptile cerebra predominately integrate olfactory or chemical data while birds are more similar to mammals. This implies that, while difficult to gauge in non-avian dinosaurs, cerebral growth and development may indicate an organism is better suited to gather and process sensory information than its more basal ancestors. This is supported by maniraptorans which experienced an enlargement of their cerebra in the Late Cretaceous (Balanoff et al., 2013, 2014, 2016, 2018a) and continues in birds where the cerebrum is second only to mammals in volumetric size (Balanoff et al., 2016).

The cerebral hemispheres of basal non-avian dinosaurs contact with the frontals. As theropods became more derived, the cerebra expanded to the parietals as well (Franzosa, 2004; Fabbri et al., 2017).

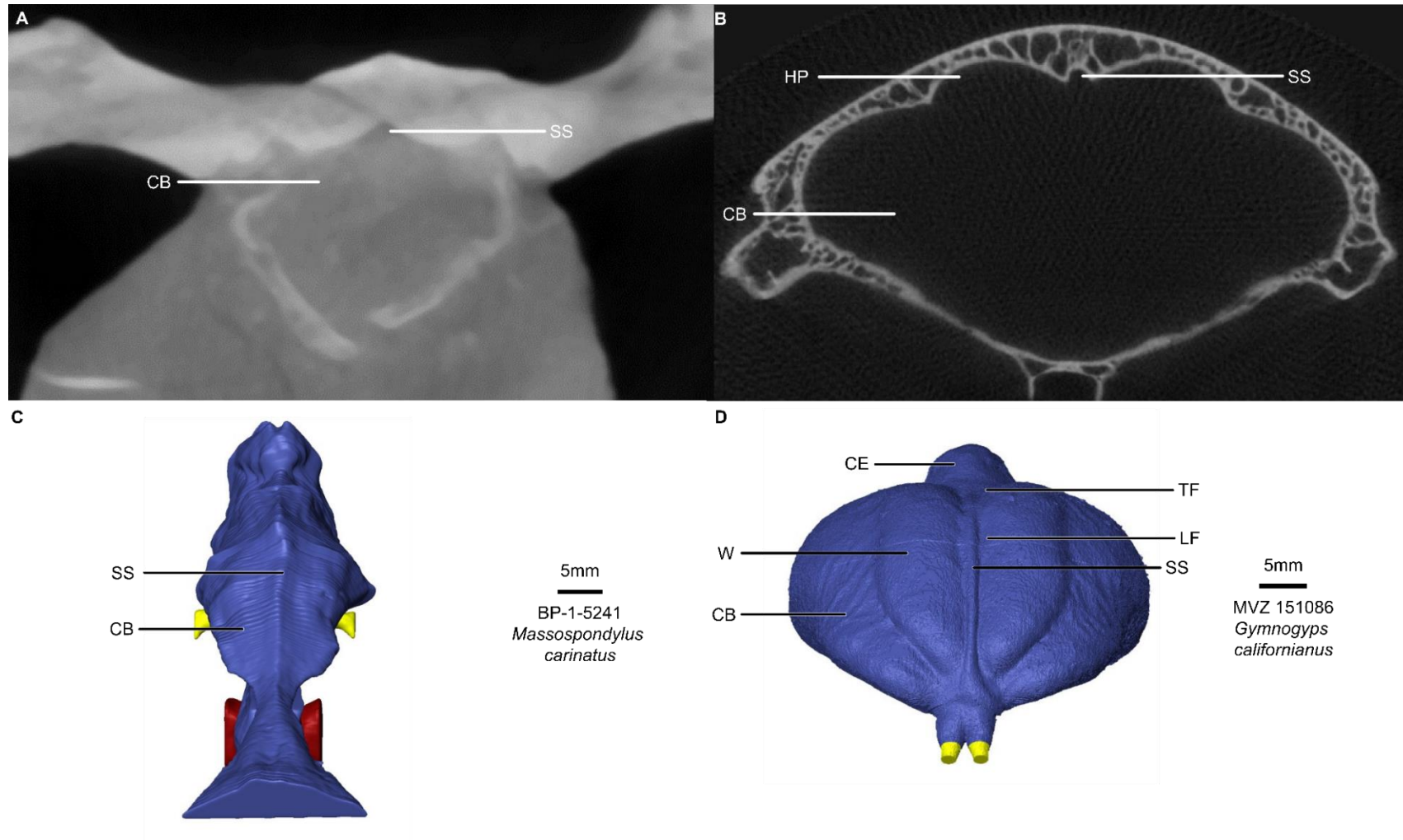


Figure 1.5 – CT data and endocasts that show differences in cerebral anatomy in basal archosaurs/non-avian dinosaurs (*Massospondylus carinatus*; A, C) and avians (*Gymnogyps californianus*; B, D). Non-avians lack the specialised dorsal expansion called the hyperpallium (named the Wulst along reconstructed endocasts). The presence of fissures is frequently obscured on basal archosaur endocasts due to thick dural coverings. Abbreviations: W, Wulst; CB, cerebrum; CE, cerebellum; HP, hyperpallium; LF, longitudinal fissure; SS, dorsal sinus; TF, transverse fissure.

1.6.5 Optic Lobes

Optic lobes of the endocast are, broadly speaking, located on the midbrain and are immediately posterior to the cerebral hemispheres but anterior to the cerebellum (Figure 1.6). The location of the optic lobes are broadly important as they are dorsally oriented in basal archosaurs and non-avian dinosaurs, but shift to a lateral configuration in derived maniraptorans (Witmer and Ridgely, 2009; Figure 4) and birds. Anatomically, the optic lobes correspond to the optic tecta of the brain. Functionally, the optic lobe – or, more correctly, the optic tectum – is responsible for collecting and interpreting visual data gathered through the eyes. The size or surface area of optic lobes in modern animals is correlated to the visual acuity of an organism. For example, diurnal, predatory birds are more reliant on vision and tend to have larger optic lobes than nocturnal, heavily specialised birds (Torres and Clarke, 2018).

Optic lobes are typically difficult or impossible to observe in non-avian, non-maniraptoran dinosaur endocasts due to coverage by the dura mater or dural venous sinuses (e.g. Franzosa and Rowe, 2005; Witmer and Ridgely, 2008; Brasier et al., 2016; Carabajal et al., 2018; Sakagami and Kawabe, 2020) and are only reliably observable in derived maniraptorans such as ornithomimids (Witmer and Ridgely, 2009) and oviraptorosaurs (Balanoff et al., 2014, 2018a).

The bones that come into contact with the optic lobes are phylogenetically controlled. Basal archosaurs and non-avian, non-maniraptoran dinosaurs are located under the frontals, but are well-hidden by soft tissues. Maniraptoran dinosaurs and birds are laterally and ventrolaterally oriented, respectively, and thus come into contact with the laterosphenoids.

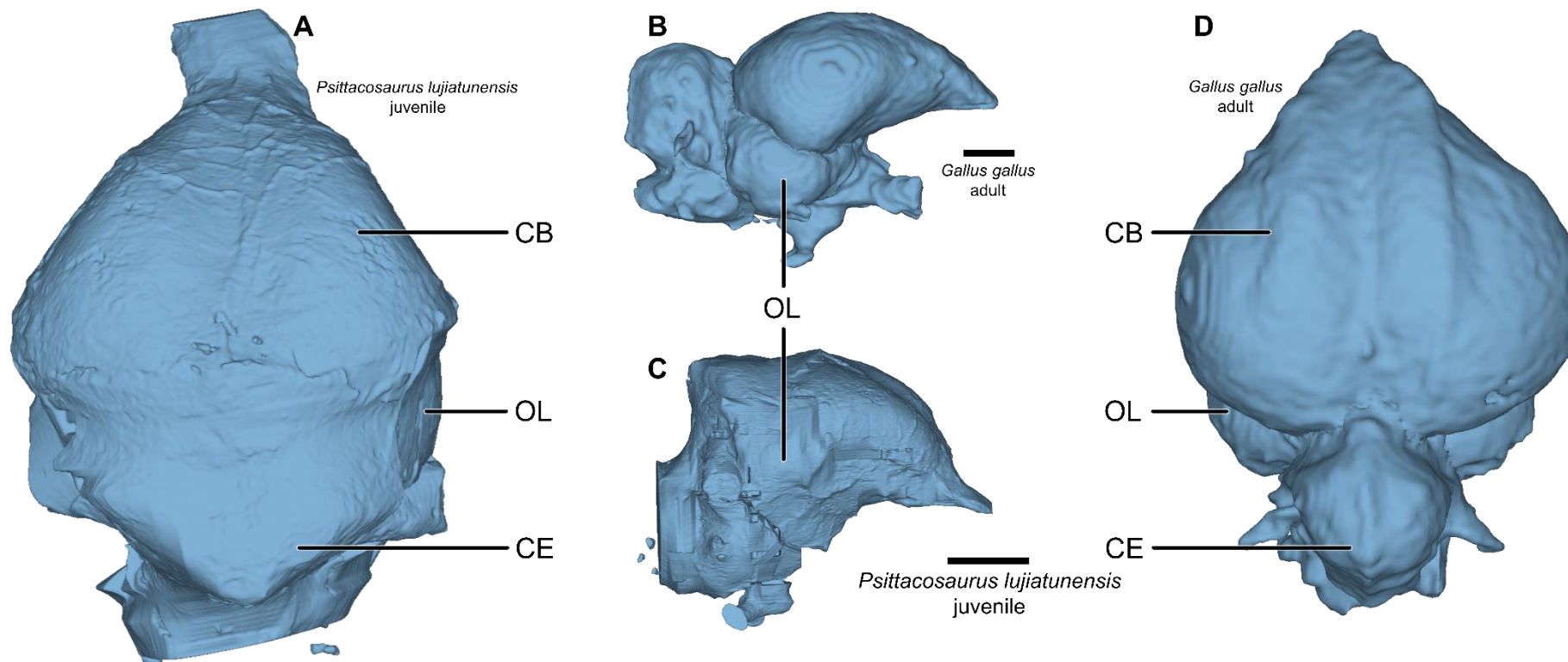


Figure 1.6 – Comparative optic lobes between *Psittacosaurus lujiatunensis* (A,C) and *Gallus gallus* (B,D). Optic lobes are located along the midbrain (as shown laterally; B,C) and are much more exaggerated in avians than non-avian dinosaurs (as shown dorsally; B,D). They are rarely visible on non-theropod dinosaurs and usually on young specimens (A,C). Scale bars = 5 mm.

1.6.5 Pituitary

The pituitary gland (also called the pituitary and pituitary body) is ventral to the cerebrum along the midbrain that connects to the body of the endocranium via the infundibulum. Pituitary glands connect to the hypothalamus through the infundibulum (Figure 1.7) and regulates which and how many hormones should be released into the body at any given moment. Posterioventrally, the internal carotid arteries are commonly preserved along the pituitary gland. The internal carotid arteries function to provide oxygenated blood to the brain and eyes.

As the source of hormonal regulation in the body, the pituitary has been the focus of a few studies – especially since the pituitary fossa is a fair representation of the pituitary gland (Edinger, 1942; Sampson and Witmer, 2007). Early work by Tilly Edinger noted that some sauropods had pituitary bodies that measured up to 10% of the total endocranial volume and linked that gigantism is potentially linked with abnormally large pituitary glands (Edinger, 1942). Further work on sauropods found that sauropods have a positive allometric relationship with body size and, as a clade, tend to have enlarged pituitaries for their brain size (Sander et al., 2011). Pituitary enlargement has been shown to evolve independently of the rest of the brain (Morhardt et al., 2017), indicating that postcranial changes in size can and are linked directly with parts of the brain. Knowing the relationship between the pituitary, brain, and postcranial body gives a better understanding how palaeoneurology, palaeobiology, and palaeoecology interact with each other and are reflected in the endocranium.

The pituitary gland is housed in the pituitary fossa that is encased within the basisphenoid.

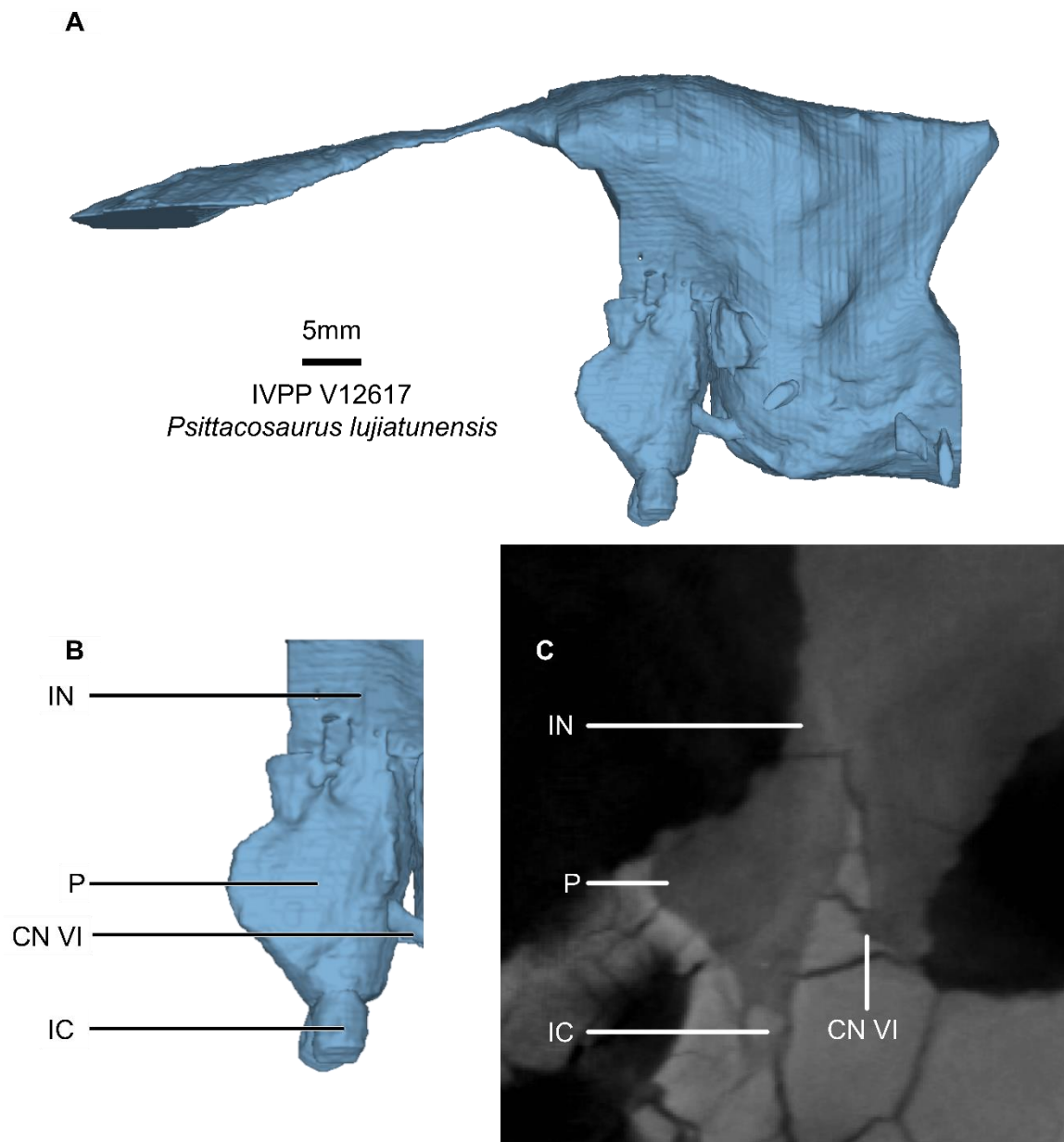


Figure 1.7 – Complete endocranium (A) of the non-ceratopsid ceratopsian dinosaur *Psittacosaurus lujiatunensis* with the pituitary area detailed (B) and the pituitary area in prior to reconstruction (C). Abbreviations: P, pituitary; IC, internal carotid; IN, infundibulum; CN VI, abducens nerve.

1.6.7 Cerebellum and Floccular Lobes

The cerebellum lies posterior to the cerebrum in vertebrates. In basal archosaurs, including most non-avian dinosaurs, the cerebrum and cerebellum are separated by the optic lobes. This changes in derived maniraptorans and birds where the cerebrum and cerebellum come in contact with each other as the optic lobes become more and more laterally oriented (Balanoff et al., 2018a). Another difference between the cerebellum of basal and derived archosaurs is that the cerebellum of basal archosaurs are covered by a thick occipital sinus (Hopson, 1979); birds lack a thickened occipital sinus and the cerebellar expansion of the endocast is a much closer approximation of the cerebellum's true form. Two projections, called floccular lobes or flocculi, extend from the cerebellum posterolaterally. Flocculi range in size between taxa but are always located along the endocranial cerebellum – when they are viewable. The dura mater in some dinosaurian taxa is thick enough around the hindbrain to obscure or completely hide surface anatomy such as the flocculi (Ballell et al., 2020).

Functionally, the cerebellum is associated with gathering movement data but also controls fine motor skills of muscles. Due to its link with movement and muscle control, the cerebellum has a close relationship to optical, visual, auditory, and somatic systems (Franzosa, 2004). This is especially true in the flocculi – the control centres of agility and balance in the brain. The size of flocculi in the fossil record are interpreted as a measure of an organism's ability to interpret somatosensory data related to speed and agility with larger flocculi implying a swift, well-balanced animal – usually a carnivore (King et al., 2020) or omnivore (Ballell et al., 2020; Müller et al., 2020). Shifts in floccular size is also interpreted as locomotory transitions in some dinosaurian taxa where locomotion changes from a bipedality to obligate quadrupedality. For example, basal sauropodomorphs are now understood to be fleet-footed bipeds with large floccular lobes in the Early Triassic (Bronzati et al., 2017; Ballell et al., 2020; Müller et al., 2020) but shift to having diminutive flocculi throughout the Mesozoic while becoming obligate quadrupedal derived sauropods of the Cretaceous (Sereno et al., 2007; Knoll et al., 2012). Some researchers have linked the size of the flocculi with other locomotory styles such as flight in pterosaurs (Witmer et al., 2003); however, more recent research shows that predicting flight styles in birds (and assumedly, pterosaurs) is much more complicated than the size of the floccular lobes (Walsh et al., 2013; Ferreira-Cardoso et al., 2017).

Dorsally, the cerebellum is bordered by the parietals and supraoccipitals. The floccular lobes are encased by the supraoccipitals and prootics of the braincase. Inside the braincase, the floccular lobes are bounded by the endosseous labyrinths (see 1.5.9).

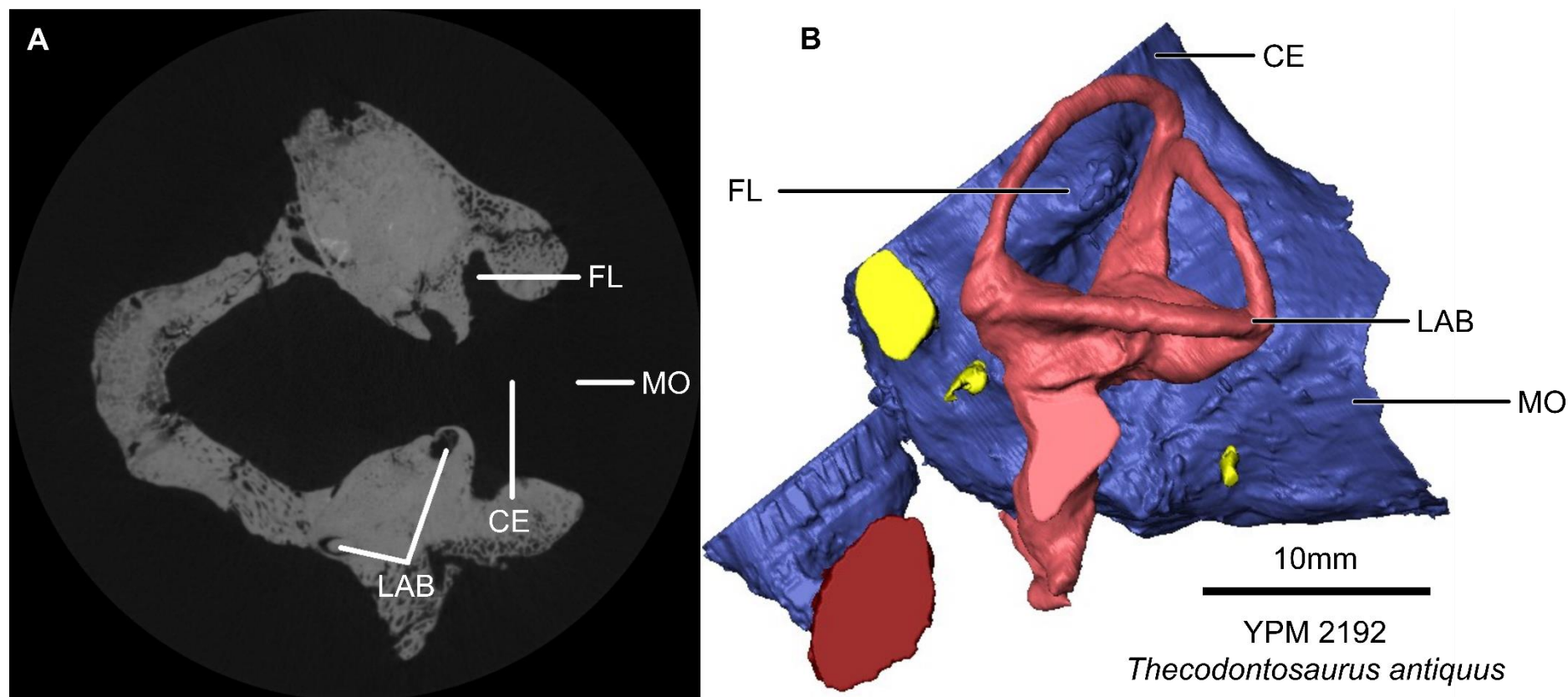


Figure 1.8 – Cerebral endocranial space within the braincase (dorsal view; A) and digitally reconstructed cerebellum (CE), floculus (FL), medulla oblongata (MO) and endosseous labyrinth (LAB) of *Thecodontosaurus antiquus* (lateral view; B). The flocculi, when present along the endocast, fit into the labyrinths as shown in B

1.6.8 Cranial Nerves

The twelve cranial nerves in dinosaurs are oriented ventrally or laterally along the ventral half of the endocast (Figure 1.3). All of them are ventrally located and will sometimes deviate laterally depending on the taxon. Each nerve is associated with a specific cephalic or somatic sense (Table 1.1) and the function of each nerve is based on the anatomy of extant archosaurs and avians. Cranial nerve nucleation points are sometimes difficult to image due to the dural envelope obscuring the surface brain anatomy in dinosaurs (Hopson, 1979). Similarly, determining the specific location where each cranial nerve innervates is near impossible since cephalic and somatic musculature is rarely preserved and, when it does fossilize, does not show how nerves attach to muscle fibres (Hopson, 1979). Innervation sites are based almost entirely off the neuroanatomy of living taxa. However, the foramina that housed cranial nerves are usually well preserved in the bones that constitute the braincase (Hopson, 1979).

Table 1.1 – List of all cranial nerves found along the non-avian dinosaur endocast and the sensory data transmitted associated with each nerve.

CRANIAL NERVE NAME	GENERALIZED FUNCTION
I - Olfactory nerve	Smell
II - Optic nerve	Sight
III - Oculomotor nerve	Fine muscle control of eye and lens; moves eyelids
IV - Trochlear nerve	Rotates eyes via muscle control
V₁ - Trigeminal nerve; ophthalmic branch	Controls senses to the face and upper skull region
V₂ - Trigeminal nerve; maxillary branch	Sensory and motor control for the maxillary region
V₃ - Trigeminal nerve; mandibular branch	Sensory and motor control for the mandibular region
VI - Abducens nerve	Moves eyes outwards via muscle control
VII - Facial nerve	Controls muscles of the face and tongue sensations
VIII - Vestibulocochlear nerve	Balance and hearing; head orientation
IX - Glossopharyngeal nerve	Sensations in the middle ear, tongue, and pharynx
X - Vagus nerve	Regulates involuntary body functions (digestion, heart rate, etc.)
XI - Accessory nerve	Supplies muscle control of the head and shoulders
XII - Hypoglossal nerve	Tongue movement and sensation

1.5.9 Endosseous Labyrinths

Endosseous labyrinths are sensory organs that gather input from two different, yet vital senses: balance and hearing. The vestibular portion of the labyrinth system detects vertical and lateral movement of the head as well as the pitch, roll, and yaw of the skull. This is done by perilymph, a viscous liquid found between the external osseous and internal membranous inner ears, moving through the semicircular canals and moving tiny hair cells in specialised anatomy called canal ampulla located at the base of each canal. As the hair cells are moved,

skull location and orientation within a 3D space is collected with the anterior, posterior, and lateral semicircular canals and sent to the brain via the vestibular branch of CN VIII. Similarly, the horizontal movement or rise and fall of the head is sensed by the utricle and saccule and transmitted along the same nerve. So as a head of an organism is moving vertically up or horizontally side-to-side, the utricle and saccule translated the movement and alerted the rest of the brain how and where the head was located in a 3D space (Rabbitt et al., 2004).

The cochlear portion of the labyrinths, the parts responsible for hearing, are represented by the cochlear duct (also called the lagena). In some fossils, the oval and round window can be viewed along the vestibule of the endosseous labyrinth (Figure 1.9). The oval window is where the stapes would contact the labyrinth and transmit sound vibrations. In life, the round window vibrates in opposition to the vibrations transmitted along the oval window. This action moves perilymph between the osseous and membranous inner ear within the cochlear duct. Cochlear ducts housed the cochlea which was made up of the basillar papillae.

As with the rest of the endocranial anatomy, the only portions of the labyrinth system that can be cast physically or digitally are the ones that left an impression within the braincase itself. In this case, only the semicircular canals and cochlea can be viewed since they had their own specialized forms within the prootics, otoccipitals, and supraoccipitals. The saccule and utricle were embedded within the vestibule and cannot be viewed due to decomposition.

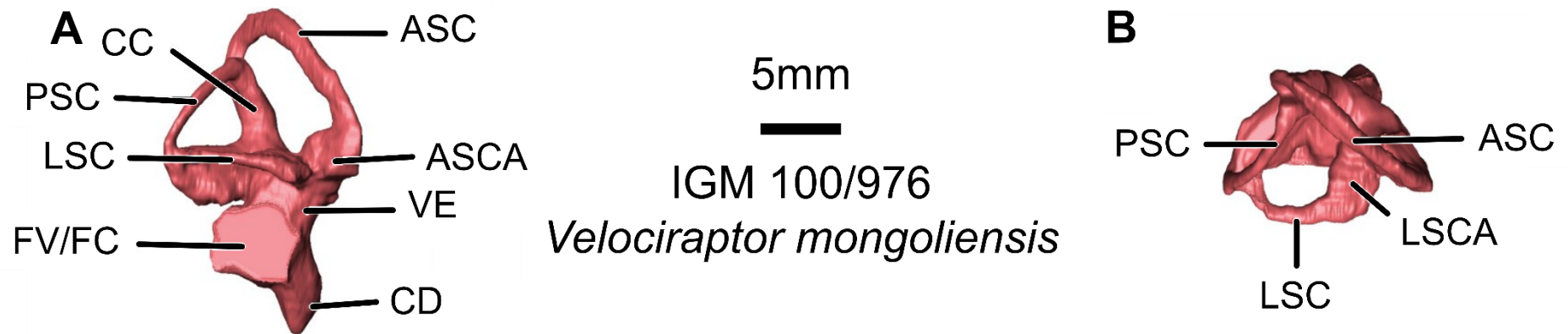


Figure 1.9 – Reconstructed right endosseous labyrinth of *Velociraptor mongoliensis* in right lateral (A) and dorsal (B) views. ASC, anterior semicircular canal; ASCA, ampulla of the anterior semicircular canal; CC, crus communis; CD, endosseous cochlear duct; VE, vestibule; FV/FC, fenestra vestibuli and fenestra cochleae (the division between the two cannot be identified); LSC, lateral semicircular canal; LSCA, ampulla of the lateral semicircular canal; PSC, posterior semicircular canal. See Figure 2.1 and 2.2. Scale bar = 5 mm

1.6.10 Flexure

Endocranial flexure refers to major areas of angle change between the forebrain, hindbrain, and midbrain when an endocast is viewed laterally and is defined as two angles depending on where along the endocast the change is occurring. These two angles are called “cephalic flexure” (the angle between the rostrocaudal axis that extends through the olfactory apparatus and the oblique axis of the midbrain) and “pontine flexure” (the angle between the rostrocaudal axis of the medulla oblongata and the oblique axis of the midbrain) (Lautenschlager and Hübner, 2013).

The degree of cephalic and pontine flexure present along non-avian dinosaur endocasts is driven by a few factors. Firstly, the size of the orbits in relation to the skull have an impact on how acute or obtuse the endocranial flexures are within the braincase (Giffin, 1989). As pointed out in Giffin (1989), smaller taxa have a larger orbit-to-absolute skull size than larger taxa do and, therefore, have less room in the braincase to accommodate an elongate brain. Lastly, the age of the individual influences the shape of the brain (see Chapter 3, for example)

Broadly speaking, the basal condition of flexure is near 180° for Archosauria and the brain is oriented along the horizontal plane (Lautenschlager and Butler, 2016). Theropods, especially those in the bird lineage, had a more intermediate brain shape where the cephalic and pontine flexure had closer to acute flexure angles. Basal and modern birds almost universally have near 90° flexure angles (Balanoff and Bever, 2017) (Figure 1.10).

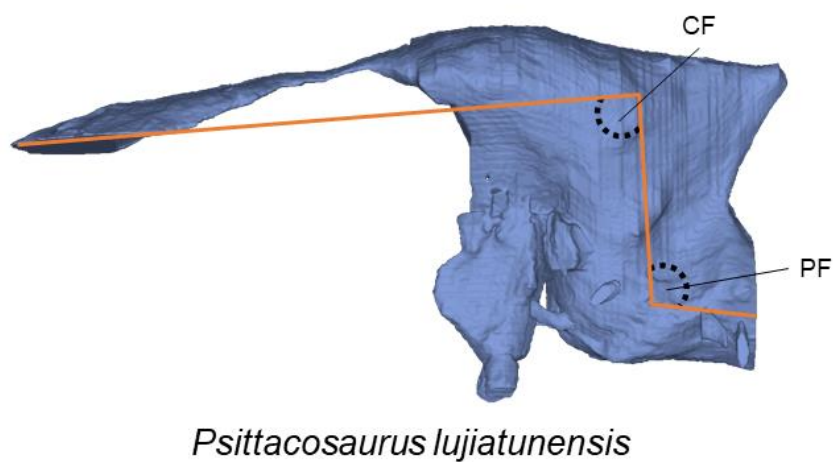
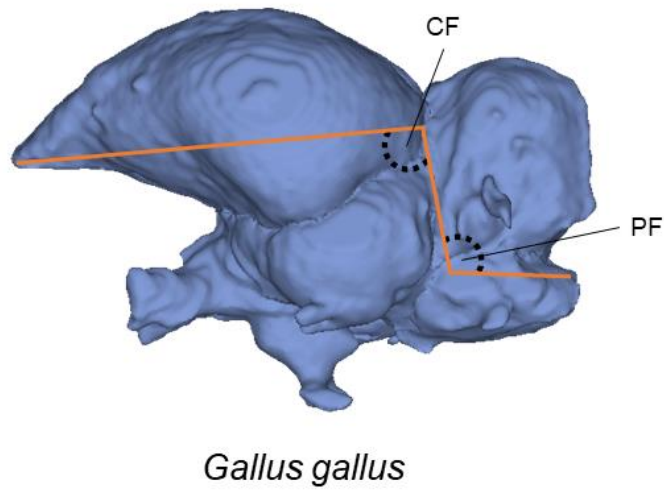
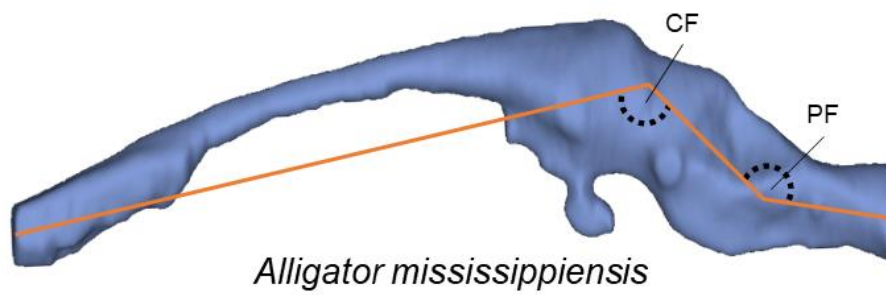


Figure 1.10 – Examples of cephalic (CF) and pontine (PF) flexure angles between different archosaurian taxa: alligators (*Alligator mississippiensis*), chickens (*Gallus gallus*), and a basal ceratopsian (*Psittacosaurus lujiatunensis*).

1.7 Dinosaur Palaeobiology and Palaeoneurology

1.7.1 Encephalisation Quotients

Endocranial anatomy can only provide so much information – with most data gathered from an endocast's anatomy pertaining to sensory function. To better understand how well a dinosaur would have interpreted its surroundings, the total endocast volume must be taken into consideration. An encephalization quotient (EQ) is a ratio calculated between the expected volume of the brain and the expected body mass of an organism (Jerison 1969; Jerison 1973; Equation 1). These transformations are used to categorize how complex the behaviour, typically interpreted as intelligence or cognitive ability in non-hominid organisms, of organisms was in relation to others.

$$EQ = \frac{E_i}{0.12P_i^{2/3}}$$

Equation 1 – General equation for an encephalization quotient. Jerison's general form of an encephalization quotient represents the ratio of an expected brain size (E_i) to an expected body size (P_i). Based on Jerison (1973) and Wharton (2002).

In extinct taxa, body size – or body volume – was calculated scaled models of species. Once a volume had been obtained, a body mass was then derived by multiplying the volume by the animal's specific gravity (Jerison, 1973; Wharton, 2002; Franzosa, 2004).

Larger EQs meant that more complex behaviour was possible or at least more likely. Quotient values larger than 1.0 means that the brain size is larger for a given body weight or size than expected. Harry Jerison's work broadly divided animals into "higher" and "lower" vertebrate groups (Figure 1.11) based on how large or small the brain volume was in comparison with an organism's respective body weight. Higher vertebrates – mammals and birds – are characterised as having brains that are large for their body weight. Lower vertebrates – reptiles and fish – are described as having brains that are smaller than expected for their body weight.

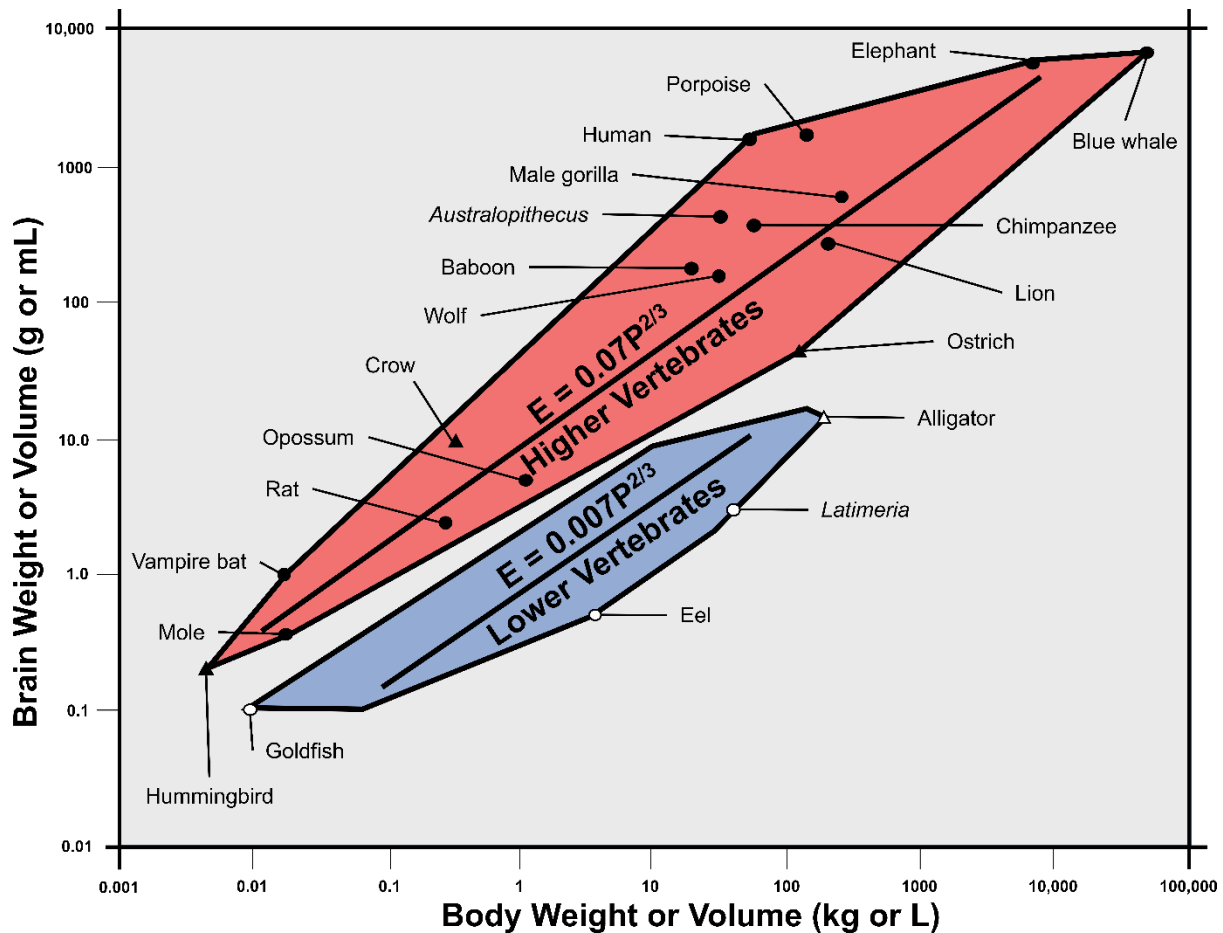


Figure 1.11 – Graph showing the ratios between brain weight and body mass in modern birds, mammals, reptiles, and fish. This visually shows the difference between what is defined as “higher” and “lower” vertebrates defined by Harry Jerison. Black circles are mammals, black triangles are birds, white triangles are reptiles, and white circles are fish. Modified from Jerison (1969).

The formula originally derived by Jerison was further derived by Grant Hurlburt into reptile (REQ) and bird (BEQ) quotients depending on how much of the endocranial was filled with neural tissue (Equation 1) (Hurlburt, 1996).

$$\text{REQ} = \frac{M_{\text{Br}}}{0.0155 * M_{\text{Bd}}^{0.553}}; \text{BEQ} = \frac{M_{\text{Br}}}{0.117 * M_{\text{Bd}}^{0.590}}$$

Equation 2 – Reptile (REQ) and bird encephalization quotients (BEQ) derived in Hurlburt (1996). M_{Br} equates to the mass of the brain of a specimen while M_{Bd} refers to body mass.

Hurlburt, unlike Jerison, sampled more thoroughly from the fossil record – although Hurlburt utilised endocranial data from literature rather than sampling endocranials directly. By adapting his equations to fit a more taxonomically diverse dataset, Hurlburt showed that dinosaur endocranials were not abnormally small but actually scaled as expected for their body size as reptiles – as was the case in Hurlburt (1996) for all of the Mesozoic reptiles he sampled. Diversifying the dinosaur dataset to include a maniraptoran, *Troodon formosus*, also had the unexpected result of showing that some dinosaurs were had larger brains than expected for

their body mass – a trait reflected in birds (if using Jerison’s original formula), the extinct avialan *Archaeopteryx*, maniraptorans, and mammals (Figure 1.12).

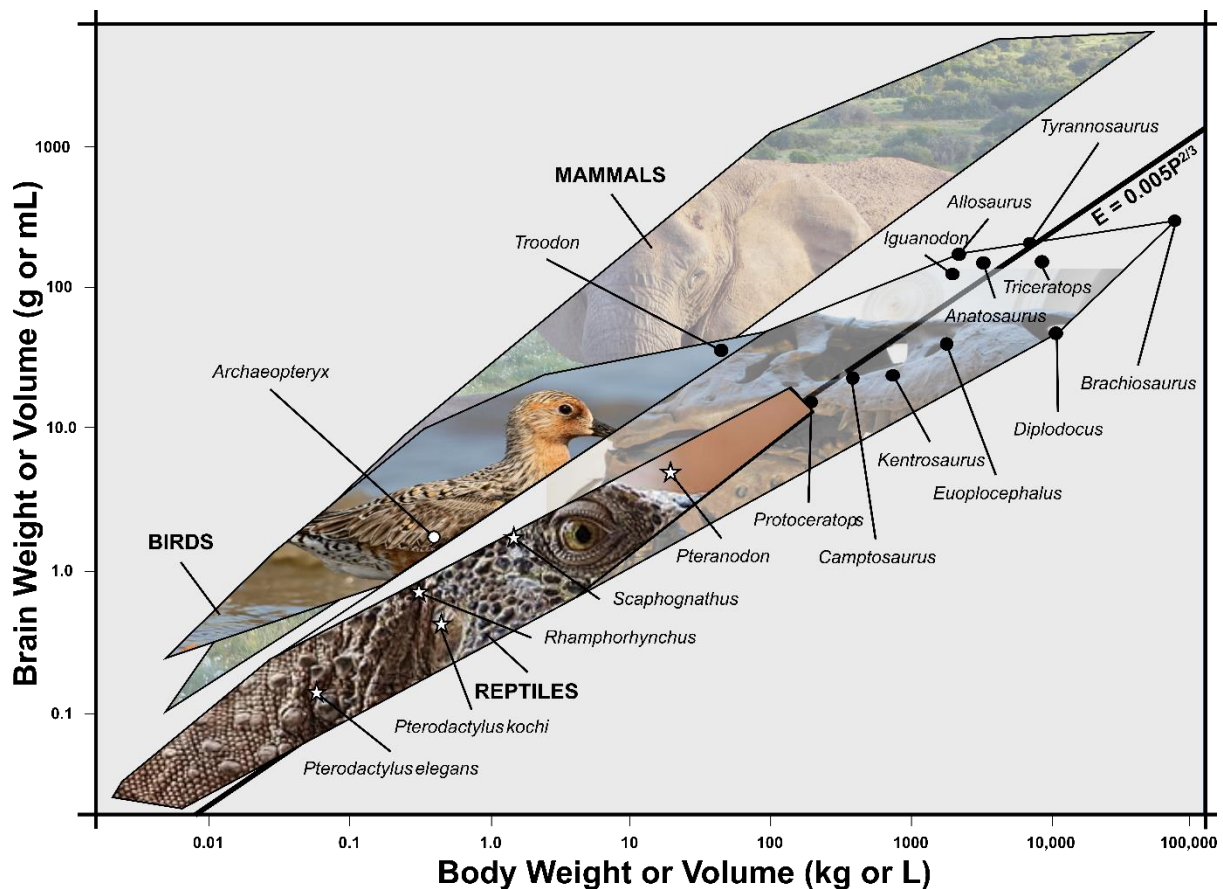


Figure 1.12 – Graph based on Hurlburt (1996) showing the locations of non-avian dinosaurs and pterosaurs plotted on top of areas already defined by extant mammals, birds, and reptiles. Dinosaurs (black circles) have brains that are expected for reptiles of their size; the same as pterosaurs (white stars) sampled for Hurlburt’s dissertation. Notably, *Archaeopteryx* (white circle) already had an above average brain for its size, further delineating it from dinosaurs. *Troodon* breaks the pattern of dinosaurs in that although it is a non-avian dinosaur, its brain-to-body size value was already more similar to birds than reptiles or non-avian dinosaurs.

Both general and derived EQs are powerful tools to help palaeoneurologists understand what size a brain should be for an animal. Calculations have been used to interpret many palaeobiological or behavioural attributes through the years such as intelligence (Jerison, 1973; Jerison et al., 1985; Franzosa, 2004), endothermy (Hopson, 1977), agility (Hopson, 1977).

The problem that plagues dinosaur palaeoneurology – and especially calculating EQs – is the uncertainty of how much the brain tissue of ancient organisms filled their braincases. If the volume of brain does not fill the braincase – which is frequently the case in adult basal archosaurs (Jirak and Janacek, 2017a) – a proper EQ cannot be measured. If assumed to be too high, then palaeontologists will falsely inflate the cognitive abilities of ancient life; too low and it is assumed that life was much too dull to carry out complex tasks – which is known to

be untrue based on modern life (Jerison, 1973). An excellent example of how assumptions of brain volume can mislead estimates can be made with dinosaurs. Arthur Dendy made the following observation while dissecting the pineal eyes of tuatara specimens in the early 1900s:

"We are not concerned here with the topographical relations of the brain [of *Sphenodon*] and its membranes in other regions, but I may be allowed to lay stress on the extraordinary disparity between the size of the brain and that of the cranial cavity. It follows that the shape of the latter can afford no reliable indication of that of the former. The same is probably true of many fossil reptiles, so that the greatest caution should be exercised in drawing conclusions from the study of casts of the cranial cavity." (Dendy, 1911; p. 237)

This statement was then applied to *Tyrannosaurus rex* when Henry Osborn studied its braincase. Osborn estimated that *Tyrannosaurus* filled only 50% of its braincase with actual brain volume (Osborn, 1912) based almost purely on the work of Arthur Dendy (Dendy, 1911). Today, it is known that tyrannosaurids are much more closely related to birds and archosaurs than *Sphenodon* thus making the 50% claim tenuous.

Modern mammals and birds fill close to 100% of the volume of their cranial cavities (Radinsky, 1968; Hopson, 1977, 1979; Evans, 2005) with actual brain tissue; however, some adult crocodilians only fill between 29% and 32% of their braincases (Jirak and Janacek 2017). The large disparity present between endocranial volume and the true volume of brain tissue in non-avian archosaurs cannot be viewed in the fossil record. This must be considered when trying to describe the brain's relationship to its respective braincase and always casts doubt on exact claims of measured volume.

Over the years, counterarguments to Arthur Dendy's claim have been made that incorporate a taxonomic viewpoint. James Hopson, for example, proposed that both modern and fossil reptiles should not be expected to exhibit linear brain-endocast relationships and some variability within and between lineages of extinct organisms should be anticipated. Hopson (1979) specifically points out that the taxonomy of extinct reptiles should reflect what is observable in extant reptiles in that the brain filled a variable amount of space within the braincase. This is to say that extinct organisms should not be expected to fill their braincases with brain tissue because some modern animals do. The inverse of this is true as well; in that extinct animals should not be assumed to partially fill their braincases simply because basal archosaurs or squamates do. Palaeoneurologists need to base their perceptions of endocranial volume off of osteological evidence because the likelihood of volume variation is almost certain; the same is true for modern organisms and should hold true for extinct taxa as

well. Osteological evidence is typically regarded as vascular vallecule impressions along the interior braincase surface (Evans, 2005). Hopson's proposal of variation in the endocranial volume of extinct organisms has been supported in saurischian dinosaurs (Evans 2005; Brasier *et al.* 2016) as well as pterosaurs (Franzosa, 2004).

1.7.2 Sensory Perception and Palaeoecology

The usefulness of palaeoneurology is apparent when the endocranial anatomy of different taxa are compared to one another. Based on the principle of proper mass (Jerison, 1973), the idea that the relative size of a brain lobe or region is indicative of how important the function of the lobe or region is, many studies have utilised endocasts to estimate the sensory abilities of non-avian dinosaurs. This is accomplished by measuring the maximal widths or ratios of an endocranial section or volume of a brain lobe.

An excellent example of this within a clade is the publication “New insights into the brain, braincase, and ear region of tyrannosaurs (Dinosauria, Theropoda), with implications for sensory organization and behaviour” (Witmer and Ridgely, 2009) in which the authors go into great descriptive and comparative detail about the neuroanatomy of tyrannosaurs and other closely related theropod taxa to demonstrate how variation in endocranial anatomy can show relationships between phylogeny, ecology, and olfaction. In this case, olfaction is clearly important to tyrannosaurs due to the olfactory apparatus's large size (Witmer and Ridgely, 2009). This was already known for *Tyrannosaurus rex* (Brochu, 2003) – though the original size estimation was overstated and reduced in Witmer and Ridgely (2009). Witmer and Ridgely (2009) demonstrated, qualitatively, that enlarged olfactory bulbs are important between different specimens of *T. rex*. Broader studies (Zelenitsky et al., 2009, 2011) have shown that by making a ratio between the greatest diameter of the olfactory bulb to that of the cerebrum and comparing it to body mass can indicate the importance of olfaction to an animal. Zelenitsky et al. (2009) showed that not all theropod olfactory bulbs are equal. For instance, basal tyrannosauroids have olfactory bulbs that were close to the average size for Theropoda such as allosauroids and ceratosaurians. Large-bodied tyrannosaurids had much larger olfactory apparatuses than predicted for their body size and show a clear trend that as tyrannosaurs evolved, they became more reliant on olfaction.

The size of the floccular lobes is frequently touted as being an indicator of agility (alongside the endosseous labyrinth) (McKeown et al., 2020) and gaze stability (Walsh et al., 2013), the ability to track an object while it or the head moves, in extinct taxa due to their connection with somatic balance and cerebellum (Bronzati et al., 2017; Ballell et al., 2020; King et al., 2020; McKeown et al., 2020; Müller et al., 2020). Taxa with linearly or volumetrically large flocculi

are interpreted as being agile with great gaze stabilization; the opposite happening with small or indistinguishable flocculi. However, there are some limits to understanding what the flocculi mean for an animal. For instance, while some interpret the agility of an animal based on the flocculi, they are not good indicators of locomotory ability (Walsh et al., 2013). Walsh et al. (2013) demonstrated that the size and volume of the flocculi was not statistically significant between volant, swimming, and flightless birds thereby indicating that size alone is not a great indicator of at least flight ability. This means that archosaur locomotory style should not be based on the flocculi alone (Witmer et al., 2003; Walsh et al., 2013; Gold and Watanabe, 2018). It should be noted that flightless birds showed the most variability among the taxa tested suggesting that the unstable nature of bipedality may be reflected in the size of flocculi (Walsh et al., 2013) therefore suggesting that agility, as a function of bipedality or quadrupedality, may be reflected in the floccular size in some part.

In summary, sizes of some neurosensory lobes can be used to infer the sensory abilities of extinct taxa – albeit sometimes only loosely. These measurements, of course, should never be used as sole evidence for palaeoecology or behaviour. Instead, features of the endocranium should be used in tandem with the skull or postcranial osteological material to infer larger, more complex behavioural patterns in extinct species. I have applied this understanding to the research presented in my thesis.

1.7.3 Ontogeny

Previous work in non-avian dinosaur palaeoneurology has covered many aspects of neuroanatomy such as endocast length, volume, ratios of size-to-body mass, and sensory capability. However, all of the trends noticed in the fossil record and brain evolutionary laws derived from endocasts lack one key element: ontogenetic growth. This is not due to ignoring data or palaeontologists not considering the importance of ontogeny in the fossil record; the omission of heterochronic shifts in non-avian dinosaur endocasts has been due to the scarcity of juvenile specimens from which minimally deformed endocasts could be made. To date, only a few papers describe anatomical and morphological shifts between endocrania of non-avian dinosaurs (Evans et al., 2009; Lautenschlager and Hübner, 2013; McKeown et al., 2020).

McKeown et al. (2020) described the cranial endocast of the tyrannosauroid *Bistahieversor sealeyi* and speculated on the differences between adult and juvenile tyrannosaur endocasts. The authors surmised that, based on the juvenile *Tyrannosaurus rex* CMNH 7541, young individuals would have had more prominent sensory lobes with identifiable optic lobes and flocculi along with more pronounced cerebral hemispheres. This would indicate that a lot of intraspecific variation observed in the endocrania of tyrannosaurs may be explained with

ontogeny. If true, then this would reflect the modern crocodilian condition where the surface anatomy of the brain steadily loses details until most are completely lost (Hu et al., 2021). Unfortunately, not enough cranial material is known from subadult tyrannosaurs to fully support this claim.

A broad study of endocranial spaces was completed by Evans et al. (2009) that incorporated four specimens of three taxa of lambeosaurine hadrosaur: a juvenile *Lambeosaurus* sp.; a juvenile and subadult *Corythosaurus* sp.; and an adult *Hypacrosaurus altispinus*. While this study focused on the elaborate cranial crests of the sample set, the endocranium of each specimen was also reconstructed and briefly described. The authors found that the cranial endocasts of juveniles were no more “brain-like” (e.g. vascularization present, clear surface anatomy) than the endocasts of the adult *Hypacrosaurus*. The juvenile taxa had larger flexure angles than the adult *Hypacrosaurus*; however, the specific changes in flexure were difficult to fully understand as none of the ontogenetic series used in the manuscript were complete and a mosaic of different lambeosaurine taxa were used. Shortened braincases between the specimens and the age of the juveniles led the authors to conclude that differences between endocrania is potentially both ontogenetically and phylogenetically driven.

The most direct endocranial changes viewable in a single species of dinosaur are described in Lautenschlager and Hübner (2013) where two digital endocasts from the ornithomimid *Dysalotosaurus lettowvorbecki* – a juvenile aged 3-4 years old and a subadult aged 12-13 years old – were compared. Though an incomplete ontogenetic series, several notable differences between the specimens were noted. As the age of the species progressed, the olfactory tract elongates, and olfactory bulb increases in size. Similarly, the cerebellum and neurovascular increases between the specimens. Within the endosseous labyrinths, the cochlear ducts do increase in size, but not enough to make a significant difference in average and best hearing frequencies. Broadly speaking, the endocast reduces its flexure angles throughout postnatal development; a trend that is strange when compared to modern archosaurs (Hu et al., 2021) and supports the patterns identified in lambeosaurine hadrosaurs (Evans et al., 2009). In *D. lettowvorbecki*, the broad changes to the length and shape of the endocast imply that growth of the endocranial anatomy was influenced not only by changes in size of the braincase but also by its shape. In other words, not only was the endocast increasing in size with development, but it was also not retaining the same static form with age.

Broadly speaking, ontogeny is a poorly studied and underutilised subsection of palaeoneurology. Since the only studies conducted have used ontogenetic series that do not

include multiple specimens that range from a young individual to a somatically mature adult, large information gaps still plague our understanding of ontogeny's effect on palaeoneurology.

Chapter 2: The endocranium and trophic ecology of *Velociraptor mongoliensis* (published in Journal of Anatomy)

2.1 Collaborative Statement

This chapter was the result of a collaborative project between Logan King (University of Bristol; designed the project, segmented the endocast, measured the labyrinths, calculated the hearing frequencies, and wrote the publication), Justin Sipla (University of Iowa; provided CT data and feedback), Justin Georgi (Midwestern University; provided CT data and feedback), Amy Balanoff (Johns Hopkins University; provided feedback), and James Neenan (Oxford Museum of Natural History; provided CT data, segmented labyrinths). I performed a majority of the work for this chapter by segmenting the endocast, comparing the endocast of IGM 100/976 to other dinosaur endocasts, made the hearing frequency calculations, wrote the initial manuscript, and edited the subsequent drafts. I completed 80% of the work in this chapter. This chapter is the product of King et al. (2020).

2.2 Abstract

Neuroanatomical reconstructions of extinct animals have long been recognized as powerful proxies for palaeoecology, yet our understanding of the endocranial anatomy of dromaeosaur theropod dinosaurs is still incomplete. Here, I used X-ray computed microtomography (μ CT) to reconstruct and describe the endocranial anatomy, including the endosseous labyrinth of the inner ear, of the small-bodied dromaeosaur, *Velociraptor mongoliensis*. The anatomy of the cranial endocast and ear were compared with non-avian theropods, modern birds, and other extant archosaurs to establish trends in agility, balance, and hearing thresholds in order to reconstruct the trophic ecology of the taxon. Our results indicate that *V. mongoliensis* could detect a wide and high range of sound frequencies (2,368–3,965 Hz), was agile, and could likely track prey items with ease. When viewed in conjunction with fossils that suggest scavenging-like behaviours in *V. mongoliensis*, a complex trophic ecology that mirrors modern predators becomes apparent. These data suggest that *V. mongoliensis* was an active predator that would likely scavenge depending on the age and health of the individual or during prolonged climatic events such as droughts.

2.3 Introduction

Velociraptor mongoliensis Osborn, 1924 is a velociraptorine dromaeosaur found in Late Cretaceous formations of China and Mongolia (Osborn, 1924; Godefroit et al., 2008) that has been made famous in recent years thanks to its portrayal in numerous Hollywood movies. *V. mongoliensis* has also been the subject of a number of cranial and postcranial

publications (Sues, 1977; Norell et al., 1997, 2004; Barsbold and Osmólska, 1999; Turner et al., 2007; Manning et al., 2009), with the cranial osteology, including the braincase, being well-known thanks to the exceptionally preserved specimens found in Mongolia (Barsbold and Osmólska, 1999). Despite this heightened attention, the endocranial anatomy of *V. mongoliensis* has not yet been described. Indeed, the endocranial anatomy of Dromaeosauridae as a whole is still relatively poorly known despite the initial osteological description of *Dromaeosaurus* having occurred almost a century ago (Matthew and Brown, 1922). Since that time, the endocast for *Bambiraptor feinbergi* (Burnham, 2004) has been partially described and portions of the endocast of *Saurornitholestes langstoni*, *V. mongoliensis*, *Tsaagan mangas*, and *Deinonychus antirrhopus* have been measured for quantitative analysis or otherwise imaged (Witmer and Ridgely, 2009; Zelenitsky et al., 2011; Balanoff et al., 2013). There is, however, a distinct lack of described endocasts with which to expand the palaeobiology of dromaeosaurs in the formal literature to date. Although a few publications have noted and discussed the implications of the large endocranial space in dromaeosaurs (Hopson, 1977; Currie, 1995; Norell et al., 2004), relating the endocranial anatomy of velociraptorine dromaeosaurs to their trophic ecology has yet to be done in any capacity.

Evidence for the trophic ecology of *V. mongoliensis*, or at least velociraptorine dromaeosaurs, is provided by a few different sources. The most famous of these, the ‘fighting dinosaurs’ of Inner Mongolia, preserves a glimpse into the predator–prey relationship between *V. mongoliensis* (IGM 100/25) and *Protoceratops andrewsi* (IGM 100/512) (Carpenter, 1998). However, two other *V. mongoliensis* specimens indicate what may be considered scavenging behaviour (Hone et al., 2010, 2012). Several previous studies have explored the connection between endocranial anatomy, palaeoecology, and behaviour within theropod dinosaurs. Medium- and large-bodied carnivorous theropods (e.g. tyrannosaurids (Witmer and Ridgely, 2009; Bever et al., 2011; Brusatte et al., 2016; Kundrát et al., 2018; McKeown et al., 2020), abelisaurids (Carabajal and Succar, 2014), carcharodontosaurids (Franzosa and Rowe, 2005; Brusatte and Sereno, 2007; Carabajal, 2010), megaraptorans (Carabajal and Currie, 2017), and allosaurids (Rogers, 1999; Gleich et al., 2005)) as well as small and medium-sized maniraptorans—e.g. oviraptorosaurs (Kundrát, 2007; Balanoff et al., 2018a), therizinosaurids (Lautenschlager et al., 2012), and others (Walsh et al., 2009; Zelenitsky et al., 2011)—have been the focus of neurosensory studies. These studies often are able to utilize structures reflected in the endocasts such as the olfactory apparatus, cochlear ducts, and optic lobes to reconstruct the posture and sensory capabilities for these extinct taxa. For instance, quantitative and comparative

analyses of tyrannosaurids have found that they had the sensory requirements for an active predatory lifestyle (Witmer and Ridgely, 2009), and semicircular canal morphologies have been found to correspond to quadrupedal and bipedal locomotor modes in dinosaurs (Georgi et al., 2013). Even in herbivorous theropods, such as *Erlikosaurus*, strong senses of smell, agility, eyesight, and hearing have been estimated (Lautenschlager et al., 2012).

With this in mind, I explored the neuroanatomy of *V. mongoliensis* (IGM 100/976) in order to better estimate the trophic ecology and sensory aptitude of this species—thus providing much needed sensory and behavioural data for dromaeosaurs. Here, I describe the anatomy of the hindbrain and inner ear of *V. mongoliensis* using cranial endocasts and compare its neuroanatomy to extant reptilian (including birds) taxa in order to place its sensory abilities into a broad palaeoecological context.

2.4 Materials, Methods, and Abbreviations

IGM 100/976 was collected as a part of the 1991 Joint Expedition of the Mongolian Academy of Sciences and American Museum of Natural History. This specimen was recovered from the Djadokhta Formation at Tugrugen Shireh, Mongolia (Norell et al., 1997) and consists of a partial skeleton, including an incomplete braincase that is missing the bones anterior to the basisphenoid and supraoccipitals (Figure 2.1A, B). The braincase is comprised of a few incomplete elements—the exoccipitals, supraoccipital, and basioccipital. These four elements are fused to form an incomplete adult endocranial space where the sutures are obliterated along the surface (Norell et al., 2004). Because of its incomplete nature, the endocast preserves the entire hindbrain but only a featureless portion of the midbrain.

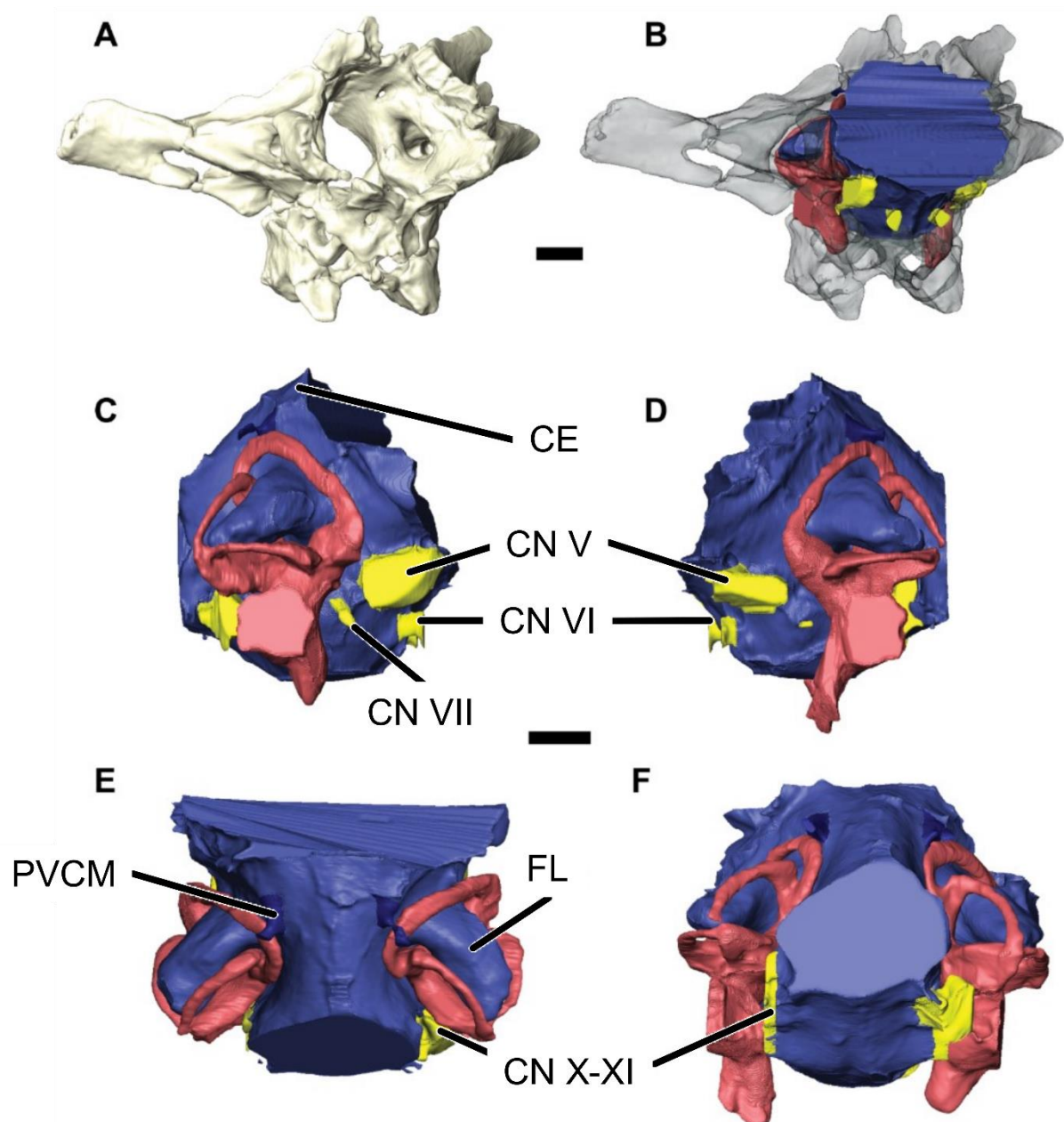


Figure 2.1 – The braincase and endocranium of *Velociraptor mongoliensis* IGM 100/976. Partial braincase in anterolateral view (A). Braincase rendered transparent (B), revealing the in situ endocast in anterolateral view. The labelled endocast is presented in the right, (C), and left (D) lateral, dorsal (E), and posterior (F) views. Brain endocast is shown in blue, veins in dark blue, cranial nerves in yellow, and endosseous labyrinth in pink. Scale bars: 5 mm. CE, cerebellum; PVCM, posterior middle cerebral vein; FL, floccular lobes; CN V, trigeminal nerve; CN VI, abducens nerve; CN VII, facial nerve; CN X–XI, shared foramina for the vagus and accessory nerves

IGM 100/976 was scanned at the University of Texas High-Resolution X-ray CT Facility in Austin, Texas, USA, producing 1024 × 1024 16-bit TIFF images. Scan parameters were as follows: 210 kV, 0.11 mA, intensity control on, high-power mode, no filter, air wedge, no offset, slice thickness 1 line (0.08506 mm), source-object distance 245 mm, 1,400 views, two samples per view, inter-slice spacing 1 line (0.08506 mm), field of reconstruction 81 mm (maximum field of view 81.8084 mm), reconstruction offset 8,700, reconstruction scale 4,000. Acquired with 31 slices per rotation and 25 slices per set. Ring-removal processing based on correction of raw sinogram data using IDL routine 'RK_SinoRingProcSimul' with parameter 'bestof5 = 11'. Reconstructed with beam-hardening coefficients (0.0, 0.6, 0.1, 0.05), and a rotation of 4 degrees. Total final slices = 450. Segmentation, reconstruction, and measurement collection were conducted in AVIZO LITE (Thermo Fisher Scientific, 9.7.0) and AMIRA 2019.1 (Thermo Fisher Scientific).

The mean and high hearing frequencies for IGM 100/976 were calculated following the method outlined in Walsh et al. (2009). To accomplish these reconstructions, I took measurements from the anterior-most extent of the basisphenoid to the posterior-most margin of the occipital condyle along with the length of the cochlear duct (Table 2.1). The two measurements were then used to calculate a cochlear duct-basisphenoid ratio and then logarithmically transformed. This normalized value was placed into pre-calculated formulae found in Walsh et al. (2009).

Institutional abbreviations: IGM—Institute of Geology in Ulaan Baatar, Mongolia; IVPP—Institute of Vertebrate Paleontology and Paleoanthropology, Beijing, China; MPC-D—Paleontological Laboratory of the Paleontological Center, Ulaan Baatar, Mongolia.

2.5 Results

2.5.1 Cranial Endocast

The identifiable regions of the brain preserved in the specimen are limited to the hindbrain: the medulla and cerebellum, including its floccular lobes. The flocculi are situated posterolaterally and orientated posteriorly at 123° (Figure 2.1C, F). The bodies of the floccular lobes are elongate, roughly circular in cross-section, and fill most of the space between the anterior and posterior semicircular canals. Each lobe extends well beyond the posterior margin of the anterior canal and almost through the posterior semicircular canal of the endosseous labyrinth. The flocculi together account for approximately 7% of the total hindbrain volume (Table 2.1).

The medulla is wider than tall and forms an almost oval shape at the foramen magnum. As seen in most other maniraptorans, the medulla is antero-posteriorly short and narrower than the rest of the hindbrain (Kundrát, 2007; Balanoff et al., 2009; Lautenschlager et al., 2012) (Table 2.1). Anteriorly, the medulla exhibits a gentle dorsolateral constriction between it and the cerebellum. Anteriorly, there is a 132.94° angle between the hindbrain and midbrain. This pontine flexure (Table 2.1) implies that the brain exhibited a gentle curvature and was not all located along the same horizontal plane. This curvature is unsurprising due to its presence in many non-maniraptoran theropods (Sampson and Witmer, 2007; Witmer and Ridgely, 2009), basal therizinosaurs (Lautenschlager et al., 2012), and oviraptorosaurs (Kundrát, 2007; Balanoff et al., 2014).

Table 2.1 – Measurements taken from the endocast of IGM 100/976. Volumes do not account for vascularization, endosseous labyrinths or cranial nerves.

Element measured	
Minimum width	14.44 mm
Maximum width	28.49 mm
Cerebellum height	26.13 mm
Cerebellum width	15.75 mm
Total endocast length	22.78 mm
Pontine flexure angle	132.94
Floccular lobe length	9.59 mm
Angle of floccular lobe	123
Total floccular lobe	0.40 g/mm ³
Total volume	5.73 g/mm ³
Cochlear duct length	11.15 mm
Basisphenoid length	34.71 mm

As a whole, few anatomical structures are preserved on the endocast of the cerebellum. The hindbrain lacks a prominent dorsal dural peak overlying the cerebellum that is found in some other maniraptorans such as *Conchoraptor* (Kundrát, 2007) and large-bodied derived tyrannosaurs (Osborn, 1924; Witmer and Ridgely, 2009; Bever et al., 2011; Brusatte et al., 2016). The absence of a large dural peak is consistent with another velociraptorine dromaeosaur, *T. mangas* (personal observation by the authors) and basal tyrannosaurs (Kundrát et al., 2018); however, it is possible that this portion of the endocast was not preserved.

2.5.2 Cranial Nerves and Vasculature

Both trigeminal nerves (CN V) are preserved; each exiting the lateral portions of the anteriormost endocast. The trigeminal is preserved as a single nerve that likely diverged into its component branches outside of the braincase as it does in other non-avian maniraptorans (Figure 2.1C, D) (Currie, 1995). The abducens nerve (CN VI) is located ventromedial to CN V (Figure 2.1C, D) and has an anterior trajectory. The endocasts of the abducens nerves are

incomplete and project anteriorly only a few millimetres before reaching the anterior limit of the braincase. A short canal for the facial nerve (CN VII) lies on the medulla at the level of the anterior edge of the endosseous labyrinth, just posterolateral to CN V. Both the vagus and accessory nerves (CN X–XI, respectively) exit a single ventrolaterally located foramen along the posterior portion of the braincase (Figure 2.1E, F). While it is located laterally near the posteriormost part of the braincase, the hypoglossal (CN XII) could not be reliably reconstructed even though the CN XII foramina are visible on the external braincase (Norell et al., 2004).

Norell et al. (2004) initially described the presence of vasculature along the interior surfaces of the braincase in this specimen of *Velociraptor*, although these could not be reconstructed digitally. The occurrence of small veins in *Velociraptor* would not be surprising considering birds and their close relatives have a thin dural envelope and a majority of their braincase filled with neural tissue (Norell et al., 2004; Evans, 2005). Little of the venous architecture is preserved—only the posterior middle cerebral veins are observable along the posterodorsal surface of the cerebellum (Figure 2.1E).

2.5.3 Endosseous Labyrinth

Both endosseous labyrinths are preserved in IGM 100/976 (Figure 2.2), although the posterior portion of the left labyrinth, i.e. where the posterior semicircular canal meets the lateral canal, is not preserved (Figure 2.2F). In many respects, the vestibular anatomy of *V. mongoliensis* is similar to that of other non-avian theropods (Balanoff et al., 2009; Witmer and Ridgely, 2009; Lautenschlager et al., 2012). Overall, the labyrinth has a somewhat triangular aspect in lateral view, with all semicircular canals being approximately orthogonal to each other. The anterior canal is taller than the posterior one and exhibits only a slight curvature until it curves sharply ventrally to help form the crus communis. The course of the anterior vertical canal is planar and has a roughly uniform lumen thickness along its entire length, except at the anterior ampulla where it meets the vestibule (Figure 2.2).

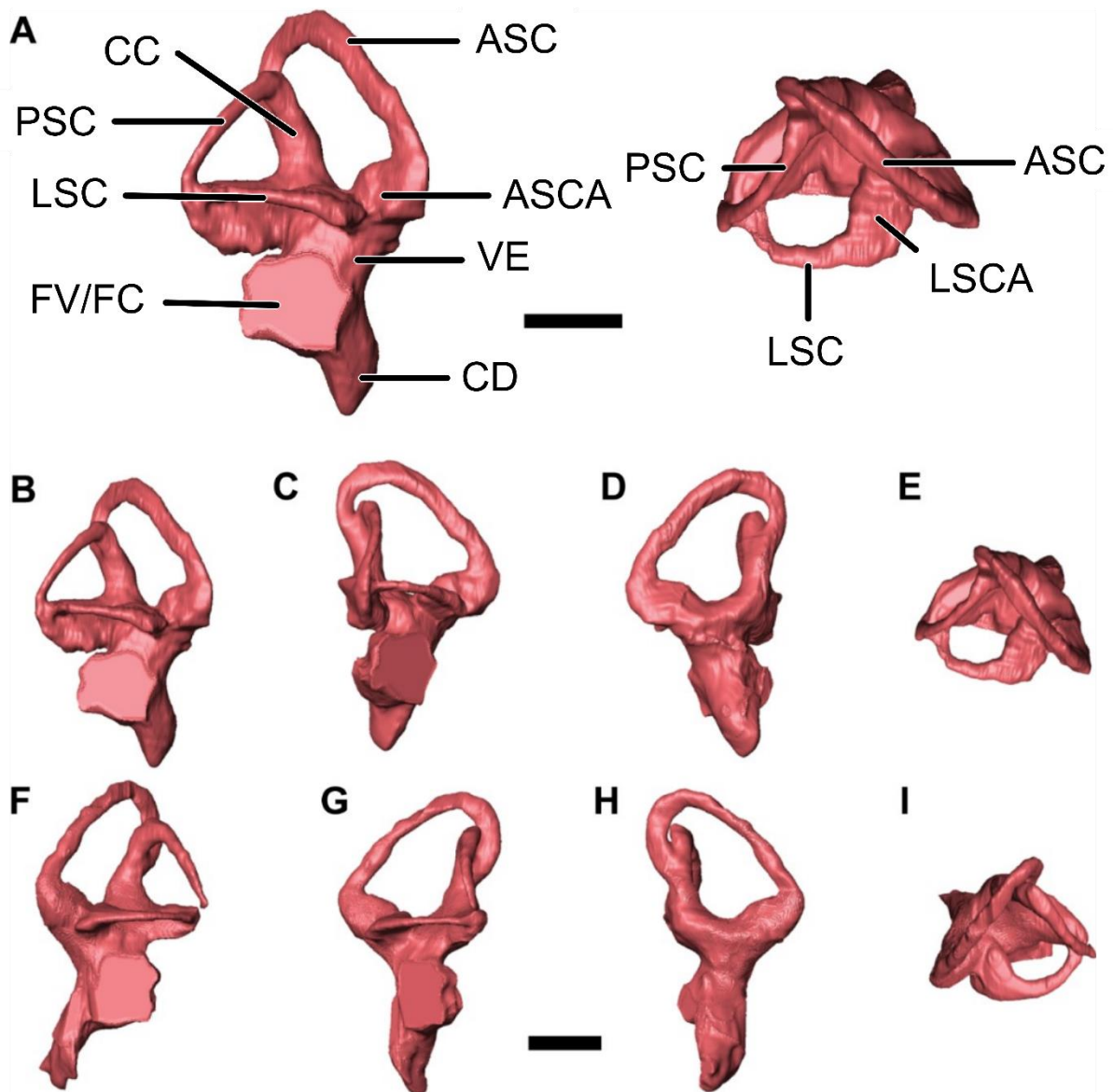


Figure 2.2 – The endosseous labyrinth of IGM 100/976. Labelled right labyrinth (A) in lateral (left) and dorsal (right) views. The right (B–E) and left (F–I) labyrinths of IGM 100/976 shown in lateral (B,F), posterior (C,G), anterior (D,H), and dorsal (E,I) views. Scale bars: 5 mm. ASC, anterior semicircular canal; ASCA, ampulla of the anterior semicircular canal; CC, crus communis; CD, endosseous cochlear duct; FV/FC, fenestra vestibuli and fenestra cochleae (the division between the two cannot be identified); LSC, lateral semicircular canal; LSCA, ampulla of the lateral semicircular canal; PSC, posterior semicircular canal

The posterior and lateral canals are approximately equal in length. The posterior canal deviates from planarity by exhibiting a slight sinusoidal curvature along its course. Although the posterior and lateral endosseous canals both appear to terminate posteriorly in a confluence (Figure 2.2), the posterior semicircular duct of the membranous labyrinth would have continued ventromedially and expanded into its component ampulla (as discussed in

Evers et al., 2019; Neenan et al., 2019), and the lateral duct would have continued medially to meet the vestibule. Similar to palaeognath birds, but previously unknown in non-avian theropods, the medial extremity of the posterior canal curves sharply ventrally and meets the crus communis in a position more anterolateral than the anterior canal (Carabajal and Succar, 2014; Benson et al., 2017).

The lateral canal emerges anteriorly from a large but dorsoventrally compressed ampulla. Its course is planar and highly curved in dorsal view, appearing to meet the vestibule at its posterior extreme just anterior to the posterior vertical canal (Figure 2.2A, E, I). As mentioned above, however, the membranous duct would have continued its loop medial to the posterior canal to meet the vestibule (e.g. Evers et al., 2019).

The cochlear duct, which would have housed the basilar papilla, the receptor organ for hearing, is relatively long in *V. mongoliensis* compared with most non-avian theropods. When measured and compared with the basisphenoid (see section 2.6.1 for details), the mean hearing frequency (2.368 Hz) and high-frequency hearing limit (3,965 Hz) can be calculated following Walsh et al., (2009). The cochlear ducts are also relatively wide and follow a similar anteriorly orientated course as the crus communis. The separation between the fenestra vestibuli and fenestra cochleae (oval and round windows, respectively) cannot be differentiated in this scan (Figure 2.2A, B, F).

2.6 Discussion and Palaeobiological Interpretations

2.6.1 Sensory Abilities of *Velociraptor*

Floccular lobes are used to maintain head and eye stability during movement within vertebrates and, as such, are frequently linked to the agility of an organism (Witmer and Ridgely, 2009). As pointed out in Walsh et al., (2013) and Ferreira-Cardoso et al., (2017), however, the size of the reconstructed flocculi do not necessarily reflect the actual volume of the lobes in life, as other anatomy (e.g. blood vessels) may have also resided within the floccular fossae, making them generally a poor indicator of flight style and ecology in birds (e.g. powered flight vs. gliding). Nevertheless, relatively large floccular fossae likely correlate with large flocculae despite extraneous anatomical structures, and Walsh et al., (2013) further postulate that enlarged flocculi in terrestrial birds could be an adaptation found in bipeds to help stabilize the unstable nature of bipedalism. It is therefore logical to interpret the floccular size in terrestrial, bipedal maniraptorans, such as dromaeosaurs, as relating to balance—with enlarged lobes corresponding to species that necessitated stable bipedal movement. The flocculi of IGM 100/976 are massive and suggest that quick movements and

a stable gaze were essential to its everyday life (Figure 2.1). Enlarged flocculi are prominent in bipedal, carnivorous or omnivorous dinosaur taxa and are frequently lost if a clade of dinosaur shifts to herbivory. For example, omnivorous basal bipedal sauropodomorphs such as *Saturnalia* and *Thecodontosaurus* are known to have large flocculi (Bronzati et al., 2017; Ballell et al., 2020) while the flocculi of herbivorous quadrupedal sauropods such as *Nigersaurus* or *Spinophosaurus* are not discernible (Serenio et al., 2007; Knoll et al., 2012). This relationship between the flocculus, locomotion, and diet fits well with the current idea that *V. mongoliensis* was a nimble predator that relied heavily on its agility while pursuing and attacking prey. Moreover, as enlarged floccular lobes have also been proposed to be indicative of strong vestibulo-ocular (VOR) and vestibulocollic (VCR) reflexes (Hopson, 1977; Witmer and Ridgely, 2009), it can be reasoned that *V. mongoliensis* was able to track moving objects easily. With that being said, because the optic lobes were not preserved it is impossible to say at this point to what degree IGM 100/976 relied on sight rather than other senses. Based on the enlarged floccular lobes, elongated semicircular canals, and large orbit size of the species, it can be assumed that the visual acuity and field of view of *V. mongoliensis* was high (Stevens, 2006; Schmitz and Motani, 2011; Torres and Clarke, 2018). This heightened optical sensitivity is not surprising considering the hypothesized predatory lifestyle of *V. mongoliensis*. When combined with its large flocculi and potentially sensitive VOR and VCR, it is likely that *V. mongoliensis* was easily able to track and pursue its prey smoothly based on its sensory neuroanatomy and stereoscopic vision (as determined from the position of the orbits).

In life, the endosseous cochlear duct of *V. mongoliensis* would have housed the basilar papilla—the auditory organ of tetrapods (Gleich et al., 2005; Walsh et al., 2009). As the length of the cochlear duct has been interpreted as a rough measurement of the basilar papilla, the length of the duct can be used as an estimator of hearing frequencies in non-avian dinosaurs (Witmer and Ridgely, 2009; Lautenschlager et al., 2012). Moreover, the relationship between the length of the cochlear duct and the basisphenoid has also been shown to correlate with hearing frequencies in modern archosaurs (Walsh et al., 2009), thus providing a way to calculate mean and high frequencies of non-avian dinosaurs. A recent study using extant turkeys demonstrated that a shape analysis of a single endosseous labyrinth can be used to represent an entire population (Cerio and Witmer, 2019); I therefore suggest that the hearing frequencies calculated in this study can be used as proxies for high and average hearing frequencies for *V. mongoliensis*. By measuring and logarithmically transforming the ratio between the cochlear duct length and the total length of the basisphenoid, a mean hearing range (2,368 Hz) and high-frequency hearing limit (3,965 Hz) was calculated for IGM 100/976—a range that is comparable to birds such as the common

raven (*Corvus corax*) and the African penguin (*Spheniscus demersus*) (Walsh et al., 2009). Unsurprisingly, the scaled anteroposterior width and length of the cochlear duct were much more similar to birds—specifically neognaths such as budgerigars (*Melopsittacus undulatus*), storks (*Ciconia ciconia*), and mute swans (*Cygnus olor*)—than to more basal archosaurs and other reptiles (Figure 2.3). Frequencies for labelled taxa are recorded in Table S2.

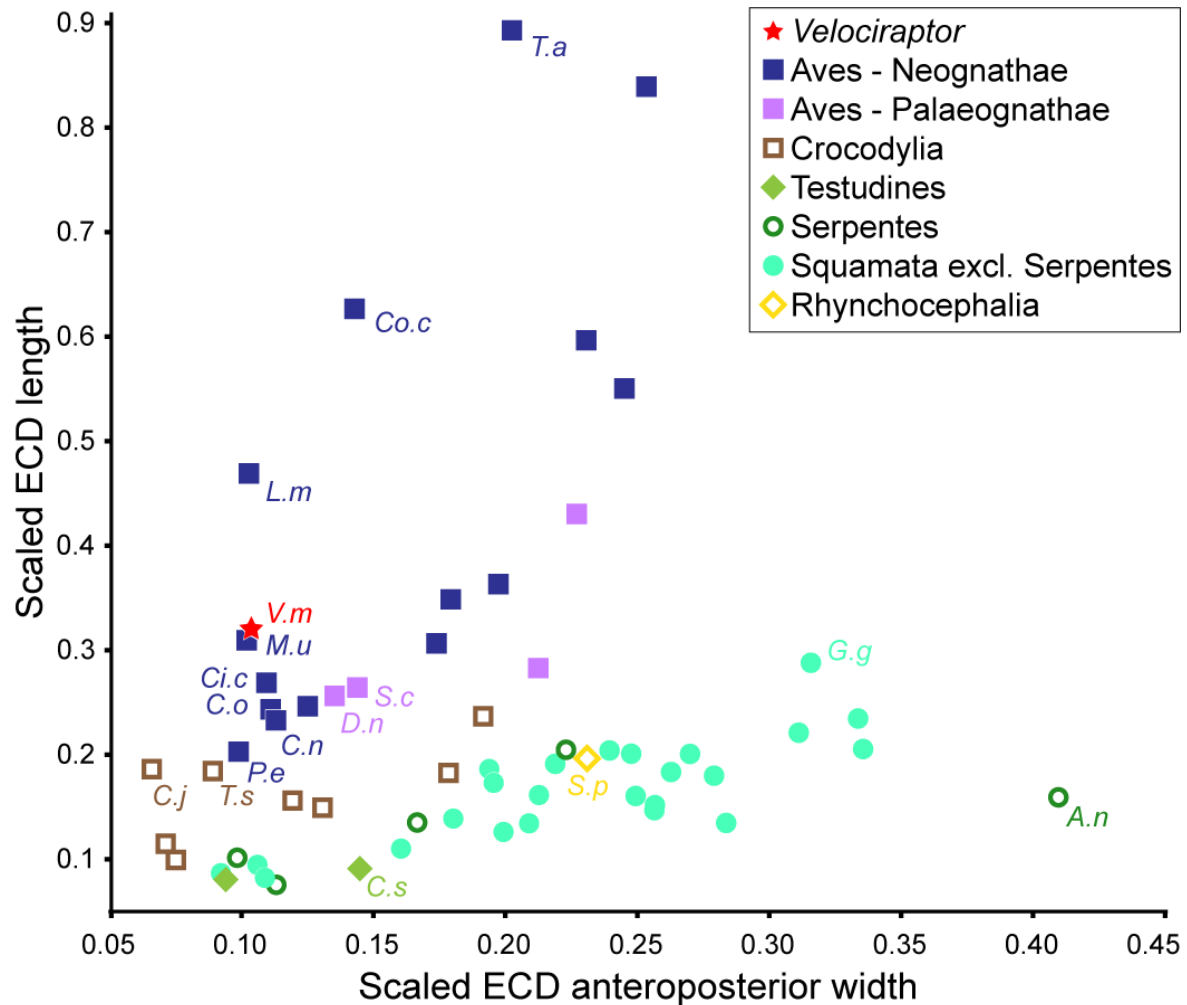


Figure 2.3 – Scaled endosseous cochlear duct (ECD) length against scaled ECD anteroposterior width, with some taxa highlighted. *Velociraptor mongoliensis* grouped more closely with birds rather than with Crocodyliformes and non-archosaurs. The scaled measurements of IGM 100/976 most closely resembled the upper range of vocal/social neognath birds. A.n, *Ahaetulla nasuta*; C.j, *Crocodylus johnstoni*; C.n, *Ciconia nigra*; C.o, *Cygnus olor*; C.s, *Chelydra serpentina*; C.i.c, *Ciconia ciconia*; Co.c, *Corvus corax*; D.n, *Dromaius novaehollandiae*; G.g, *Gymnodactylus geckoides*; L.m, *Luscinia megarhynchos*; M.u, *Melopsittacus undulatus*; P.e, *Psittacus erithacus*; S.c, *Struthio camelus*; S.p, *Sphenodon punctatus*; T.a, *Tyto alba*; T.s, *Tomistoma schlegelii*; V.m, *Velociraptor mongoliensis*. Modified from Walsh et al. (2009)

Our results indicate that *V. mongoliensis* could hear, hunt, and perhaps vocalize most efficiently in the range of 2,400 Hz. When compared with other maniraptorans for which data are available, the mean hearing frequency of *V. mongoliensis* is high. For instance, the mean and high hearing frequencies estimated for the basally diverging therizinosaur *Falcarius utahensis* are 1,630 Hz and 4,000 Hz, respectively (Lautenschlager

et al., 2012). Similarly, the frequency range of the more derived therizinosaurid *Erlikosaurus andrewsi* has a high range between 1,600 and 4,000 Hz (Lautenschlager et al., 2012). Although the mean frequency range of *V. mongoliensis* is notably higher than that of therizinosaurs, the high-frequency values are roughly the same.

The elongate nature of the cochlear duct supports the hypothesis that *V. mongoliensis* was capable of detecting a wide range of sounds, indicating that hearing was likely an important sensory system in this taxon (Manley, 1990; Walsh et al., 2009; Witmer and Ridgely, 2009; Brusatte et al., 2016; Carabajal et al., 2016). In fact, IGM 100/976 plots closest to the socially vocal learner *Melopsittacus undulatus* (budgerigar), making it feasible that *V. mongoliensis* utilized hearing in social interactions as well as active predation (Figure 2.3).

2.6.2 The Trophic Ecology of *Velociraptor*

Dinosaur feeding styles, such as predation vs. scavenging, have been a topic of popular interest in the past but remain difficult to diagnose in the fossil record (Holtz Jr., 2008). Our current understanding of the trophic ecology of *V. mongoliensis* is provided by several sources. The most famous of these, the ‘fighting dinosaurs’ (IGM 100/25) of Mongolia, preserves what has been interpreted by some palaeontologists as a predation attempt of a *Velociraptor* on a *Protoceratops* (Carpenter, 1998). However, further evidence has emerged in recent years suggesting that *V. mongoliensis* was not an obligate predator. This includes *Velociraptor* tooth marks on bones, which have been interpreted as late stage scavenging, and the preserved gut contents of a subadult individual (Hone et al., 2010, 2012). Each of these specimens indicate that scavenging was a part of the trophic ecology of *V. mongoliensis*. The neuroanatomical results described in this study help flesh out the degree to which scavenging contributed to the diet of *V. mongoliensis*.

Our current understanding of the neuroanatomy of *V. mongoliensis* suggests that predation likely made up a large part of its diet. As with therizinosaurs and oviraptorosaurs, IGM 100/976 possesses relatively enlarged flocculi (Figure 2.1; Lautenschlager et al., 2012; Balanoff et al., 2018). However, the flocculi of IGM 100/976 surpass those of observed therizinosaurs and almost completely fill the interior space between the semicircular canals. Enlarged flocculi have been used to predict prey tracking capabilities and may imply that the species had an acute vestibulo-ocular reflex (Walsh et al., 2013). This evidence in conjunction with the wide field of binocular vision, extended hearing range (as determined

from this study), and skeletal morphology indicates that rather than being equally or more reliant on scavenging, *V. mongoliensis* was well-equipped to be an active predator.

The fossil record, however, indicates that scavenging was at least a small part of the diet in *V. mongoliensis* (Hone et al., 2010, 2012). Opportunistic scavenging is supported by gut contents recovered from MPC-D100/54 that include a 75-mm-long bone of an unidentified pterosaur. Whether this represents an act of osteophagy or scavenging due to an injury or its small size, it is probable that the pterosaur was dead prior to being eaten, given its incomplete nature. In the case of IVPP V16137, a probable *Protoceratops*, multiple bone fragments including a dentary, exhibited bite marks characteristic of velociraptorine dromaeosaurs. Velociraptorine teeth (IVPP V16138) were also found in association with IVPP V16137, further indicating that a velociraptorine dromaeosaur was feeding on the carcass of IVPP V16137. Some of these tooth drag marks found along the anterior portion of the dentary suggest that this was an instance of late-stage scavenging by *V. mongoliensis* due to the lack of significant muscle mass located along a dentary during life. While this evidence for scavenging can be interpreted as being somewhat circumstantial, I accept that the specimens nevertheless show enough evidence to be considered acts of scavenging rather than active predation based on the conclusions of previous studies (Hone et al., 2010, 2012).

This type of flexible hunting strategy is not surprising given that modern predator diets are a spectrum rather than an 'either/or' scenario in which seasonality, fitness, and other ecological constraints are the primary drivers (Mattisson et al., 2016). Here, I propose the fossil evidence indicates a scavenging behaviour that complimented an active predatory lifestyle—similar to what can be found in the modern biota. Modern predators, including predatory birds such as *Aquila chrysaetos*, often resort to changes in hunting behaviour, or even scavenging, when prolonged weather patterns, injury or ontogenetic stage forces them to find alternative food sources (Tjernberg, 1981; Marchetti and Price, 1989; Wilmers et al., 2003; Mattisson et al., 2016). It follows that the neuroanatomy of *V. mongoliensis* suggests a behaviour that is adapted for active predation (Carpenter, 1998); however, young or injured individuals and those experiencing dietary constraints brought on by local climate would have actively sought out carcasses for an easy meal.

2.7 Conclusions

In this chapter, a partial endocast and both endosseous labyrinths of *Velociraptor mongoliensis*, IGM 100/976, were reconstructed in order to describe the anatomy of the midbrain, hindbrain, and inner ears of the species; better understand how the species interpreted its surroundings; and clarify its trophic ecology.

Neuroanatomically, the most notable features are the enlarged floccular lobes that project laterally from the cerebellum and pass almost completely through the vestibular portion of the endosseous labyrinths. The cochlear ducts of the endosseous labyrinths are long, consisting of almost half of the total height of the endosseous labyrinths. Together, the flocculi and cochlear ducts give supporting neurological evidence for an active predacious lifestyle for *V. mongoliensis*. When neuroanatomical data is compared with fossils that suggest scavenging was present in *V. mongoliensis*' trophic ecology, a clearer picture of dietary patterns becomes clear. Despite being neurologically primed for predacious carnivory, *V. mongoliensis* would have resorted to scavenging should local climate, age of the individual, or injury prevented an individual from hunting.

This chapter is indicative of the limits present in the study of endocasts. For example, supporting or refuting the gregarious nature – the social or hierarchical behaviour of an animal – of dromaeosaurs is impossible from the endocast alone. Social behaviour is further hindered by a lack of evidence for social or pack hunting among *V. mongoliensis* (e.g. large amounts of tooth shedding at a kill site as interpreted for *Deinonychus antirrhopus*). An enlarged endocast with a large cerebrum do indicate that social intraspecies interactions were possible for the clade; however, this same brain set up is true for other maniraptorans and some large-bodied theropods for which no fossil evidence of gregariousness has ever been provided. Recent research has provided evidence for a more solitary dromaeosaur lifestyle but not solid evidence for pack behaviour has been found for any dromaeosaurid.

Chapter 3: Ontogenetic endocranial shape change in alligators and ostriches and implications for the development of the non-avian dinosaur endocranium (published in *The Anatomical Record*, corresponding author)

3.1. Collaborative Statement

This project was initially a master's project for Krishna Hu – which I co-advised and designed. The chapter presented here is based on the resulting publication which was a collaboration between Krishna Hu, Cheyenne Romick (Ohio University; provided data), David Dufeu (Marian University; provided data), and Lawrence Witmer (Ohio University; shared data and gave feedback on manuscript), Thomas Stubbs (University of Bristol; assisted with RStudio coding), Emily Rayfield (University of Bristol; reviewed manuscript drafts and provided feedback), and Michael Benton (University of Bristol; reviewed manuscript drafts and provided feedback). I did most of the work to make the project publishable after the completion of the MSc project. I rewrote the manuscript, redrafted some of the images in RStudio, made corrections to the comparative anatomy, and edited the ensuing drafts. In converting this to a publishable paper – Hu et al. (2020) – and thesis chapter, I completed 80% of the work.

3.2 Abstract

Birds and crocodiles show radically different patterns of brain development, and it is of interest to compare these to determine the pattern of brain growth expected in dinosaurs. Here, I provide atlases of 3D brain (endocast) reconstructions for *Alligator mississippiensis* (alligator) and *Struthio camelus* (ostrich) through ontogeny, prepared as digital restorations from CT scans of stained head and dry skull specimens. Our morphometric analysis confirms that ostrich brains do not change significantly in shape during postnatal growth, whereas alligator brains unfold from a cramped bird-like shape in the hatchling to an elongate, straight structure in the adult. I confirm that birds exhibit paedomorphic dinosaur endocranial traits such as retaining an enlarged and compact brain shape in the adult, whereas crocodiles show peramorphic traits where the brain elongates with growth as the skull elongates. These atlases of ontogenetic stages of modern bird and crocodilian endocrania provide a basis for comparison of non-avian dinosaur endocasts and consideration of the divergence of the “avian” and “crocodilian” modes of brain development and heterochronic change on phylogenies.

3.3 Introduction

Ever since the American dinosaur discovery rush of the late 19th century, paleontologists have reported dinosaurian endocasts (Marsh, 1880, 1884b, 1890, 1896). However, it took some time before paleobiologists began to make inferences about the paleoneurology of non-avian dinosaurs and other extinct archosaurs (Edinger, 1951; Jerison, 1973; Buchholtz and Seyfarth, 1999). Archosauria is a clade whose living members are crocodilians and birds, together with the extinct dinosaurs and pterosaurs. Endocasts can provide evidence of development, paleoecology, and paleobiology of extinct taxa (Edinger, 1951; Jerison, 1973; Rogers, 1999; Lautenschlager and Hübner, 2013; Balanoff et al., 2014). For example, inferred structures of the brains of pterosaurs and extinct birds have been used to explore the link between flight and sensory processing (Witmer et al., 2003; Ashwell and Scofield, 2008; Picasso et al., 2009). There is growing interest in understanding what changes in endocranial shape mean for paleobiology, including sensory neurology (Lautenschlager et al., 2012). Dinosaur endocasts are commonly compared to the brains of crocodilians and birds (Witmer and Ridgely, 2008b; Evans et al., 2009; Carabajal, 2012; Balanoff et al., 2014; Nomura and Izawa, 2017), but few publications describe such comparisons through ontogeny, and so cannot offer insights into heterochronic shifts in endocranial development within Archosauria.

Macroevolutionary questions around the archosaurian skull and brain have been brought into focus by the hypothesis that birds retain an apparently juvenile skull and brain shape into adulthood, with large eyes, a short snout, and large brain (Bhullar et al., 2012; Wang et al., 2017). Crocodilians, on the other hand, show elongation of the snout and brain throughout development. If both living lineages of archosaurs show such differences in cranial development, how does the endocranial growth in non-avian dinosaurs? In particular, when did dinosaurs switch from a “reptilian” to an “avian” developmental pattern of skull and brain, and did this happen as a single shift, or in a more complex manner? Indeed, is the alligator developmental pattern akin to that of the ancestral archosaur, or has it too diverged from that ancestor?

Our aim is to provide some comparative materials from modern taxa that can form the basis of an understanding of how the brains of modern crocodilians and birds develop. With that information, linking brain proportions and details of anatomy at different stages of ontogenetic growth in crocodilians and birds, the two major clades that bracket non-avian dinosaurs phylogenetically, paleontologists can make comparisons to their fossil materials and work out whether or not all dinosaurs show the same developmental and heterochronic aspects of brain size, shape and anatomy, whether they follow the “crocodilian” pattern of development, the “avian” pattern of development, or something else altogether. Since alligators and ostriches

are some of the most frequently used and most well understood anatomical analogues, I compare the endocrania of both taxa to the other to find common trends in modern archosaurian endocranial morphology. Here, I compare shape, flexure, and anatomical differences between ontogenetic series of *Alligator mississippiensis* and *Struthio camelus* endocrania.

3.4 Materials and Methods

3.4.1 Describing fossil brains: terminology

In neuroanatomy, the cranial endocast refers to the internal cast of the braincase that outlines the general shape of a brain, and in particular the dural envelope (Dufeu et al., 2012; Lautenschlager and Hübner, 2013). Since endocranial tissue is not typically preserved in the fossil record, the shape and surface anatomy of the endocast is vital evidence for studying the brains of extinct animals (Rogers, 1999; Evans et al., 2009). Here, I use endocasts of alligator and ostrich to permit direct comparison with endocasts from extinct relatives.

It is important to note that endocasts are the sum total of all soft tissue inside the braincase and thus do not often reflect the actual size of the brain itself. Adult crocodilians, for instance, have brains that occupy 40% or less of the endocranial cavity (Hopson, 1979; Jirak and Janacek, 2017a), whereas in birds most of the endocranial cavity is filled with brain tissue (Iwaniuk and Nelson, 2002; Watanabe et al., 2019). However, the morphology of endocasts shows that they generally retain the overall shape of the brains they house, regardless of differences in size between the two (Watanabe et al., 2019). Nonetheless, the fact that the size, shape, and volume of the braincase are not equivalent is important in reconstructing fossil brains, and in making any estimates concerning brain form or function of extinct animals (Corfield et al., 2008; Lautenschlager and Hübner, 2013).

Here, I use the terms “brain” and “endocast” but prefer the latter as I am actually describing the internal space surrounded by braincase bones rather than the actual brain tissue. I use the term “endocast” explicitly for fossil examples and for cases where I mean the space inside the endocranium, and “brain” to refer to the contained organ. Similarly, all fossae or foramina that were partially or completely filled with brain tissue in life are referred to by their anatomical name (e.g., the pituitary fossa is called the pituitary).

3.4.2 Sample: Source and age composition

I selected alligators and ostriches as representatives of crocodilians and birds respectively because specimens were available and easily obtainable, largely through wildlife farms.

Further, the specimens are large enough for handling and scanning, and they are much-studied taxa that have long been regarded as exemplar taxa.

Thirteen *Alligator mississippiensis* and thirteen *Struthio camelus* specimens were selected to cover the total posthatchling ontogenetic series for each taxon. Our sample of thirteen scanned specimens per taxon is small, with single specimens representing well-spaced growth stages of each taxon, but the trends are clear and match qualitative and quantitative comparisons between groups.

Alligator data (n = 13) was sourced from Dufeu et al. (2012) and (Dufeu and Witmer (2015) (see Table 3.1 for a full specimen list). Ontogenetic stages for the alligator span from approximately 1-month posthatching to a large adult over 5-years-old. All alligator specimens were provided as cadaveric salvage specimens by the Rockefeller Wildlife Refuge (Louisiana Department of Wildlife and Fisheries, Grand Chenier, Louisiana, USA. Seven fully segmented specimens were used in a 3D morphometric analysis while all 13 were used to compare anatomy between specimens of different ages.

Table 3.1 – Master list of specimens used for this study and the relevant scan parameters. Specimens noted with superscript were either specifically made for this project¹ or used for the PCA². All were used for comparative anatomy

Taxon	Specimen #	Age	Energy (kV)	Resolution (µm)	Amps (µA)
<i>Alligator mississippiensis</i>	OUGC 10117	<1 month	80	45	450
<i>Alligator mississippiensis</i>	OUGC 10606 ²	~ 1 month	80	45	450
<i>Alligator mississippiensis</i>	OUGC 10390	10 months	60	92	450
<i>Alligator mississippiensis</i>	OUGC 10391	10 months	60	92	450
<i>Alligator mississippiensis</i>	OUGC 10385 ²	11 months	60	92	450
<i>Alligator mississippiensis</i>	OUGC 10386	11 months	60	92	450
<i>Alligator mississippiensis</i>	OUGC 10387 ²	11 months	60	92	450
<i>Alligator mississippiensis</i>	OUGC 10388	11 months	60	92	450
<i>Alligator mississippiensis</i>	OUGC 10389 ²	1 year	60	92	450
<i>Alligator mississippiensis</i>	OUGC 10629	2-3 years	120	625	200-300
<i>Alligator mississippiensis</i>	OUGC 9761 ²	~4 years	120	625	200-300
<i>Alligator mississippiensis</i>	USNM 211233 ²	~5 years	120	625	200-300
<i>Alligator mississippiensis</i>	USNM 211232 ²	>5 years	120	625	200-300
<i>Struthio camelus</i>	2-weeks-old ^{1,2}	2 weeks	195	36	172
<i>Struthio camelus</i>	OUGC 10463	~2 weeks	80	45	450
<i>Struthio camelus</i>	4-weeks-old ^{1,2}	4 weeks	180	41	235
<i>Struthio camelus</i>	OUGC 10521	~1 month	80	92	450
<i>Struthio camelus</i>	OUGC 10518	~1 month	80	92	450
<i>Struthio camelus</i>	OUGC 10519	~2 months	80	90	450
<i>Struthio camelus</i>	12-weeks-old ^{1,2}	4 months	180	46	235
<i>Struthio camelus</i>	OUGC10517	~4 months	80	92	450
<i>Struthio camelus</i>	5-months-old ^{1,2}	5 months	230	52	220
<i>Struthio camelus</i>	OUGC 10630	~1 year	80	90	450
<i>Struthio camelus</i>	OUGC 10661	~1 year	80	300	450
<i>Struthio camelus</i>	OUGC 10491	~1 year	120-140	625	200-300
<i>Struthio camelus</i>	36-months-old ^{1,2}	3 years	237	86	350

The ostrich specimens ($n = 13$) were obtained from multiple sources. Seven segmented endocasts were from Romick (2013), one from Witmer and Ridgely (2008), and five were digitally reconstructed specifically for this project (see Table 3.1 for a full specimen list). Specimens scanned for this project were ethically purchased from a Bulgarian farm as husbandry by-products. Like the alligators, the ostriches covered the entire ontogenetic series— from a 2-weeks posthatching specimen to a large 3-yearold adult. Similarly, seven of the individuals were used for a morphometric analysis and all were used to compare anatomy between different ontogenetic stages.

Both growth series span from hatchling to adult, but I cannot match the particular stages as developmentally equivalent, as I had to use specimens that were available and, importantly, that had age information (many museum specimens do not). Bearing in mind that ostriches reach skeletal maturity in about 3 years and sexual maturity in 4–5 years (Cooper, 2005) and alligators reach sexual maturity in 11–15 years for females and 8–12 years for males, and skeletal maturity at 25–35 years (Wilkinson et al., 2016), calendar years cannot be used as markers of equivalent ontogenetic stages. With a hatchling at one end and an adult at the other, I can simply present the known ages of my individual specimens and not make any claim for equivalence between the examples of each species.

3.4.3 3D reconstruction

Alligators imaged in this study were scanned at the Ohio University MicroCT Scanning facility (see Table 1 for scan parameters). All of the alligator endocasts were premade endocasts so no further scanning or segmentation was needed for the specimens. The alligator dataset was incorporated in the present study as prerendered .obj files.

Ostriches from Romick (2013) were scanned at the Ohio University MicroCT Scanning facility. The endocast from Witmer and Ridgely (2008), OUVC 10491, was scanned at O'Bleness Memorial Hospital. The ostrich skulls scanned for this project were done so with the Nikon XT H 225ST CT scanner in the Bristol Palaeobiology Research Group at the University of Bristol. Each scan set was filtered with a 0.5 mm copper filter (a 0.25 mm tin filter was used with the 3-year-old ostrich), and 3,141 projections were created with 2x frame averaging (see Table 1 for all ostrich scan parameters). Once the CT images had been saved as TIFF image stacks, they were transferred into Avizo Lite (v.9.7.0) for 3D reconstruction. The CT slices were interpolated at every five slices using Avizo's segmentation editor.

The endocast reconstructions were saved as .obj files and converted to .ply files to ensure compatibility with RStudio.

3.4.4 Measurements and Morphometrics

I measured the cephalic and pontine flexure angles of each endocast in a 2D plane on the left lateral images, using ImageJ v1.46 (Figure 3.1A, B). Definitions of the angles from Hopson (1979) and Lautenschlager and Hübner (2013, p. 2045): “the pontine flexure was measured as the angle between the long (rostrocaudal) axis of the medulla oblongata and the oblique axis of the midbrain indicated by the caudal outline of the cerebellum; the cephalic flexure was measured as the angle between the long (rostrocaudal) axis through the cerebral hemispheres and the oblique axis of the midbrain” (as illustrated by Lautenschlager and Hübner (2013), Figure 3.1).

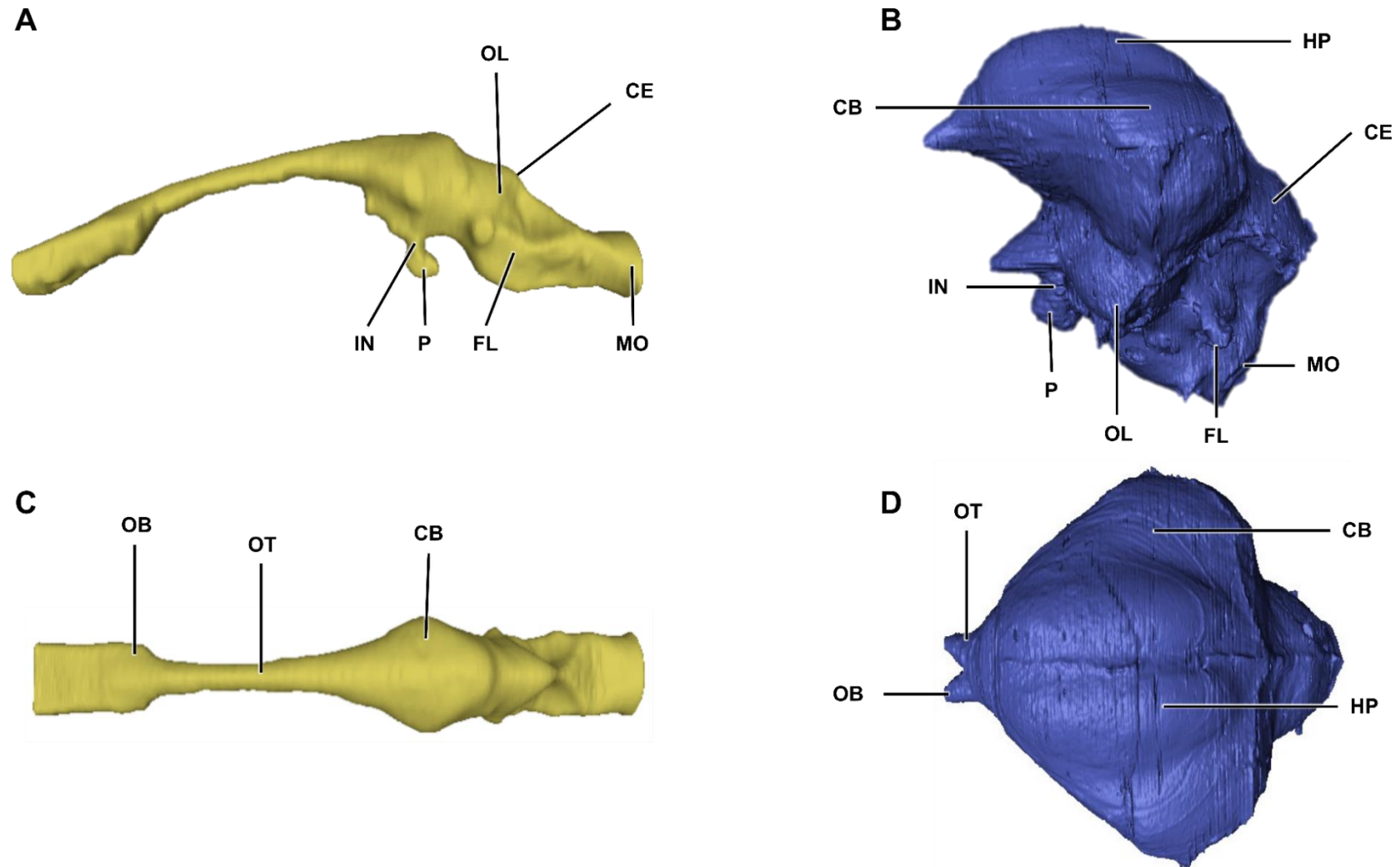


Figure 3.1 – Left lateral and dorsal views of an *Alligator mississippiensis* (A, C) and *Struthio camelus* (B, D) endocast. Relevant anatomy has been labelled on each specimen to demonstrate key differences between each endocast. Note the Wulst, the dorsal expansion of the ostrich forebrain that is unique to avians. P, pituitary body/gland; W, Wulst; CE, cerebellum; CB, cerebral hemispheres/cerebrum; IN, infundibulum; OB, olfactory bulb; OT, olfactory tract. Endocasts are not to scale

I also carried out a 3D geometric analysis of each endocast model using 17 landmarks at specific points of anatomy along each endocast and 57 semilandmarks to outline endocranial morphology along the sagittal plane (Figure 3.2). The semilandmarks were slid during alignment. The 17 landmark sites are, in sequence, olfactory tract (right lateral), olfactory bulb (right lateral, center, left lateral), olfactory tract (left lateral), cerebral hemisphere (lower right lateral, upper right lateral, top, upper left lateral, lower left lateral), pituitary (ventral), cerebral hemisphere (caudal), cerebellum (caudal), flocculus (left, right), medulla oblongata (dorsal, ventral). The exact locations of these 17 landmarks in multiple views of the endocasts of alligator and ostrich are shown in Figure 3.2.

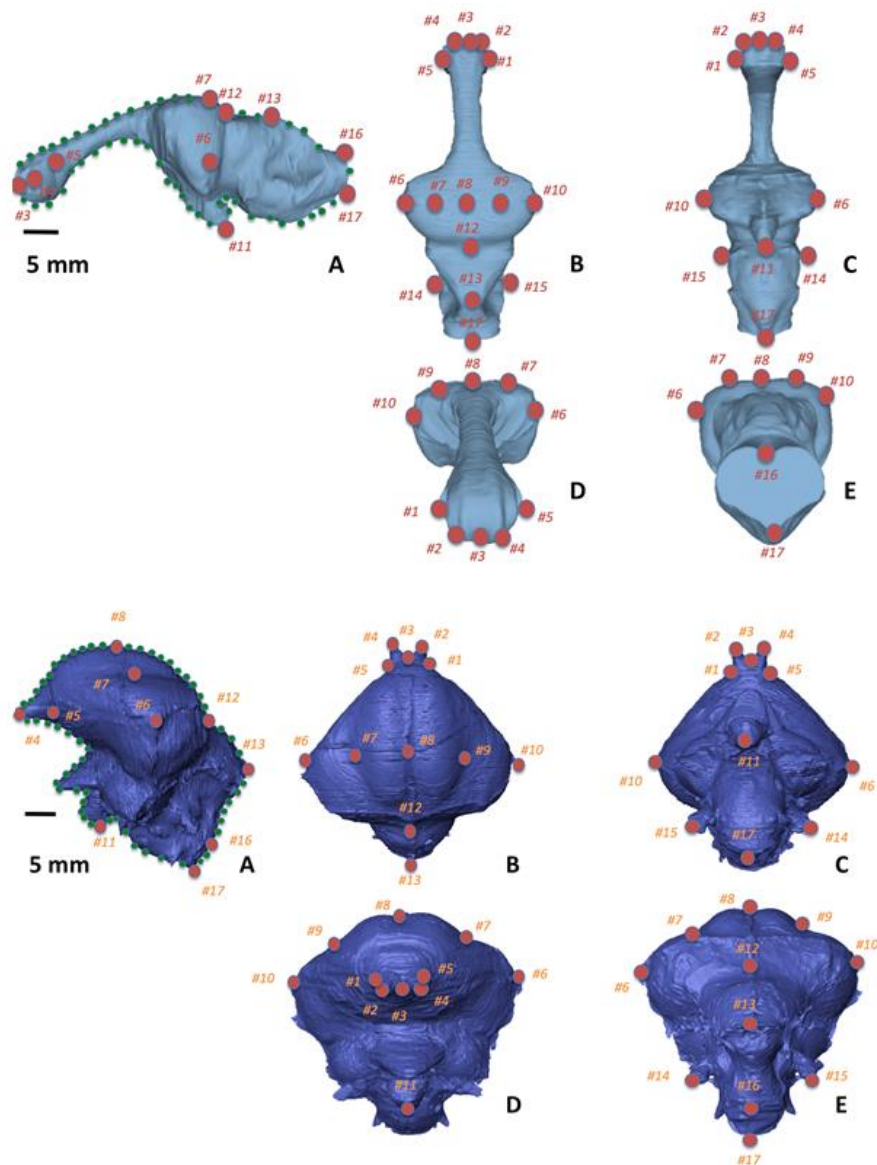


Figure 3.2 – Landmarks used for specimens in this chapter. Numbered natural landmarks are orange; semilandmarks are green.

Natural landmarks were selected based on anatomical points shared between all specimens and both taxa (Figure 3.2; orange points). Semilandmarks were placed on the sagittal plane along the midline of the endocasts to better understand elongation trends at the point of bilateral symmetry (Figure 3.2; green points). By using natural landmarks and semilandmarks, anatomy and symmetry can be used to get the highest degree of shape accuracy between specimens and taxa.

To get a sense of how portions of the endocast were developing in relation to each other, the widths of the olfactory bulbs, cerebral hemispheres, and cerebellum were taken at the widest points of each lobe or set of lobes. Each measurement was taken in dorsal view in order to capture the widest aspect of each measurement, using ImageJ. The measurement values were either logarithmically normalized or a ratio was made between the olfactory bulbs or cerebellum and the cerebral hemispheres to prevent skewed graphs due to large size differences between ostrich and alligator endocasts. These new values were then plotted to see how endocranial widths of neurosensory portions of the endocast developed in relation to shape and age.

Landmarks were added digitally to the specimens using RStudio with the package “geomorph” (Adams and Otárola-Castillo, 2013). Then, using the same package, a Generalized Procrustes Analysis was carried out to eliminate the effects of size, orientation, and translation of the endocasts. I then conducted a principal component analysis (PCA) using the geomorph and plotted morphospaces based on principal component axes 1 and 2.

3.5 Results

3.5.1 Surface anatomy of the adult alligator endocast

The general structure of an alligator endocast is of the typical crocodilian form (Figure 3.1A, C) in that it is long, narrow, and linearly organized in lateral view (Rogers, 1999), a plesiomorphic trait shared also with fish, amphibians and other basal amniotes (Rogers, 1998). Here, the olfactory apparatus comprises two large, elliptical bulbs and a long, thin tract (Figure 3.1A, C). The olfactory apparatus is noticeably longer than and almost as wide as the relatively smaller cerebrum caudally. The cerebral hemispheres are the widest portion of the endocast, though they are only 10% wider than the olfactory bulb. Without the development of the Wulst seen in the ostrich, the dorsal peaks of the cerebral hemispheres in the alligator are not as prominent.

Most of the midbrain of *A. mississippiensis* appears to be modest in size when compared to the forebrain and hindbrain. The optic lobes are arranged caudally to the cerebral hemispheres and rostrally to the cerebellum but become less prominent throughout ontogeny and are not as clearly visible in alligators as they are in ostriches (Figure 3.1A, B). The pituitary is the only part of the forebrain that protrudes ventrally as a distinctive feature within the dural envelope (Figure 3.1B).

Along the hindbrain, the cerebellum is situated caudally to the cerebral hemispheres as a relatively smaller region (Figure 3.1A). The flocculi are not present along the lateral surface of the endocast due to their small size. The medulla oblongata is the caudalmost portion of the endocast that has a roughly circular cross-section and extends ventrally and caudally to the flocculi (Figure 3.1A, C).

The endocast of the juvenile alligator approximates the shape of the brain itself, but only a small portion of the endocranial volume is taken up by the brain in an adult alligator, with estimates that the crocodilian brain takes up ~30–40% of the space (Hopson, 1977; Jirak and Janacek, 2017a) or 52–99% of the space (Watanabe et al., 2019) depending on the age of the specimen.

3.5.2 Surface anatomy of the adult ostrich brain

The adult ostrich endocranium (Figure 3.1B, D) shows a compact S-shaped curve in which the forebrain is situated rostradorsally to the rest of the brain regions and the hindbrain is positioned along the caudoventral axis - a typical structure for birds (Kawabe et al., 2013). The olfactory apparatus comprises two small elliptical bulbs, which are complemented by an equally short tract (Figure 3.1D). The small size of olfactory region contrasts with the much larger, rounded cerebral hemispheres just caudal to the olfactory apparatus. As in alligators, the cerebral hemispheres of the ostrich are both the widest aspect of the endocast and the largest portion in dorsal view (Figure 3.1C, D).

The optic lobes are enlarged and tightly packed ventrally to the cerebral hemispheres (Figure 3.1B); this is another trait shared among most birds that reflects their increased reliance upon vision (Jones et al., 2007). Ventrally to the cerebral hemispheres, the pituitary gland is displaced rostroventrally as another small projection of the midbrain (Figure 3.1B).

The cerebellum is a large, rounded region of the brain that is situated between the medulla oblongata dorsally and the cerebral hemispheres caudally (Figure 3.1B). The flocculi project laterally from the cerebellum as small protrusions with elliptical cross-sections (Figure 3.1B). The medulla oblongata is relatively small compared to the rest of the endocast and forms a curve at the rostral section below the midbrain (Figure 3.1B).

The ostrich brain, as in most birds, occupies the majority of space within the braincase, with a brain-to-braincase volume that is negligibly different (Iwaniuk and Nelson, 2002; Watanabe et al., 2019). Therefore, the endocast provides a reasonable approximation for brain volume and size.

3.5.3 Comparative anatomy of adult alligator and ostrich endocasts

Adult alligators and ostriches show several fundamental differences in the overall shape and layout of their endocasts. The endocast of an adult alligator is rostrocaudally elongated while an ostrich brain is more rounded and condensed in shape (Figure 3.1B, D). This rounded avian shape arises from lower cephalic and pontine flexure angles, reflecting the fact that avian brains do not elongate rostrocaudally with development. The different ratios of dural volume to brain volume in alligators and ostriches not only affect our interpretations of actual brain volumes, but also the details of surface anatomy that may be observed. The greater ratio of neural tissue to dural volume in the ostrich means that the endocranial surface of an adult ostrich is more likely to show signs of vascular valliculae or suture patterns than an alligator.

Considering regional differences, the olfactory bulbs and tract are much larger and longer, respectively, in alligators than ostriches (Figure 3.1A, C). The cerebral hemispheres of the ostrich are more enlarged than in the alligator (Figure 3.1B, D). The expansion of the cerebral hemispheres and the development of a Wulst in birds expands the brain laterally and dorsally and makes for an enlarged forebrain in the ostrich ontogenetic series, traits that are absent in crocodilians. While there are some shape variations, the pituitary and infundibulum are similar in both taxa. The pituitary always extends ventrally from the infundibulum, and the infundibulum separates the pituitary from the main body of the forebrain (Figure 3.1A, C). The enlargement of the forebrain in the ostrich pushes the optic lobes from a dorsolateral position (Figure 3.1A, C), as seen in alligators and basal archosaurs, to a ventrolateral orientation (Figure 3.1B, D) along the midbrain. Hindbrain structures diverge in shape: the cerebellum forms a dorsal expansion that is rounded in the ostrich but more triangular in the alligator when viewed dorsally (Figure 3.1C, D); floccular casts extend mediolaterally from the cerebellum in the ostrich but are absent in alligators (Figure 3.1A–D); and the medulla oblongata is larger than the forebrain and midbrain in the alligator and extends further than in the ostrich (Figure 3.1A, B).

3.8 Cephalic and pontine flexure angles

Both the cephalic and pontine flexure points of the *Alligator mississippiensis* ontogenetic series show consistent linear expansion throughout development. Both angle measurements

begin below 90 and increase to beyond 120 (Table 3.2). By the time adulthood is reached, the cephalic and pontine flexures have increased by up to 51.9%. Increased flexure indicates that the elongation of the endocast is not only a lengthening of the endocranium but also an “unfolding” of the brain as the fore- and hindbrain change position in relation to the oblique axis of the brain itself.

Table 3.2 – Cephalic and pontine flexure angles measured from select ostrich and alligator endocasts

Specimen	Age	Cephalic Flexure	Pontine Flexure
<i>Alligator mississippiensis</i>	<1 month	80	45
<i>Alligator mississippiensis</i>	10 months	80	45
<i>Alligator mississippiensis</i>	1 year	60	92
<i>Alligator mississippiensis</i>	4 years	60	92
<i>Alligator mississippiensis</i>	>5 years	60	92
<i>Struthio camelus</i>	2 weeks	195	36
<i>Struthio camelus</i>	4 weeks	80	45
<i>Struthio camelus</i>	12 weeks	180	41
<i>Struthio camelus</i>	5 months	80	92
<i>Struthio camelus</i>	3 years	80	92

On the other hand, *Struthio camelus* exhibits a very conservative flexure change through its life. In our my study specimens I found a decrease in both cephalic and pontine flexures by a couple of degrees before a slight rise, thus returning the adult value to close to what was seen in the 2-week-old (Table 3.2). These unchanging brain flexure angles indicate that ostriches are morphologically paedomorphic, retaining juvenile endocranial shapes throughout their life.

3.6 Ontogenetic development of the alligator endocranium

3.6.1 Forebrain

When comparing the ontogenetic stages of *A. mississippiensis*, the greatest changes in the forebrain are rostrocaudal lengthening of the olfactory bulbs, tract, and cerebral hemispheres. In the neonate specimen (Figure 3.3A–E), the olfactory apparatus comprises elongated tracts and bulbs, though still relatively short and small compared to those of an adult alligator (Figure 3.7A). Both the olfactory tract and bulbs continue to increase in size and length throughout all life stages until they comprise approximately half the total endocranial length (Figures 3.3–3.7A, B). Also, as demonstrated in the 10-monthold specimen onwards (Figures 3.4–3.7A–D), the olfactory tract appears to shrink in width between the rostralmost portion of the cerebral hemispheres and the caudalmost portion of the olfactory bulbs.

The cerebrum in the neonate is clearly distinctive from the endocranial components caudal to it as the cerebrum shows a caudally expanded elliptic shape in lateral view. Dorsally, the cerebral hemispheres are the widest aspect of the endocast (Figure 3.3A). Between the 10-

month-old and yearling specimens (Figures 3.4A–D and 3.5A–D), the rostral portions of the cerebral hemispheres become pyriform as they lead to the narrow olfactory tract. Sagittally, the hemispheres in the first three life stages are taller than they are wide (Figures 3.3–3.5A–D) but become more equal in size later in life (Figures 3.6A–D and 3.7A–D).

While it is small and difficult to distinguish in the neonate (Figure 3.3A, C), the pituitary gland gradually becomes more demarcated from the rest of the ventral portions of the forebrain as the infundibulum narrows to form the pituitary's droplet shape. The pituitary body maintains the same position just rostral to the medulla oblongata throughout life (Figures 3.3–3.7A, C).

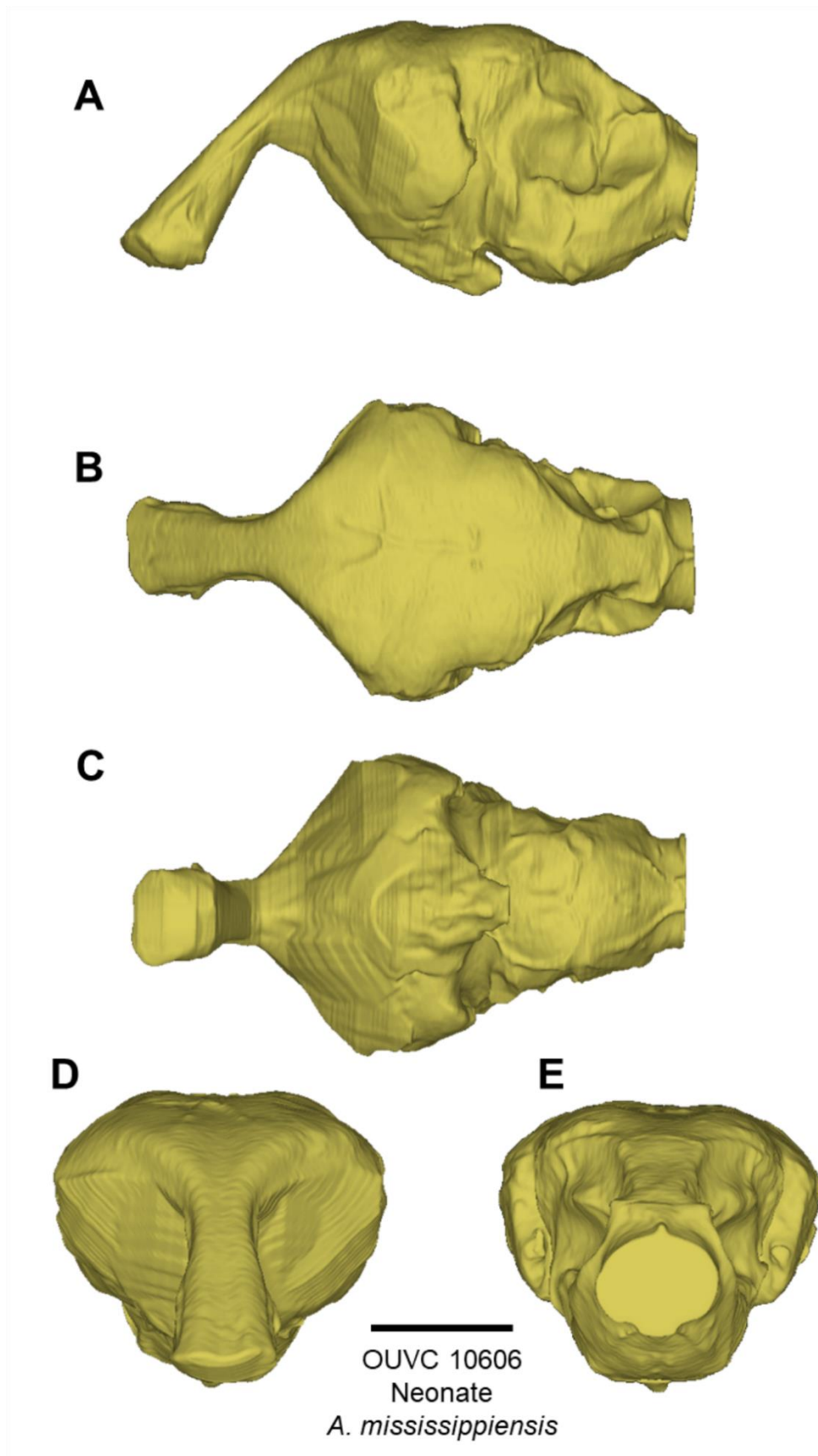


Figure 3.3 – A neonatal alligator endocast in (A) lateral, (B) dorsal, (C) ventral, (D) anterior, and (E) posterior views. Scale bar = 5 mm

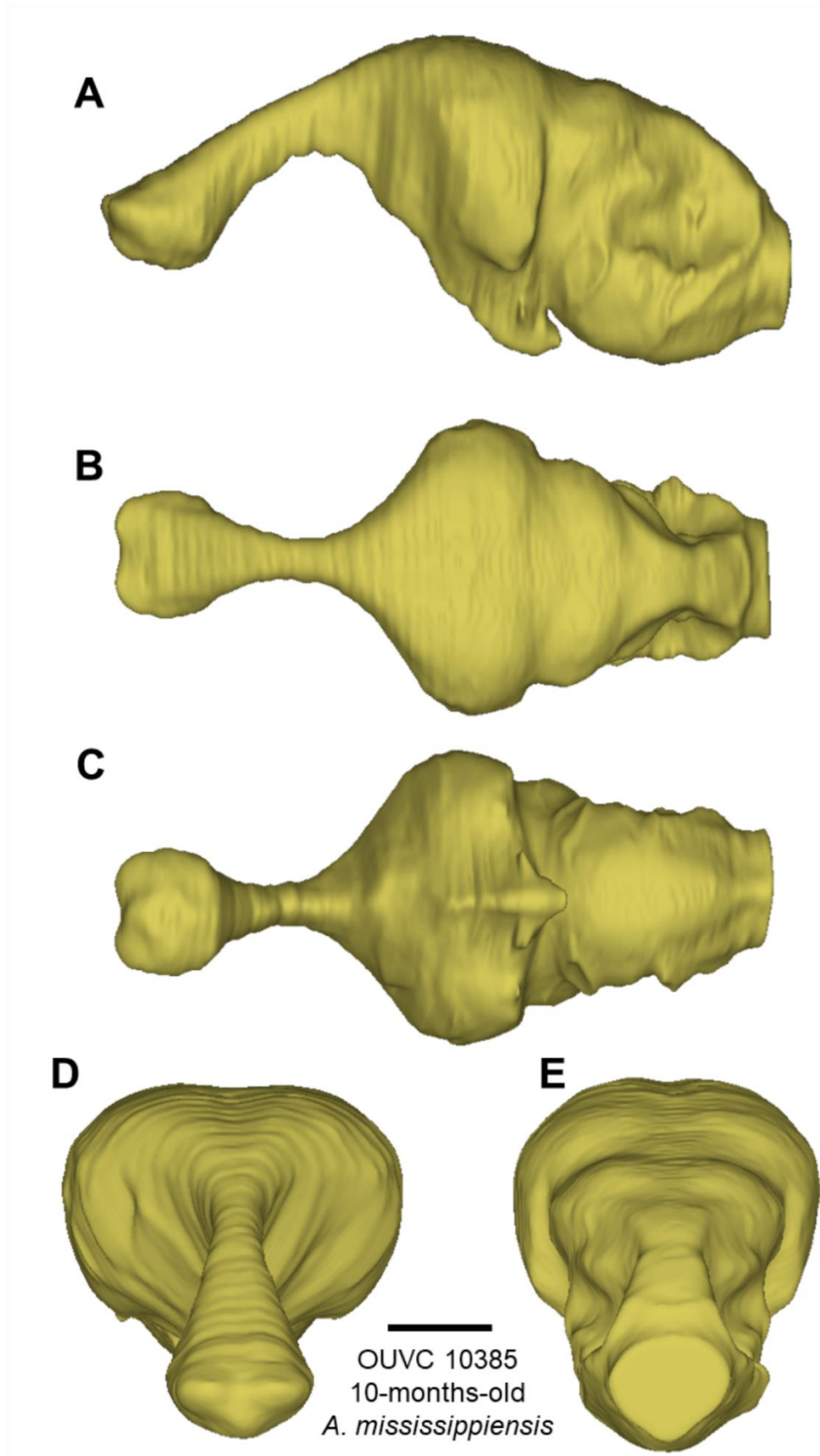


Figure 3.4 – A 10-month-old alligator endocast in (A) lateral, (B) dorsal, (C) ventral, (D) anterior, and (E) posterior views. Scale bar = 5 mm

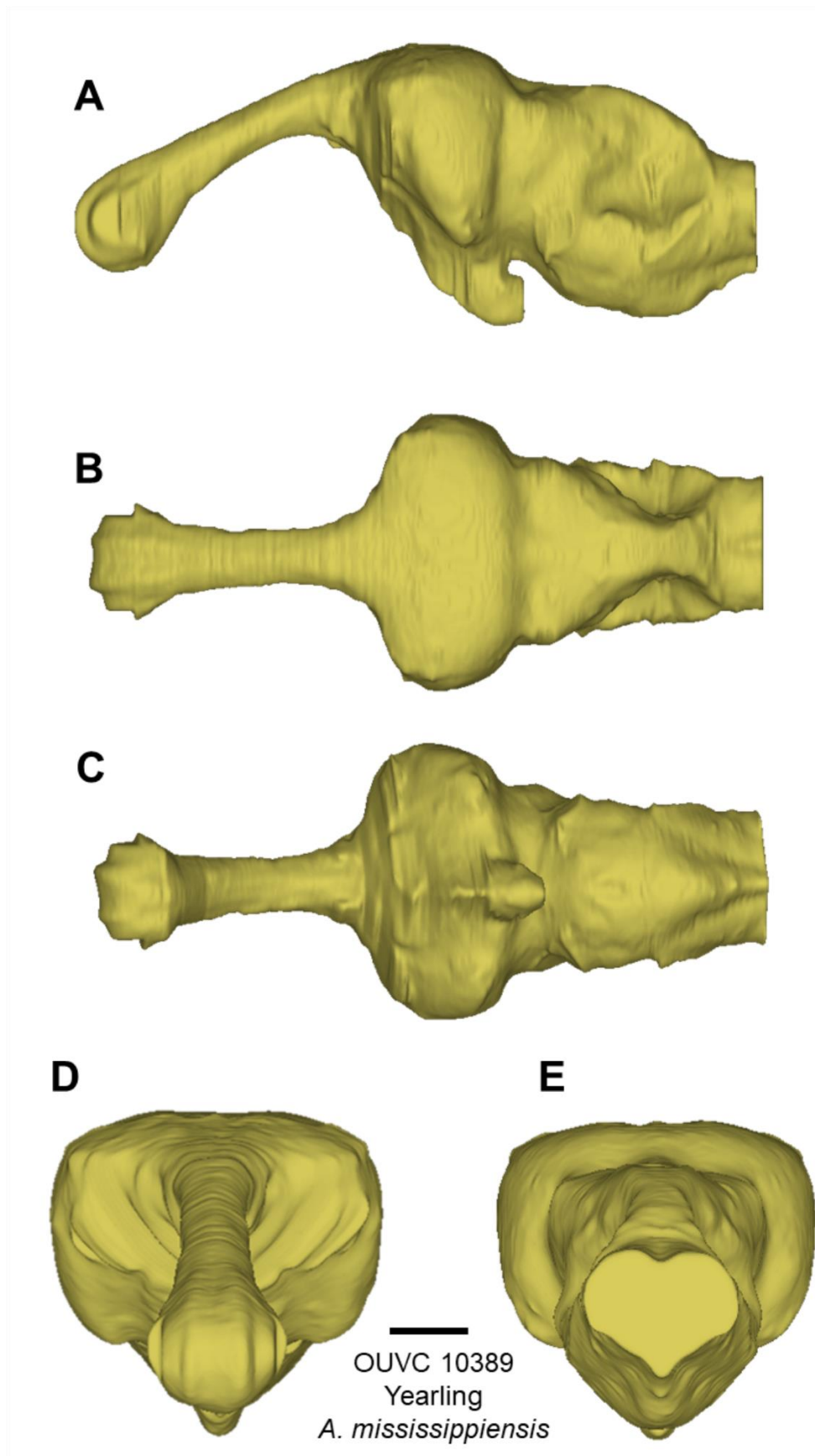


Figure 3.5 – A 1-year-old alligator endocast in (A) lateral, (B) dorsal, (C) ventral, (D) anterior, and (E) posterior views. Scale bar = 5 mm

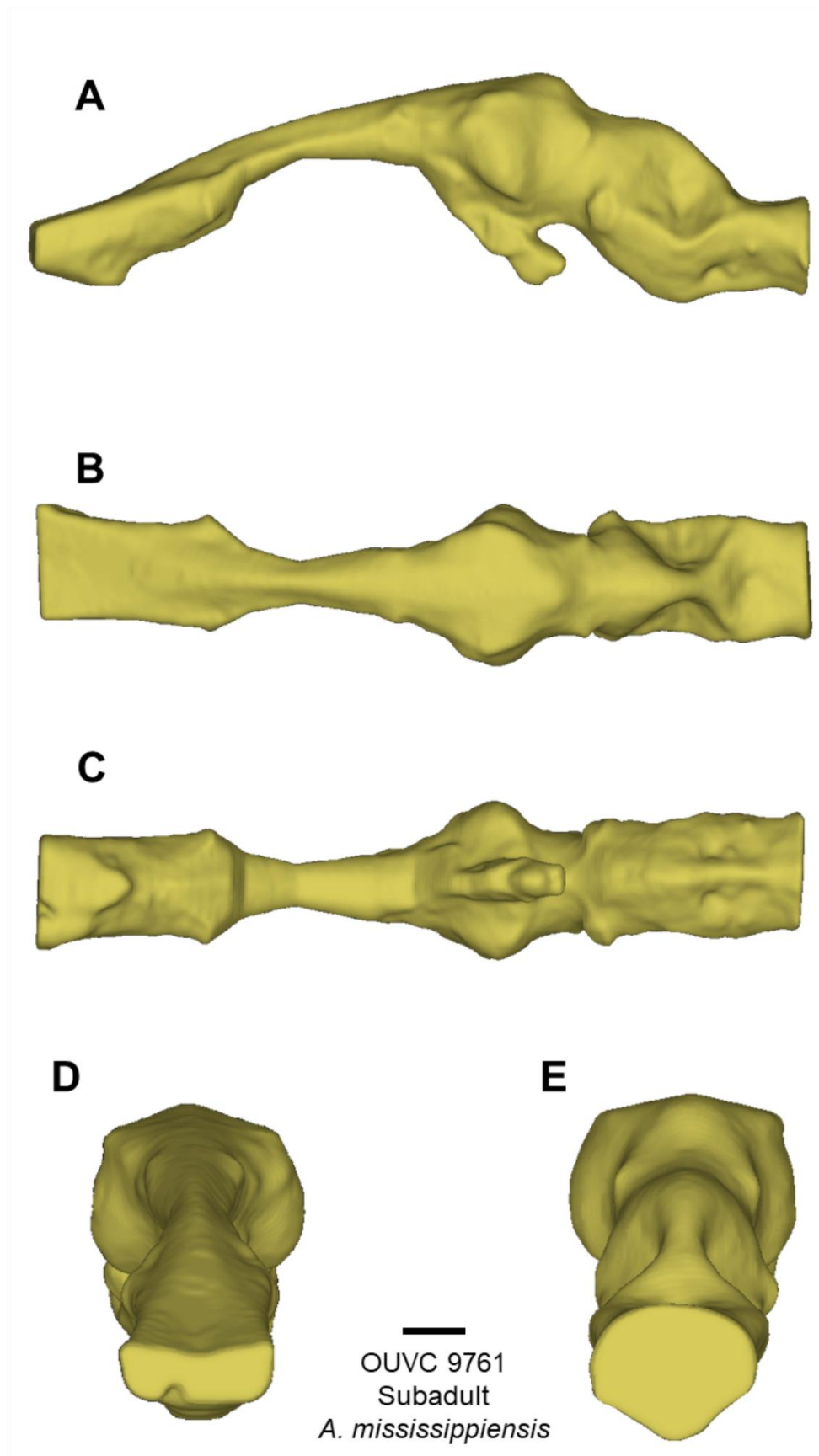


Figure 3.6 – A subadult (3 to 4-year-old) alligator endocast in (A) lateral, (B) dorsal, (C) ventral, (D) anterior, and (E) posterior views. Scale bar = 5 mm

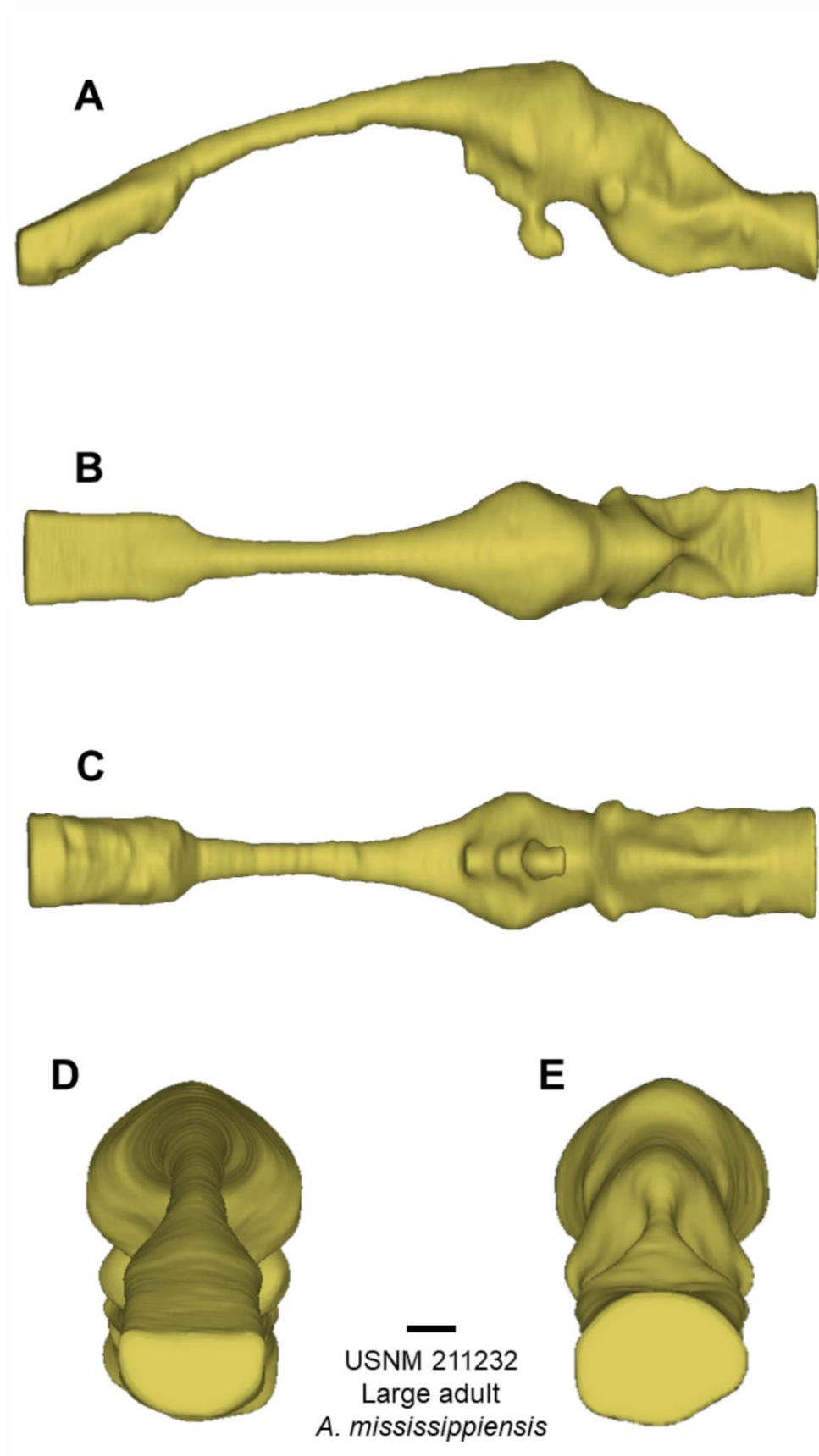


Figure 3.7 – A large adult (≥ 5 -year-old) alligator endocast in (A) lateral, (B) dorsal, (C) ventral, (D) anterior, and (E) posterior views. Scale bar = 5 mm

3.6.2 Midbrain

The overall appearance of the midbrain in *A. mississippiensis* changes through ontogeny. The optic lobes begin as prominent dorsolateral eminences but are entirely covered in the dural envelope and become obscured with age (Figures 3.3A, B and 3.7A, B). By the reduction of contact points between the optic lobes and braincase during development, and with the growth of overlying venous sinuses with age, both lobes become less distinct through ontogeny before becoming nearly invisible in adults (Dufeu et al., 2012). Laterally, the space between the cerebrum and cerebellum occupied by the optic lobes is initially large compared to the area directly ventral that leads to the pituitary gland (Figures 3.3–3.5A, B). These two portions of the midbrain, devoted to optic lobes and pituitary, become more equivalent in size in the subadult and adult (Figures 3.6 and 3.7A, B), which also coincides with reduction in height and width of the cerebrum.

3.6.3 Hindbrain

The hindbrain of *A. mississippiensis* changes as expected for a basal archosaur. The cerebellum shows the least amount of shape or relative size change, and yet in all specimens minor changes through ontogeny make the structure more compact and cone-like (Figures 3.3–3.7A–C, E). However, the amount of shape change is difficult to ascertain as the dural envelope obscures much of the dorsal surface between the midbrain and hindbrain. The medulla oblongata undergoes a much more significant change in shape. Accompanied by the pontine flexure angle change, the medulla oblongata shows noticeable rostrocaudal growth in response to exoccipital expansion throughout ontogeny. The medulla oblongata elongates throughout an alligator's lifetime, though not to the same extent as the olfactory tract (Figures 3.3–3.7E).

3.7 Ontogenetic development of the ostrich endocranium

3.7.1 Forebrain

In all *S. camelus* specimens, the forebrain is well-developed. The olfactory bulb and tract in the 2-week-old (Figure 3.8A) shows the relative size and shape seen in the older specimens with all possessing short olfactory tracts and small bulbs (Figure 3.8B–E).

The cerebral hemispheres show an increase in size and expand transversely between the 2-week-old and the 12-week-old (Figures 3.8–3.9A, C). This increase in cerebrum size corresponds to a rostrocaudal expansion in the hindbrain between 2 and 12 weeks of age. This expansion causes a reduction in height difference between the tops of the cerebral hemispheres and the cerebellum as *S. camelus* grows to 12 weeks of age (Figure 3.9C). By

5 months, however, the cerebral hemispheres have expanded dorsally with the development of the Wulst. The increase in the size of the Wulst causes the hemispheres to extend more dorsally than the cerebellum and develop a shape similar to that in the 2-week-old. Despite these small changes in relative size and shape of the cerebral hemispheres during growth, the overall shape of the brain changes little during ontogeny (Figure 3.11).

The pituitary gland begins facing ventrally from the rest of the endocast. During growth, the region expands in all directions from the ventralmost part of the forebrain. Pituitary expansion is first noticed in the 4-week-old (Figure 3.9B). Through most of ontogeny, the pituitary faces ventrally; however, the pituitary of the 36-monthold specimen (Figure 3.12E) rotates approximately 45° rostrally.

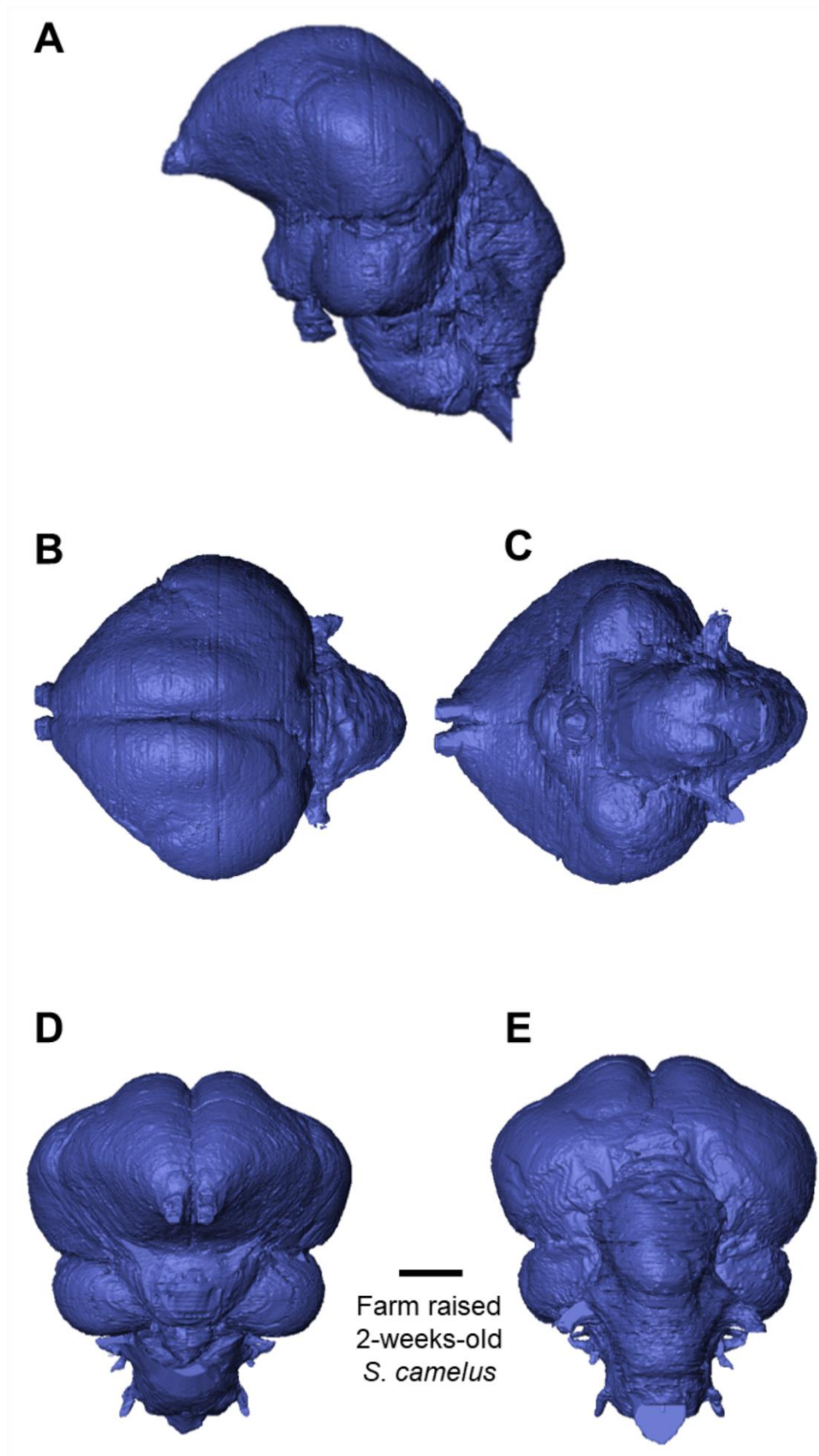


Figure 3.8 – Two-week-old posthatching ostrich endocranium in (A) lateral, (B) dorsal, (C) ventral, (D) anterior, and (E) posterior views. Scale bar = 5 mm

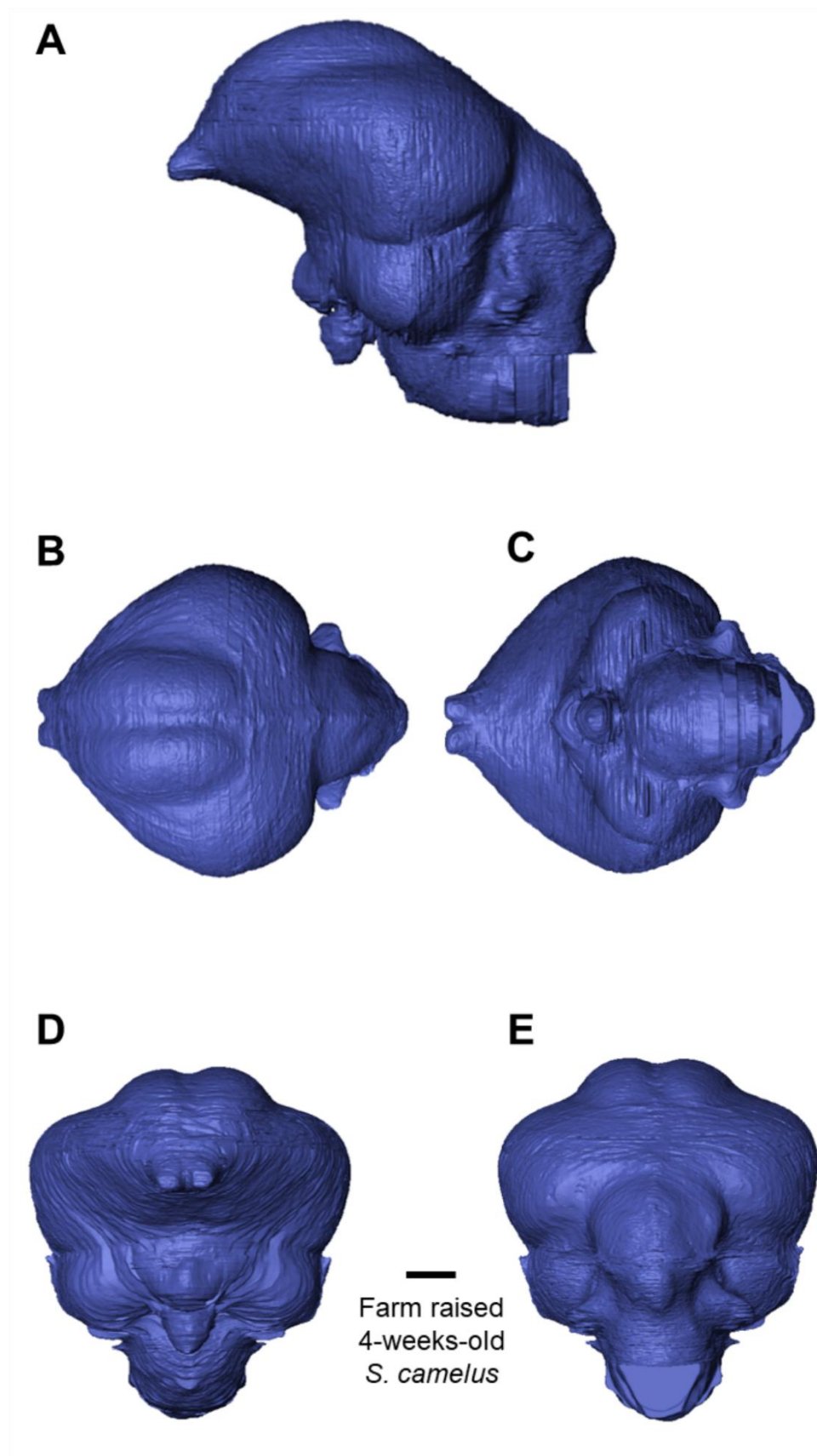


Figure 3.9 – Four-week-old posthatching ostrich endocranium in (A) lateral, (B) dorsal, (C) ventral, (D) anterior, and (E) posterior views. Scale bar = 5 mm

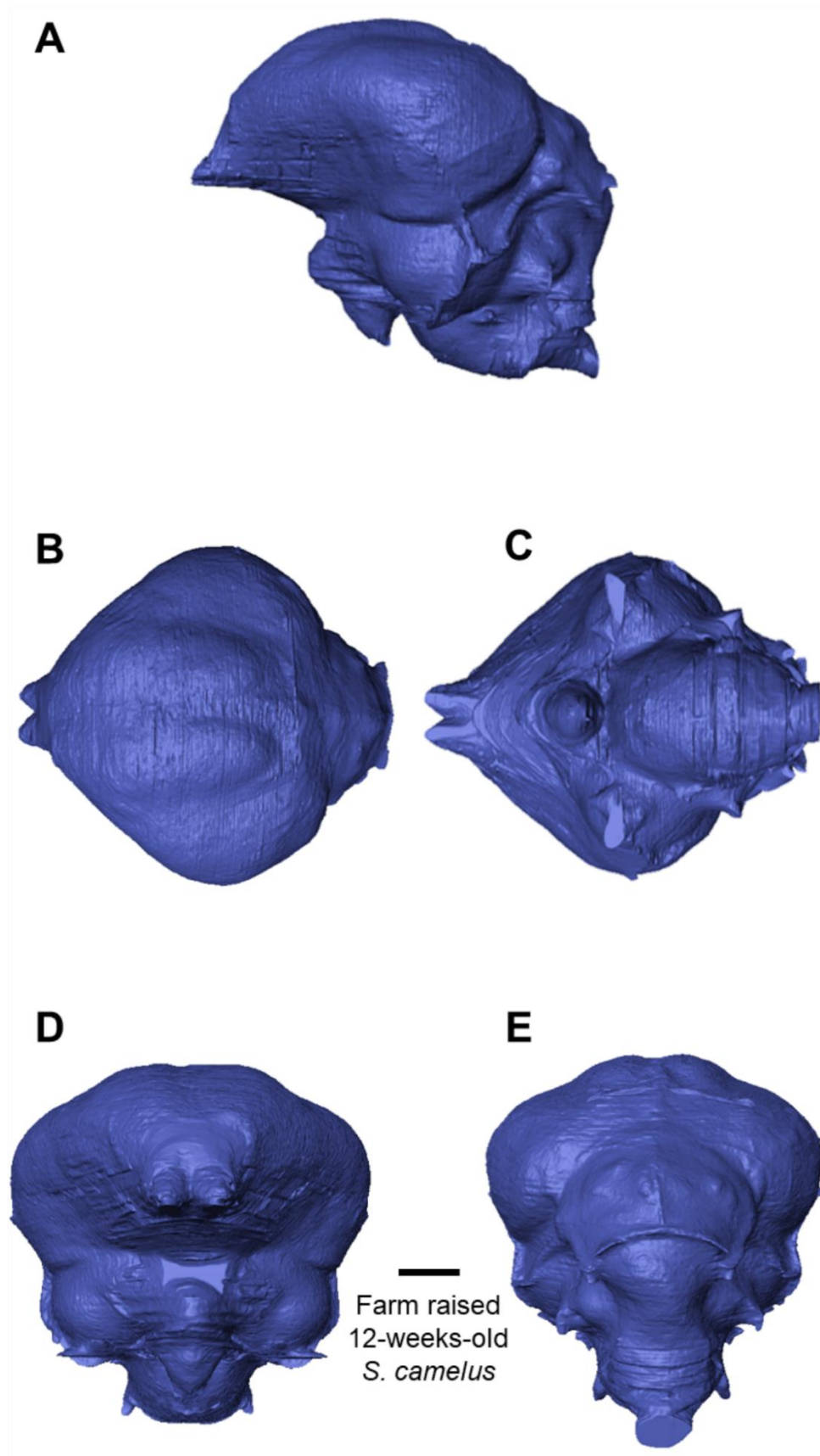


Figure 3.10 – Twelve-week-old posthatching ostrich endocranium in (A) lateral, (B) dorsal, (C) ventral, (D) anterior, and (E) posterior views. Scale bar = 5 mm

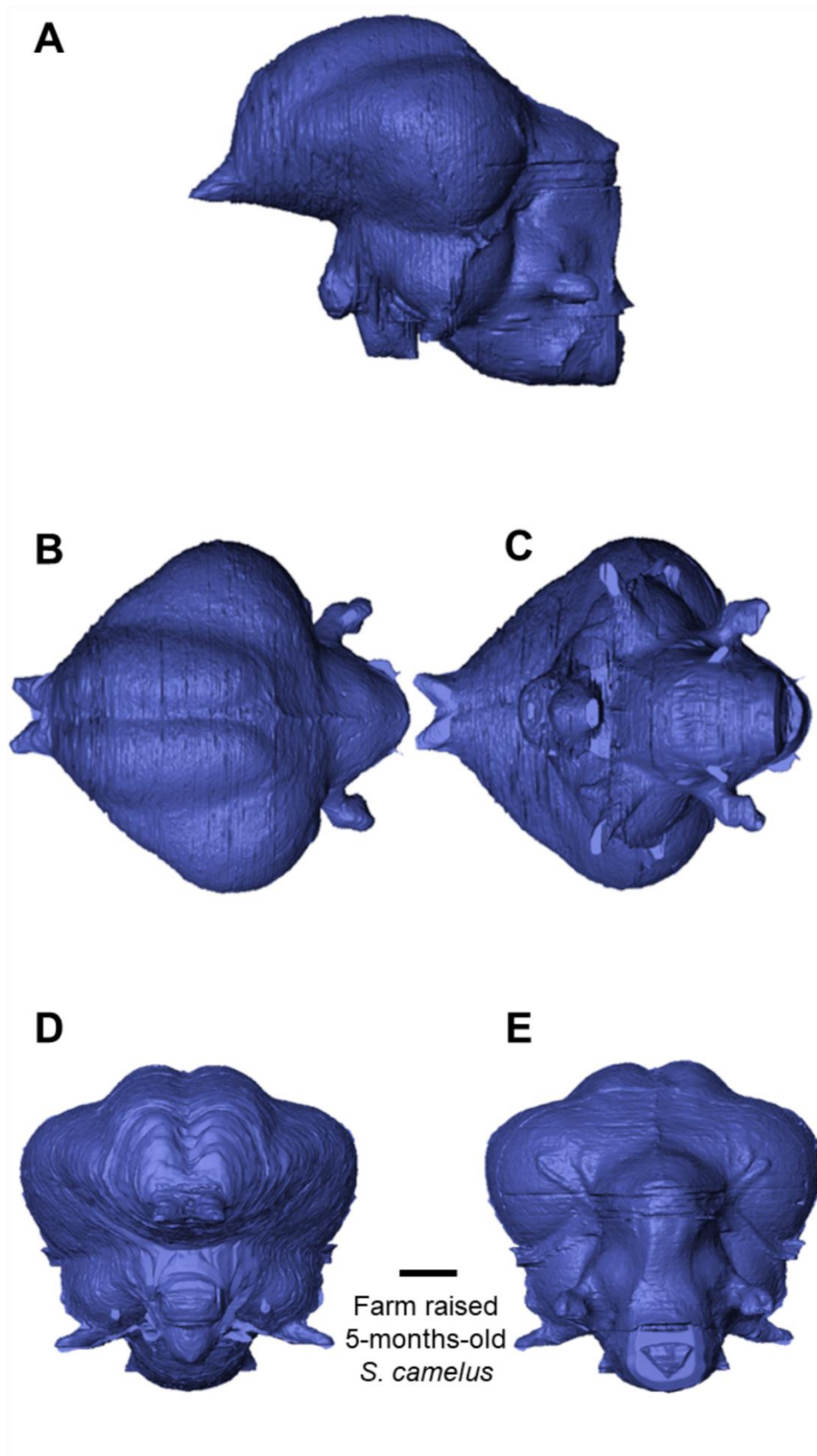


Figure 3.11 – Five-month-old posthatching ostrich endocast in (A) lateral, (B) dorsal, (C) ventral, (D) anterior, and (E) posterior views. Scale bar = 5 mm

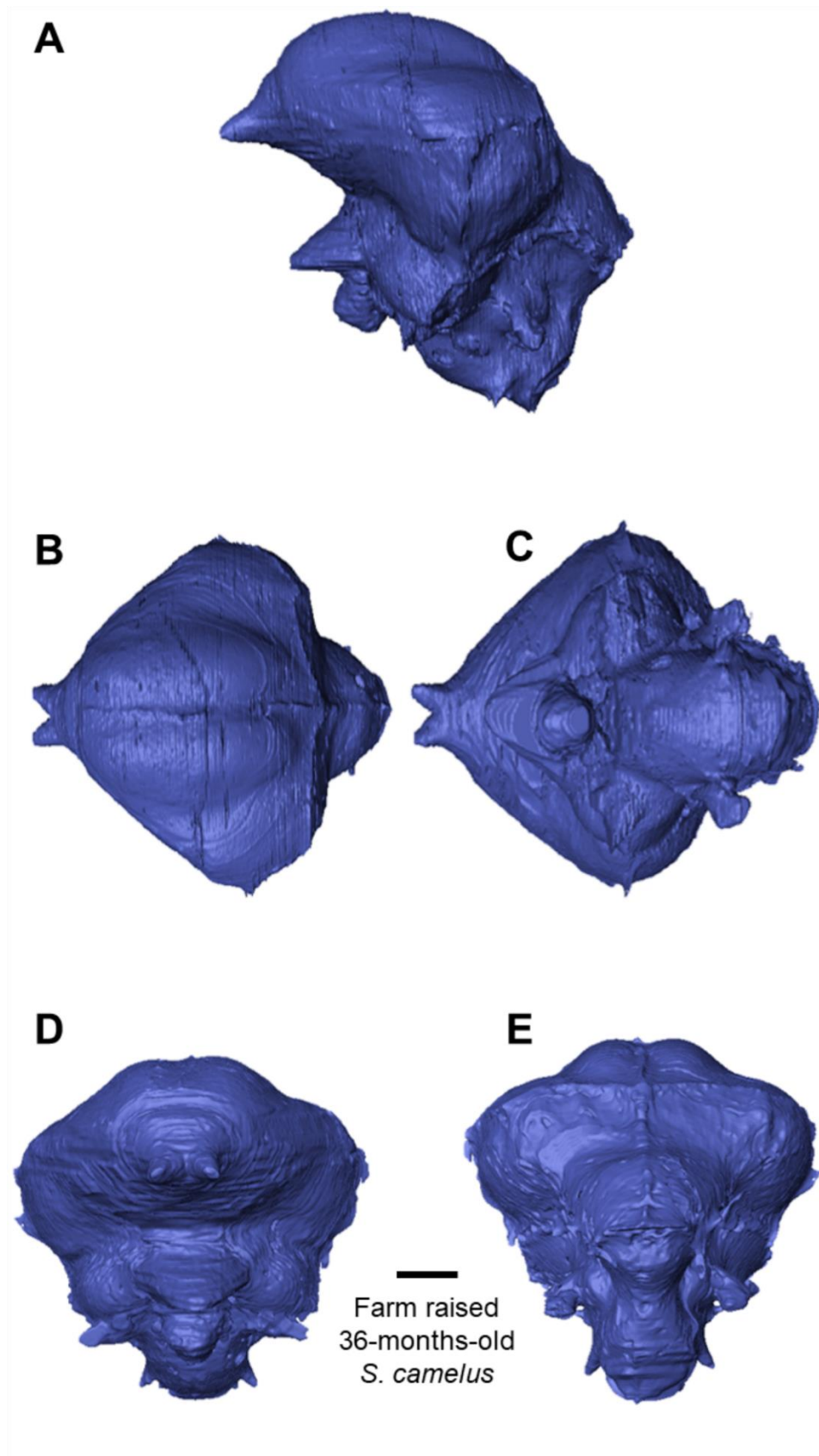


Figure 3.12 – A 36-month-old posthatching ostrich endocranium in (A) lateral, (B) dorsal, (C) ventral, (D) anterior, and (E) posterior views. Scale bar = 5 mm

3.7.2 Midbrain

The only point of interest in the midbrain of *S. camelus* is the optic lobes. These are easily identified in the youngest specimen (Figure 3.8A) as rounded features positioned directly ventral to the cerebral hemispheres. The optic lobes do not change much in overall shape during growth, but they shift rostrally between the 5-month-old and 36-month-old specimens (Figure 3.12D, E).

3.7.3 Hindbrain

Among the specimens visualized in this study, both the pons and medulla oblongata exhibit little change in relative size or shape (Figure 3.8A–E), however, there is notable change in the cerebellar region (broadly referred to here as the cerebellum). With age, the cerebellum follows a trend similar to the cerebral hemispheres in that it changes up to the age of 12-weeks-old (Figure 3.10C) before shifting back to something closer to its youngest form. The cerebellum expands rostrocaudally between 2 weeks and 12 weeks of age (Figures 3.8–3.10A, C). Furthermore, as seen in the three youngest specimens, the relative height of the cerebellum gradually comes closer to that of the cerebral hemispheres.

The cerebellum slows growth between 12 weeks and 5 months of age, and instead the caudal portion becomes more angular in shape. During this same period of growth, the Wulst begins expanding on the dorsal surface of the cerebral hemispheres. Thus, the relative positioning of the cerebellum is lowered, as shown in the 36-month-old, which is very similar in form to the 2-week-old (Figure 3.8A, E). Across all specimens, the shapes of the flocculi accompanying the cerebellum remain largely unchanged.

3.9 Brain growth with age and body mass

Birds and crocodilians show markedly different trajectories of growth in brain size and shape. Because of their rapid growth to skeletal maturity in 3 years, ostrich body mass follows a compressed logistic curve, with modest growth in the first 6 months, and then a rapid rise to adult size in years 2–3 (Figure 3.13A). Alligator body mass increases apparently more steadily over time, and still has not achieved full size by 10 years; thus reflecting earlier observations that alligators keep growing long past sexual maturity at around 10–12 years to finally cease growth at 25–35 years old (Wilkinson et al., 2016). The summaries of brain shape change (Figure 3.13B, C) show how substantially the alligator brain changes in shape in comparison to the ostrich brain. Both alligator and ostrich start life with their brains folded back into a small, posteriorly located region behind the enlarged orbit and eye and, whereas the alligator brain (Figure 3.13B) lengthens rostrocaudally and the posterior part straightens out (much

increased pontine and cephalic flexure angles), the ostrich brain (Figure 3.13C) changes little in shape through its entire posthatching ontogeny.

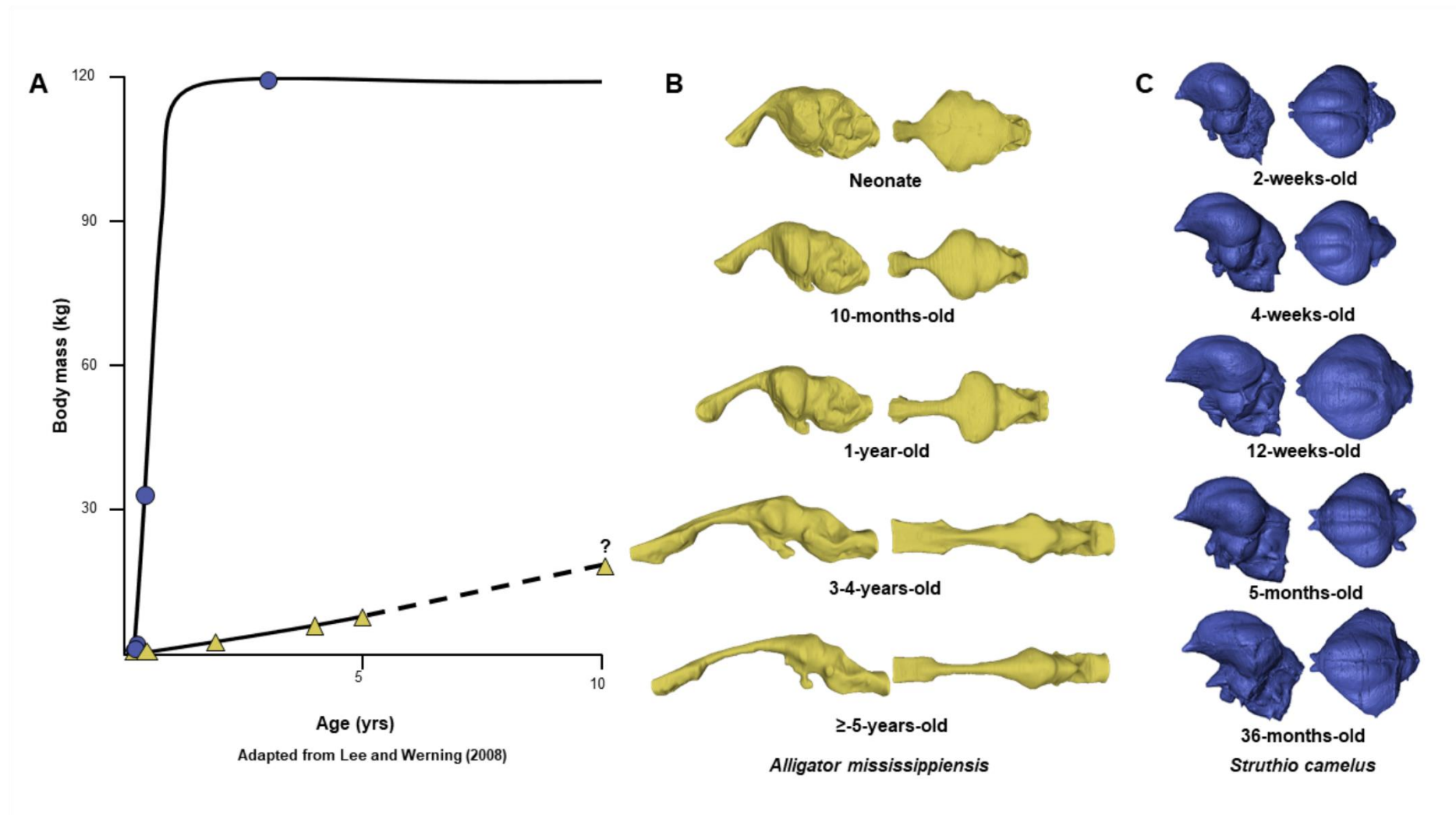


Figure 3.13 – Growth in body size and brain shape for alligator and ostrich. Body size growth curves for ostriches and alligators (A). The question mark and dotted line on the alligator growth curve indicates a projected growth pattern, as they continue to increase their body size throughout their lifetime. The endocasts of alligators (B) and ostriches (C) shown to uniform length so shape changes are highlighted

3.10 Geometric morphometrics

In the morphospace derived from the PCA, the first (PC1) and second (PC2) principal components encapsulate 92.51% of total variance—86.5% in PC1 and 6.01% in PC2. When all endocasts that represent the growth stages of the alligator and the ostrich are plotted, they occupy distinct regions of morphospace (Figure 3.14). The data points in the ostrich morphospace are closer together and more tightly packed than the alligator—as is expected for an endocranial shape that does not change much through ontogeny. Datapoints for the alligators are more spread out reflecting the overall differences in shape between all the ontogenetic stages.

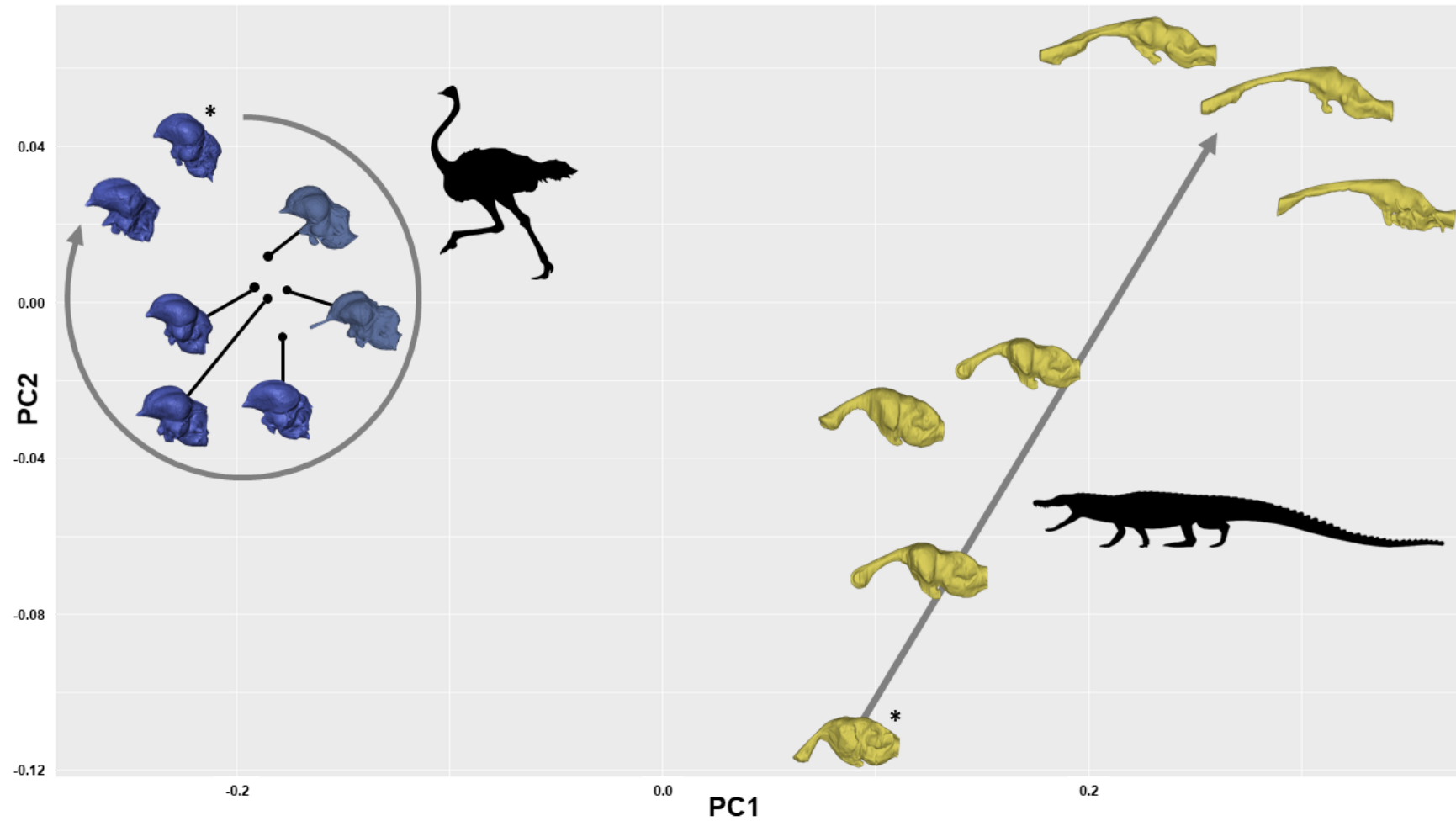


Figure 3.14 – Brain shape change trajectories in morphospace based on landmark data. Brain shape for both ostrich (left) and alligator (right) are always distinctive and do not occupy the same portions of morphospace. The trajectory for the ostrich (left, blue) is tight and curves round, suggesting brain shape in the adult is most similar to that of the hatchling. The trajectory for the alligator (right, yellow) is open and unidirectional, showing continuing shape change in uniform directions, particularly the unfolding of the posterior part of the brain and overall substantial rostrocaudal elongation. Youngest specimens marked with an asterisk. Grey arrow indicated age increase in alligators. Endocasts not to scale.

The differentiation between alligator and ostrich in morphospace is unsurprising based on the large amount of shape change observable between the adults of both taxa and ontogenies. PC1 documents differences in elongation patterns between ostriches and alligators (Figure 3.14). Shape change is dominated by PC1 (Figure 3.14) and is driven by the craniocaudal elongation of the endocast. Elongation is most evident in the alligators where the ontogenetic stages are arranged in a less densely packed pattern thus reflecting a trajectory of continuing shape change through posthatching ontogeny, becoming more and more elongated, especially along the olfactory tract and bulbs, towards the right-hand end of PC1. The ontogenetic sequence of ostrich specimens shows a tightly packed grouping of data, with the youngest specimen plotting near—and reflecting a very similar shape exhibited by—the 5-month-old and 36-month-old. This similarity in shape between ostriches is explained by the forebrain shifting position only slightly and only minor changes in flexure that lacks any kind of major elongation (Figures 3.13C and 3.14).

3.11 Discussion

3.11.1 Endocranial change through ontogeny

Our study highlights the substantial differences between adult alligator and ostrich endocasts as well as unique endocranial modifications that occur throughout ontogeny between the two taxa. In alligators, the large change in the olfactory bulb and tract could imply a change to smell and chemoreception during growth (Weldon and Ferguson, 1993), but that is yet to be established; indeed the shape change might indicate little about changing sensory function. The enlargement of the medulla oblongata, on the other hand, likely corresponds with the need to control breathing and heart rate: necessary adaptations for an amphibious lifestyle typical of most adult crocodilians. But again, it is unclear whether these functions change during ontogeny as brain shape changes.

Struthio camelus shows much less change in the overall shape of its endocast. The olfactory apparatus and medulla oblongata do not significantly change in relative size through ontogeny. The cerebral hemispheres expand less in the rostrocaudal direction than laterally. The enlargement of the cerebral hemispheres in *S. camelus* may conform with the fact that movement and motor control are significant aspects of the life of an ostrich (Breazile and Hartwig, 1989; Peng et al., 2010). Additionally, though the cerebellum does not show much change in size or shape through ontogeny, it is always relatively larger than in the alligator. A static cerebellum through ontogeny suggests that balance, coordination and voluntary movement are also important in the life of an ostrich throughout growth, just as in flying birds (Maderspacher, 2017). Furthermore, little postnatal ontogenetic variation in the brain of birds

is not unique to ostriches but is supported in chickens as well (Kawabe et al., 2015). The major driver of brain shape variation in chickens does not come from massive changes in anatomical size or scaling but rather from the rotation of the telencephalon, myelencephalon, and cerebellum (Kawabe et al., 2015). Ontogenetic studies of modern archosaur endocrania remains an understudied branch of neuroanatomy with only a few peer-reviewed sources describing the interplay of ontogeny, anatomy, morphology, and shape change in archosaurs (Dufeu et al., 2012; Romick, 2013; Dufeu and Witmer, 2015; Kawabe et al., 2015; Jirak and Janacek, 2017a; Watanabe et al., 2019).

These observations are all further supported by the flexure angle measurements. In *S. camelus*, the values change very little, but they follow a negative trend until the middle specimen before shifting positively, describing a negative parabola if plotted against age. Meanwhile the values of *A. mississippiensis* display continuous positive changes in the angles as the crocodilian brain “unfolds” (Beyrand et al., 2019). To summarize, not only do the endocast shapes between an adult *S. camelus* and *A. mississippiensis* differ, but so do the rates at which they change.

The primary difference in shape between the two exemplar taxa – the elongation of the endocast – is more typical of basal archosaurs than birds with adult endocrania being longer than juveniles. From this we can infer that changes in the shape of modern archosaur endocrania is both phylogenetically as well as ontogenetically driven. This is explored further in non-avian dinosaurs in Chapter 4 and Chapter 5 of this thesis.

3.11.2 Heterochrony and the archosaur endocranium

The endocrania of alligators and ostriches experience very different patterns of shape change and anatomical development throughout their life cycles. Ostriches reach skeletal maturity rapidly, in approximately 3 years (Cooper, 2005) and their endocranial widths (here defined as the maximal width across any given region of the endocast) reflect the same fast postcranial growth (Figure 3.15A, D). In the first year of life, the olfactory bulbs, cerebral hemispheres, and cerebellum all develop rapidly and continue to expand with age. Alligators, on the other hand, develop more slowly than birds and only reach sexual maturity at 11–15 years for females and 8–12 years for males (Wilkinson et al., 2016) depending on body size. As they age, alligators show a steady increase in endocranial width values (Figure 3.15B–D) indicating that portions of the brain that can be measured develop at a constant pace before plateauing with adulthood. These developmental patterns reflect the speed at which the respective taxa reach maturity. Comparing the logarithmically normalized values indicates that the endocranial widths of the olfactory bulbs, cerebrum, and cerebellum of both taxa develop as expected.

That is to say that while the development of the cerebellum is similar in both taxa (Figure 3.15D), olfactory bulb width (Figure 14C), and olfactory tract lengths (Figures 3.7B–D and 3.12B–D), increase much more rapidly in alligators. Specific accelerated growth along the olfactory bulbs indicates that the sensory development of alligators and ostriches are independent of their peramorphic and paedomorphic endocranial development when neural processing centres of the endocast are measured.

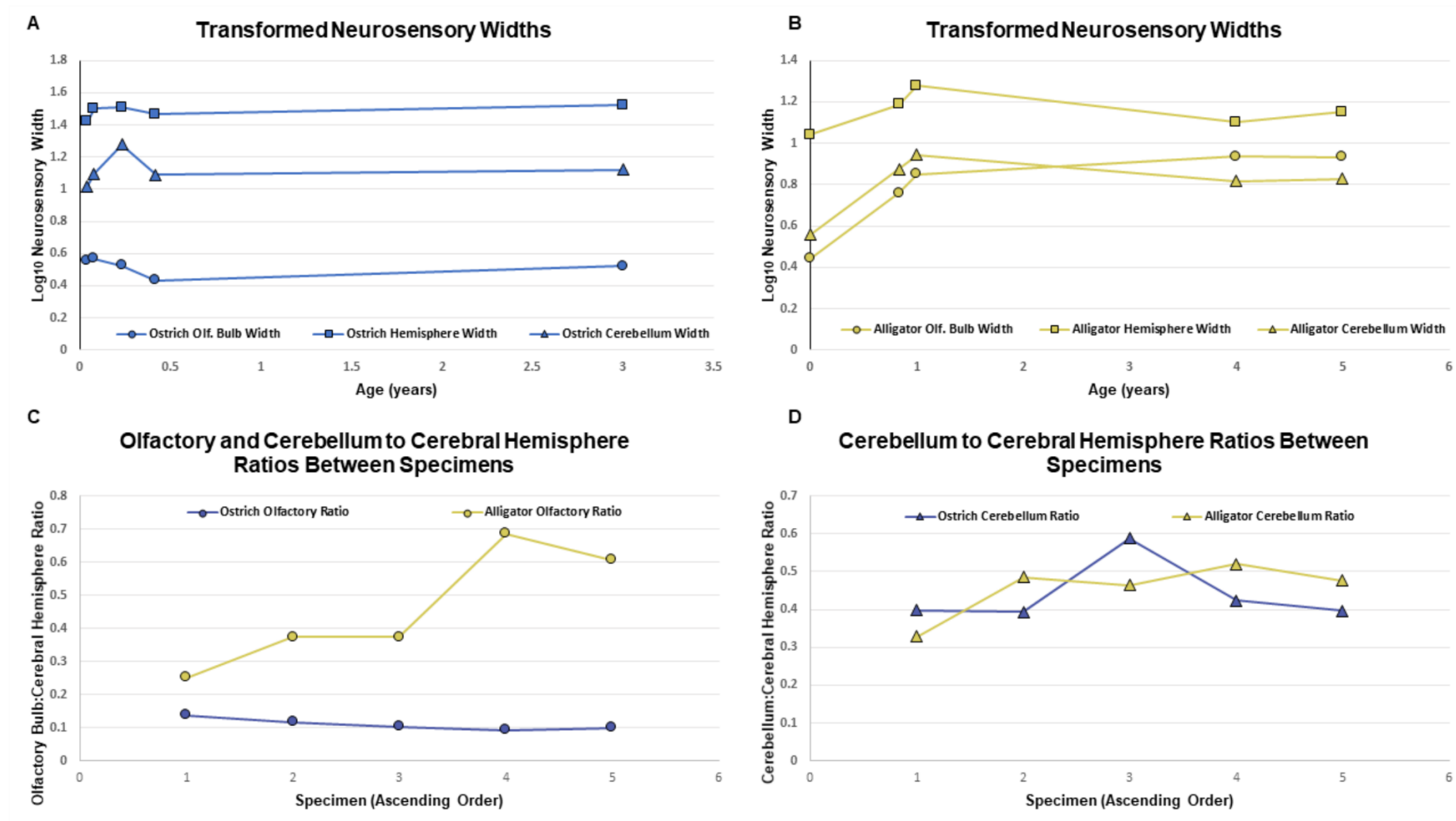


Figure 3.15 – Graphs showing how the logarithmically transformed olfactory bulb, cerebral hemisphere, and cerebellum widths of birds (A) and alligators (B) change with age. In order to better understand what these endocranial width transformations mean, ratios between the olfactory bulbs and cerebral hemispheres (C) and cerebellum and cerebral hemispheres (D) were made for both taxa

Brain growth in birds shows evidence for paedomorphosis. Because the ontogenetic span of birds is shorter than that of crocodilians, and possibly shorter than that of their ancestors, neoteny is most likely ruled out as the possible heterochronic mode, because neoteny depends on slow developmental rates over about the same ontogenetic span as in the ancestor. Shorter ontogenetic trajectories point to progenesis (early onset of sexual maturity) or post-displacement (delayed onset of ontogeny) as two feasible paedomorphic modes, and evidence from modern avian development points to progenesis as the dominant heterochronic mode in bird skulls (Bhullar et al., 2016).

3.11.3 Implications for non-avian dinosaurs

The key questions that arise from this study are whether the crania and brains of non-avian dinosaurs are more like birds or crocodilians, and if there is a transition, where and when did it take place? The answers are likely to be complex, and indeed there is no reason that all dinosaurs should show one or other pattern. If the avian endocranial developmental pattern is paedomorphic, paedomorphic endocranial growth might have been achieved stepwise. Ontogenetic series of fossils may help resolve the nature of the transition and its various steps through the phylogeny of Dinosauria.

Very few non-avian dinosaurs preserve an ontogenetic series of endocasts (Evans et al., 2009; Lautenschlager and Hübner, 2013), and to date, endocranial ontogeny has been described for only one example, *Dysalotosaurus lettowvorbecki* (Lautenschlager and Hübner, 2013). Throughout its ontogeny the endocast of *D. lettowvorbecki* changes not only in size but also in shape. For example, between the juvenile and subadult specimens, the flexure angles decrease in size as the endocast becomes more compact with age (Lautenschlager and Hübner, 2013). Lack of endocranial elongation aside, *D. lettowvorbecki* has developmental traits that are expected within basal archosaurs or are observed directly in the alligator ontogenetic series. The olfactory apparatus elongates anteriorly with age, a prominent dorsal dural peak develops, and the cerebral hemispheres do not undergo extreme expansion (Lautenschlager and Hübner, 2013). It is evidently not as simple as identifying an entirely avian or an entirely crocodilian ontogenetic pattern in dinosaurs.

3.12 Conclusions

The amount of endocranial shape change between ostriches (*Struthio camelus*) and alligators (*Alligator mississippiensis*) is both qualitatively and quantitatively large. As the endocranium ages, it either experiences an almost constant rostrocaudal elongation (*A. mississippiensis*) or remains relatively unchanged, retaining in a juvenile shape throughout adulthood (*S.*

camelus). Endocranial shape change includes shifts in the flexure points of the endocast as well, with the angles changing by 44° to 52° throughout posthatching ontogeny in the alligator. Ostriches, on the other hand, show only 0.25° to 1.64° change of flexure angles, and a similar statistical shape between the endocasts of juveniles and adults. Alligators also show regional shape changes in the endocast through ontogeny: the olfactory bulbs and tracts elongate with age, the cerebral hemispheres do not expand as much when compared to the rest of the endocast, and dural tissues substantially thicken with time. On the other hand, ostriches show a significant expansion of the cerebral hemispheres and cerebellum early in life and maintain the size of these lobes throughout their lifespan.

Understanding how and when ontogenetic changes occur in two extant exemplar archosaurs helps us to model patterns in non-avian dinosaur endocranium development. Since scannable 3D dinosaur braincases are so rare in the fossil record, our understanding of endocranial development through ontogeny in dinosaurs is extremely incomplete. One of the few ontogenetic series that is available for a non-avian dinosaur, *Dysalotosaurus lettowvorbecki*, shows that shape and flexure points—when compared to modern taxa—can be misleading. The general shape for *D. lettowvorbecki* is distinctive but does not show exaggerated elongation nor does it keep a pedomorphic shape, thus diverging from extant analogues. Also, both the cephalic and pontine flexure angles decrease with age, indicating that shape and flexure are not clear indicators of developmental pattern in a dinosaurian endocast. Here, I suggest that anatomical factors (e.g., development or lack of cerebral peaks, elongation of the olfactory apparatus, broadening of cerebral hemispheres) should be considered in addition to shape or flexure when determining ontogenetic patterns and possible heterochrony.

Chapter 4: Ontogenetic trends in the endocranium of *Psittacosaurus lujiatunensis*

4.1 Collaborative Statement

This chapter is a collaborative effort that includes Zhao Qi (Institute of Vertebrate Paleontology and Paleoanthropology; provided data), Emily Rayfield (University of Bristol; gave feedback and edited drafts), and Michael Benton (University of Bristol; gave feedback and edited drafts). I have done a majority of the work by segmenting all of the endocasts, measuring linear distances and flexure angles, comparing the anatomy between endocasts, as well as writing and editing the chapter. I estimate that I have completed 95% of the work for this chapter myself. This chapter has not been published yet.

4.2 Abstract

Endocranial ontogenetic series of dinosaurs are rare and seldomly contain more than two or three endocasts thus limiting our understanding of how dinosaur neuroanatomy develops postnatally. Here, I describe the anatomy and measure the endocranial widths and flexure variation in an ontogenetic series of *Psittacosaurus lujiatunensis* – a basal non-ceratopsid ceratopsian. Anatomically, the endocrania described show a mix of avian and basal archosaur-like traits where the endocast anatomy of *P. lujiatunensis* shifts bird-like and crocodilian-like throughout postnatal development. In terms of flexure, the development of the *P. lujiatunensis* neurocranium matches no modern archosaur developmental trends. These results have two major implications for dinosaur palaeoneurology: adult specimens should be used in broad macroevolutionary studies and that the ontogenetic form of a non-avian dinosaur endocast should not be assumed based on its phylogenetic relationship.

4.3 Introduction

Palaeoneurology of non-avian dinosaurs has predominantly focused on single descriptions of reconstructed – or, more rarely, natural (Brasier et al., 2016; Carabajal et al., 2018) – endocasts with comparisons to other taxa (for example, Rogers, 1999; Franzosa and Rowe, 2005; Carabajal, 2010; Lauters et al., 2013; Bronzati et al., 2017; Zhang et al., 2019) or broad trends in evolution between closely related clades (Witmer and Ridgely, 2009; McKeown et al., 2020). The advent, refinement, and increased use of computed tomography (CT) scanning and digital reconstruction has greatly increased the amount of endocranial information available to researchers (Racicot, 2016). But even with newer methods of endocranial reconstruction, the ontogenetic development of the dinosaurian endocast

remains poorly understood due to the fragmentary fossil record of young individuals (Bever et al., 2011; Lautenschlager and Hübner, 2013; McKeown et al., 2020).

Psittacosaurus, a genus of incredibly species-rich ceratopsians from the Early Cretaceous (c. 125–100 Ma) of China, Mongolia, and Russia (Napoli et al., 2019), gives an unprecedented opportunity to study the cranial remains of young juveniles – especially those of *Psittacosaurus lujiatunensis* (Zhao et al., 2013a). *P. lujiatunensis* is known from hundreds of specimens all from a single stratigraphic level and locality, the Lujiatun Unit (c. 125.7 Ma) around the village of Lujiatun in Liaoning Province (Rogers et al., 2015), and most are unusually well-preserved and uncrushed because they were buried in rapidly accumulating ash deposits, hence the name of the site, the ‘Chinese Pompeii’ (Zhao et al., 2013a; Bullar et al., 2019). These hundreds of specimens have provided evidence of ontogenetic shifts in braincase osteology (Bullar et al., 2019), postural shifts in the species throughout somatic maturation (Zhao et al., 2013), and age segregated behaviour (Zhao et al., 2013a) thanks to small amounts of juvenile and subadult specimens found throughout the Yixian Formation. Access to non-destructive modelling methods and skulls from all ontogenetic stages allows for unprecedented examples of how the neurocranium changes anatomically and morphologically with age alongside the behaviour and palaeobiology of *P. lujiatunensis*.

Previous work has explored the osteological changes that occur between juvenile posthatchling and adult specimens of *P. lujiatunensis* (Bullar et al., 2019) to better understand how the braincase and endosseous labyrinths change form throughout ontogenetic development. Bullar et al. (2019) describes that even though braincase anatomy is typically conservative between closely related adult taxa, a surprising amount of morphometric change can occur in certain bones of the braincase throughout the lifetime of a non-avian dinosaur. In their study, *P. lujiatunensis* was used to illustrate just how the cranium changes with age (Figure 4.1, 4.2). The results show that much of the change that occurs in the braincase is focused around the laterosphenoids, parietals, supraoccipital, paroccipital processes, and basal tubera (Figure 4.1). Increases in size to the laterosphenoids, parietals, and basal tubera give added length to the skull and braincase of the adult while expansions to the posterior braincase along the basal tubera and paroccipital processes make the skull broader along the posterior skull.

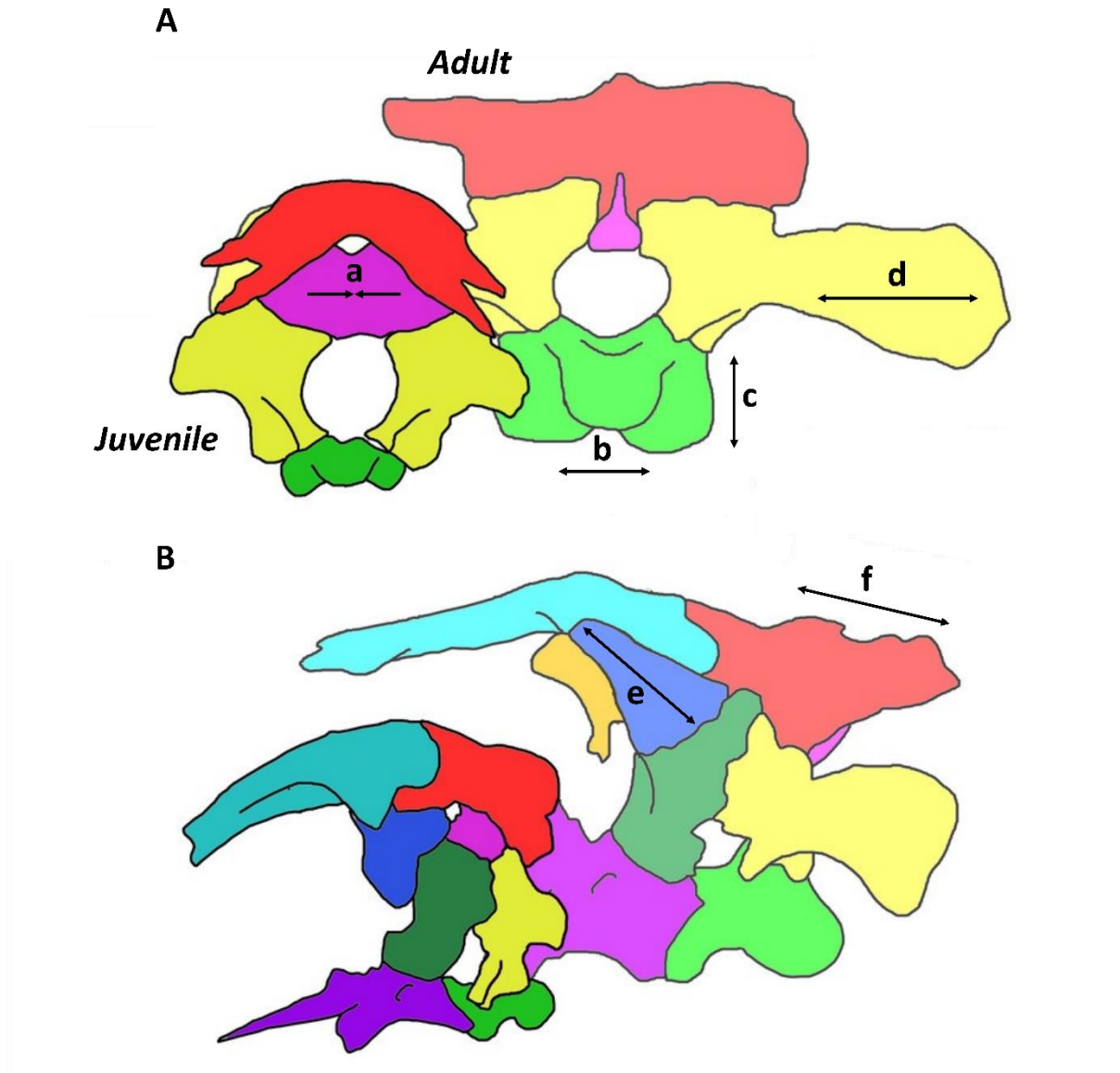


Figure 4.1 – Line drawings of a juvenile and adult *Psittacosaurus lujiatunensis* braincase in posterior (A) and left lateral (B) views. Changes in bone size or form are summarised as a shrinking of the supraoccipital (pink; a), an increase in the width (green; b) and height (green; c) of the basal tubera, lateral expansion of the paroccipital processes (yellow; d) elongation of the laterosphenoids (blue; e) and lengthening of the parietals (red; f). Braincases not to scale. Modified from Bullar et al. (2019).

Internally, the endosseous labyrinths undergo subtle changes that give more detail about the palaeobiology of *P. lujiatunensis* that change with time. Bullar et al. (2019) calculated the angle between the lateral semicircular canal and palate. The lateral semicircular canal is held parallel to the ground in life (Witmer et al., 2003) therefore giving a glimpse into how the species would have held their heads in respect to the ground. Understanding the relationship between the lateral semicircular canals and palate of *P. lujiatunensis* and the ground allows palaeontologists to calculate how the angle of the skull changes with age. As ontogeny progresses, the angle between the palate and lateral semicircular canals narrows to the point that the skull is held nearly horizontal to the ground in adulthood (Figure 4.2).

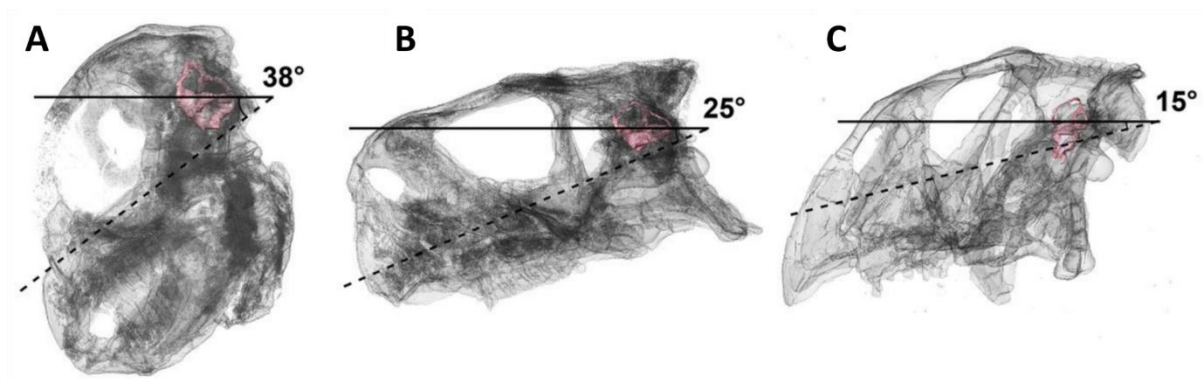


Figure 4.2 – Skulls of a posthatchling (A), juvenile (B), and adult (C) *Psittacosaurus lujiatunensis* with their respective calculated head angles. Note how the angle becomes smaller with age signifying a change in how *P. lujiatunensis* held its head throughout life. Figure modified from Bullar et al. (2019). Skulls not to scale.

The work of Bullar et al. (2019) detailed how the osteology of the braincase changed with age; however, the soft tissue of the interior braincase was not reconstructed for the study. Here, the endocranium has been reconstructed from five well-preserved *P. lujiatunensis* skulls to better understand how the endocast of a species changed between a sub-yearling juvenile and a 10-years-old somatically mature adult (Zhao et al., 2013). This chapter seeks to define how the morphology and anatomy of the *P. lujiatunensis* endocranium changes with ontogeny and explore what the neurosensory width changes mean for sensory perception or behaviour in the species.

4.4 Materials, Methods, and Institutional Abbreviations

Three specimens, a sub-yearling, juvenile, and adult skulls, are housed at IVPP. The two subadult skulls are housed at PKUP. Ages of the specimens were calculated based on femoral osteohistology in prior research (Zhao et al. 2013b).

All of the skulls used for this chapter were scanned with a micro-computed tomography scanner at the Institute of Vertebrate Paleontology and Paleoanthropology in Beijing, China (see Table 4.1 for scan parameters). Avizo 9.3 (FEI Visualization Sciences Group) was used to segment the endocrania. Relevant areas of the internal braincase were digitally highlighted in Avizo on each 2D CT slice and slowly made into a 3D image by combining all of the 2D highlighted areas together. ImageJ (v1.52) was used to measure flexure points and make linear measurements. Graphing was carried out in RStudio (v3.6.3). Ostrich data used in this chapter was the same data generated for Chapter 3. Alligator data was sourced from Dufeu and Witmer (2015) and Romick (2013).

Table 4.1 – Scan parameters used for all psittacosaur used throughout this chapter.

Specimen Number	Resolution (µm)	Voltage (kV)
IVPP V15451	21.96	130
IVPP V12731	37.64	140
PKUP 1053	160	440
PKUP 1054	160	440
IVPP V12617	160	140

After making digital endocranial models, linear measurements were taken across the maximal distance of the olfactory, cerebral, and cerebellar lobes. The cephalic and pontine flexure points were measured in two different areas. Cephalic flexure was defined and measured as the angle between the anteriormost extent of the olfactory bulbs, the posteriormost extent of the cerebral hemispheres, and the floccular lobes. Pontine flexures were measured as the angle between the centre of the medulla oblongata, the floccular lobes, and the posteriormost extent of the cerebral hemispheres.

A linear measurement across the maximal width of the olfactory bulb, cerebrum, and cerebellum was made to understand how the main neurosensory areas of the endocast developed between each ontogenetic stage. Linear measurements were used in lieu of volumes for two reasons. First, there is inconsistent preservation across the psittacosaur endocasts – specifically along the anterior floor of the braincase. Generally speaking, the preservation between the endocasts is sufficient enough define anatomy along the dorsal and lateral surfaces. The orbitosphenoids are only partially preserved in IVPP V15451 and wholly missing in IVPP V12731 thus making volumetric measurements unreliable between young specimens. Volumetric uncertainty is especially evident along the olfactory bulbs where large amounts of shape variation occur in modern non-avian archosaur taxa (Hu et al., 2021). Secondly, there is evidence of a thickening dural envelope with age based on the disappearance of anatomical features (e.g. optic lobes, longitudinal/transverse fissures) along the dorsal surface and midbrain. Neither of these issues invalidate the measurements made from the endocasts, however, they do call into question how helpful volume measurements would be – especially in an ontogenetic series where large amounts of change (e.g. thickening of the dural envelope) can be expected with age.

Institutional abbreviation: IVPP—Institute of Vertebrate Paleontology and Paleoanthropology, Beijing, China; PKUP—Peking University Paleontological Collections, Beijing, China.

4.5 Anatomy of the Developing Endocranial Form of *Psittacosaurus lujiatunensis*

4.5.1 IVPP V15451: Sub-Yearling (<1-Year-Old)

The olfactory tract is similar to those found in juvenile alligators in that it is elongate and would have borne two small olfactory bulbs anteriorly; however, the olfactory bulbs of IVPP V15451 are not well-preserved. A ventral view of the frontals shows an expansion at the anterior margin, but the true extent of the bulbs is unknown due to the lack of fully preserved frontals (Bullar et al., 2019). More mature specimens of *Psittacosaurus lujiatunensis* show enlarged olfactory bulbs that are more similar to those found in basal archosaurs and even large-bodied coelurosaurs when compared to their body size (Zhou et al., 2007). Indentations along the frontal bones of IVPP V15451 show that enlarged olfactory bulbs would have been expected in young individuals of *P. lujiatunensis*.

Both cerebral hemispheres (= cerebrum) are roughly pyriform in dorsal view and project ventrally in a gentle curve. Together, they are remarkably wide (10.5 mm across the posterodorsal margin, Table 4.2), representing 70.4% of the endocast length. Cerebral widths decrease to 31.2% in the adult. Medially, the longitudinal fissure separates the cerebral hemispheres. Posteriorly, the transverse fissure separates the cerebrum from the cerebellum.

Table 4.2 – List of measurements from identifiable sources of brain anatomy across the entire ontogenetic series of *P. lujiatunensis* endocasts.

Specimen	Age (Years)	Endocast Length	Olf. Bulb Width	Cerebrum Width	Cerebellum Width
IVPP V15451	<1	14.9	3.8	10.5	7.8
IVPP V12731	2	30.5	5.4	14.3	9.1
PKUP V1053	7	92.0	7.8	19.6	8.4
PKUP V1054	8	84.7	6.5	19.5	11.6
IVPP V12617	10	78.1	10.4	24.3	15.3

Along the midbrain, a swelling is present on the right side of the IVPP V15451 endocast, the optic lobes (OL, Figure 4.3C). The optic lobes are laterally located compared to the dorsal surface, and the presence of optic lobes in a juvenile non-avian, non-theropod dinosaur suggests that either the dura mater has yet to thicken and remains a thin membrane in the juvenile, or the venous sinuses have yet to develop and mask their appearance beneath the dura mater (Dufeu et al., 2012). Adult birds have a thinner dura mater than adult modern

crocodilians, whereas juvenile crocodilians retain a thin dura (Dufeu et al., 2012; Jirak and Janacek, 2017) meaning that this trait might be expected also in juvenile non-avian dinosaurs. Ventrally, a small pituitary gland projects from a short infundibulum. Internal carotid arteries project posteroventrally from the pituitary with almost 180° between the arteries.

The cerebellum makes a rough triangular shape that sweeps back posteriorly and measures 7.8 mm at its widest point (Figure 4.3A). Over the life of *P. lujiatunensis*, the size of the cerebellum more than doubles (15.3 mm). Typically, a dural peak would be present dorsally along the cerebellum, but a dislodged supraoccipital prevented the reconstruction of the cerebellum's posterior margin – if one were present. The medulla oblongata (MO, Figure 1E) marks the posterior-most extent of the endocast and, in IVPP V15451, forms a roughly oval shape ventral to the cerebellum.

Almost no peripheral anatomy such as cranial nerves (CN) are preserved along the endocast. Poorly preserved peripheral anatomy is most likely due to the poor ossification of the braincase due to the young age of the specimen. Bullar et al. (2019) indicates that a partial foramen for CN V (trigeminal nerve) was formed by the laterosphenoids and prootic, but this was not clear along the endocast. The only cranial nerve partially preserved was CN XII (the hypoglossal nerve).

Table 4.3 – List of all cephalic and pontine flexure angles from the entire ontogenetic series of *P. lujiatunensis* endocasts.

Specimen	Age (Years)	Cephalic Flexure	Pontine Flexure
IVPP V15451	<1	82.1°	89.6°
IVPP V12731	2	138.7°	138.7°
PKUP V1053	7	138.2°	148.4°
PKUP V1054	8	133.9°	140.1°
IVPP V12617	10	88.1°	88.9°

The cephalic and pontine flexure angles of IVPP V15451 are well below those found in adult crocodilians (Dufeu et al., 2012; Jirak and Janacek, 2017) and reflect the fact that the endocast is compressed in an S-shaped configuration. Flexure angles vary substantially throughout ontogeny in alligators (Dufeu et al., 2012) but not in birds. Notably, IVPP V15451 has a pontine flexure that is more similar to birds of any somatic age and only similar to alligators that are less than one year of age.

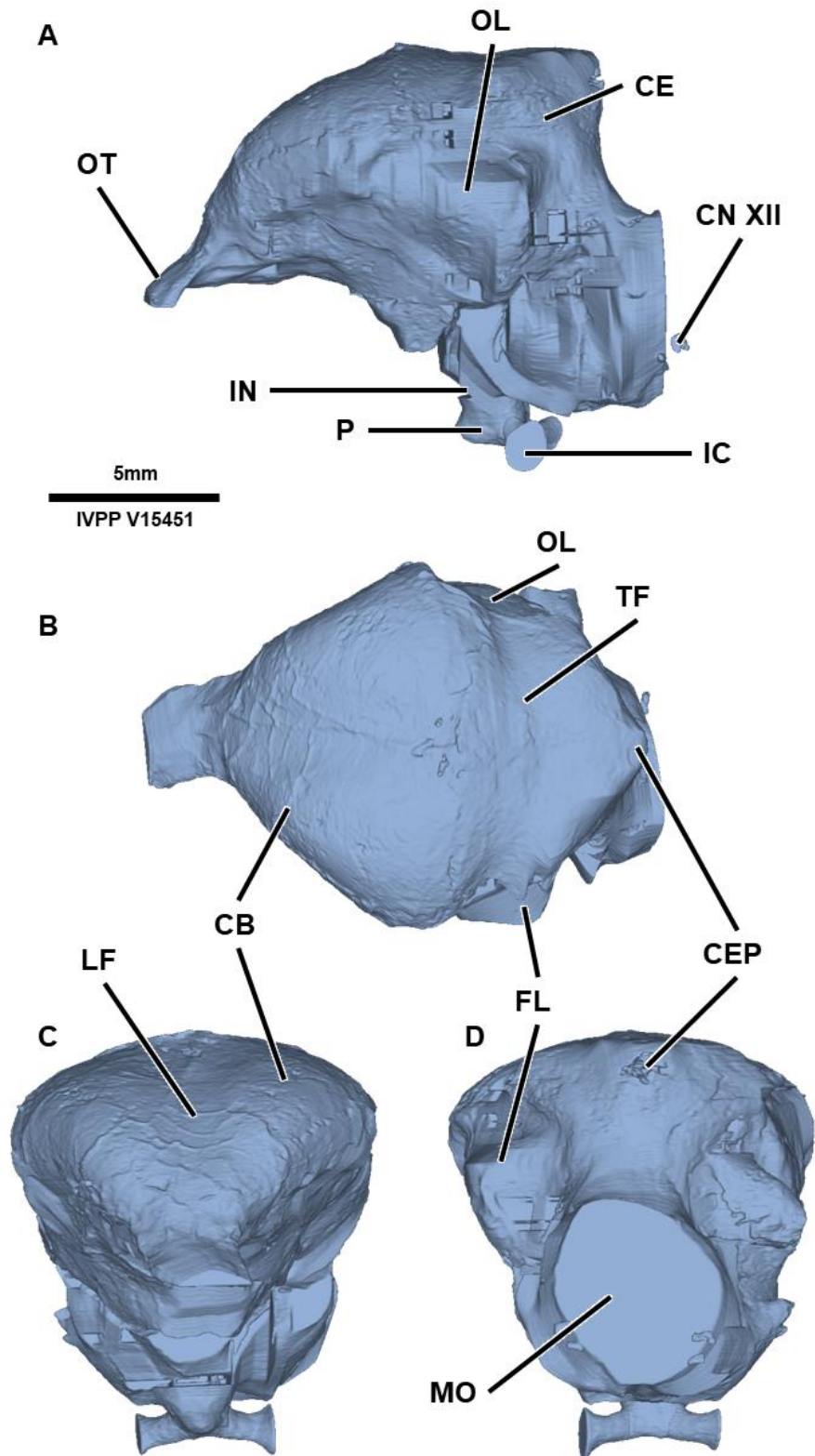


Figure 4.3 – Lateral (A), dorsal (B), anterior (C), and posterior (D) views of the segmented endocast of IVPP V15451. P, pituitary; CB, cerebellum; CE, cerebrum; IC, internal carotid artery; IN, infundibulum; FL, flocculus; LF, longitudinal fissure; MO, medulla oblongata; OB, olfactory bulb; OT, olfactory tract; TF, transverse fissure; CEP, cerebral protuberance; CN XII, hypoglossal nerve

4.5.2 IVPP V12731: Juvenile (2-Years-Old)

The olfactory bulbs are complete in IVPP V12731 (Figure 4.4A-C) and are represented by a flared, hourglass-shaped attachment point to a short olfactory tract when viewed in dorsal view (Figure 4.4B). Across their widest point, the olfactory bulbs measure 5.4 mm. Dorsally, the olfactory bulbs are bound by the frontal bones. The ventral floor of the braincase that supported the olfactory apparatus in life was not preserved in IVPP V12731 thus preventing additional measurements.

The forebrain is only partially preserved as the laterosphenoids were only partly fossilised. As such, the cerebrum shape is not dorsoventrally uniform and only the dorsal and dorsolateral margins of the cerebrum were reliably preserved. When viewed dorsally, the cerebrum maintains a pyriform shape much like IVPP V15451 though the longitudinal and transverse fissures are difficult to distinguish in IVPP V12731 (Figure 4.4B). Maximally, the cerebral hemispheres measure 14.3 mm across (Table 4.2). Due to dorsoventral compression, the contact point between the cerebrum and midbrain is mildly flattened.

Poor preservation makes much of the anatomy along the midbrain difficult to diagnosis – especially laterally (Figure 4.4A). Dorsally, two hemispherical protuberances can be viewed along the midbrain near the cerebellum (Figure 4.4B). Based on the anatomy of IVPP V15451, these are interpreted as optic lobes. Their original location along the midbrain is called into question due to taphonomic distortion. Along the bottom of the midbrain, a thick infundibulum projects the more developed pituitary ventrally at nearly a right angle. Aside from the presence of optic lobes, the midbrain is unremarkable in IVPP V12731.

The reconstructed hindbrain – the cerebellum, flocculi, medulla oblongata – is much less distorted than the forebrain and midbrain (Figure 4.4B, D). Dorsally, the cerebellum area broadest just above the flocculi and tapers posteriorly. The flocculi are large and project mediolaterally from the cerebellum (Figure 4.4 A, B, D). The bones of the braincase are only slightly separated posteriorly between the parietals and supraoccipitals. Due to the partial separation of the braincase, the cartilaginous expansion of the cerebellum (CEP, Figure 4.4 A, B) is difficult to distinguish when viewed laterally but can be observed in dorsal view.

No peripheral anatomy was preserved along IVPP V12731 due to the poor preservation of the braincase floor.

Even with the dorsoventral compression, the flexure angles of IVPP V12731 reflect the pattern observed in PKUP V1053 and PKUP 1054 (Table 4.3). This is to say that the flexure angles almost double and the endocast goes from having cephalic and pontine right angles to the

endocast almost being arranged all along the same plane (compare Figure 4.3A to Figure 4.4A).

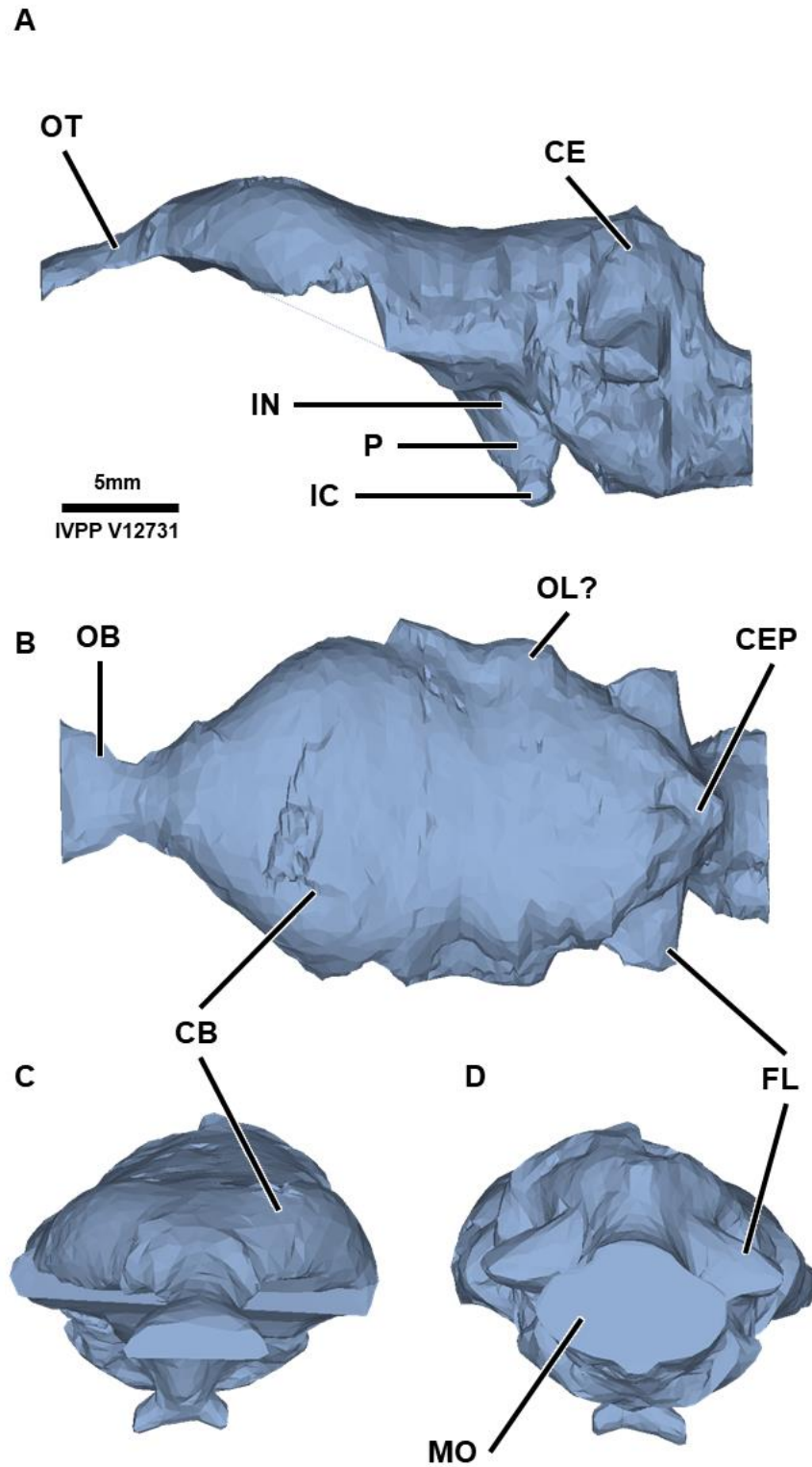


Figure 4.4 – Lateral (A), dorsal (B), anterior (C), and posterior (D) views of the segmented endocast of IVPP V12731. P, pituitary; CB, cerebellum; CE, cerebrum; IC, internal carotid artery; IN, infundibulum; FL, flocculus; MO, medulla oblongata; OB, olfactory bulb; OL?, optic lobe?, OT, olfactory tract; CEP, cerebral protuberance

4.5.3 PKUP V1053: Sub-Adult (7-Years-Old)

Anteriorly, the olfactory bulbs are attached to a stocky olfactory tract. Both bulbs measure 7.8 mm across (Table 4.2). There is a dural ridge running dorsally along the olfactory tract and the individual olfactory bulbs are not visible due to a thick dural envelope (Figure 4.5A, B). The olfactory bulbs appear to be thin in profile due to poor preservation along the ventral margin of the olfactory bulbs (Figure 4.5A).

The cerebrum is located just posterior to the olfactory tract and is roughly oval in shape when viewed dorsally (Figure 4.5A). Laterally, the cerebrum appears to be thin or dorsally compressed (Figure 4.5B) because of the poor preservation of the braincase floor present throughout most of the psittacosaur endocasts used in this chapter. Across its widest point, the cerebrum measures 19.6 mm (Figure 4.5A). Neither the longitudinal nor transverse fissures are viewable along the dorsal surface (Figure 4.5B).

The midbrain is unremarkable with no clear anatomy visible along it (Figure 4.5A, D). Since the dural envelope has thickened with age, and since the dural envelope greatly thickens along the midbrain (Jirak and Janacek, 2017), the usual anatomy visible (e.g. optic lobes) are not observable (Figure 4.5A, B). Ventrally, the infundibulum and pituitary are partially preserved, but the internal carotids are fully preserved (Figure 4.5A, C).

The hindbrain of PKUP V1053 is one of the most detailed cerebellar regions of all the psittacosaur endocasts reconstructed for this project. At its widest point, the cerebellum is 8.4 mm wide (Table 4.2). The dural expansion is situated dorsally to the cerebellum and sweeps back posteriorly (Figure 4.5A, B, D). The caudal middle cerebral vein protrudes from the apex of the dural expansion and is oriented posteriorly (Figure 4.5A-D). This vein is missing from the other endocasts due to the preservation and taphonomic distortion along the parietals. Inferior to the cerebellum is the flocculi (Figure 4.5D). The flocculi are nearly indistinguishable along the endocast, most likely due to the dura. They are only observable when the endocast is viewed posteriorly (Figure 4.5D). Posteriorly, the medulla oblongata is subtriangular in cross-section (Figure 4.5D).

Four cranial nerves are preserved along the endocast. Posterior to the pituitary, CN V protrudes mediolaterally (Figure 4.5A). Inferior to CN V, CN VI project anteriorly on both sides of the pituitary (Figure 4.5A, C). On the right side of the endocast, CN VII projects laterally and is located posterior to CN V. Mediolaterally, part of CN XII projects posteriorly from the medulla oblongata (Figure 4.5A, B, D).

The cephalic and pontine flexure of PKUP V1053 continues the trend established in IVPP V12731 in that the angles exceed the near 90° found in IVPP V15451 (Table 4.3).

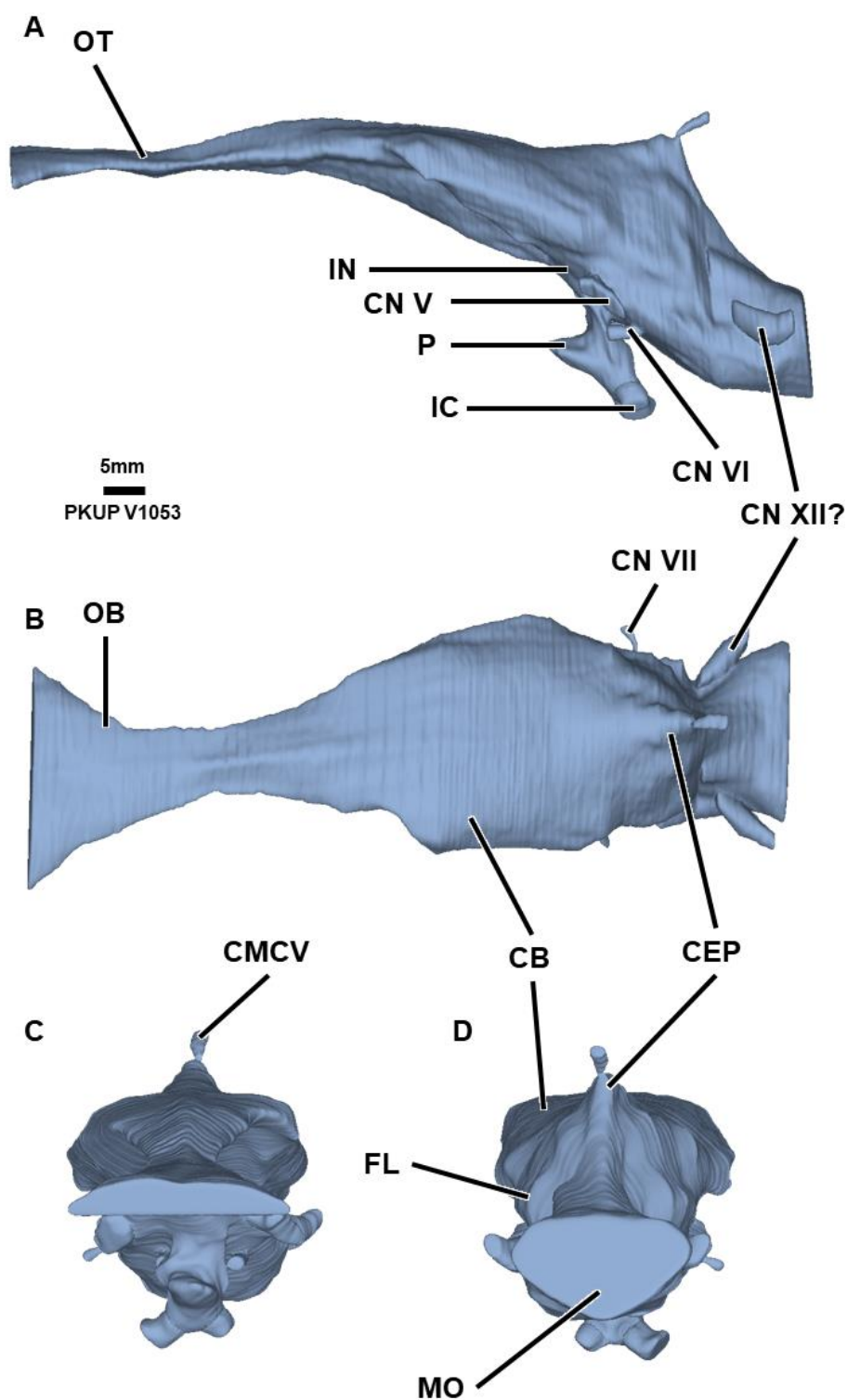


Figure 4.5 – Lateral (A), dorsal (B), anterior (C), and posterior (D) views of the segmented endocast of PKUP V1053. P, pituitary; CB, cerebellum; CE, cerebrum; IC, internal carotid artery; IN, infundibulum; FL, flocculus; MO, medulla oblongata; OB, olfactory bulb; OT, olfactory tract; CEP, cerebral protuberance; CMCV, caudal middle cerebral vein; CN V, trigeminal nerve; CN VI, abducens nerve; CN VII, facial nerve; CN XII?, hypoglossal nerve?

4.5.4 PKUP V1054: Sub-Adult (8-Years-Old)

The olfactory bulbs appear flattened due to the lack preservation along the ventral portion of the olfactory apparatus. The dorsal and lateral margins preserved the top and widths of the bulbs, respectively, giving an accurate idea of their true shape. Together, the olfactory bulbs measure 6.5 mm across (Table 4.2) the widest point and both are attached at the end of a thin olfactory tract (Figure 4.6A, B).

The longitudinal fissure between the cerebral hemispheres cannot be viewed due to the enlarged dural envelope around the cerebrum (Figure 4.6B). Dorsally, the cerebrum is triangular in shape and narrows in width towards the olfactory tract (Figure 4.6B). Ventrally, along the forebrain and midbrain junction, the only nucleation point of CN II in all the psittacosaur endocasts (Figure 4.6A). The partially preserved CN II projects anteriorly, would have diverged, entered the orbits through a foramen, and terminated at posterior margin of the eyes.

As with most endocasts from older psittacosaurid specimens, not much surface anatomy can be viewed along the midbrain, and this is especially true with PKUP V1054. The locations of the optic lobes are completely indistinguishable. Ventrally, a faint infundibulum along the floor of the endocast is visible, but the pituitary and internal carotid arteries were not preserved (Figure 4.6A, C).

The hindbrain preserves the most endocranial anatomy of PKUP V1054. Dorsally, the cerebellum is narrow, measures 19.5 mm across and its widest point (Table 4.2), and merges seamlessly with the dural expansion posteriorly (Figure 4.6A, B, D). Mediolaterally, floccular lobes create small protuberances but not much can be told about how small or large the flocculi are due to the influence of the dural expansion (Figure 4.6B, D). Posteriorly, the medulla oblongata is quasi-diamond shaped (Figure 4.6D).

Broadly speaking, the endocast of PKUP V1054 has very little peripheral anatomy preserved when compared to other endocasts (e.g. IVPP V12617, Figure 4.7). Not much taphonomic distortion is present so the flexure angles are very well-preserved (Figure 4.6A; Table 4.3). The cephalic and pontine flexure is 133.9° and 140.1°, respectively. A slight reduction in flexure indicates that, since the seventh year of age, *P. lujiatunensis* begins to rearrange its endocranial morphology.

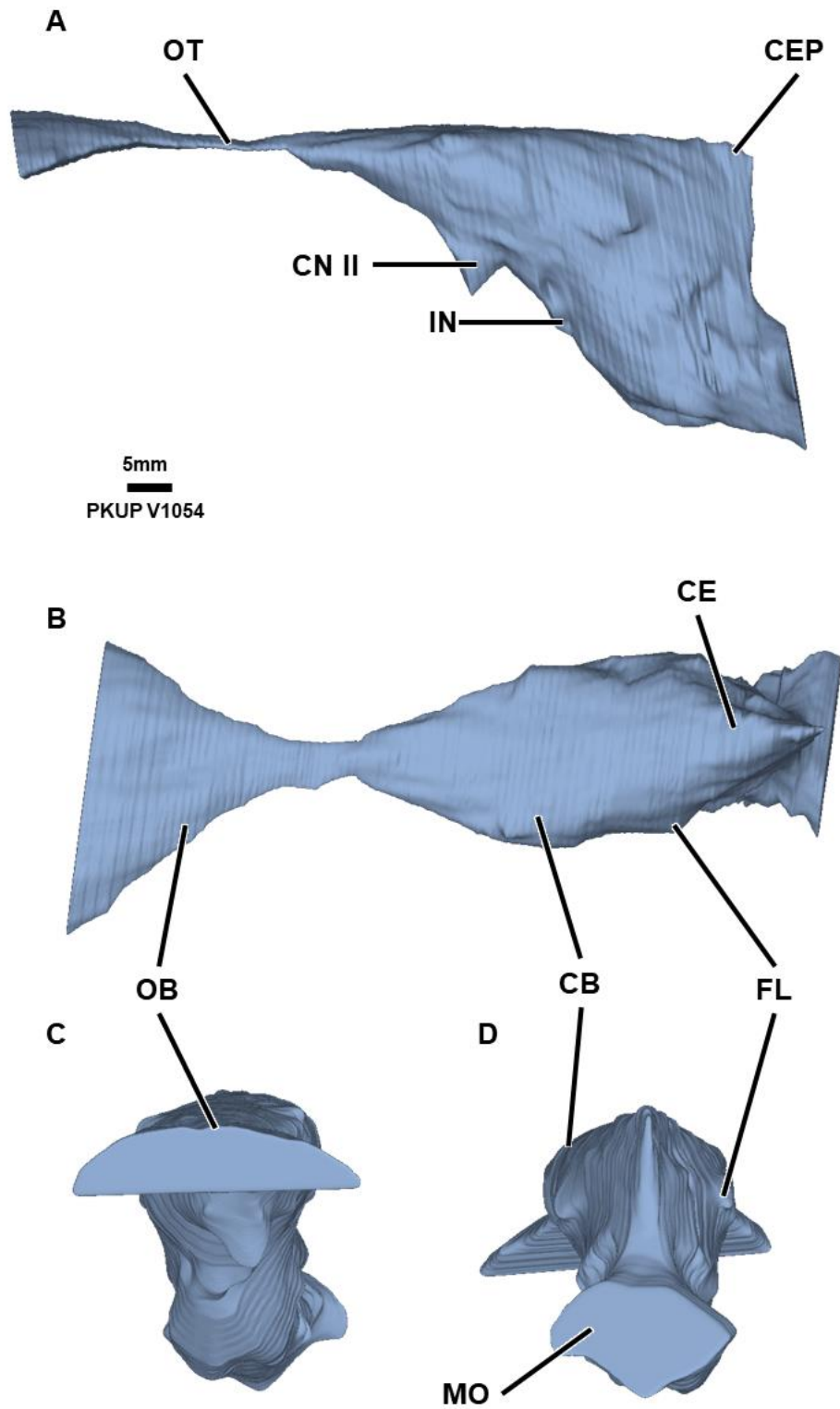


Figure 4.6 – Lateral (A), dorsal (B), anterior (C), and posterior (D) views of the segmented endocast of PKUP V1054. CB, cerebellum; CE, cerebrum; IN, infundibulum; FL, flocculus; MO, medulla oblongata; OB, olfactory bulb; OT, olfactory tract; CEP, cerebral protuberance; CN II, olfactory nerve

4.5.5 IVPP V12617: Adult (10-Years-Old)

The olfactory bulbs of IVPP V12617 measures 10.4 mm across (Figure 4.7A, Table 4.2) and seamlessly merges into the nasal cavity. Posteriorly, the olfactory tract attaches directly to the anteriormost margin of the cerebrum, but it is offset left laterally when viewed dorsally (Figure 4.7B). Aside from the ventral part of the midbrain, the slightly offset olfactory tract is the only distorted section of the endocast.

The cerebrum ends abruptly anteriorly at the meeting point between the cerebrum and olfactory apparatus (as seen in Napoli et al., (2019); Figure 4.7B). Dorsally, the cerebrum has lost the pyriform or diamond shape observed in the younger specimens. Neither cerebral hemisphere nor the longitudinal fissure is viewable; most likely due to the increase in thickness of the dural envelope (Figure 4.7B). Across the widest point of the cerebrum, the dorsal surface, it measures 24.3 mm across (Table 4.2).

Along the midbrain, not much is viewable – again, most likely due a developed dural envelope. The only viewable midbrain anatomy is ventrally oriented. The infundibulum is short but stocky and attaches to an enlarged pituitary (Figure 4.7B). Inferior to the pituitary are the internal carotid arteries which diverge at a sub-90° angle (Figure 4.7C). The right lateral half of the ventral midbrain anatomy is the poorly preserved, but the left half is preserved well enough that anatomy can be identified (Figure 4.7C).

Hindbrain anatomy is very well-preserved (Figure 4.7D). Dorsally, the cerebellum merges seamlessly with the cerebrum anteriorly and sweeps posteriorly to an elongated dural expansion – though IVPP V12617 lacks a caudal middle cerebral vein on the apex of the dural expansion (Figure 4.7B, D). The flocculi are mediolaterally oriented and appear to be reduced when compared to the younger specimens, especially IVPP V15451 and IVPP V12731 (Figure 4.4A vs. Figure 4.7A). Measuring how absolute the reduction in the flocculi size is in IVPP V12617 is impossible to measure since the dural envelope increases in size with age. Posteriorly, the medulla oblongata is roughly oval in shape (Figure 4.7D).

Peripheral anatomy is best preserved in IVPP V12617. A total of four cranial nerves are preserved with all being located along the hindbrain (Figure 4.7A-D). Posterior to the infundibulum and pituitary, CN V is partially preserved on both sides. Both CN VI are preserved just inferior to CN V. Posterior to both CN V and CN VI are both CN VII. Further posterior and just anterior to the medulla oblongata are two branches of CN XII (Figure 4.7A-D).

Flexure angles along IVPP V12617 have returned to the near 90° cephalic and pontine flexure found in IVPP V15451 (Table 4.3),

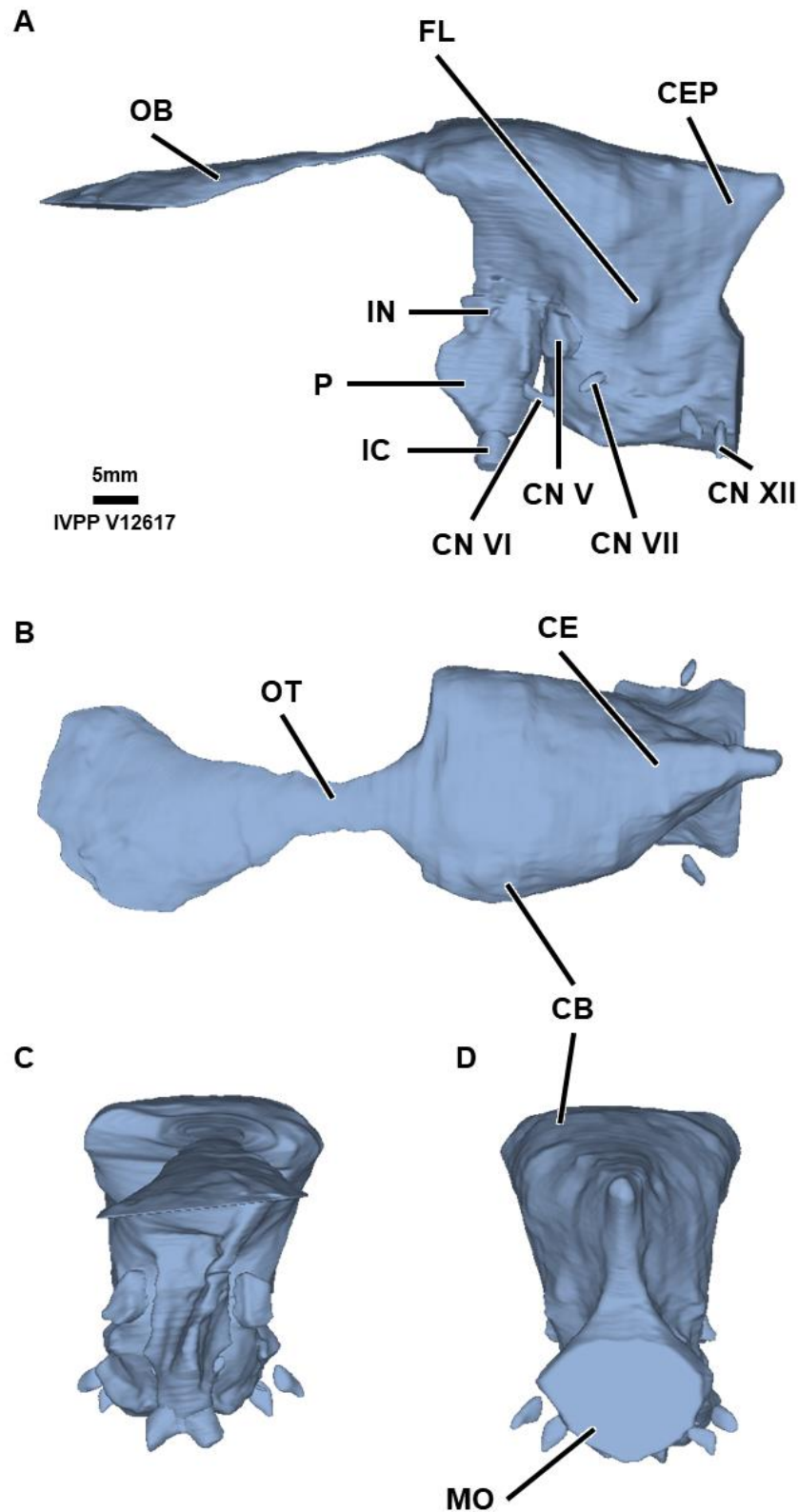


Figure 4.7 – Lateral (A), dorsal (B), anterior (C), and posterior (D) views of the segmented endocast of IVPP V12617. P, pituitary; CB, cerebellum; CE, cerebrum; IC, internal carotid artery; IN, infundibulum; FL, flocculus; MO, medulla oblongata; OB, olfactory bulb; OT, olfactory tract; CEP, cerebral protuberance; CN V, trigeminal nerve; CN VI, abducens nerve; CN VII, facial nerve; CN XII, hypoglossal nerve

4.6 Olfactory, Cerebral, and Cerebellar Shifts in the Species and Their Implications

4.6.1 Olfactory Growth

The olfactory capabilities of organisms are, in palaeoneurology, gauged by the size of the olfactory bulbs (Witmer and Ridgely, 2009; Zelenitsky et al., 2009, 2011). In life, the olfactory bulbs contain mitral cells – cells that gather scent data – that gather scent data from the nasal cavity through olfactory receptors and send it further into the brain along mitral axons (i.e. the olfactory tract) (Blanchart et al., 2006; Muroyama et al., 2016). Grigg et al. (2012) found that this anatomy is the same in birds and even increases by up in organisms that depend on carrion for their food – thus demonstrating that, in animals that require a high olfactory acuity, large olfactory bulbs are key for success. The subadult endocast of *Psittacosaurus lujiatunensis* has demonstrated that, for its size, the species had an olfactory bulb size comparable to large-bodied theropods (Zhou et al., 2007). Ecologically, the need for a high olfactory acuity within *P. lujiatunensis* can be debated as an adaptation to an herbivorous diet or for predator avoidance. Regardless of the need for acute olfaction, recent research shows that the species had, at least in almost mature individuals, large olfactory bulbs (Zhou et al., 2007).

The olfactory bulbs of birds are notably reduced when compared to other archosaur taxa (Wenzel, 1971, 1987) (see Chapter 3) – with the notable exception being carrion eating birds (e.g. Cathartidae) where the olfactory bulbs are massive relative to the rest of the brain (Grigg et al., 2012). Stable, enlarged olfactory bulbs are reflected in this study in that there is very little absolute change in the widths of the olfactory bulbs among birds (Table 4.4). Crocodilians are almost the exact opposite of birds in that their olfactory bulbs experience a much larger change throughout ontogeny (Figure 4.8). When compared to extant archosaurs, *P. lujiatunensis* displays olfactory bulbs growth patterns that are much more similar to crocodilians than birds where the olfactory bulbs are enlarged early in life and continue to increase throughout the life of the species (Figure 4.8). Zhou et al. (2007) explains that, in predacious dinosaurs, enlarged olfactory bulbs reflect a higher reliance on olfaction. When the olfactory bulbs of *Tyrannosaurus rex* were measured and plotted as a function age, the growth pattern and trendline are nearly identical to that of *P. lujiatunensis* (Figure 4.8).

Table 4.4 – Age and olfactory bulb width data (with logarithmically corrected values for both) for ostriches, chickens, alligators, caiman, and *Psittacosaurus*, respectively, used throughout this project. Another dinosaur, *Tyrannosaurus*, was added to test how closely the absolute and normalised widths of large-bodied predacious theropods compare with those of *P. lujiatunensis*.

Taxon	Age	Log ₁₀ Age	Olf. Bulb Width (mm)	Log ₁₀ Olf. Bulb Width
<i>Struthio camelus</i>	2 weeks	-1.420216403	3.6	0.55594044
<i>Struthio camelus</i>	4 weeks	-1.113509275	3.7	0.56749689
<i>Struthio camelus</i>	12 weeks	-0.63638802	3.4	0.52504481
<i>Struthio camelus</i>	5 months	-0.379863945	2.7	0.43216727
<i>Struthio camelus</i>	3 years	0.477121255	3.3	0.51995918
<i>Gallus gallus</i>	1 day	-2.522878745	1.5	0.17926446
<i>Gallus gallus</i>	30 days	-1.096910013	2.8	0.44388855
<i>Gallus gallus</i>	46 days	-0.886056648	3.4	0.53135116
<i>Gallus gallus</i>	86 days	-0.638278164	2.8	0.44932409
<i>Gallus gallus</i>	119 days	-0.48148606	2.0	0.29994290
<i>Alligator mississippiensis</i>	<1 month	-1.301029996	2.8	0.44059426
<i>Alligator mississippiensis</i>	10 months	-0.079354999	5.8	0.76027166
<i>Alligator mississippiensis</i>	1 year	0	7.1	0.84923509
<i>Alligator mississippiensis</i>	4 years	0.602059991	8.6	0.93555765
<i>Alligator mississippiensis</i>	5+ years	0.698970004	8.6	0.93227078
<i>Caiman crocodilus</i>	2 years	0.301029996	5.7	0.75694024
<i>Caiman crocodilus</i>	3 years	0.477121255	11.1	1.07921744
<i>Caiman crocodilus</i>	7 years	0.84509804	12.0	1.07921744
<i>Psittacosaurus lujiatunensis</i>	<1 year	-0.037630664	3.8	0.58331215
<i>Psittacosaurus lujiatunensis</i>	2 years	0.301029996	5.4	0.72916479
<i>Psittacosaurus lujiatunensis</i>	7 years	0.84509804	7.8	0.89181612
<i>Psittacosaurus lujiatunensis</i>	8 years	0.903089987	6.5	0.81190998
<i>Psittacosaurus lujiatunensis</i>	10 years	1	10.4	1.01527591
<i>Tyrannosaurus rex</i>	7 years	0.84509804	33.5	1.52439612
<i>Tyrannosaurus rex</i>	20 years	1.301029996	50.7	1.70500796
<i>Tyrannosaurus rex</i>	23 years	1.361727836	51.7	1.71332250
<i>Tyrannosaurus rex</i>	28 years	1.447158031	46.3	1.66595603

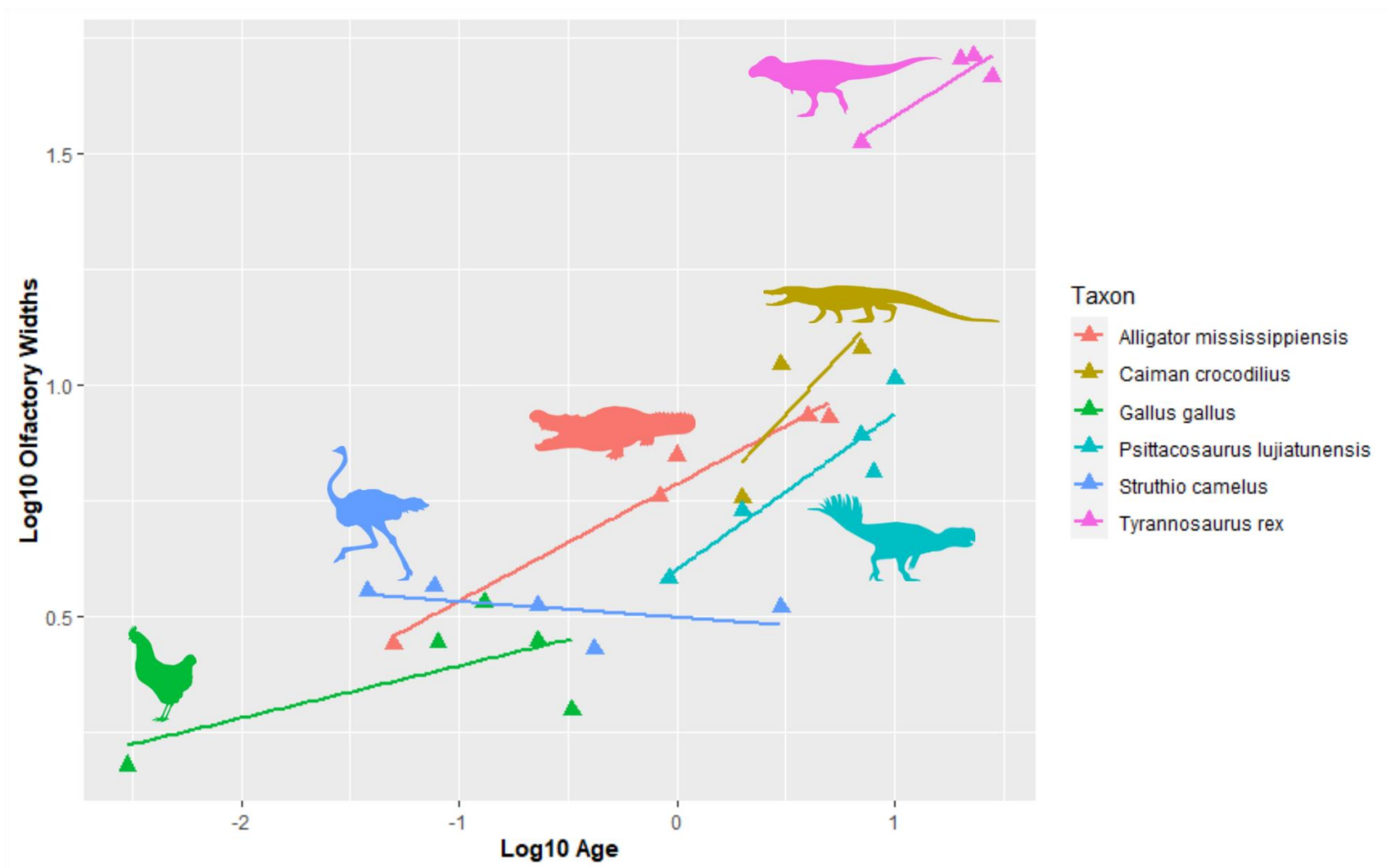


Figure 4.8 – Logarithmically normalised widths of *Psittacosaurus lujiatunensis* olfactory bulbs compared with birds (*Struthio camelus* and *Gallus gallus*) and crocodilians (*Alligator mississippiensis* and *Caiman crocodilus*). The tyrannosaurid *Tyrannosaurus rex* was added to give a sense of how the olfactory bulbs from *P. lujiatunensis* developed when compared to large-bodied, predacious theropod.

4.6.2 Cerebrum Development

The cerebrum is the centre of processing neurosensory information collected from around the body and where sensory data in this project are interpreted. This includes collection and interpretation of hearing (Kettler and Carr, 2019), cognitive function (Briscoe et al., 2018), and olfaction. Typically, measurements across the cerebrum are interpreted as the total width of both cerebral hemispheres (e.g. Franzosa and Rowe, 2005; Witmer and Ridgely, 2009; Lautenschlager et al., 2012; Lautenschlager and Hübner, 2013; Cruzado-Caballero et al., 2015). The cerebrum is variable in both absolute size and relative size when compared to the total endocranial length. Not enough ontogenetic series of dinosaurian taxa have been compared prior to this study to understand what absolute cerebrum width increases mean between ontogenetic stages of any given dinosaur. Prior to this study, only one other study had measured the cerebrum from more than one ontogenetic stage of a single species (Lautenschlager and Hübner, 2013).

Chickens and ostriches have enlarged cerebral widths when compared to the rest of the taxa used in this study in terms of absolute size. Of the two, ostriches have the largest cerebral width as well as the largest increase in size during their ontogenetic development by a small margin (Table 4.5). Adult chickens and birds have a cerebrum that is 92.3% and 70.5% the total length of the endocranial length, a typical trait in birds where the cerebrum is exaggerated in size (Larsson et al., 2000; Bever et al., 2011; Balanoff et al., 2014). The crocodylians have smaller cerebra than the birds – to the point that the adult alligator's cerebrum does not reach the size of the one found in the youngest juvenile ostrich (Figure 4.9; Table 4.5). While the ontogenetic series is incomplete in the caiman, the trend is continued where the cerebrum is still not as large as the one found in some of the chickens and never reaches the size of the cerebra found in ostriches (Figure 4.9; Table 4.5). As expected, the cerebrum-to-endocranial length ratio is much smaller in alligators and caiman than birds at 18.2% and 29.7%, respectively. *P. lujiatunensis* has an interesting relationship between all of the other taxa measured in that the cerebral width of the juvenile is similar in size to a juvenile alligator, however, the adult's cerebrum is larger than that of the oldest chicken used in the study (Figure 4.9; Table 4.5). In other words, even though a juvenile *P. lujiatunensis* has a cerebrum with an absolute width comparable to a juvenile alligator, an adult exceeds expectations by being more comparable to at least some adult birds than adult basal archosaurs. This also means that the non-avian *P. lujiatunensis* experiences a much more dynamic cerebral expansion than birds and crocodylians throughout its life – a fact that is clear when the normalised width values are plotted against normalised ages of individuals (Figure 4.9). Even with its explosive cerebral expansion, *P. lujiatunensis* does follow the

typical non-avian archosaur trend of having a small cerebrum-to-endocranial length as an adult at only 31.2%.

An enlarged cerebrum, and hence heightened ability to interpret surround sensory input, is not surprising in young *P. lujiatunensis* in light of evidence for complex behaviour in the fossil record (Zhao et al., 2013a). It is possible that enlarged cerebra in juvenile psittacosaurids may be linked with niche partitioning, age segregation, or tangentially related with locomotion (Zhao et al., 2013a; Zhao et al., 2013b). Postulating or linking what size disparities in the cerebrum means for *P. lujiatunensis* is difficult to do as identifying meaningful behaviour differences in brain size of modern animals is challenging. Since the cerebrum is used in integrating information gathered from the other brain regions, the only way to gauge how changes in behaviour correspond with age and brain growth would be to directly observe behaviour in *P. lujiatunensis*. Since direct observations of behaviour are impossible in the fossil record, the cerebral size differences between the specimens of this chapter are best left interpreted as purely ontogenetic (see Chapter 5 for more details on ontogeny and the non-avian dinosaur brain).

Table 4.5 – Age and cerebral width data (with logarithmically corrected values for both) for ostriches, chickens, alligators, caiman, and *Psittacosaurus*, respectively, used throughout this project.

Taxon	Age	Log ₁₀ Age	Cerebrum Width (mm)	Log ₁₀ Cerebrum Width
<i>Struthio camelus</i>	2 weeks	-1.420216403	26.2	1.41859956
<i>Struthio camelus</i>	4 weeks	-1.113509275	31.7	1.50094965
<i>Struthio camelus</i>	12 weeks	-0.63638802	32.3	1.50945791
<i>Struthio camelus</i>	5 months	-0.379863945	29.1	1.46438521
<i>Struthio camelus</i>	3 years	0.477121255	33.4	1.52386348
<i>Gallus gallus</i>	1 day	-2.522878745	15.2	1.18061325
<i>Gallus gallus</i>	30 days	-1.096910013	20.0	1.30202773
<i>Gallus gallus</i>	46 days	-0.886056648	24.0	1.38013885
<i>Gallus gallus</i>	86 days	-0.638278164	24.5	1.38897105
<i>Gallus gallus</i>	119 days	-0.48148606	21.9	1.3397892
<i>Alligator mississippiensis</i>	<1 month	-1.301029996	11.0	1.0413532
<i>Alligator mississippiensis</i>	10 months	-0.079354999	15.4	1.18760532
<i>Alligator mississippiensis</i>	1 year	0	18.9	1.27721943
<i>Alligator mississippiensis</i>	4 years	0.602059991	12.6	1.09992223
<i>Alligator mississippiensis</i>	5+ years	0.698970004	14.1	1.14955779
<i>Caiman crocodilius</i>	2 years	0.301029996	16.5	1.21698356
<i>Caiman crocodilius</i>	3 years	0.477121255	19.2	1.28366299
<i>Caiman crocodilius</i>	7 years	0.84509804	21.0	1.32221929
<i>Psittacosaurus lujiatunensis</i>	<1 year	-0.037630664	10.5	1.02102382
<i>Psittacosaurus lujiatunensis</i>	2 years	0.301029996	14.3	1.15563963
<i>Psittacosaurus lujiatunensis</i>	7 years	0.84509804	19.6	1.29254403
<i>Psittacosaurus lujiatunensis</i>	8 years	0.903089987	19.5	1.29007915
<i>Psittacosaurus lujiatunensis</i>	10 years	1	24.3	1.38535599

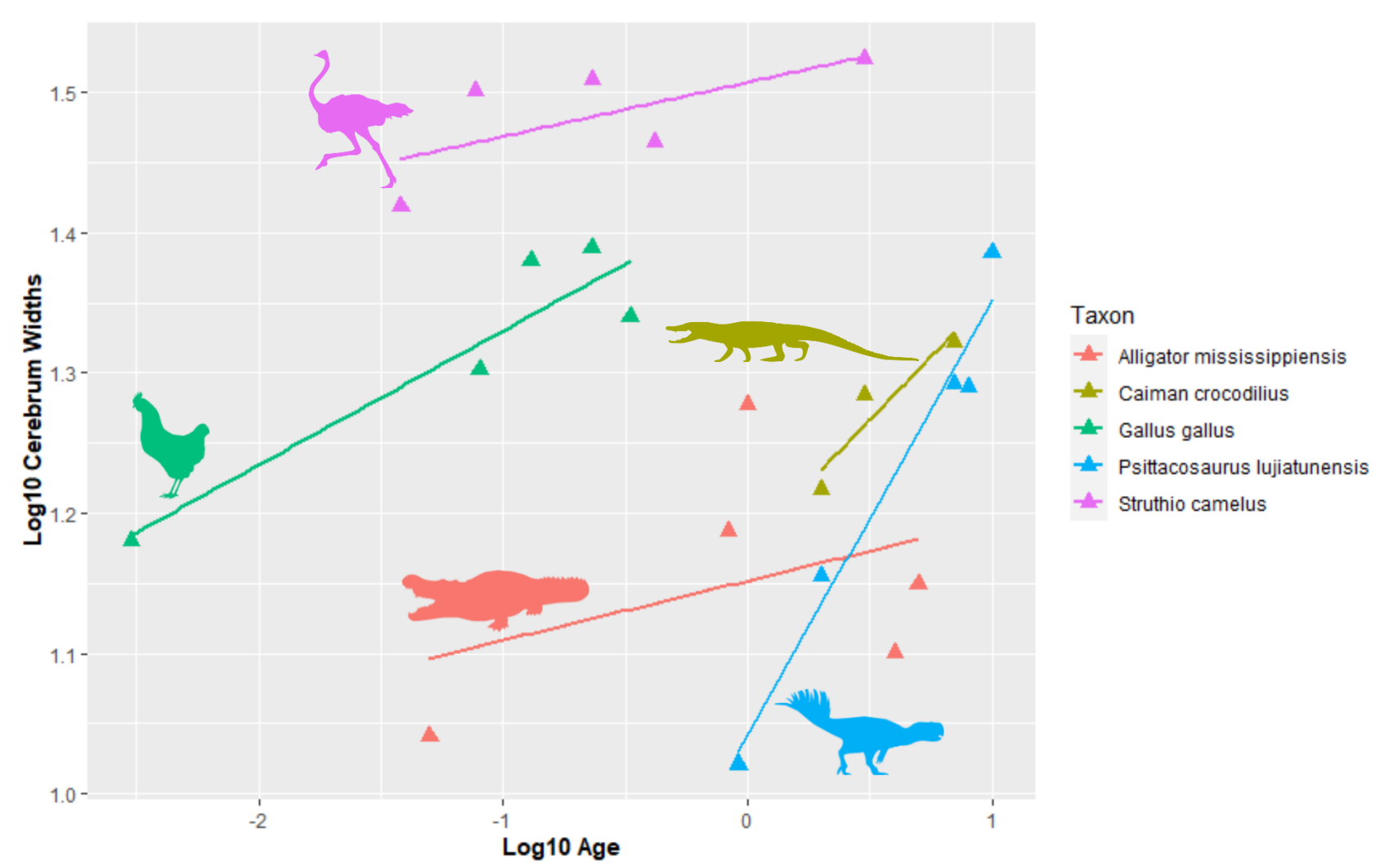


Figure 4.9 – Logarithmically normalised widths of *Psittacosaurus lujiatunensis* cerebra compared with birds (*Struthio camelus* and *Gallus gallus*) and crocodilians (*Alligator mississippiensis* and *Caiman crocodilus*).

4.6.3 Growth of the Cerebellum

The hindbrain region of endocasts is comprised of multiple parts that control various aspects of balance, speed, and hearing in life. Hearing and balance data are collected and transmitted by the vestibular portion of the inner ear and CN VIII, respectively. The cerebellum works with the cerebrum to create a sense of perception, control motor skills, and understand where the body and head are in a 3D space (Paulin, 1993; Wilson et al., 1995; Benson et al., 2017; Beckinghausen and Sillitoe, 2019). The inner ears of *P. lujiatunensis* are a part of the braincase and have been the focus of a previous ontogenetic study (Bullar et al., 2019), they were excluded from this project.

The cerebellar region of chickens and ostriches are, expectedly, typically wider than either crocodilian (Figure 4.10, Table 4.6) with chickens have narrower cerebral widths than ostriches. Both have a fairly steady increase in cerebellar widths with time, but the cerebrum never doubles in size. The cerebellar region of the endocast is 38.5% and 39.7% the width of the cerebrum in chickens and ostriches, respectively. Alligators and caiman show a general trend in cerebellar growth but have smaller widths. Caiman are the only crocodilian used in the study that are as large as birds and even then, only the largest caiman specimen had a cerebellum width close to a chicken in size (Figure 4.10). Both alligators and caiman have a higher cerebellum-to-cerebrum width ratio when compared to birds with 47.6% and 45.5%, respectively. The difference in cerebellum-to-cerebrum ratios is due to the smaller cerebrum found in non-avian archosaurs. The cerebellar width of the *P. lujiatunensis* specimens' doubles over ontogeny – a trait that is more similar to crocodilians than birds (Table 4.6), however, the absolute widths are closer to birds. Similarities between cerebellar regions are made clear when the normalised cerebellar values are compared among taxa (Figure 4.10).

Table 4.6 – Age and cerebellar width data (with logarithmically corrected values for both) for ostriches, chickens, alligators, caiman, and *Psittacosaurus*, respectively, used throughout this project.

Taxon	Age	Log ₁₀ Age	Cerebral Width (mm)	Log ₁₀ Cerebral Width
<i>Struthio camelus</i>	2 weeks	-1.420216403	10.4	1.01811772
<i>Struthio camelus</i>	4 weeks	-1.113509275	12.5	1.09558775
<i>Struthio camelus</i>	12 weeks	-0.63638802	19.0	1.27843348
<i>Struthio camelus</i>	5 months	-0.379863945	12.3	1.09106873
<i>Struthio camelus</i>	3 years	0.477121255	13.3	1.12247801
<i>Gallus gallus</i>	1 day	-2.522878745	6.2	0.79155031
<i>Gallus gallus</i>	30 days	-1.096910013	7.8	0.8925398
<i>Gallus gallus</i>	46 days	-0.886056648	8.8	0.94438396
<i>Gallus gallus</i>	86 days	-0.638278164	9.3	0.96717342
<i>Gallus gallus</i>	119 days	-0.48148606	8.4	0.82556991
<i>Alligator mississippiensis</i>	<1 month	-1.301029996	3.6	0.55870857
<i>Alligator mississippiensis</i>	10 months	-0.079354999	7.5	0.8736112
<i>Alligator mississippiensis</i>	1 year	0f	8.8	0.94448267
<i>Alligator mississippiensis</i>	4 years	0.602059991	6.6	0.81637389
<i>Alligator mississippiensis</i>	5+ years	0.698970004	6.7	0.82749851
<i>Caiman crocodilius</i>	2 years	0.301029996	4.9	0.6863681
<i>Caiman crocodilius</i>	3 years	0.477121255	7.4	0.86646457
<i>Caiman crocodilius</i>	7 years	0.84509804	9.7	0.98533664
<i>Psittacosaurus lujiatunensis</i>	<1 year	-0.037630664	7.8	0.89030922
<i>Psittacosaurus lujiatunensis</i>	2 years	0.301029996	9.1	0.96047078
<i>Psittacosaurus lujiatunensis</i>	7 years	0.84509804	8.4	0.92551836
<i>Psittacosaurus lujiatunensis</i>	8 years	0.903089987	11.6	1.06531824
<i>Psittacosaurus lujiatunensis</i>	10 years	1	15.3	1.18378215

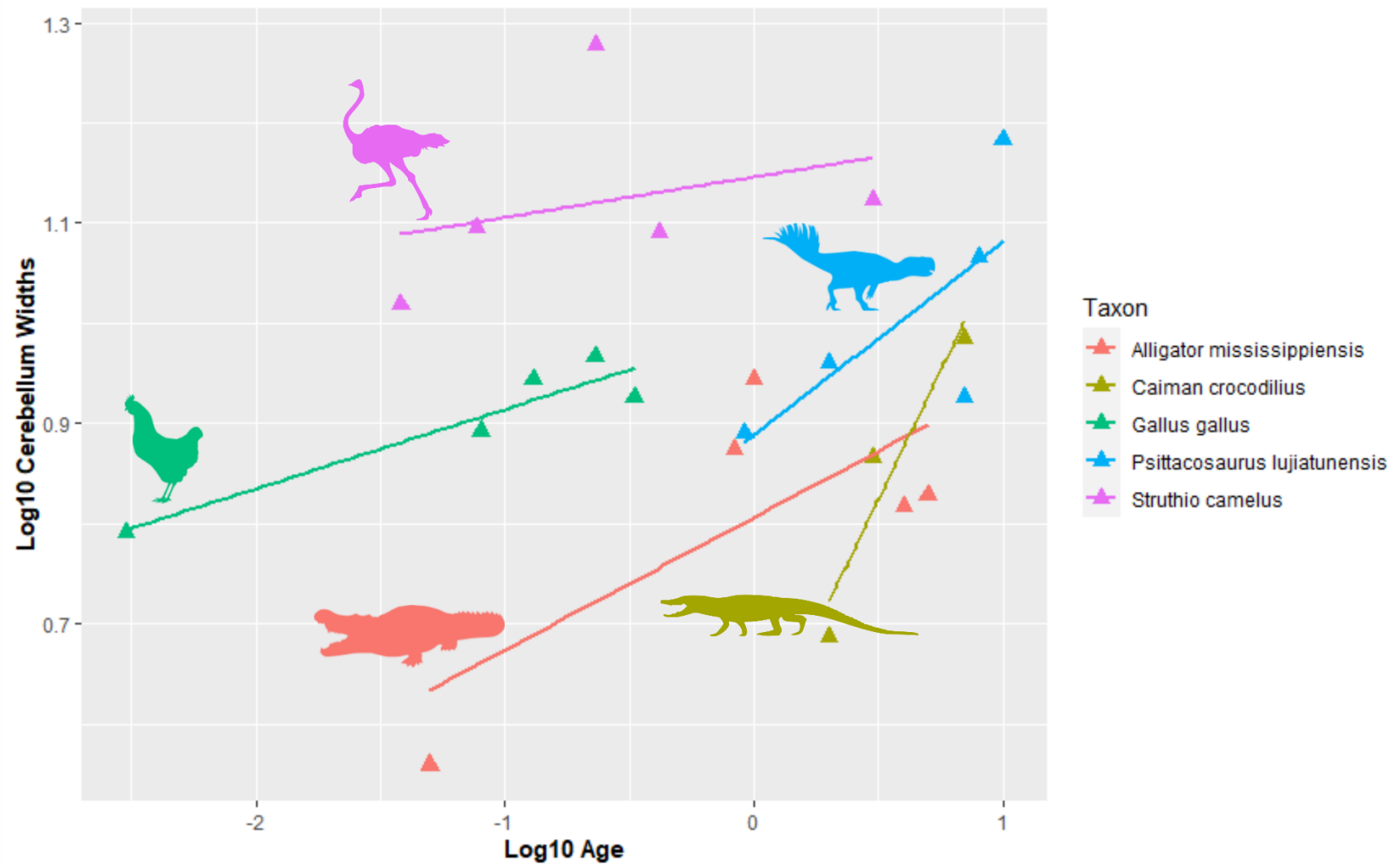


Figure 4.10 – Logarithmically normalised widths of *Psittacosaurus lujiatunensis* cerebellar regions compared with birds (*Struthio camelus* and *Gallus gallus*) and crocodilians (*Alligator mississippiensis* and *Caiman crocodilus*).

4.7 Endocranial Flexure and the Variable Morphology of the *Psittacosaurus*

Endocast

One of the most interesting aspects of the *P. lujiatunensis* endocast through ontogeny is that it does not reflect the patterns of flexure change observed in exemplar archosaurs (see Chapter 3). Rather than continually expanding the flexure angles or maintaining similar flexure values through life, the cephalic and pontine flexure of *P. lujiatunensis* begins as near 90°, expands to approximately 140° in juvenile and subadult stages, and returns to near 90° at somatic maturity. This elongation and then contraction of flexure diverges from modern archosaurs where cephalic and pontine flexures follow specific patterns along phylogenetic relationships (e.g. alligators always elongate their endocasts with ontogeny; see Chapter 3). Evidence shows that members of Dinosauria had much more variable endocranial flexure angles than extant archosaurs (Figure 4.11, 4.10), It is too early to say if flexure patterns found in non-avian dinosaurs are phylogenetic, osteological, or ecomorphological in nature due to too many gaps in the ontogenetic fossil record.

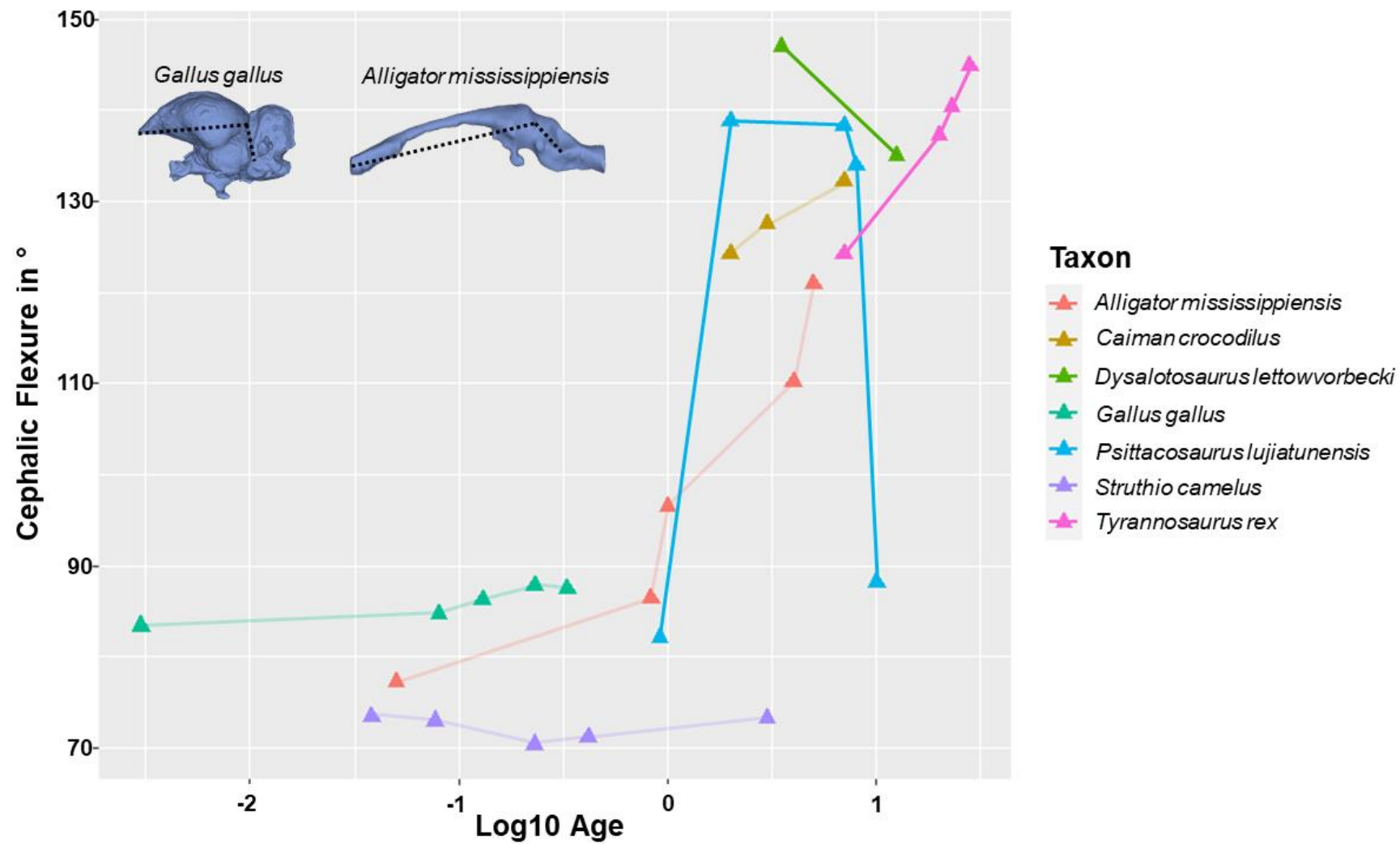


Figure 4.11 – Cephalic flexure angles (in degrees) plotted against logarithmically corrected ages of crocodilians, birds, and non-avian dinosaurs – *P. lujiatunensis* included.

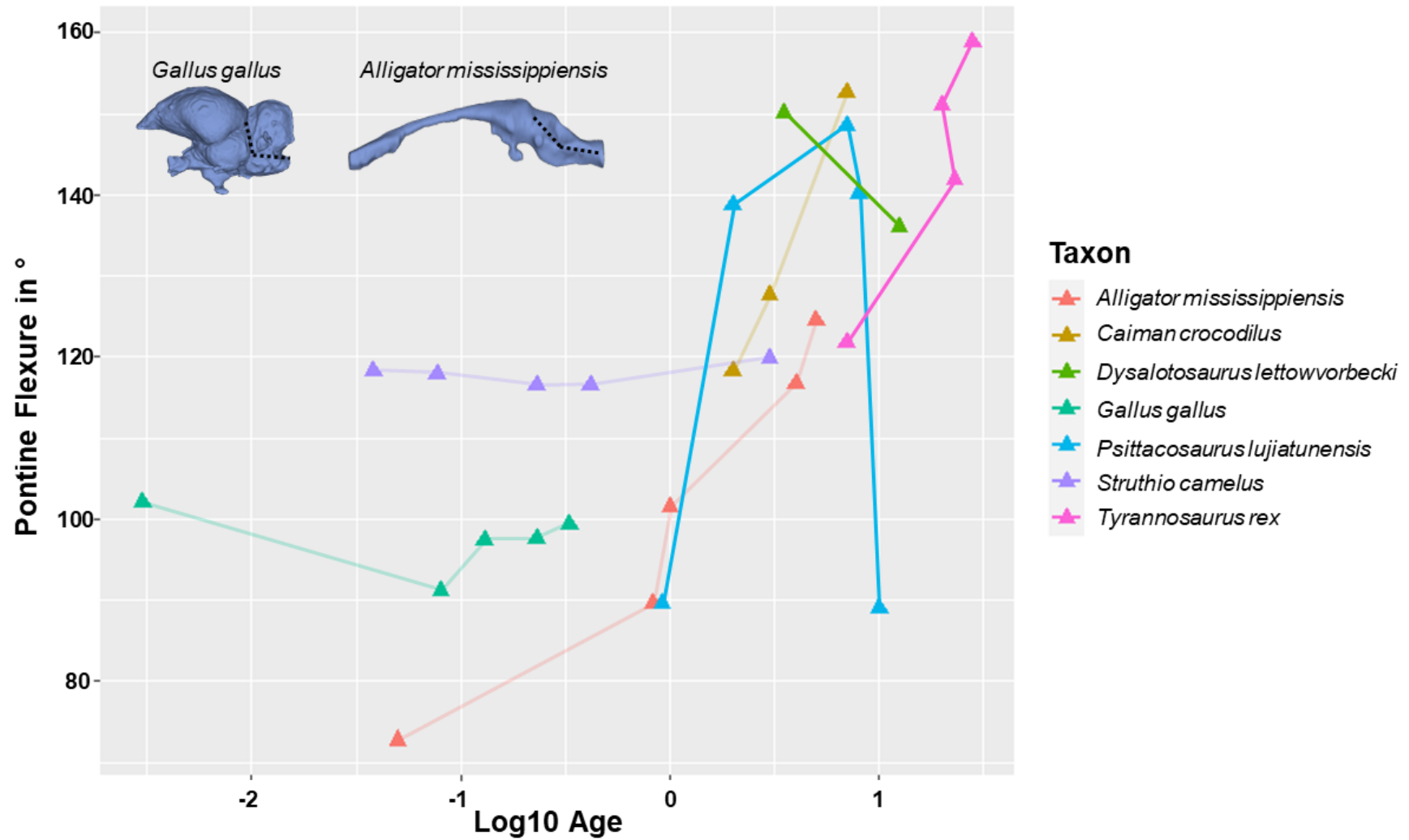


Figure 4.12 – Pontine flexure angles (in degrees) plotted against logarithmically corrected ages of crocodilians, birds, and non-avian dinosaurs – *P. lujiatunensis* included. Note that angles are similar between cephalic flexure angles from the same species of the same ontogenetic stages, however, neither flexure angle of non-avian dinosaurs do not always reliably favour other archosaur taxa.

Variation in the psittacosaur endocranial morphology indicates that, just because exemplar archosaurs demonstrate certain flexure traits throughout ontogeny, the same should not be expected from all members of Archosauria in the fossil record. Zhou et al. (2007), for example, used PKUP V1053 to represent *P. lujiatunensis* in a phylogeny of ceratopsian dinosaurs for endocranial evolution (Figure 4.8). It is now understood, however, that PKUP V1053 is not a somatically mature adult and therefore does not represent a fully developed endocranial; a specimen like IVPP V12617 should be used to represent the complete *P. lujiatunensis* (Figure 4.13). Knowing this, the implications for our understanding of archosaurian endocranial evolution are huge. Without taking ontogeny into account, a misrepresentation of an endocranial's anatomy and morphology will be made and potentially mislead macroevolutionary studies in the future.

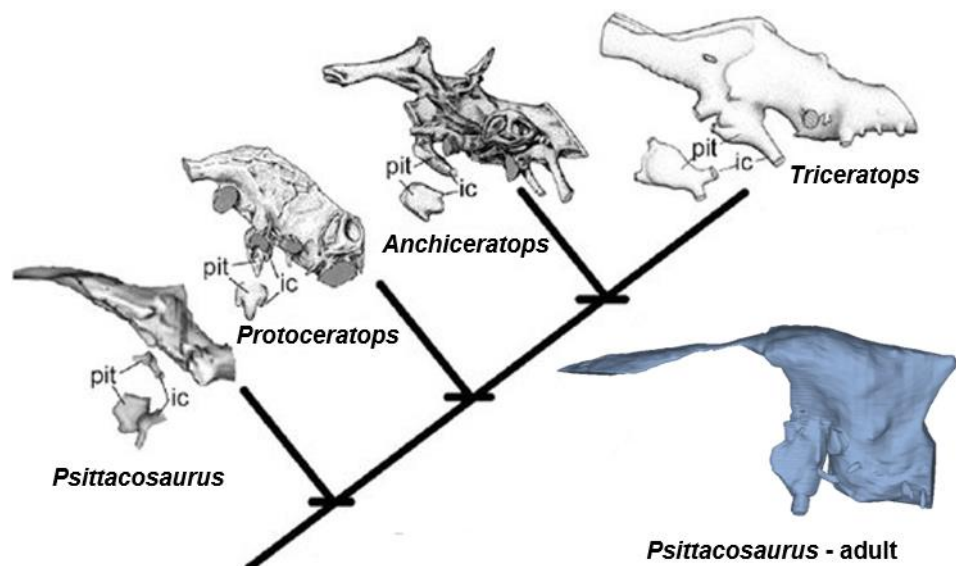


Figure 4.13 – Cladogram modified from Zhou et al. (2007) that shows how PKUP V1053's endocranial fits with others within Ceratopsia. PKUP V1053 has been found to be a subadult based on osteohistology and does not reflect the morphology that should be expected in an adult such as IVPP V12617 (blue).

4.8 Conclusions

Comparisons between sub-yearling, juvenile, subadult, and adult *Psittacosaurus lujiatunensis* endocranial anatomy indicate that the morphology was highly variable and the endocranials share traits with both birds and crocodilians. Most notably, the ontogenetic changes can be summarised as (i) the olfactory bulbs are always large and continue to increase in size, (ii) the cerebrum is as wide as a chicken's in a sub-yearling psittacosaur but the cerebrum-to-endocranial length ratio lessens with time, (iii) the cerebellum increases in width throughout

the life of *P. lujiatunensis*, and (iv) the cephalic and pontine flexure angles of the endocast “unfold” and “refold” as the endocranium elongates and reshapes itself.

The relationships between the neurosensory widths taken for this project and their implication for behaviour and neurosensory ability are difficult to discern by themselves; however, postcranial remains, cranial osteology, and interspecies comparisons help to interpret what increases along the neurosensory lobes mean for *P. lujiatunensis*. For instance, the olfactory bulb width of the youngest *P. lujiatunensis* is larger than that found in either bird from any ontogenetic stage used in this study. By the time psittacosaur reaches adulthood, the olfactory bulbs more than triple in size. This tripling of size allows for additional area where more mitral cells can form within the olfactory bulb and more olfactory receptors within the epithelium can collect scent data in the nasal cavity. An increase in olfactory size translates to an increase in olfactory acuity as the olfactory bulbs increased with age. This supports the results found in Zelenitsky et al. (2009) where olfactory acuity was expressed as the ratio between the greatest width of the olfactory bulbs and cerebrum in theropods. In this study, the olfactory bulb widths are much smaller than theropods (in both absolute and normalised terms) but were very comparable to crocodilians (Fig 4.6). Since olfaction is an important aspect of extant crocodilians based on their large olfactory bulbs (Hu et al., 2021) and a nasal cavity that is almost completely lined with olfactory epithelium (Hansen, 2007).

Of all three neurosensory portions of the *P. lujiatunensis* endocast that were measured, the cerebrum is the most difficult to interpret in terms of implications for changes in developmental behaviour or palaeoecology. Difficulty in interpreting the cerebrum is, in part, due to the cerebrum being a collection point and processing centre for sensory data from all over the brain. Large changes that occur in the size of the cerebrum can be attributed to more acute or faster processing speed due to more neurons available to interpret sensory data. What cerebrum size means for *P. lujiatunensis*, whose ontogenetic cerebral size shift is the largest in any archosaur used in this project, is debatable but can possibly be related to changes in behaviour through time. *P. lujiatunensis* is one of the few dinosaurs for which there is sufficient evidence of changes in both postural and social behaviour during ontogeny (Zhao et al., 2013). Considering the amount of increase that happens in the cerebrum of *P. lujiatunensis*, it is possible that changes in senses, sociality, or behaviour may have necessitated a larger, more effective area of the brain to process new sensory data input. Sociality and behaviour associated with the cerebrum are difficult to measure due to the inability to directly observe behavioural changes in the fossil record and due to the understudied nature of ontogeny's effect on hemispheric anatomy in modern archosaurs. So, in summary, the enormous growth of the cerebrum in *P. lujiatunensis* can potentially be attributed to the need for processing of

new sensory inputs gained through development, but this is currently inconclusive for reasons that are beyond the scope of this project.

The cerebellum massively increases in width and implies that fine motor skills, such as balance, may have increased between the juvenile stage to adulthood. Cerebellar changes in *P. lujiatunensis* is supported in Zhao et al. (2013) where forelimb-to-hindlimb ratios change with age and the species shifts from a quadruped to biped. A shift in centre of gravity and posture would require neuroanatomy that accounted for shifts in balance – this primarily being the cerebellar area of the brain and the brainstem (Beckinghausen and Sillitoe, 2019; Surgent et al., 2019). An enlarged cerebellum that continues to grow into adulthood allows for an increasing volume of grey and white matter within the brain to supply more area of the brain with neurons dedicated to receiving, transporting, and interpreting slight changes in balance experienced throughout the body. Since the shift from quadrupedality to bipedality begins at approximately one-year-old and finishes at five-years-old (Zhao et al., 2013) the significant increase in the cerebellar width found in psittacosaur (Figure 4.10) helps to support the postural shift proposed by Zhao et al. (2013).

The cephalic and pontine flexure angles throughout psittacosaur ontogeny is not similar to any archosaur that was measured for this chapter. Flexure change could indicate two things. First, non-avian dinosaurs diverge from the flexure patterns found throughout modern birds and crocodilians. Considering the variability of the skull between related species and throughout ontogenetic series (Horner and Goodwin, 2006; Hübner and Rauhut, 2010; Bullar et al., 2019), which is not surprising as the braincase osteology and brain are known to move with each other (Fabbri et al., 2017). This is to say that changes in the braincase in non-avian dinosaurs are much more extreme or are completely different from the patterns observed in today's archosaurs. Secondly, the age driven shape reconfiguration of the *P. lujiatunensis* endocast really highlights how little is known about endocranial flexure and what these changes in endocranial morphology found in the early stages of non-avian dinosaurs mean on a broad macroevolutionary scale. Either way, this chapter provides evidence that the endocranial morphology of non-avian dinosaurs change with age – sometimes drastically. This is to say that non-adult specimens should not be representative of the species when used in macroevolutionary studies.

Broad neuroanatomical examinations of the ornithischian endocranium are still very much understudied. Comparative studies are limited to ornithopods (Evans et al., 2009; Farke et al., 2013; Lautenschlager and Hübner, 2013) with ceratopsian research being limited to single descriptions of endocasts from a single ontogenetic stage (Zhou et al., 2007; Napoli et al., 2019; Zhang et al., 2019; Sakagami and Kawabe, 2020) or the ontogeny of the braincase

surrounding the endocast (Bullar et al., 2019). This study represents the first use of endocasts from a single ornithischian species to observe changes across an entire ontogenetic series of any ornithischian – ceratopsian or otherwise. The results of this study indicate that little is actually known about what happens to the non-avian dinosaur endocast throughout ontogeny – especially in under sampled dinosaurs such as ceratopsians. Due to this, the ontogenetic stage of an individual specimen’s endocast must be taken into account in order to gain a more complete picture of endocranial morphology, palaeobiology, and behaviour of non-avian dinosaurs.

Chapter 5: The avian nature of the juvenile *Psittacosaurus lujiatunensis* endocast and its implications

5.1 Collaborative Statement

This chapter is a collaborative effort between Zhao Qi (Institute of Vertebrate Paleontology and Paleoanthropology; provided data), Soichiro Kawabe (Fukui Prefectural University; provided data), David Dufeu (Marian University; provided data and gave feedback about the project), Emily Rayfield (University of Bristol; gave feedback and edited drafts), and Michael Benton (University of Bristol; gave feedback and edited drafts). I segmented the *Psittacosaurus* endocasts, wrote the chapter, measured the specimens, made the images, and have edited the chapter. I have done 90% of the work in completing this chapter. This chapter is in review with Current Biology.

5.2 Abstract

Birds, non-avian dinosaurs, and crocodilians comprise Archosauria alongside pterosaurs; a clade whose evolution is partially defined by the anatomy and morphology of the skull and brain. The adult bird skull and endocranium is similar to that of a juvenile theropod, non-avian dinosaur and this has been explained by the retention of juvenile characters (paedomorphosis). Did an endocranial paedomorphic shift occur with the origin of birds or, if it applies to non-avian dinosaurs as a whole, did it arise much earlier in Dinosauria? Here, I explore aspects of this evolutionary shift in the juvenile and adult skulls and brains of the ornithischian dinosaur *Psittacosaurus lujiatunensis*. I demonstrate that sub-yearling psittacosaurus possessed morphological and anatomical features similar to adult birds and changes in neuroanatomy may be related to ontogenetic shifts in locomotion. Through ontogeny, the *Psittacosaurus* brain initially elongated anteriorly, apparently replicating the basal archosaurian or crocodilian pattern, and then shortened and folded back to replicate the avian pattern. Brain and head development in *Psittacosaurus* follows neither the avian nor the crocodilian model, but shares elements of both, thus indicating considerable complexity in endocranial development and evolution across Dinosauria as a whole, representing more than simply a 'bird' or 'crocodilian' model.

5.3 Introduction

Evolution of form in plants and animals depends on complex interactions of natural selection, ecomorphology, and genomic regulation (Lautenschlager, 2014; Knapp et al., 2018; Hughes and Finarelli, 2019). Different developmental stages from embryo to adult may be subject to various modes of selection based on body size and adaptations (McNamara, 2012). This is

overlaid by evolutionary-developmental interactions, usually termed heterochrony. Heterochrony includes cases where adults retain juvenile characteristics (paedomorphosis) and cases where adults show additional steps of development compared to their ancestors (peramorphosis) (Plateau and Foth, 2020). The evolution of birds has often been said to involve paedomorphosis, in the reduction of body size when compared to their dinosaurian ancestors, but also in changes in head shape when compared to crocodilians, and to many non-avian dinosaurs. In fact, the bird skull is much more complex, showing a mix of paedomorphic (Bhullar et al., 2012, 2016) and peramorphic (Plateau and Foth, 2020) characteristics when compared to non-avian theropods.

These observations on living birds and crocodilians leave open many questions about how these complex heterochronic shifts took place, and requires a study of extinct relatives, primarily non-avian. It is a challenge to study the brains and sensory organs of extinct animals, but CT scanning now allows palaeontologists to penetrate inside well-preserved fossils, image the enclosed braincase, and reconstruct the associated internal soft tissue structures (Racicot, 2016).

Current understanding of the neurosensory (Zelenitsky et al., 2009, 2011) and endocranial evolution of birds stems from comparisons to non-avian dinosaur taxa; however, these observations and measurements are made from large or adult non-avian theropods (Larsson et al., 2000; Kundrát, 2007; Zelenitsky et al., 2009, 2011; Bever et al., 2011; Balanoff et al., 2014, 2018) and extinct birds (Dominguez et al., 2004; Kurochkin et al., 2006, 2007; Milner and Walsh, 2009; Zelenitsky et al., 2011; Walsh et al., 2016; Walsh and Knoll, 2018; Plateau and Foth, 2020). Studying the skulls and brains of adults of extinct birds and non-avian dinosaurs provides some information, but for full understanding of heterochrony full developmental sequences are required; and not only that, but developmental sequences for which there are sufficient well-preserved, uncrushed and complete skulls of as many ontogenetic stages as possible from hatchling to adult. To date, ontogenetic exploration has been possible only for a very small number of ornithischian dinosaurs such as ornithomimids (Evans et al., 2009; Farke et al., 2013; Lautenschlager and Hübner, 2013). *Psittacosaurus*, a genus of species-rich ceratopsians from the Early Cretaceous (c. 125–100 Ma) of China, Mongolia, and Russia (Napoli et al., 2019), provides an opportunity to study the cranial remains of young juveniles – especially those of *Psittacosaurus lujiatunensis* (Zhao et al., 2013a). *P. lujiatunensis* is known from hundreds of specimens all from a single stratigraphic level and locality, the Lujiatun Unit (c. 125.7 Ma) around the village of Lujiatun in Liaoning Province. Most specimens are unusually well preserved and uncrushed, as they were buried

in rapidly accumulating ash deposits, hence the nickname of the site, the ‘Chinese Pompeii’ (Rogers et al., 2015).

Here, I explore how a juvenile non-avian, non-theropod dinosaur endocast compares with the adult of the species, and whether the implied heterochronic changes in *P. lujiatunensis* can be interpreted as either crocodilian or avian, or something else altogether. To do this, I describe an endocast from a sub-yearling *P. lujiatunensis* (IVPP V15451) and measure the widths of the olfactory bulbs, cerebral hemispheres, and cerebellum as well as the cephalic and pontine flexure points. The endocranial anatomy of IVPP V15451 and its respective widths and flexure points are compared to the morphology of a subadult and adult endocast of *P. lujiatunensis*. I also compare the abbreviated ontogenetic series of *P. lujiatunensis* to endocranial ontogenies of ostriches, alligators, and chickens to test how similar the morphology of IVPP V15451 is to extant basal archosaurs and birds. Adult endocasts of *Archaeopteryx lithographica* and *Cerebavis cenomanica* are included to extend the range of comparable taxa beyond extant analogues.

5.4. Materials and Methods

5.4.1 Endocasts

Alligator endocasts were provided by Lawrence Witmer and David Dufeu from previous research projects (Dufeu et al., 2012; Dufeu and Witmer, 2015). Similarly, Soichiro Kawabe provided all chicken data referenced in this manuscript (Kawabe et al., 2015). Ostrich endocasts were from ethically sourced from Bulgarian farms by Emily Rayfield and segmented as a part of Krishna Hu’s MSc in Palaeobiology thesis work at the University of Bristol. Zhao Qi provided all *Psittacosaurus* skull CT data and Logan King segmented all datasets at the University of Bristol.

5.4.2 Scanning and segmentation

IVPP V15451, PKUP V1053, and IVPP V12617 were scanned using the Chinese Academy of Sciences micro-computed tomography 450kV scanner (450-TY-ICT) at the Institute of Vertebrate Paleontology and Paleoanthropology, Beijing, China. IVPP V15451 was scanned at 130 kV with a voxel resolution of 92.61 μm . The skull of PKUP V1053 was scanned at 440 kV and has a voxel resolution of 160 μm . Finally, IVPP V12617 was scanned at 140 kV with a voxel resolution of 160 μm . The endocasts were segmented at the University of Bristol’s Tomography Lab with Avizo Lite (Thermo Fisher Scientific, v.9.7.0). Endocasts were from the specimens used in Chapter 4 of this thesis.

The ostrich skulls used for this project were scanned with a Nikon XT H 225ST CT scanner at the University of Bristol. All scan sets were filtered with a 0.5 mm copper filter (the oldest ostrich required a 0.25 tin filter). All endocranial models were made in Avizo Lite (Thermo Fisher Scientific, v9.7.0) at the University of Bristol's Tomography Lab. Scan energy and resolution varied between each specimen: 2-weeks-old (195 kV, 36 μm), 4-weeks-old (180 kV, 41 μm), 12-weeks-old (180 kV, 46 μm), 5-months-old (220 kV, 52 μm), and 3-years-old (237 kV, 86 μm). Endocasts were made from skulls scanned for Chapter 3 of this thesis.

Chicken skulls were μMRI scanned with a 1.5-T MRmini SA (MRTechnology, Inc) at Ehime University. Two different diameter radiofrequency coils – 30 mm or 38.5 mm – were used depending on the size of the specimen. Segmentation was carried out with Amira visualization software (Mercury Computer Systems, v.5.3.2). All chicken skulls were gathered from Kawabe et al., (2015).

Small alligator skulls (OUVC 10606, 10385, and 10389) were scanned at the Ohio University MicroCT Scanning facility with GE eXplor Locus *in vivo* Small Animal MicroCT Scanner. The CT parameters varied between each individual: OUVC 10606 (80 kV, 45 μm), OUVC 10385 (60 kV, 92 μm), OUVC 10389 (60 kV, 92 μm), OUVC 9761 (120 kV, 625 μm), and USNM 211232 (120 kV, 625 μm). Large skulls (OUVC 9761 and USNM 211232) were scanned at OhioHealth O'Bleness Hospital with a GE Lightspeed Ultra MultiSlice CT scanner. Segmentation of the alligator CT data was carried out with Amira (Mercury-TGS, v.4.1) and were scanned for Dufeu and Witmer, (2015).

5.4.3 Age estimation

The ages for all modern taxa used for this study were recorded from farms (ostriches, alligators), brood data (chickens), or from museum collection data where skulls were gathered for CT scanning (alligators). Ages for *P. lujiatunensis* were estimated from long bone osteohistology (Zhao et al., 2013) and from the size of the skull and the degrees of fusion of cranial bones (Bullar et al., 2019) (Table 5.1).

Table 5.1 – Master list of the specimen flexure angles and ages used for this chapter

Specimen	Taxon	Cephalic Flexure (°)	Pontine Flexure (°)	Age (years)
IVPP V15451	<i>P. lujiatunensis</i>	82.1	89.6	<1
IVPP V12731	<i>P. lujiatunensis</i>	138.7	138.7	2
PKUP V1053	<i>P. lujiatunensis</i>	138.2	148.4	7
PKUP V1054	<i>P. lujiatunensis</i>	133.9	140.1	8
IVPP V12617	<i>P. lujiatunensis</i>	88.1	88.9	10
OUGC 10606	Alligator	77.2	72.7	0.08
OUGC 10385	Alligator	86.5	89.6	0.83
OUGC 10389	Alligator	96.5	101.4	1
OUGC 9761	Alligator	110.2	116.7	4
USNM 211232	Alligator	121.0	124.5	5
2-weeks-old	Ostrich	73.5	118.2	0.04
4-weeks-old	Ostrich	73.0	117.9	0.08
12-weeks-old	Ostrich	70.4	116.4	0.23
5-months-old	Ostrich	71.2	116.4	0.42
3-years-old	Ostrich	73.3	119.8	3
1-day-old	Chicken	83.4	102.1	0
30-days-old	Chicken	84.7	91.2	0.08
46-days-old	Chicken	86.3	97.4	0.13
86-days-old	Chicken	87.8	97.5	0.23
119-days-old	Chicken	87.4	99.3	0.33

5.4.4 Linear measurements

The endocasts made in Avizo Lite were exported as .obj files for 2D linear measurement in ImageJ (1.52p). ImageJ was chosen for measuring linear distances and flexure angles. Ratios were made by comparing the smaller widths (olfactory bulbs, cerebellum) to the maximum endocranial width across the cerebrum. Cerebral hemisphere ratios were made by comparing the maximal width across the cerebrum to the total endocast length. The angle tool in ImageJ was used to measure flexure angles (Table 5.1).

5.5 Results

The olfactory tract is similar to those found in juvenile alligators in that it is not dorsally obstructed by the cerebrum and would have contained two small anteriorly located olfactory bulbs; however, the olfactory bulbs of IVPP V15451 are not well-preserved. (Figure 5.1). A ventral view of the frontals shows an expansion at the anterior margin, but the true extent of the bulbs is unknown due to poor preservation along the ventral surface of the anterior frontals (Bullar et al., 2019). More mature specimens of *Psittacosaurus lujiatunensis* show

enlarged olfactory bulbs that are more similar to those found in basal archosaurs and even large-bodied coelurosaurs when compared to their body size (Zhou et al., 2007). Faint indentations along the anterior portion of the frontal bones of IVPP V15451 show that enlarged olfactory bulbs would have been expected in young individuals of *P. lujiatunensis*.

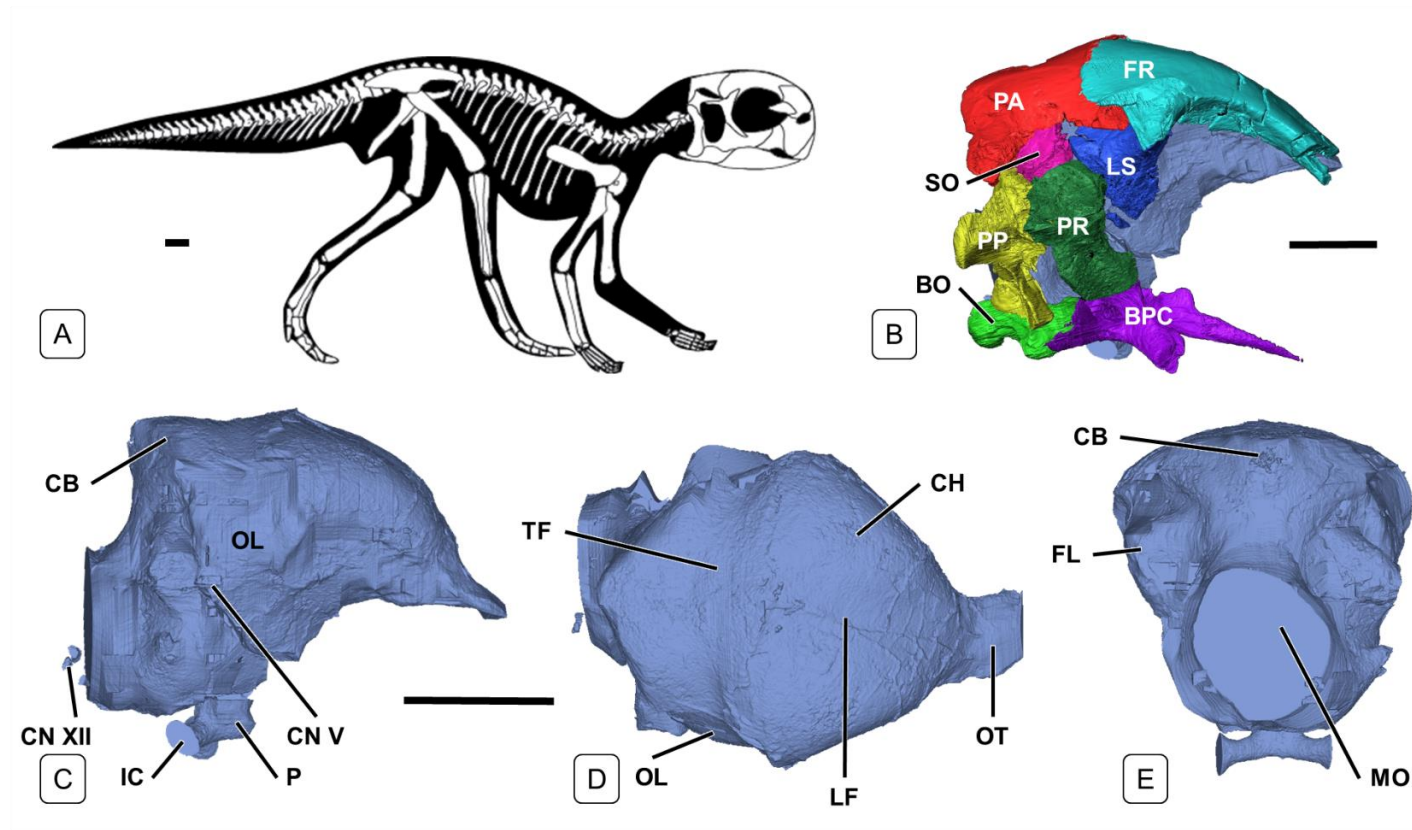


Figure 5.1 – Figure 2. Line-drawing of a sub-yearling *Psittacosaurus lujiatunensis* (A) and the segmented braincase of IVPP V15451 (B). The segmented endocast of IVPP V15451 is shown in right lateral (C), dorsal (D), and posterior (E) views to show anatomy relevant to this study. Braincase abbreviations: BO, basioccipital; FR, frontal; LS, laterosphenoids; PA, parietal; PP, paroccipital process; PR, prootic; SO, supraoccipital; BPC, basisphenoid-parasphenoid process. Endocast abbreviations: CB, cerebellum; CN V, trigeminal nerve; CN XII, hypoglossal nerve; FL, floccular lobe; IC, internal carotid arteries; LF, longitudinal fissure; MO, medulla oblongata; OL, optic lobe; OT, olfactory tract; P, pituitary; TF, transverse fissure. Skeletal artwork (A) of *P. lujiatunensis* credited to Simon Powell. The segmented braincase (B) was adapted from Bullar et al. (2019). Scale bar = 5 mm

The olfactory bulbs, even though badly damaged and partially missing in IVPP V15451, are much larger than in *S. camelus* and similar in size to *A. mississippiensis*. This pattern is continued throughout the life of *P. lujiatunensis* where olfactory bulb widths increase through ontogeny rather than remain the same relative size as in *S. camelus*. When the data for all three taxa are graphed for all five ontogenetic specimens, olfactory bulb development in *P. lujiatunensis* follows a trend similar to *A. mississippiensis* (Figure 2A) and indicates that, even though the endocranium of IVPP V15451 is similar to the avian form, developmental changes in the olfactory bulbs more closely resemble those of crocodilians. An enlarged olfactory bulb is indicative that even early in life *P. lujiatunensis* had an olfactory sensitivity more akin to alligators than birds in general (barring birds with specialized olfactory senses such as members of Cathartiformes, Falconiformes, and Accipitriformes) (Potier, 2019; Potier et al., 2019).

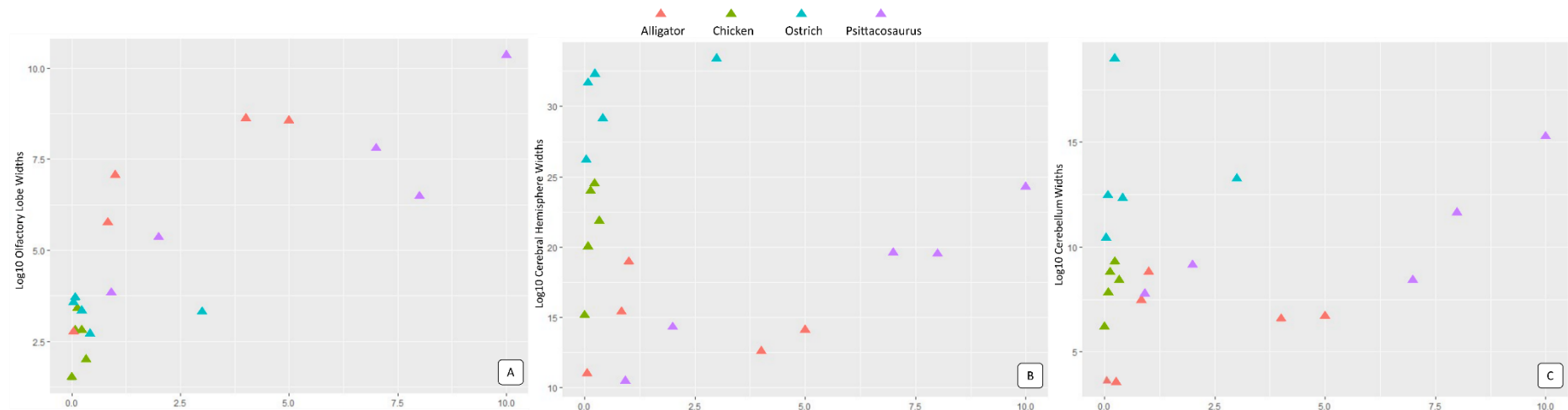


Figure 5.2 – Normalized widest diameter measurements of olfactory bulbs (A), cerebral hemispheres (B), and cerebellum (C) along ontogenetic series of endocasts from *Alligator mississippiensis* (red), *Psittacosaurus lujiatunensis* (green), and *Struthio camelus* (blue). Neuroanatomy development is variable across taxa with no clear comparison that can be drawn between exemplar non-avian archosaurs, birds, and the extinct ceratopsian *P. lujiatunensis* throughout growth.

The cerebrum width of IVPP V15451 comprises 70.4% of the total endocranial length – much larger than the 38.9% in *A. mississippiensis* juveniles of an approximately similar age, and especially much larger than the 31.2% value in ostriches. Ostriches have an expanded cerebrum early in life (96% of the total endocranial length; see Table 5.2 for a master list of widths and ratios) but only lose a small fraction of cerebral width when compared to total length (92.3%) throughout development. In *P. lujiatunensis*, cerebral expansion occurs early in life much as in birds (Figure 2B).

Table 5.2 – Master list of the total length of their endocranial, maximal olfactory bulb width, maximal cerebral hemisphere width, and maximal cerebellum width. Ratios of the maximal widths were made by comparing them to the widest aspect of the cerebral hemispheres¹ or the total length of the endocranial²

Specimen	Taxon	Tot. Length	Olf. Width	% ¹	Ch. Width	% ²	Ce. Width	% ¹
IVPP V15451	<i>P. lujiatunensis</i>	14.9	3.8	36.5	10.5	70.4	7.8	74.0
IVPP V12731	<i>P. lujiatunensis</i>	30.5	5.4	37.5	14.3	46.9	9.1	63.8
PKUP V1053	<i>P. lujiatunensis</i>	92.0	7.8	39.7	19.6	21.3	8.4	43.0
PKUP V1054	<i>P. lujiatunensis</i>	84.7	6.5	33.3	19.5	23.0	11.6	59.6
IVPP V12617	<i>P. lujiatunensis</i>	78.1	10.4	42.7	24.3	31.2	15.2	62.9
OUGC 10606	Alligator	20.3	2.6	25.1	10.9	54.2	3.6	32.9
OUGC 10385	Alligator	33.7	5.8	37.4	15.4	45.7	7.5	48.5
OUGC 10389	Alligator	48.6	7.1	37.3	18.9	38.9	8.8	46.5
OUGC 9761	Alligator	59.9	8.6	68.5	12.6	21.0	6.6	52.1
USNM 211232	Alligator	77.4	8.6	60.6	14.1	18.2	6.7	47.6
2-weeks-old	Ostrich	27.3	3.6	13.7	26.2	96.0	10.4	39.8
4-weeks-old	Ostrich	40.1	3.7	11.7	31.7	79.0	12.5	39.3
12-weeks-old	Ostrich	36.4	3.4	10.4	32.3	88.8	19.0	58.7
5-months-old	Ostrich	35.1	2.7	9.3	29.1	83.0	12.3	42.3
3-years-old	Ostrich	36.2	3.3	9.9	33.4	92.3	13.3	39.7
1-day-old	Chicken	17.0	1.5	10.0	15.2	89.2	6.2	40.8
30-days-old	Chicken	23.0	2.8	13.9	20.0	87.2	7.8	40.0
46-days-old	Chicken	27.0	3.4	14.2	24.0	88.9	8.8	36.7
86-days-old	Chicken	35.0	2.8	11.5	24.5	70.0	9.2	37.9
119-days-old	Chicken	31.0	2.0	9.1	21.9	70.5	8.4	38.5

Ontogenetic development of the cerebellar maximal width of *P. lujiatunensis* shows a very different pattern than birds and crocodilians (Figure 2C). The cerebellum in ostriches and chickens develops rapidly to the point of being enlarged and rounded in post-hatchlings before slowing down as adulthood approaches thus creating a prominent expansion along the dorsoposterior surface of the endocranial. Alligators show slower cerebellum development overall, but still growth slows towards maturity. The cerebellum of *P. lujiatunensis* is unique compared to modern archosaurs in that it displays a more protracted growth phase instead of having a spike of growth early in post-hatching development. Continued cerebellar growth may reflect the shift from quadrupedality to bipedality in older juveniles (Zhao et al., 2013) since alligators and birds are always quadrupedal and bipedal, respectively, with no shifts in

hindlimb locomotion. A modified pattern of development in the cerebellum of *P. lujiatunensis* is consistent with the ontogenetic shift from an obligate quadrupedal stance to a bipedal stance (Zhao et al., 2013), however, the exact nature of cerebellar change remains uncertain due to a lack of a modern archosaur exemplar that shifts its locomotory stance during ontogeny. Considering that the increase in cerebellum width only occurs after the fifth year of age, this gives neuroanatomical support for a postural shift and helps to explain why the plotted cerebellum development varies so much from the extant exemplars (Figure 3C).

Comparing the shifts in widths of major portions of the endocranium among alligators, ostriches, and *P. lujiatunensis* indicates that the timing of endocranial (and therefore brain) development had a myriad of triggers. Intra- and interspecific allometric differences among the endocrania measured here can be accounted for by ontogenetic variation, phylogenetic relationships, and ecomorphological roles associated with each section of the brain. The variability among specimens at different ages is evidence that even though ecomorphology and phylogeny of a specimen may be known, the assessment of the neurosensory ability of a species may not be accurate if ontogenetic stage is not considered. Furthermore, as evidenced by *P. lujiatunensis*, the overall form of an endocranium is dependent on ontogeny just as much as phylogeny (Figure 2, second row). None of the neuroanatomical widths mirrors the avian-like growth curve of *P. lujiatunensis* (Erickson et al., 2009).

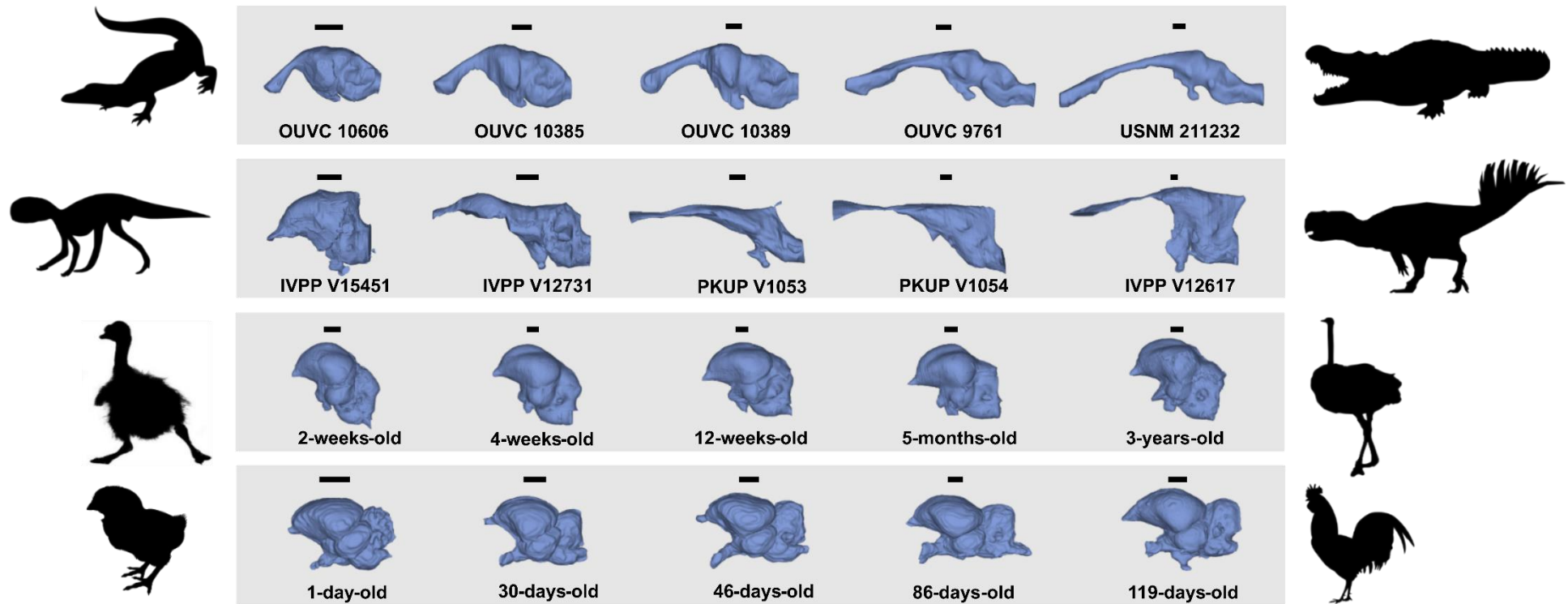


Figure 5.3 – Figure 3. Archosaur brains through ontogeny: *Alligator mississippiensis* (first row), *Psittacosaurus lujiatunensis* (second row), *Struthio camelus* (third row), and *Gallus gallus* (fourth row). The endocast of *Psittacosaurus* demonstrates growth patterns that are most similar to avians early in life (e.g. expanded cerebrum, $\leq 90^\circ$ flexure angles) but incorporates more non-avian archosaur traits with age (e.g. endocranial elongation, enlarged olfactory bulbs). Ontogenetic development of the *P. lujiatunensis* endocast ends with a refolded form that superficially resembles both avian and non-avian archosaur endocranial morphologies. Age increases from juveniles (left) to adults (right). The older *P. lujiatunensis* endocasts were made from a 7-years-old individual (PKUP V1053; middle) and 10-years-old individual (IVPP V12617; right). Scale bars = 5 mm.

5.6 Discussion

Considering that the endocranial morphology of non-avian dinosaurs is highly dependent on its ontogenetic stage, our understanding of the avian form can become clearer. The avian brain shows a few unique features when compared to the generalized archosaur brain. These traits include a reduced pair of olfactory bulbs (Balanoff et al., 2018), near 90° cephalic and pontine flexures (i.e. an “S-shaped” endocranium), a deep, enlarged cerebrum (Balanoff et al., 2018; Gold and Watanabe, 2018; Walsh and Knoll, 2018), and a set of lateral or anterolaterally located optic lobes (Witmer and Ridgely, 2009; Balanoff et al., 2018; Gold and Watanabe, 2018; McKeown et al., 2020). Of this anatomy, the hatchling IVPP V15451 displays near or sub-90° cephalic and pontine flexure angles, an enlarged cerebrum compared to the total endocranial length, and laterally located optic lobes. Because the bird skull can be considered as a paedomorphic theropod skull in shape (Bhullar et al., 2012) and implies that paedomorphic constraints are also affecting the brain. Indeed, the modern bird braincase is even more bulbous and paedomorphic than that of early avialans (Bhullar et al., 2016). The shape of the bird brain indicates that Aves have continued a paedomorphic endocranial trend that was already well in place in Avialae and that avian brain evolution is a mosaic of paedomorphic and plesiomorphic characters.

Our study of endocranial ontogeny in *Psittacosaurus*, a taxon that is phylogenetically far removed from theropods and birds, shows that many traits previously assumed to be avian or avian-like may occur much more widely throughout Dinosauria, particularly in juvenile specimens. At a minimum, it should be noted that characters that are termed “bird-like” (e.g. small flexure angles, an enlarged cerebrum, laterally oriented optic lobes) are present in at least some non-avian, non-theropod dinosaurs that are young (<1 year of age). An S-shape, or at least non-linear endocranial arrangement, is present in juvenile non-avian, non-dinosaur archosaurs (e.g. alligators) with varying degrees of flexure (Dufeu et al., 2012). An enlarged cerebrum, making up greater than 50% of the endocranial length, is present in at least some post-hatchling juveniles of non-avian dinosaurs and avians, but is lost in basal archosaurs (McKeown et al., 2020). Interestingly, and possibly most importantly, prominently visible laterally situated optic lobes were previously thought to be an avian, or at least derived theropod, character (Gold and Watanabe, 2018) but are present in the juvenile, IVPP V15451. Enlarged fore- and hindbrain structures have been suggested to push the optic lobes from a dorsolateral position to a ventrolateral one in some maniraptorans (Balanoff et al., 2014). In IVPP V15451, this happens because the braincase is compact and the forebrain already enlarged; and it is the same in birds, which have morphometrically paedomorphic skulls (Bhullar et al., 2012) and both an enlarged cerebrum and cerebellum (Gold and Watanabe, 2018). As evidenced in many non-avian dinosaurs (including IVPP

V15451), juvenile skulls are relatively anteroposteriorly shorter than adult skulls (Bhullar et al., 2016; Wang et al., 2017; Woodruff et al., 2018). Based on the anatomy of the endocast of IVPP V15451, I hypothesize that the paedomorphic nature of the avian and avialan endocast can be traced deeper in the phylogenetic tree of non-avian dinosaurs than the origin of theropods and includes characters (e.g. an expanded cerebrum and a S-shape) that are found in at least some juvenile ornithischians all the way up to derived theropods (Balanoff et al., 2014, 2018) and even avialans and avians such as *Archaeopteryx lithographica* and *Cerebavis cenomanica*, respectively (Figure 4). This supports the suggestion that the avian skull (including the braincase and endocast) is morphometrically similar to those found in juvenile theropods. The results of this chapter imply that in non-avian dinosaurs, ontogeny creates aesthetically bird-like endocranial morphology. This bird-like endocranial morphology is then exaggerated in later theropods where the bird brain form mirrors the paedomorphic nature of the skull.

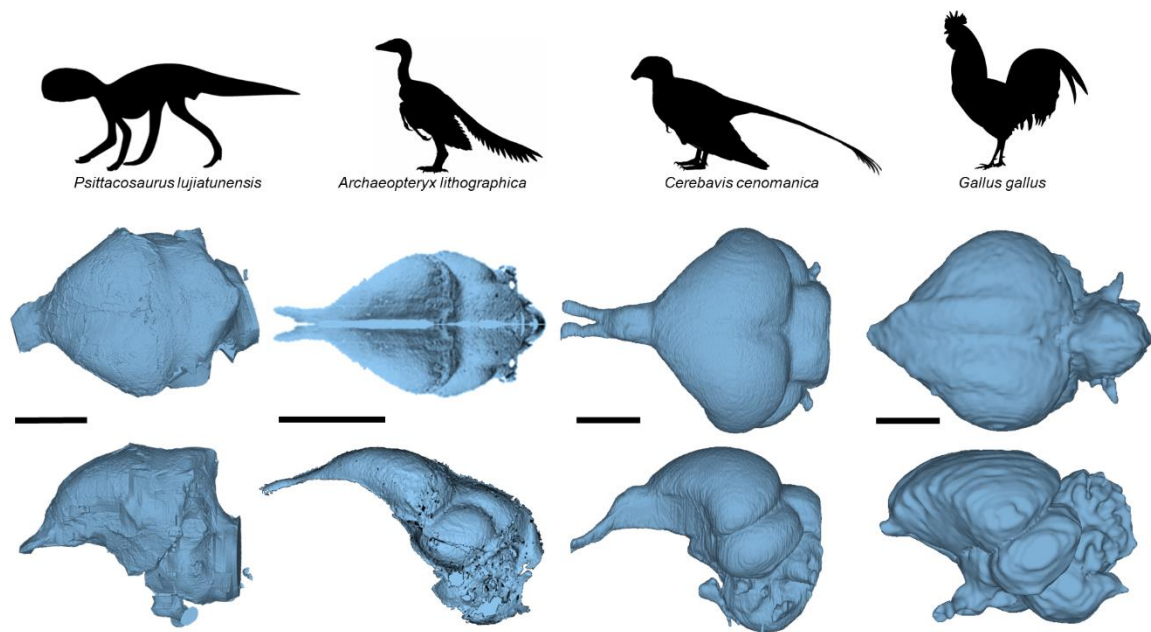


Figure 5.4 – Comparative endocasts from a juvenile non-theropod, non-avian dinosaurs (*Psittacosaurus lujiatunensis*, IVPP V15451), an avialan (*Archaeopteryx lithographica*), an extinct avian (*Cerebavis cenomanica*), and an extant avian (*Gallus gallus*). Note the enlarged cerebrum and optic lobe location on each specimen. Scale bars = 5mm

Why would the brain in *Psittacosaurus* seemingly elongate from avian-like to crocodilian-like in the first part of its development, and then apparently revert to a shortened, more avian-like form in the adult? Morphological shifts as extreme as this are likely because adult *Psittacosaurus* have an anteroposteriorly shortened skull; for example, some species of *Psittacosaurus* have skulls where the preorbital area of the skull comprises only 40% of the total skull length (Averianov et al., 2006), a shorter value than in adult large-bodied derived

ceratopsians (Horner and Goodwin, 2006). The shortening of the adult psittacosaur skull is presumably related to the lack of a bony crest and nose horn in the genus. Derived ceratopsians, such as *Triceratops*, follow an allometrically positive growth pattern where the nasal horn and parietal crest drastically change through time (Horner and Goodwin, 2006). As *Triceratops* aged, the cranium changed as the nasal horn and bony shield shifted from small protrusions along the anterior and posterior skull, respectively, with a short anteroposterior length (Goodwin et al., 2006; Horner and Goodwin, 2006). By the time adulthood was reached, both the nasal horn and posterior shield were prominent features on an elongated skull (Horner and Goodwin, 2006). The elongation and ornamentation that is prominent in derived ceratopsians affects the bones that directly contact the endocranium (e.g. parietals, frontals, sphenoid complex) and may influence the morphology of the endocranium with age. Since the genus *Psittacosaurus* does not have significant craniofacial ornamentation and the skull remains short throughout ontogeny, the adult skull retains a shape that strongly favours the juvenile morphology even though some cranial bones grew at different rates (Bullar et al., 2019). Since *Psittacosaurus* does not have major dorsoventral heightening of the cranium nor skull elongation associated with a parietal shield and nasal horn modification, respectively, the soft tissues of the endocranium did not undergo the same level of peramorphic modification seen in basal archosaurs, thus retaining a bird-like or modified avian style of endocranial morphology in both infancy and adulthood (Figure 5.3, 5.4).

The presence of the longitudinal and transverse fissures (Figure 1D) and visible optic lobes in juvenile psittacosaurids, suggest a tightly constrained internal space as these same features are noticeable on avialan and avian endocrasts due to their thin dural envelope and short paedomorphic skulls with confined braincases; however, neither can be detected in crocodylians older than one year of age. As crocodylians mature, the dural envelope increases in thickness (Jirak and Janacek, 2017) to the point that fine anatomy becomes obscured and parts of the brain become decoupled from the braincase, causing the endocrast to be less informative of underlying neural structures in places such as the midbrain (Jirak and Janacek, 2017). The young ontogenetic age of IVPP V15451 corresponds with a dural envelope that is more representative of the underlying neural structures and reveals a strongly flexed, S-shaped brain. For this reason, it appears to be bird-like in morphology even though it is phylogenetically far removed from theropods and avians. Because IVPP V15451 also looks like sub-yearling alligators and birds with their tighter flexure angles and higher cerebrum-to-endocranial ratios, this provides strong support for the deep paedomorphic history of the avian-style endocranium.

If these comparative anatomical points are confirmed in future neuroanatomical studies, especially in avialans, then it would mean that a pair of dramatically reduced olfactory bulbs, evidence for a dural envelope congruent with the underlying neuroanatomy throughout ontogeny, and an overall brain form that does not drastically change between post-hatching and somatic maturation are some of the few truly “avian” characters shared between endocasts of non-avian dinosaurs and extant birds. All other anatomical changes that I have noted in *Psittacosaurus* should be considered paedomorphic morphological holdovers from non-avian dinosaurs or plesiomorphic characters from deeper within Archosauria.

5.7 Conclusions

The expanded cerebral hemispheres and S-shaped morphology found in adult forms of avians and avialans represent a paedomorphic anteroposterior flexure of the braincase – as represented by the ceratopsian *Psittacosaurus lujiatunensis*. This interpretation supports recent work that indicates a paedomorphic relationship between the skull shapes of non-avian theropods and modern birds (Bhullar et al., 2012). Based on the closer phylogenetic relationship between *P. lujiatunensis* and extant crocodilians, the bird-like characters observed on the endocast of IVPP V15451 are unrelated to the extant avian condition and should be considered as examples of paedomorphic characters that date at least from the origin of Dinosauria. I hypothesize that the avialan and modern avian endocranial form follows the same paedomorphic trend as the bird skull and juvenile non-avian dinosaurs: the expanded cerebrum and near 90° flexure angles reflect the paedomorphic nature of the bird skull. If the endocasts of avialans and birds are paedomorphic, then the expansion of the cerebrum found in avians, avialans, and juvenile theropods is not unique to Theropoda. Instead, cerebral expansion has been maintained from multiple juvenile non-avian dinosaurs that can be traced back throughout archosaurs as a juvenile trait. This would indicate that early exaggerated cerebral expansion can be traced back to non-theropod Dinosauria considering that these patterns are found in young ornithischians such as *P. lujiatunensis* and only becomes prominent in adult forms of Maniraptora and Aves.

The endocranial ontogenetic series of *P. lujiatunensis* demonstrates how its brain shape and anatomy becomes modified throughout development. Over the span of the first decade of the animal’s life, the endocast morphology of *P. lujiatunensis* traverses from bird-like to crocodilian-like and back to a modified bird-like form where, in juveniles, the dural envelope was thin and the brain was tightly fitted inside the braincase. Even though psittacosaurus are not closely related to theropods and birds, I suggest that the endocasts of young, post-hatching individuals reflect the deep paedomorphic origins of some endocranial characteristics seen in modern birds, and both modern and fossil birds have further modified

the ontogenetic growth series of skull and brain to retain a broadly paedomorphic pattern to adulthood.

Chapter 6: Conclusions and Impact

6.1 Conclusions

Chapter 1:

- The subfield of palaeoneurology was formed with brain size, brain volume, and body size at the forefront of its development.
- Previous palaeoneurologists have established series of rules and derived formulae that help explain the relationship between brain size and evolutionary success for many different taxa throughout time – non-avian dinosaurs included.
- Replication methods for endocasts have varied throughout palaeoneurology and trend towards less destructive techniques with time, especially with the widespread use of CT scanning. Regardless of the method used, palaeoneurology is constrained by the preservation – or lack thereof – of braincases in the fossil record.
- When non-avian dinosaur endocasts are made, neurosensory anatomical points of interest can be interspecifically and intraspecifically compared between taxa to establish how sensory abilities change through time and with evolution.
- A key point that is understudied or wholly missing from many discussions on brain-braincase volume ratios or macroevolutionary trends in the endocranium of non-avian dinosaurs is ontogeny and how heterochrony may impact our understanding of dinosaur palaeoneurology.

Chapter 2:

- The partial endocast of a *Velociraptor mongoliensis* specimen, IGM 100/976, provides neuroanatomical support for the proposed predatory nature of the species. Large floccular lobes imply an acute sense of agility that matches well with the assumed palaeoecology of the species.
- The cochlear ducts of the endosseous labyrinths provide a means to calculate mean and high hearing ranges for *V. mongoliensis*. Hearing ranges calculated for IGM 100/976 further support the proposed predatory nature of the species since their hearing was closer to birds than archosaurs – thus indicating vocalizations were important during life. How this was used (e.g. socially, prey location) is still a matter of debate.
- This chapter demonstrates that there are limits to what can and cannot be derived from cranial endocasts. For instance, sensory inferences (i.e. agility, hearing) can be made, but some assumed behaviours – such as gregariousness – are reliant more on postcranial fossils than endocrania.

Chapter 3:

- Ontogenetic trends in endocranial development are understudied among modern archosaur taxa and have left significant gaps in our understanding of comparative anatomy. This has been partially bridged by comparing the anatomical and morphological variation throughout the postnatal growth of alligators (*Alligator mississippiensis*) and ostriches (*Struthio camelus*) – two of the most commonly used archosaurs that are compared with non-avian dinosaurs.
- Alligator endocasts always have a pair of large olfactory bulbs that increase in size in both absolute terms and relative to the widest aspect of the cerebrum. Ostriches begin smaller in terms of absolute size and actually decrease in size with respect to the cerebrum through life.
- Broadly speaking, the morphological differences between alligator and ostrich endocasts can be divided into elongation and flexure. Avian endocasts retain the same general shape throughout their life along with their small $\sim 90^\circ$ flexure angles. Basal archosaurs, such as alligators, have endocasts and flexure angles that constantly elongate throughout their lives.
- This chapter implies that the endocranial form of non-avian dinosaurs was not static, evolutionarily nor ontogenetically speaking. As such, palaeoneurologists should not expect a species of non-avian dinosaur to display the same neuroanatomical features throughout life.

Chapter 4:

- Five different endocasts were sampled from different ontogenetic stages (of the basal ceratopsian *Psittacosaurus lujiatunensis*).
- The complete ontogenetic series of endocasts from *P. lujiatunensis* reveals that even though the species is more closely related to basal archosaurs such as alligators and caiman, their endocranial morphology should not be assumed to mimic basal archosaurs.
- Endocranial morphology drastically changes in *P. lujiatunensis* throughout postnatal ontogeny from a condensed form with $\sim 90^\circ$ flexure angles to an elongate shape in subadults with flexure angles above 130° before returning to near right angles in somatically mature adults.
- Neurosensory lobes of the *P. lujiatunensis* endocasts were linearly measured, logarithmically normalised, and compared to the age of different archosaur taxa (*Alligator mississippiensis*, *Caiman crocodylus*, *Struthio camelus*, and *Gallus gallus*)

to see how the development of the lobes compare between taxa and developmental stages.

- The olfactory bulbs of *P. lujiatunensis* compare much more closely to basal archosaurs than birds in that the maximal width of the bulbs are always larger than either of the oldest birds and even the youngest alligator used in the study. Zhou et al. (2007) noted that, for their size, the olfactory bulbs rival the size of those found in tyrannosaurs. When *Tyrannosaurus rex* was added to the olfactory size data, the normalised widths of tyrannosaurs were still larger than both basal archosaurs and *P. lujiatunensis*.
- The cerebral widths of *P. lujiatunensis* show the most growth between taxa. In the sub-yearling psittacosaur, the comparative width is smaller than the youngest alligator, but by adulthood the widths rival the size of adult chickens (though ostriches always remained larger than any other archosaur).
- Cerebellar widths of young psittacosaur compare with adult crocodilians and chickens. By adulthood, *P. lujiatunensis* has a normalised cerebellar width that is larger than adult ostriches.
- All of these morphological and anatomical comparisons indicate that the ontogenetic stage of a specimen needs to be taken into consideration when describing palaeoneuroanatomy. Otherwise, the morphology of an endocast from an immature archosaur may not reflect the adult endocranial form. This creates issues when tracing the evolutionary trends in non-avian dinosaurs and somatically mature adults should be used in macroevolutionary studies.
- When paired with the results from Chapter 3, this chapter confirms that the ontogenetic stage of a non-avian dinosaur's endocast is a driver of endocranial form. Moreover, this chapter indicates that some dinosaur endocrania deviate from the pattern demonstrated by exemplar modern archosaur taxa – thus suggesting that there are limits to predicting endocranial form in extinct organisms based on modern specimens.

Chapter 5:

- The endocast of the juvenile-most *P. lujiatunensis* superficially favours that found in birds with its low flexure angles resulting in a S-shape and expanded cerebrum. This is a case of both convergent evolution and, in the case of avians, pedomorphosis.
- An enlarged cerebrum is a trait typically found in juvenile archosaurs. The presence of a cerebrum that is 70% of the total endocranial length is the same as that found in

chickens and almost double the size of an alligator's cerebrum of the same approximate age.

- The optic lobe on a juvenile *P. lujiatunensis* – a rarity for non-avian, non-maniraptoran dinosaurs – is laterally oriented. Although the position of the optic lobes is not as ventrolateral as in birds, it is located more lateral than the dorsally oriented ones found in juvenile alligators.
- The flexure angles of the sub-yearling juvenile *P. lujiatunensis* strongly favour the cephalic and pontine flexure angles found in chickens and ostriches of all ages and only sub-yearling alligators.
- Logarithmically corrected growth of the olfactory bulbs of *P. lujiatunensis* throughout ontogeny mirrors alligators. Ostriches' widths are diminutive when compared to alligators and psittacosaurus.
- Conversely, the corrected widths of the cerebrum in *P. lujiatunensis* are in the range of ostriches whereas the alligators were much smaller.
- Interestingly, the widths of the cerebellar regions of psittacosaurus starts in the range of alligators but ends in the range of ostriches.
- This study supports recent work that states the bird skull is paedomorphic since the bird brain expresses exaggerated juvenile characters found in non-avian dinosaurs: approximately 90° flexure angles, a cerebrum larger than 50% of the total endocranial length, and laterally situated optic lobes.
- Furthermore, being phylogenetically far removed from Theropoda, the avian-like nature of young ceratopsians like *P. lujiatunensis* suggests that endocranial forms in birds can be traced further back in Dinosauria than just Theropoda.

6.2 Summary and impact

The impact of this thesis to the field of palaeoneurology can be summarised in three parts. This thesis diverges from past studies that focus on volume or encephalization quotients. An overarching theme throughout this thesis is that endocrania from different ontogenetic stages of non-avian dinosaurs have the potential to be highly variable in terms morphology and surface anatomy – even in a single species. Variation between endocrania demonstrates that qualitative comparative studies are important tools to assess an endocast's plasticity through postnatal development as well as evolution. For example, the partial endocast of *Velociraptor mongoliensis* used in Chapter 2 of this thesis lacks both the completeness and number of specimens to provide statistical evidence for ecomorphological data as it only preserves the hindbrain region and inner ears. Instead, the partial endocast

can qualitatively be compared with other closely related non-avian dinosaur endocasts, modern taxa with dietary preferences similar to what is assumed for *V. mongoliensis*, and postcranial fossils from the species to reach meaningful broad conclusions about palaeobiology.

Due to endocranial variation within non-avian dinosaurs, a developmental pattern should not be assumed throughout an ontogenetic series. This thesis shows postnatal development follows trends in exemplar archosaur taxa – either elongation or minimal morphological change. Moreover, the ontogenetic stage of a specimen should be taken into consideration in neuroanatomical projects. If an endocast is reconstructed from a subadult (or younger) individual, it is possible that the morphology represented in an endocast from a younger individual will not be representative of a fully mature endocast. This has the potential to heavily skew the results of a macroevolutionary study and our understanding of how the endocranium changes through time. Since palaeoneurologists' understanding of endocranial form and function is intrinsically linked to modern analogues, a broader knowledge of ontogenetic data from modern taxa must also be derived. Work accomplished to complete this thesis has indicated that our understanding of how ontogeny impacts the form of endocasts is either understudied in modern taxa or almost unknown. Being understudied potentially skews how dinosaur ontogeny and evolution are related to each other neuroanatomically. For this reason, the key takeaways from Chapter 3 and Chapter 4 are to illuminate how little is known about the ontogeny of archosaur endocranium and to reveal that some dinosaurs may diverge from modern archosaur patterns in endocranial development.

Our understanding of modern archosaur neuroanatomy is heavily based on theropods. This is due mostly to the sheer number of theropodan endocasts made and their relationships to modern archosaurs. Chapter 5 demonstrates that ontogeny can be just as important – if not more so – than phylogeny and reveals that more comparisons need to be made between both non-theropod endocasts and from juvenile non-avian dinosaurs. An investigation into the endocast of a juvenile *Psittacosaurus lujiatunensis* highlights the need for further exploration as the bird-like attributes in a non-avian, non-theropod endocast are unexpected. Since the bird like form of the juvenile *P. lujiatunensis* endocast supports the claim that birds have paedomorphic skulls, new questions now arise. How do the endocasts of juvenile sauropods, the sister taxa of theropods, compare with birds? Is the link between avian features and juvenile non-avian dinosaur braincases even restricted to the split between Saurischia and Ornithischia? If not, how far back within Dinosauria or Archosauria do

paedomorphic trends extend? All of these questions require new palaeoneurological investigations that extend beyond Theropoda.

6.3 Future work

In the future, the impact of ontogeny on palaeoneurology will be expanded by scanning, reconstructing, and comparing endocranial series from more diverse members of Dinosauria. To date, only the above-described *P. lujiatunensis* series of endocasts has allowed for observing more than two or three endocrania from an ontogenetic series at a time. I will utilize ontogenetic series of endocrania from specimens that have either never been sampled before or are underrepresented in palaeoneurology to broaden the scope of ontogeny's impact on neuroanatomy to beyond just psittacosaur. Select theropods, ornithomimids, other ceratopsians, and sauropodomorphs have minimally deformed braincases from different ontogenetic stages that can be sampled for future projects.

Furthermore, comparative ontogenetic series of endocasts from extant archosaurs are almost non-existent in the literature – a reoccurring problem that I faced throughout my PhD projects. I, along with collaborators, will work towards increasing the number of archosaur taxa from which endocrania can be compared with for future projects. As a result, this will give a broader baseline from which to compare the anatomy and morphology of non-avian dinosaur endocrania.

Chapter 7: References

- Adams, D. C., and E. Otárola-Castillo. 2013. Geomorph: an r package for the collection and analysis of geometric morphometric shape data. *Methods in Ecology and Evolution* 4:393–399.
- Ashwell, K. W. S., and Z. Scofield. 2008. Big birds and their brains: Paleoneurology of the New Zealand moa. *Brain, Behavior and Evolution* 71:151–166.
- Averianov, A. O., A. V. Voronkevich, S. V. Leshchinskiy, and A. V. Fayngertz. 2006. A ceratopsian dinosaur *Psittacosaurus sibiricus* from the Early Cretaceous of West Siberia, Russia and its phylogenetic relationships. *Journal of Systematic Palaeontology* 4:359–395.
- Balanoff, A. M., and G. S. Bever. 2017. The role of endocasts in the study of brain evolution; pp. 223–241 in J. H. Kaas (ed.), *Evolution of Nervous Systems*, 2nd ed. vol. 1. Elsevier, Oxford.
- Balanoff, A. M., G. S. Bever, and M. A. Norell. 2014. Reconsidering the avian nature of the oviraptorosaur brain (Dinosauria: Theropoda). *PLOS ONE* 9:e113559.
- Balanoff, A. M., J. B. Smaers, and A. H. Turner. 2016. Brain modularity across the theropod–bird transition: testing the influence of flight on neuroanatomical variation. *Journal of Anatomy* 229:204–214.
- Balanoff, A. M., G. S. Bever, T. B. Rowe, and M. A. Norell. 2013. Evolutionary origins of the avian brain. *Nature* 501:93–96.
- Balanoff, A. M., M. A. Norell, A. V. C. Hogan, and G. S. Bever. 2018a. The endocranial cavity of oviraptorosaur dinosaurs and the increasingly complex, deep history of the avian brain. *Brain, Behavior and Evolution* 91:125–135.
- Balanoff, A. M., M. A. Norell, A. V. C. Hogan, and G. S. Bever. 2018b. The endocranial cavity of oviraptorosaur dinosaurs and the increasingly complex, deep history of the avian brain. *Brain, Behavior, and Evolution* 91:125–135.
- Balanoff, A. M., X. Xu, Y. Kobayashi, Y. Matsufune, and M. Norell. 2009. Cranial osteology of the theropod dinosaur *Incisivosaurus gauthieri* (Theropoda, Oviraptorosauria). *American Museum Novitates* 3651:1–35.
- Ballell, A., J. L. King, J. M. Neenan, E. J. Rayfield, and M. J. Benton. 2020. The braincase, brain and palaeobiology of the basal sauropodomorph dinosaur *Thecodontosaurus antiquus*. *Zoological Journal of the Linnean Society*.
- Barsbold, R., and H. Osmólska. 1999. The skull of *Velociraptor* (Theropoda) from the Late Cretaceous of Mongolia. *Acta Palaeontologica Polonica* 44:189–219.
- Beckinghausen, J., and R. V. Sillitoe. 2019. Insights into cerebellar development and connectivity. *Neuroscience Letters* 688:2–13.
- Benson, R. B. J., E. Starmer-Jones, R. A. Close, and S. A. Walsh. 2017. Comparative analysis of vestibular ecomorphology in birds. *Journal of Anatomy* 231:990–1018.

Bever, G. S., S. L. Brusatte, A. M. Balanoff, and M. A. Norell. 2011. Variation, variability, and the origin of the avian endocranium: insights from the anatomy of *Alioramus altai* (Theropoda: Tyrannosauroidae). PLOS ONE 6:e23393.

Beyrand, V., D. F. A. E. Voeten, S. Bureš, V. Fernandez, J. Janáček, D. Jiráček, O. Rauhut, and P. Tafforeau. 2019. Multiphase progenetic development shaped the brain of flying archosaurs. Scientific Reports 9:1–15.

Bhullar, B.-A. S., M. Hanson, M. Fabbri, A. Pritchard, G. S. Bever, and E. Hoffman. 2016. How to make a bird skull: Major transitions in the evolution of the avian cranium, paedomorphosis, and the beak as a surrogate hand. Integrative and Comparative Biology 56:389–403.

Bhullar, B.-A. S., J. Marugán-Lobón, F. Racimo, G. S. Bever, T. B. Rowe, M. A. Norell, and A. Abzhanov. 2012. Birds have paedomorphic dinosaur skulls. Nature 487:223–226.

Bianki, V. L. 1983. Hemisphere specialization of the animal brain for information processing principles. The International Journal of Neuroscience 20:75–89.

Blanchart, A., J. A. D. Carlos, and L. López-Mascaraque. 2006. Time frame of mitral cell development in the mice olfactory bulb. Journal of Comparative Neurology 496:529–543.

Brasier, M. D., D. B. Norman, A. G. Liu, L. J. Cotton, J. E. H. Hiscocks, R. J. Garwood, J. B. Antcliff, and D. Wacey. 2016. Remarkable preservation of brain tissues in an Early Cretaceous iguanodontian dinosaur. Geological Society, London, Special Publications 448:SP448.3.

Breazile, J. E., and H.-G. Hartwig. 1989. Central nervous system; pp. 485–566 in Form and function in birds. vol. 4. Academic Press, New York.

Briscoe, S. D., C. B. Albertin, J. J. Rowell, and C. W. Ragsdale. 2018. Neocortical association cell types in the forebrain of birds and alligators. Current Biology 28:686–696.

Brochu, C. A. 2003. Osteology of *Tyrannosaurus rex*: insights from a nearly complete skeleton and high-resolution computed tomographic analysis of the skull. Journal of Vertebrate Paleontology 22:1–138.

Bronzati, M., O. W. M. Rauhut, J. S. Bittencourt, and M. C. Langer. 2017. Endocast of the Late Triassic (Carnian) dinosaur *Saturnalia tupiniquim*: implications for the evolution of brain tissue in Sauropodomorpha. Scientific Reports 7:1–7.

Brusatte, S. L., and P. C. Sereno. 2007. A new species of *Carcharodontosaurus* (Dinosauria: Theropoda) from the Cenomanian of Niger and a revision of the genus. Journal of Vertebrate Paleontology 27:902–916.

Brusatte, S. L., A. Averianov, H.-D. Sues, A. Muir, and I. B. Butler. 2016. New tyrannosaur from the mid-Cretaceous of Uzbekistan clarifies evolution of giant body sizes and advanced senses in tyrant dinosaurs. Proceedings of the National Academy of Sciences 113:3447–3452.

Buchholtz, E. A., and E.-A. Seyfarth. 1999. The gospel of the fossil brain: Tilly Edinger and the science of paleoneurology. Brain Research Behavior 48:351–361.

Buchholtz, E. A., and E.-A. Seyfarth. 2001. The study of “fossil brains”: Tilly Edinger (1897–1967) and the beginnings of paleoneurology. BioScience 51:674–682.

Bullar, C. M., Q. Zhao, M. J. Benton, and M. J. Ryan. 2019. Ontogenetic braincase development in *Psittacosaurus lujiatunensis* (Dinosauria: Ceratopsia) using micro-computed tomography. *PeerJ* 7:e7217.

Burnham, D. A. 2004. New information of *Bambiraptor feinbergi* (Theropoda: Dromaeosauridae) from the Late Cretaceous of Montana; pp. 67–111 in Feathered Dragons: Studies on the Transition from Dinosaurs to Birds. Indiana University Press, Bloomington.

Carabajal, A. P. 2010. Cranial endocast of the carcharodontosaurid theropod *Giganotosaurus carolinii* Coria & Salgado, 1995. *Neues Jahrbuch Für Geologie Und Paläontologie - Abhandlungen* 258:249–256.

Carabajal, A. P. 2012. Neuroanatomy of titanosaurid dinosaurs from the Upper Cretaceous of Patagonia, with comments on endocranial variability within Sauropoda. *The Anatomical Record* 295:2141–2156.

Carabajal, A. P., and C. Succar. 2014. The endocranial morphology and inner ear of the abelisaurid theropod *Aucasaurus garridoi*. *Acta Palaeontologica Polonica* 60:141–144.

Carabajal, A. P., and P. J. Currie. 2017. The braincase of the theropod dinosaur *Murusraptor*: osteology, neuroanatomy and comments on the paleobiological implications of certain endocranial features. *Ameghiniana* 54:617–640.

Carabajal, A. P., Y.-N. Lee, and L. L. Jacobs. 2016. Endocranial morphology of the primitive nodosaurid dinosaur *Pawpawsaurus campbelli* from the Early Cretaceous of North America. *PLOS ONE* 11:e0150845.

Carabajal, A. P., R. A. Coria, P. J. Currie, and E. B. Koppelhus. 2018. A natural cranial endocast with possible dicraeosaurid (Sauropoda, Diplodocoidea) affinities from the Lower Cretaceous of Patagonia. *Cretaceous Research* 84:437–441.

Carpenter, K. 1998. Evidence of predatory behavior by carnivorous dinosaurs. *Gaia* 15:135–144.

Cerio, D. G., and L. M. Witmer. 2019. Intraspecific variation and symmetry of the inner-ear labyrinth in a population of wild turkeys: implications for paleontological reconstructions. *PeerJ* 7:e7355.

Cobb, S., and T. Edinger. 1962. The brain of the emu (*Dromaeus novaehollandiae*, Lath) I. Gross anatomy of the brain and pineal body. *Breviora* 170:1–18.

Cooper, R. G. 2005. Growth in the ostrich (*Struthio camelus* var. *domesticus*). *Animal Science Journal* 76:1–4.

Corfield, J. R., J. M. Wild, M. E. Hauber, S. Parsons, and M. F. Kubke. 2008. Evolution of brain size in the palaeognath lineage, with an emphasis on New Zealand ratites. *Brain, Behavior and Evolution* 71:87–99.

Cruzado-Caballero, P., J. Fortuny, S. Llacer, and J. I. Canudo. 2015. Paleoneuroanatomy of the European lambeosaurine dinosaur *Arenysaurus ardevoli*. *PeerJ* 3:e802.

Currie, P. J. 1995. New information on the anatomy and relationships of *Dromaeosaurus albertensis* (Dinosauria: Theropoda). *Journal of Vertebrate Paleontology* 15:576–591.

Cuvier, G. 1835. Recherches Sur Les Ossements Fossiles: Où l'on Rétablit Les Caractères de Plusieurs Animaux Dont Les Révolutions Du Globe Ont Détruit Les Espèces, 4. éd. E. d'Ocagne, Paris, 488 pp.

Dendy, A. 1911. On the structure, development and morphological interpretation of the pineal organs and adjacent parts of the brain in the tuatara (*Sphenodon punctatus*). Phil. Trans. R. Soc. Lond. B 201:227–331.

Dominguez, P., A. Milner, R. Ketcham, J. Cookson, and T. Rowe. 2004. The avian nature of the brain and inner ear of *Archaeopteryx*. Nature 430:666–669.

Dufeu, D. L., and L. M. Witmer. 2015. Ontogeny of the middle-ear air-sinus system in *Alligator mississippiensis* (Archosauria: Crocodylia). PLOS ONE 10:e0137060.

Dufeu, D. L., A. C. Morhardt, and L. M. Witmer. 2012. Ontogenetic change in the cranial endocast and endosseous labyrinth of American alligator (*Alligator mississippiensis*): Implications for the interpretation of extinct archosaurs. Journal of Vertebrate Paleontology 32:1.

Edinger, T. 1929. Die fossilen Gehirne. Ergebnisse Der Anatomie Und Entwicklungsgeschichte 28:1–249.

Edinger, T. 1942. The pituitary body in giant animals fossil and living: a survey and a suggestion. The Quarterly Review of Biology 17:31–45.

Edinger, T. 1948. Evolution of the Horse Brain. Geological Society of America, 192 pp.

Edinger, T. 1951. The brains of the Odontognathae. Evolution 5:6–24.

Edinger, T. 1955. Hearing and smell in cetacean history. Monatsschrift Für Psychiatrie Und Neurologie 129:37–58.

Edinger, T. 1962. Anthropocentric misconceptions in paleoneurology. Medical Society in the City of New York 19:56–107.

Edinger, T. 1975. Paleoneurology 1804-1966: An Annotated Bibliography. Springer Science & Business Media, 258 pp.

Erickson, G. M., P. J. Makovicky, B. D. Inouye, C.-F. Zhou, and K.-Q. Gao. 2009. A life table for *Psittacosaurus lujiatunensis*: initial insights into ornithischian dinosaur population biology. The Anatomical Record 292:1514–1521.

Evans, D. C. 2005. New evidence on brain-endocranial cavity relationships in ornithischian dinosaurs. Acta Palaeontologica Polonica 50:617–622.

Evans, D. C., R. Ridgely, and L. M. Witmer. 2009. Endocranial anatomy of lambeosaurine hadrosaurids (Dinosauria: Ornithischia): A sensorineural perspective on cranial crest function. The Anatomical Record 292:1315–1337.

Evers, S. W., J. M. Neenan, G. S. Ferreira, I. Werneburg, P. M. Barrett, and R. B. J. Benson. 2019. Neurovascular anatomy of the protostegid turtle *Rhinochelys pulchriceps* and comparisons of membranous and endosseous labyrinth shape in an extant turtle. Zoological Journal of the Linnean Society 187:800–828.

- Fabbri, M., N. Mongiardino Koch, A. C. Pritchard, M. Hanson, E. Hoffman, G. S. Bever, A. M. Balanoff, Z. S. Morris, D. J. Field, J. Camacho, T. B. Rowe, M. A. Norell, R. M. Smith, A. Abzhanov, and B.-A. S. Bhullar. 2017. The skull roof tracks the brain during the evolution and development of reptiles including birds. *Nature Ecology & Evolution* 1:1543–1550.
- Farke, A. A., D. J. Chok, A. Herrero, B. Scolieri, and S. Werning. 2013. Ontogeny in the tube-crested dinosaur *Parasaurolophus* (Hadrosauridae) and heterochrony in hadrosaurids. *PeerJ* 1:e182.
- Ferreira-Cardoso, S., R. Araújo, N. E. Martins, G. G. Martins, S. Walsh, R. M. S. Martins, N. Kardjilov, I. Manke, A. Hilger, and R. Castanhinha. 2017. Floccular fossa size is not a reliable proxy of ecology and behaviour in vertebrates. *Scientific Reports* 7:1–11.
- Franzosa, J., and T. Rowe. 2005. Cranial endocast of the Cretaceous theropod dinosaur *Acrocanthosaurus atokensis*. *Journal of Vertebrate Paleontology* 25:859–864.
- Franzosa, J. W. 2004. Evolution of the brain in Theropoda (Dinosauria). Ph.D., The University of Texas at Austin, Austin, Texas, 357 pp.
- Georgi, J. A., J. S. Sipla, and C. A. Forster. 2013. Turning semicircular canal function on its head: dinosaurs and a novel vestibular analysis. *PLOS ONE* 8:e58517.
- Giffin, E. B. 1989. Pachycephalosaur paleoneurology (Archosauria: Ornithischia). *Journal of Vertebrate Paleontology* 9:67–77.
- Gleich, O., R. J. Dooling, and G. A. Manley. 2005. Audiogram, body mass, and basilar papilla length: correlations in birds and predictions for extinct archosaurs. *Naturwissenschaften* 92:595–598.
- Godefroit, P., P. J. Currie, L. Hong, S. C. Yong, and D. Zhi-Ming. 2008. A new species of *Velociraptor* (Dinosauria: Dromaeosauridae) from the Upper Cretaceous of northern China. *Journal of Vertebrate Paleontology* 28:432–438.
- Gold, M. E. L., and A. Watanabe. 2018. Flightless birds are not neuroanatomical analogs of non-avian dinosaurs. *BMC Evolutionary Biology* 18:190.
- Goodwin, M. B., W. A. Clemens, J. R. Horner, and K. Padian. 2006. The smallest known *Triceratops* skull: new observations on ceratopsid cranial anatomy and ontogeny. *Journal of Vertebrate Paleontology* 26:103–112.
- Grigg, N. P., J. M. Krilow, C. Gutierrez-Ibanez, D. R. Wylie, G. R. Graves, and A. N. Iwaniuk. 2012. Anatomical evidence for scent guided foraging in the turkey vulture. *Scientific Reports* 7:17408.
- von Haller, V. A. 1762. *Elementa Physiologiae Corporis Humani*. Sumptibus M. M. Bousquet et Sociorum, Lausannae, 596 pp.
- Hansen, A. 2007. Olfactory and solitary chemosensory cells: two different chemosensory systems in the nasal cavity of the American alligator, *Alligator mississippiensis*. *BMC Neuroscience* 8:64.

- Holtz Jr., T. R. 2008. A critical reappraisal of the obligate scavenging hypothesis for *Tyrannosaurus rex* and other tyrant dinosaurs; pp. 371–396 in *Tyrannosaurus rex* the Tyrant King. Indiana University Press, Bloomington.
- Hone, D., T. Tsuihiji, M. Watabe, and K. Tsogtbaatr. 2012. Pterosaurs as a food source for small dromaeosaurs. *Palaeogeography, Palaeoclimatology, Palaeoecology* 331–332:27–30.
- Hone, D., J. Choiniere, C. Sullivan, X. Xu, M. Pittman, and Q. Tan. 2010. New evidence for a trophic relationship between the dinosaurs *Velociraptor* and *Protoceratops*. *Palaeogeography, Palaeoclimatology, Palaeoecology* 291:488–492.
- Hopson, J. A. 1977. Relative brain size and behavior in archosaurian reptiles. *Annual Review of Ecology and Systematics* 8:429–448.
- Hopson, J. A. 1979. Paleoneurology; pp. 39–146 in *Biology of the Reptilia*, C. Gans, R.C. Northcutt, and P. Ulinski. vol. 9. Academic Press Inc., New York, New York.
- Horner, J. R., and M. B. Goodwin. 2006. Major cranial changes during *Triceratops* ontogeny. *Proceedings of the Royal Society B: Biological Sciences* 273:2757–2761.
- Hu, K., J. L. King, C. A. Romick, D. L. Dufeu, L. M. Witmer, E. J. Rayfield, and M. J. Benton. 2021. Ontogenetic endocranial shape change in alligators and ostriches and its implications for the development of the non-avian dinosaur endocranium. *The Anatomical Record*.
- Hübner, T. R., and O. W. M. Rauhut. 2010. A juvenile skull of *Dysalotosaurus lettowvorbecki* (Ornithischia: Iguanodontia), and implications for cranial ontogeny, phylogeny, and taxonomy in ornithomimid dinosaurs. *Zoological Journal of the Linnean Society* 160:366–396.
- Hughes, G. M., and J. A. Finarelli. 2019. Olfactory receptor repertoire size in dinosaurs. *Proceedings of the Royal Society B: Biological Sciences* 286:20190909.
- Hurlburt, G. R. 1996. Relative brain size in recent and fossil amniotes: determination and interpretation. Ph.D., University of Toronto, Toronto pp.
- Iwaniuk, A. N., and J. E. Nelson. 2002. Can endocranial volume be used as an estimate of brain size in birds? *Canadian Journal of Zoology* 80:16–23.
- Jarvik, E. 1954. On the visceral skeleton in *Eusthenopteron*, with a discussion of the parasphenoid and palatoquadrate in fishes. *Kungl. Svenska Vetenskapsakademiens Handlingar* 4:1–104.
- Jerison, H. J. 1955. Brain to body ratios and the evolution of intelligence. *Science* 121:447–449.
- Jerison, H. J. 1961. Quantitative analysis of evolution of the brain in mammals. *Science* 133:1012–1014.
- Jerison, H. J. 1969. Brain evolution and dinosaur brains. *The American Naturalist* 103:575–588.
- Jerison, H. J. 1973. *Evolution of the Brain and Intelligence*. Academic Press, New York, 482 pp.

Jerison, H. J., H. B. Barlow, and L. Weiskrantz. 1985. Animal intelligence as encephalization. *Philosophical Transactions of the Royal Society of London. B, Biological Sciences* 308:21–35.

Jirak, D., and J. Janacek. 2017. Volume of the crocodilian brain and endocast during ontogeny. *PLOS ONE* 12:e0178491.

Jones, M. P., K. E. Pierce, and D. Ward. 2007. Avian vision: a review of form and function with special consideration to birds of prey. *Journal of Exotic Pet Medicine* 16:69–87.

Kawabe, S., S. Matsuda, N. Tsunekawa, and H. Endo. 2015. Ontogenetic shape change in the chicken brain: implications for paleontology. *PLOS ONE* 10:e0129939.

Kawabe, S., T. Shimokawa, H. Miki, S. Matsuda, and H. Endo. 2013. Variation in avian brain shape: relationship with size and orbital shape. *Journal of Anatomy* 223:495–508.

Kettler, L., and C. E. Carr. 2019. Neural maps of interaural time difference in the American alligator: a stable feature in modern archosaurs. *Journal of Neuroscience* 39:3882–3896.

King, J. L., J. S. Sipla, J. A. Georgi, A. M. Balanoff, and J. M. Neenan. 2020. The endocranium and trophic ecology of *Velociraptor mongoliensis*. *Journal of Anatomy* 237:861–869.

Knapp, A., R. J. Knell, A. A. Farke, M. A. Loewen, and D. W. E. Hone. 2018. Patterns of divergence in the morphology of ceratopsian dinosaurs: sympatry is not a driver of ornament evolution. *Proceedings of the Royal Society B: Biological Sciences* 285:20180312.

Knoll, F., and D. Schwarz-Wings. 2009. Palaeoneuroanatomy of *Brachiosaurus*. *Annales de Paléontologie* 95:165–175.

Knoll, F., L. M. Witmer, F. Ortega, R. C. Ridgely, and D. Schwarz-Wings. 2012. The braincase of the basal sauropod dinosaur *Spinophorosaurus* and 3D reconstructions of the cranial endocast and inner ear. *PLOS ONE* 7:e30060.

Kondrashova, T., J. Blanchard, L. Knoche, J. Potter, and B. A. Young. 2020. Intracranial pressure in the American Alligator (*Alligator mississippiensis*): reptilian meninges and orthostatic gradients. *Journal of Comparative Physiology. A, Neuroethology, Sensory, Neural, and Behavioral Physiology* 206:45–54.

Kundrát, M. 2007. Avian-like attributes of a virtual brain model of the oviraptorid theropod *Conchoraptor gracilis*. *Naturwissenschaften* 94:499–504.

Kundrát, M., X. Xu, M. Hančová, A. Gajdoš, Y. Guo, and D. Chen. 2018. Evolutionary disparity in the endoneurocranial configuration between small and gigantic tyrannosauroids. *Historical Biology* 0:1–15.

Kurochkin, E. N., S. V. Saveliev, A. A. Postnov, E. Pervushov, and E. V. Popov. 2006. On the brain of a primitive bird from the Upper Cretaceous of European Russia. *Paleontological Journal* 40:655–667.

Kurochkin, E. N., G. J. Dyke, S. V. Saveliev, E. M. Pervushov, and E. V. Popov. 2007. A fossil brain from the Cretaceous of European Russia and avian sensory evolution. *Biology Letters* 3:309–313.

- Larsson, H. C. E., P. C. Sereno, and J. A. Wilson. 2000. Forebrain enlargement among nonavian theropod dinosaurs. *Journal of Vertebrate Paleontology* 20:615–618.
- Lautenschlager, S. 2014. Morphological and functional diversity in therizinosaur claws and the implications for theropod claw evolution. *Proceedings of the Royal Society of London B: Biological Sciences* 281:20140497.
- Lautenschlager, S., and T. Hübner. 2013. Ontogenetic trajectories in the ornithischian endocranium. *Journal of Evolutionary Biology* 26:2044–2050.
- Lautenschlager, S., and R. J. Butler. 2016. Neural and endocranial anatomy of Triassic phytosaurian reptiles and convergence with fossil and modern crocodylians. *PeerJ* 4.
- Lautenschlager, S., E. J. Rayfield, P. Altangerel, L. E. Zanno, and L. M. Witmer. 2012. The endocranial anatomy of Therizinosauria and its implications for sensory and cognitive function. *PLOS ONE* 7:e52289.
- Lauters, P., M. Vercauteren, Y. L. Bolotsky, and P. Godefroit. 2013. Cranial endocast of the lambeosaurine hadrosaurid *Amurosaurus riabinini* from the Amur Region, Russia. *PLOS ONE* 8:e78899.
- Maderspacher, F. 2017. Evolution: Flight of the ratites. *Current Biology* 27:R110–R113.
- Manley, G. A. 1990. The peripheral hearing organ in birds; pp. 206–252 in *Peripheral Hearing Mechanisms in Reptiles and Birds*, 1st ed. Springer, Verlag Berlin Heidelberg.
- Manning, P. L., L. Margetts, M. R. Johnson, P. J. Withers, W. I. Sellers, P. L. Falkingham, P. M. Mummery, P. M. Barrett, and D. R. Raymont. 2009. Biomechanics of dromaeosaurid dinosaur claws: application of X-ray microtomography, nanoindentation, and finite element analysis. *The Anatomical Record* 292:1397–1405.
- Marchetti, K., and T. Price. 1989. Differences in the foraging of juvenile and adult birds: the importance of developmental constraints. *Biological Reviews* 64:51–70.
- Marsh, O. C. 1873. Notice of a new and remarkable fossil bird. *Annals and Magazine of Natural History* 11:80.
- Marsh, O. C. 1874. Small size of the brain in tertiary mammals. *Annals and Magazine of Natural History* 14:167–167.
- Marsh, O. C. 1880. *Odontornithes: A Monograph on the Extinct Toothed Birds of North America*. U.S. Government Printing Office, 201 pp.
- Marsh, O. C. 1881. Principal characters of American Jurassic dinosaurs, Part V. *American Journal of Science Series 3 Vol.* 21:417–423.
- Marsh, O. C. 1884a. Principal characters of American Jurassic dinosaurs; Part VII, on the Diplodocidae, a new family of the Sauropoda. *American Journal of Science* 27:161–167.
- Marsh, O. C. 1884b. Principal characters of American Jurassic dinosaurs; Part VIII, the order Theropoda. *American Journal of Science* 27:329–340.
- Marsh, O. C. 1886. *Dinocerata: A Monograph of an Extinct Order of Gigantic Mammals*. U.S. Government Printing Office, 522 pp.

- Marsh, O. C. 1889. Notice of gigantic horned Dinosauria from the Cretaceous. American Journal of Science Series 3 Vol. 38:173–176.
- Marsh, O. C. 1890. Additional characters of the Ceratopsidae, with notice of new Cretaceous dinosaurs. American Journal of Science Series 3 Vol. 39:418–426.
- Marsh, O. C. 1891. The gigantic Ceratopsidæ, or horned dinosaurs, of North America. Geological Magazine 8:193–199.
- Marsh, O. C. 1896. The Dinosaurs of North America. United States Geological Survey, Washington D. C., 133–244 pp.
- Matthew, W. D., and B. Brown. 1922. The family Deinodontidae, with notice of a new genus from the Cretaceous of Alberta. Bulletin of the American Museum of Natural History 46:367–385.
- Mattisson, J., G. R. Rauset, J. Odden, H. Andrén, J. D. C. Linnell, and J. Persson. 2016. Predation or scavenging? Prey body condition influences decision-making in a facultative predator, the wolverine. Ecosphere 7:e01407.
- McKeown, M., S. L. Brusatte, T. E. Williamson, J. A. Schwab, T. D. Carr, I. B. Butler, A. Muir, K. Schroeder, M. A. Espy, J. F. Hunter, A. S. Losko, R. O. Nelson, D. C. Gautier, and S. C. Vogel. 2020. Neurosensory and sinus evolution as tyrannosauroid dinosaurs developed giant size: Insight from the endocranial anatomy of *Bistahieversor sealeyi*. The Anatomical Record 303:1043–1059.
- McNamara, K. J. 2012. Heterochrony: the evolution of development. Evolution: Education and Outreach 5:203–218.
- Milner, A. C., and S. A. Walsh. 2009. Avian brain evolution: new data from Palaeogene birds (Lower Eocene) from England. Zoological Journal of the Linnean Society 155:198–219.
- Morhardt, A. C., R. Ridgely, and L. M. Witmer. 2017. Gross Anatomical Brain Region Approximation (GABRA): a new landmark-based approach for estimating brain regions in dinosaurs and other archosaurs. Federation of American Societies for Experimental Biology 31:251.2-251.2.
- Müller, R. T., J. D. Ferreira, F. A. Pretto, M. Bronzati, and L. Kerber. 2020. The endocranial anatomy of *Buriolestes schultzi* (Dinosauria: Saurischia) and the early evolution of brain tissues in sauropodomorph dinosaurs. Journal of Anatomy.
- Muroyama, Y., A. Baba, M. Kitagawa, and T. Saito. 2016. Olfactory sensory neurons control dendritic complexity of mitral cells via notch signaling. PLOS Genetics 12:e1006514.
- Napoli, J. G., T. Hunt, G. M. Erickson, and M. A. Norell. 2019. *Psittacosaurus amitabha*, a new species of ceratopsian dinosaur from the Ondai Sayr locality, Central Mongolia. American Museum Novitates 2019:1–36.
- Neenan, J. M., K. E. J. Chapelle, V. Fernandez, and J. N. Choiniere. 2018. Ontogeny of the *Massospondylus* labyrinth: implications for locomotory shifts in a basal sauropodomorph dinosaur. Palaeontology 62:255–265.

Newton, E. T. 1888. On the skull, brain, and auditory organ of a new species of pterosaurian *Scaphognathus purdoni*, from the upper Lias near Whitby, Yorkshire. Phil. Trans. R. Soc. Lond. B 179:503–537.

Nomura, T., and E.-I. Izawa. 2017. Avian brains: Insights from development, behaviors and evolution. *Development, Growth & Differentiation* 59:244–257.

Norell, M. A., P. Makovicky, and J. M. Clark. 1997. A *Velociraptor* wishbone. *Nature* 389:447.

Norell, M. A., P. J. Makovicky, and J. M. Clark. 2004. The braincase of *Velociraptor*, pp. 133–143 in *Feathered Dragons: Studies on the Transition from Dinosaurs to Birds*. Indiana University Press, Bloomington.

Osborn, H. F. 1912. Crania of *Tyrannosaurus* and *Allosaurus*. *American Museum of Natural History Memoirs* 1:1–30.

Osborn, H. F. 1924. Three new Theropoda, *Protoceratops* zone, central Mongolia. *American Museum Novitates* 144:1–12.

Paulin, M. G. 1993. The role of the cerebellum in motor control and perception. *Brain, Behavior and Evolution* 41:39–50.

Peng, K.-M., Y. Feng, G. Zhang, H. Liu, and H. Song. 2010. Anatomical study of the brain of the African ostrich. *Turkish Journal of Veterinary and Animal Sciences* 34:235–241.

Picasso, M. B. J., C. Tambussi, and M. T. Dozo. 2009. Neurocranial and brain anatomy of a Late Miocene eagle (Aves, Accipitridae) from Patagonia. *Journal of Vertebrate Paleontology* 29:831–836.

Plateau, O., and C. Foth. 2020. Birds have peramorphic skulls, too: anatomical network analyses reveal oppositional heterochronies in avian skull evolution. *Communications Biology* 3:1–12.

Potier, S. 2019. Olfaction in raptors. *Zoological Journal of the Linnean Society* 1–10.

Potier, S., O. Duriez, A. Célérier, J.-L. Liegeois, and F. Bonadonna. 2019. Sight or smell: Which senses do scavenging raptors use to find food? *Animal Cognition* 22:49–59.

Rabbitt, R. D., E. R. Damiano, and J. W. Grant. 2004. Biomechanics of the semicircular canals and otolith organs; pp. 153–201 in S. M. Highstein, R. R. Fay, and A. N. Popper (eds.), *The Vestibular System*. Springer Handbook of Auditory Research Springer, New York, NY.

Racicot, R. 2016. Fossil secrets revealed: X-ray CT scanning and applications in paleontology. *The Paleontological Society Papers* 22:21–38.

Radinsky, L. B. 1968. A new approach to mammalian cranial analysis, illustrated by examples of prosimian primates. *Journal of Morphology* 124:167–179.

Rogers, C. S., D. W. E. Hone, M. E. McNamara, Q. Zhao, P. J. Orr, S. L. Kearns, and M. J. Benton. 2015. The Chinese Pompeii? Death and destruction of dinosaurs in the Early Cretaceous of Lujiatun, NE China. *Palaeogeography, Palaeoclimatology, Palaeoecology* 427:89–99.

Rogers, S. W. 1998. Exploring dinosaur neuropaleobiology: computed tomography scanning and analysis of an *Allosaurus fragilis* endocast. *Neuron* 21:673–679.

Rogers, S. W. 2000. *Allosaurus*, crocodiles, and birds: evolutionary clues from spiral computed tomography of an endocast. *The Anatomical Record* 257:162–173.

Romick, C. A. 2013. Ontogeny of the brain endocasts of ostriches (Aves: *Struthio camelus*) with implications for interpreting extinct dinosaur endocasts. Ohio University, Athens, 47 pp.

Ruse, M. 2019. Why did the *Stegosaurus* have plates, or is biology second-rate because it thinks in terms of ends? *Humanities Journal of Valparaíso* 0:9–25.

Sakagami, R., and S. Kawabe. 2020. Endocranial anatomy of the ceratopsid dinosaur *Triceratops* and interpretations of sensory and motor function. *PeerJ* 8:e9888.

Sampson, S. D., and L. M. Witmer. 2007. Craniofacial anatomy of *Majungasaurus crenatissimus* (Theropoda: Abelisauridae) from the Late Cretaceous of Madagascar. *Journal of Vertebrate Paleontology* 27:32–104.

Sander, P. M., A. Christian, M. Clauss, R. Fechner, C. T. Gee, E.-M. Griebeler, H.-C. Gunga, J. Hummel, H. Mallison, S. F. Perry, H. Preuschoft, O. W. M. Rauhut, K. Remes, T. Tütken, O. Wings, and U. Witzel. 2011. Biology of the sauropod dinosaurs: the evolution of gigantism. *Biological Reviews* 86:117–155.

Sanders, R. K., and D. K. Smith. 2005. The endocranium of the theropod dinosaur *Ceratosaurus* studied with computed tomography. *Acta Palaeontologica Polonica* 50:601–616.

Schmitz, L., and R. Motani. 2011. Nocturnality in dinosaurs inferred from scleral ring and orbit morphology. *Science* 332:705–708.

Schuchert, C. 1938. Biographical memoir of Othniel Charles Marsh 1831–1899. *National Academy of Sciences* 20:1–78.

Sereno, P. C., J. A. Wilson, L. M. Witmer, J. A. Whitlock, A. Maga, O. Ide, and T. A. Rowe. 2007. Structural extremes in a Cretaceous dinosaur. *PLOS ONE* 2:e1230.

Sollas, W. J. 1904. A method for the investigation of fossils by serial sections. *Philosophical Transactions of the Royal Society of London. B, Biological Sciences* 196:259–265.

Stevens, K. A. 2006. Binocular vision in theropod dinosaurs. *Journal of Vertebrate Paleontology* 26:321–330.

Sues, H.-D. 1977. The skull of *Velociraptor mongoliensis*, a small cretaceous theropod dinosaur from Mongolia. *Paläontologische Zeitschrift* 51:173–184.

Surgent, O. J., O. I. Dadalko, K. A. Pickett, and B. G. Travers. 2019. Balance and the brain: A review of structural brain correlates of postural balance and balance training in humans. *Gait & Posture* 71:245–252.

Tjernberg, M. 1981. Diet of the golden eagle *Aquila chrysaetos* during the breeding season in Sweden. *Ecography* 4:12–19.

- Torres, C. R., and J. A. Clarke. 2018. Nocturnal giants: Evolution of the sensory ecology in elephant birds and other palaeognaths inferred from digital brain reconstructions. *Proceedings of the Royal Society B: Biological Sciences* 285:20181540.
- Turner, A. H., P. J. Makovicky, and M. A. Norell. 2007. Feather quill knobs in the dinosaur *Velociraptor*. *Science* 317:1721–1721.
- Walsh, S. A., and F. Knoll. 2018. The Evolution of Avian Intelligence and Sensory Capabilities: The Fossil Evidence; pp. 59–69 in E. Bruner, N. Ogihara, and H. C. Tanabe (eds.), *Digital Endocasts: From Skulls to Brains.*, . Replacement of Neanderthals by Modern Humans Series Springer Japan, Tokyo.
- Walsh, S. A., A. C. Milner, and E. Bourdon. 2016. A reappraisal of *Cerebavis cenomanica* (Aves, Ornithurae), from Melovodka, Russia. *Journal of Anatomy* 229:215–227.
- Walsh, S. A., P. M. Barrett, A. C. Milner, G. Manley, and L. M. Witmer. 2009. Inner ear anatomy is a proxy for deducing auditory capability and behaviour in reptiles and birds. *Proceedings of the Royal Society of London B: Biological Sciences* 276:1355–1360.
- Walsh, S. A., A. N. Iwaniuk, M. A. Knoll, E. Bourdon, P. M. Barrett, A. C. Milner, R. L. Nudds, R. L. Abel, and P. D. Sterpaio. 2013. Avian cerebellar floccular fossa size is not a proxy for flying ability in birds. *PloS One* 8:e67176.
- Wang, S., J. Stiegler, R. Amiot, X. Wang, G. Du, J. M. Clark, and X. Xu. 2017. Extreme ontogenetic changes in a ceratosaurian theropod. *Current Biology* 27:144–148.
- Watanabe, A., P. M. Gignac, A. M. Balanoff, T. L. Green, N. J. Kley, and M. A. Norell. 2019. Are endocasts good proxies for brain size and shape in archosaurs throughout ontogeny? *Journal of Anatomy* 234:291–305.
- Weldon, P. J., and M. W. Ferguson. 1993. Chemoreception in crocodilians: anatomy, natural history, and empirical results. *Brain, Behavior and Evolution* 41:239–245.
- Wenzel, B. M. 1971. Olfaction in birds; pp. 432–448 in J. E. Amoore, M. G. J. Beets, J. T. Davies, T. Engen, J. Garcia, R. C. Gesteland, P. P. C. Graziadei, K.-E. Kaissling, R. A. Koelling, J. LeMagnen, P. MacLeod, D. G. Moulton, M. M. Mozell, D. Ottoson, T. S. Parsons, S. F. Takagi, D. Tucker, B. M. Wenzel, and L. M. Beidler (eds.), *Olfaction in Birds.*, . Handbook of Sensory Physiology Springer Berlin Heidelberg, Berlin, Heidelberg.
- Wenzel, B. M. 1987. The olfactory and related systems in birds. *Annals of the New York Academy of Sciences* 519:137–149.
- Wharton, D. 2002. The evolution of the avian brain. Ph.D., University of Bristol, Bristol, 352 pp.
- Wilkinson, P. M., T. R. Rainwater, A. R. Woodward, E. H. Leone, and C. Carter. 2016. Determinate growth and reproductive lifespan in the American Alligator (*Alligator mississippiensis*): Evidence from long-term recaptures. *Copeia* 104:843–852.
- Wilmers, C. C., D. R. Stahler, R. L. Crabtree, D. W. Smith, and W. M. Getz. 2003. Resource dispersion and consumer dominance: scavenging at wolf- and hunter-killed carcasses in Greater Yellowstone, USA. *Ecology Letters* 6:996–1003.

Wilson, V. J., R. Boyle, K. Fukushima, P. K. Rose, Y. Shinoda, Y. Sugiuchi, and Y. Uchinoll. 1995. The vestibulocollic reflex. *Journal of Vestibular Research* 5:147–170.

Witmer, L. M., and R. C. Ridgely. 2008a. Structure of the brain cavity and inner ear of the centrosaurine ceratopsid dinosaur *Pachyrhinosaurus* based on CT scanning and 3D visualization; pp. 117–144 in In: Currie PJ, Langstone Jr W, Tanke DH, editors. *A New Horned Dinosaur from an Upper Cretaceous Bone Bed in Alberta*. National Research Council of Canada, Ottawa.

Witmer, L. M., and R. C. Ridgely. 2008b. The paranasal air sinuses of predatory and armored dinosaurs (Archosauria: Theropoda and Ankylosauria) and their contribution to cephalic structure. *The Anatomical Record* 291:1362–1388.

Witmer, L. M., and R. C. Ridgely. 2009. New insights into the brain, braincase, and ear region of tyrannosaurs (Dinosauria, Theropoda), with implications for sensory organization and behavior. *The Anatomical Record* 292:1266–1296.

Witmer, L. M., S. Chatterjee, J. Franzosa, and T. Rowe. 2003. Neuroanatomy of flying reptiles and implications for flight, posture and behaviour. *Nature* 425:950–953.

Woodruff, D. C., T. D. Carr, G. W. Storrs, K. Waskow, J. B. Scannella, K. K. Nordén, and J. P. Wilson. 2018. The smallest diplodocid skull reveals cranial ontogeny and growth-related dietary changes in the largest dinosaurs. *Scientific Reports* 8:1–12.

Zelenitsky, D. K., F. Therrien, and Y. Kobayashi. 2009. Olfactory acuity in theropods: palaeobiological and evolutionary implications. *Proceedings of the Royal Society of London B: Biological Sciences* 276:667–673.

Zelenitsky, D. K., F. Therrien, R. C. Ridgely, A. R. McGee, and L. M. Witmer. 2011. Evolution of olfaction in non-avian theropod dinosaurs and birds. *Proceedings. Biological Sciences* 278:3625–3634.

Zhang, Q.-N., J. L. King, D.-Q. Li, Y.-M. Hou, and H.-L. You. 2019. Endocranial morphology of *Auroraceratops* sp. (Dinosauria: Ceratopsia) from the Early Cretaceous of Gansu Province, China. *Historical Biology* 1–6.

Zhao, Q., M. J. Benton, X. Xu, and P. M. Sander. 2013a. Juvenile-only clusters and behaviour of the Early Cretaceous dinosaur *Psittacosaurus*. *Acta Palaeontologica Polonica* 59:827–833.

Zhao, Q., M. J. Benton, C. Sullivan, P. Martin Sander, and X. Xu. 2013b. Histology and postural change during the growth of the ceratopsian dinosaur *Psittacosaurus lujiatunensis*. *Nature Communications* 4:1–8.

Zhou, C.-F., K.-Q. Gao, R. C. Fox, and X.-K. Du. 2007. Endocranial morphology of psittacosaur (Dinosauria: Ceratopsia) based on CT scans of new fossils from the Lower Cretaceous, China. *Palaeoworld* 16:285–293.

Supplementary Information

Table S1 – Comprehensive table of named taxa from which cranial endocasts are known. Taxa are separated into genus and species, first appearance in the fossil record (FAD), last appearance in the fossil record (LAD), clade, the lowest phylogenetic level available that groups large amounts of taxa, and continent where the species is found.

Genus/species	FAD	LAD	Clade	Lowest broad phylogenetic level	Continent
<i>Iguanodon bernissartensis</i>	126	122	Cerapoda	Iguanodontidae	Europe
<i>Mantellisaurus atherfieldensis</i>	130	125	Cerapoda	Iguanodontidae	Europe
<i>Secernosaurus koeneri</i>	85	66	Cerapoda	Saurolophinae	South America
			Cerapoda	Dryosaurid	
<i>Dysalotosaurus lettowvorbecki</i>	152	151		Iguanodontian	North America
<i>Corythosaurus casuarius</i>	77	75	Cerapoda	Lambeosaurinae	North America
<i>Edmontosaurus regalis</i>	73	66	Cerapoda	Saurolophinae	North America
<i>Parasaurolophus walker</i>	76.5	73	Cerapoda	Lambeosaurinae	North America
<i>Hypacrosaurus altispinus</i>	75	67	Cerapoda	Lambeosaurinae	North America
<i>Lambeosaurus lambei</i>	76	75	Cerapoda	Lambeosaurinae	North America
<i>Gryposaurus notabilis</i>	80	75	Cerapoda	Saurolophinae	North America
<i>Kundurosaurus nagorny</i>	67	66	Cerapoda	Saurolophinae	Europe
<i>Telmatosaurus transsylvanicus</i>	70	66	Cerapoda	Basal Hadrosaur	Europe
<i>Arenysaurus ardevoli</i>	66	66	Cerapoda	Lambeosaurinae	Europe
<i>Amurosaurus riabinini</i>	70	66	Cerapoda	Lambeosaurinae	Europe
<i>Auroraceratops rugosus</i>	126	115	Cerapoda	Neoceratopsia	China
<i>Stegoceras validum</i>	77.5	74	Cerapoda	Pachycephalosauridae	North America
<i>Pachycephalosaurus wyomingensis</i>	70	66	Cerapoda	Pachycephalosauridae	North America
<i>Pachyrhinosaurus canadensis</i>	73.5	68.5	Cerapoda	Neoceratopsia	North America
<i>Psittacosaurus lujiatunensis</i>	126	101	Cerapoda	Ceratopsia	Asia
<i>Triceratops horridus</i>	68	66	Cerapoda	Neoceratopsia	North America
<i>Stegosaurus stenops</i>	155	150	Thyreophora	Stegosauria	North America
<i>Kentrosaurus aethiopicus</i>	152	152	Thyreophora	Stegosauria	Africa
<i>Kunbarrasaurus ieveri</i>	105	99	Thyreophora	Ankylosauria	Australia
<i>Euoplocephalus tutus</i>	76	75	Thyreophora	Ankylosauria	North America
<i>Tarchia kielanae</i>	75	70	Thyreophora	Ankylosauria	Asia
<i>Talarurus plicatospineus</i>	102	86	Thyreophora	Ankylosauria	Asia
<i>Bissektipelta archibaldi</i>	92	90	Thyreophora	Ankylosauria	Asia
<i>Cedarpelta bilbeyhallorum</i>	116	109	Thyreophora	Ankylosauria	North America
<i>Hungarosaurus tormai</i>	85	85	Thyreophora	Ankylosauria	Europe
<i>Panoplosaurus mirus</i>	76	76	Thyreophora	Ankylosauria	North America
<i>Pawpawsaurus campbelli</i>	100	100	Thyreophora	Ankylosauria	North America
<i>Struthiosaurus austriacus</i>	85	66	Thyreophora	Ankylosauria	Europe
<i>Struthiosaurus transylvanicus</i>	85	66	Thyreophora	Ankylosauria	Europe
<i>Thecodontosaurus antiquus</i>	203	201	Sauropodomorpha	Basal Sauropodomorpha	Europe
<i>Buriolestes schultzi</i>	233	233	Sauropodomorpha	Basal Sauropodomorpha	South America
<i>Saturnalia tupiniquim</i>	233	233	Sauropodomorpha	Basal Sauropodomorpha	South America
<i>Plateosaurus engelhardti</i>	214	204	Sauropodomorpha	Basal Sauropodomorpha	Europe
<i>Cetiosaurus oxoniensis</i>	167	167	Sauropodomorpha	Sauropoda	Europe
<i>Nigersaurus taqueti</i>	115	105	Sauropodomorpha	Sauropoda	Africa
<i>Massospondylus carinatus</i>	200	183	Sauropodomorpha	Basal Sauropodomorpha	Africa
<i>Diplodocus longus</i>	154	152	Sauropodomorpha	Sauropoda	North America
<i>Shunosaurus lii</i>	159	159	Sauropodomorpha	Sauropoda	Asia
<i>Barosaurus lentus</i>	152	150	Sauropodomorpha	Sauropoda	North America
<i>Camarasaurus supremus</i>	155	145	Sauropodomorpha	Sauropoda	North America
<i>Malawisaurus dixeyi</i>	125	93.9	Sauropodomorpha	Sauropoda	Africa
<i>Giraffatitan brancai</i>	150	145	Sauropodomorpha	Sauropoda	Africa
<i>Tornieria africana</i>	150	150	Sauropodomorpha	Sauropoda	Africa
<i>Dicraeosaurus hansemanni</i>	155	150	Sauropodomorpha	Sauropoda	Africa
<i>Apatosaurus ajax</i>	152	151	Sauropodomorpha	Sauropoda	North America

<i>Amargasaurus cazau</i>	129	122	Sauropodomorpha	Sauropoda	South America
<i>Spinophorosaurus nigerensis</i>	167	167	Sauropodomorpha	Sauropoda	Africa
<i>Sarmientosaurus musacchioi</i>	95	95	Sauropodomorpha	Sauropoda	South America
<i>Lohuecotitan pandafilandi</i>	72	72	Sauropodomorpha	Sauropoda	Europe
<i>Brachiosaurus altithorax</i>	154	153	Sauropodomorpha	Sauropoda	North America
<i>Coelophysis bauri</i>	196	196	Theropoda	Coelophysidae	North America
<i>Citipati osmolskae</i>	75	71	Theropoda	Oviraptorosauria	Asia
<i>Incisivosaurus gauthieri</i>	126	126	Theropoda	Oviraptorosauria	Asia
<i>Falcarius utahensis</i>	139	134	Theropoda	Therizinosauria	North America
<i>Nothronychus mckinleyi</i>	92	91	Theropoda	Therizinosauria	North America
<i>Erlikosaurus andrewsi</i>	96	89	Theropoda	Therizinosauria	Asia
<i>Velociraptor mongoliensis</i>	75	71	Theropoda	Dromaeosauridae	Asia
<i>Bambiraptor feinbergi</i>	72	72	Theropoda	Dromaeosauridae	North America
<i>Deinonychus antirrhopus</i>	115	108	Theropoda	Dromaeosauridae	North America
<i>Halszkaraptor escuilliei</i>	75	71	Theropoda	Dromaeosauridae	Asia
<i>Gallimimus bullatus</i>	70	70	Theropoda	Ornithomimidae	Asia
<i>Struthiomimus altus</i>	77	66	Theropoda	Ornithomimidae	North America
<i>Troodon formosus</i>	77.5	76.5	Theropoda	Troodontidae	North America
<i>Zanabazar junior</i>	70	70	Theropoda	Troodontidae	Asia
<i>Allosaurus fragilis</i>	155	145	Theropoda	Allosauridae	North America
<i>Dilong paradoxus</i>	126	126	Theropoda	Tyrannosauroidae	Asia
<i>Alioramus altai</i>	70	70	Theropoda	Tyrannosauridae	Asia
<i>Timurlengia euotica</i>	92	90	Theropoda	Tyrannosauroidae	Asia
<i>Bistahieversor sealeyi</i>	74.5	74.5	Theropoda	Tyrannosauroidae	North America
<i>Gorgosaurus libratus</i>	76.6	75.1	Theropoda	Tyrannosauridae	North America
<i>Daspletosaurus torosus</i>	77	74	Theropoda	Tyrannosauridae	North America
<i>Tarbosaurus bataar</i>	70	70	Theropoda	Tyrannosauridae	Asia
<i>Tyrannosaurus rex</i>	68	66	Theropoda	Tyrannosauridae	North America
<i>Ceratosaurus nasicornis</i>	153	148	Theropoda	Ceratosauridae	North America
<i>Acrocanthosaurus atokensis</i>	116	110	Theropoda	Carcharodontosauridae	North America
<i>Carcharodontosaurus saharicus</i>	100.5	93.9	Theropoda	Carcharodontosauridae	Africa
<i>Giganotosaurus carolinii</i>	98	97	Theropoda	Carcharodontosauridae	South America
<i>Majungasaurus crenatissimus</i>	70	66	Theropoda	Abelisauridae	Africa
<i>Viavenator exxoni</i>	86	83	Theropoda	Abelisauridae	South America
<i>Abelisaurus comahuensis</i>	80	80	Theropoda	Abelisauridae	South America
<i>Skorpiovenator bustingorryi</i>	95	95	Theropoda	Abelisauridae	South America
<i>Carnotaurus sastrei</i>	71	71	Theropoda	Abelisauridae	South America
<i>Aucasaurus garridoi</i>	85	80	Theropoda	Abelisauridae	South America
<i>Irritator challengeri</i>	110	110	Theropoda	Spinosauridae	South America
Aves	121	0	---	---	Worldwide
Pseudosuchia	250	0	---	---	Worldwide

At the broadest phylogenetic level, non-avian dinosaur endocasts are represented by Cerapoda (constitutes 23% of the total dataset), Thyreophora (14%), Sauropodomorpha (24%), and Theropoda (39%).

Table S2 – Comparative list of hearing ranges from extant reptiles, birds, and *Velociraptor mongoliensis*. All modern values are taken from Walsh et al. (2009). The hearing frequencies for *V. mongoliensis* were calculated for Chapter 2 of this thesis.

Genus	High range (Hz)	Mean (Hz)
<i>Crocodylus acutus</i>	2700	1650
<i>Alligator mississippiensis</i>	900	550
<i>Caiman crocodylus</i>	1700	1150
<i>Chelonia mydas</i>	350	325
<i>Chelydra serpenta</i>	800	600
<i>Sphenodon punctatus</i>	700	450
<i>Gekko gekko</i>	4780	2610
<i>Ptyodactylus hasselquistii</i>	2200	1400
<i>Hemitheconyx caudicinctus</i>	1580	1010
<i>Podarcis scicula</i>	2500	1750
<i>Gerrhonotus multicarinatus</i>	2400	1800
<i>Tiliqua rugosa</i>	3800	2100
<i>Chalcides ocellatus</i>	1700	1150
<i>Varanus niloticus</i>	1100	950
<i>Gambelia (Crotaphytus) wislizenii</i>	400	500
<i>Anolis sagrei</i>	1800	1100
<i>Uromastyx hardwickii</i>	2700	1650
<i>Diplometopon zarudnyi</i>	800	1100
<i>Tyto alba</i>	9000	5000
<i>Melopsittacus undulatus</i>	6700	3650
<i>Dromaius novaehollandiae</i>	3420	1790
<i>Spheniscus demersus</i>	3400	2300
<i>Corvus sp.</i>	4900	2550
<i>Taeniopygia guttata</i>	4700	3350
<i>Velociraptor mongoliensis</i>	3965	2368

Other publications generated during my thesis:

Landi, D., **J. L. King**, Q. Zhao, E. J. Rayfield, and M. J. Benton. 2021. Testing for a dietary shift in the Early Cretaceous ceratopsian dinosaur *Psittacosaurus lujiatunensis*. Palaeontology. DOI: 10.1111/pala.12529

Ballel-Mayoral, A., **J. L. King**, J. Neenan, E. J. Rayfield, and M. J. Benton. 2020. “The braincase, brain, and paleobiology of the basal sauropodomorph dinosaur *Thecodontosaurus*”. Zoological Journal of the Linnean Society. DOI: 10.1093/zoolinnean/zlaa157

King, J. L. and Super, K. 2019. “First instance of a small *Xiphactinus* (Teleostei: Ichthyodectiformes) specimen from the Niobrara Chalk of western Kansas: new information on ichthyodectid ontogeny”. Historical Biology DOI: 10.1080/08912963.2019.1623212

Zhang, Q.-N., **J. L. King**, H.-L. You, D. Q. Li, and Y. M. Hou. 2019. “Brain morphology of *Auroraceratops* sp. (Dinosauria: Ceratopsia) based on CT scans from the Early Cretaceous of Gansu province, China”. Historical Biology, DOI: 10.1080/08912963.2019.1588893